AD-A144 949 AN INVESTIGATION OF THE SOLUBILITY AND DIFFUSIVITY OF CHROMIUM IN GALLIUM ARSENIDE(U) ADVANCED RESEARCH AND APPLICATIONS CORP SUNNYVALE CA T J MAGEE ET AL. 1/3

UNCLASSIFIED 23 MAY 84 N00014-80-C-0482 F/G 7/4 NL

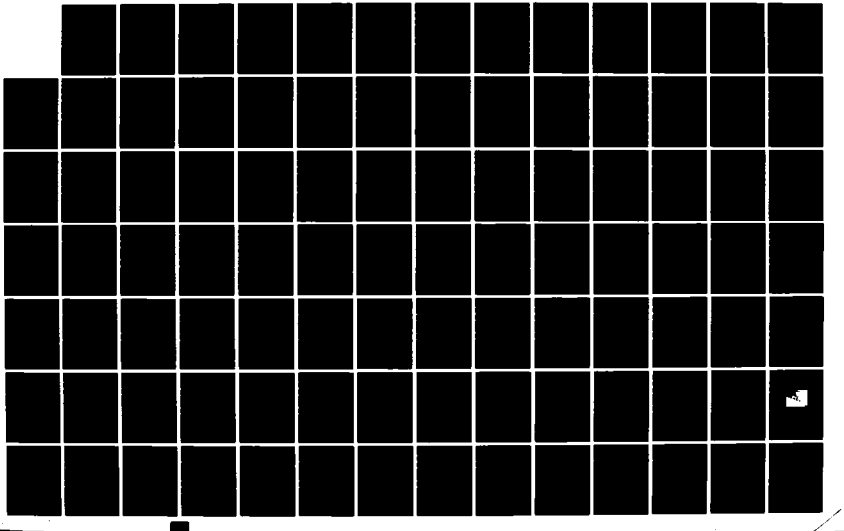

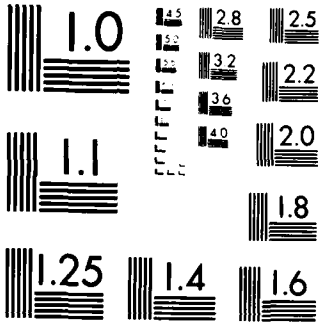

AN INVESTIGATION OF THE SOLUBILITY AND DIFFUSIVITY OF CHROMIUM IN GALLIUM ARSENIDE

SPECIAL INTERIM TECHNICAL REPORT
FOR THE PERIOD 02/07/81 THROUGH 01/31/84

PREPARED FOR:

DEFENSE ADVANCED RESEARCH PROJECTS AGENCY
1400 WILSON BOULEVARD
ARLINGTON, VA 22209

ATTENTION: DR. R. A. REYNOLDS
MR. S. ROOSILD

OFFICE OF NAVAL RESEARCH
800 NORTH QUINCY STREET
ARLINGTON, VA 22217

ATTENTION: MR. M. N. YODER

ADVANCED RESEARCH AND APPLICATIONS CORPORATION

Unclassified

SECURITY CLASSIFICATION OF THIS PAGE (When Data Entered)

REPORT DOCUMENTATION PAGE	READ INSTRUCTIONS BEFORE COMPLETING FORM
1. REPORT NUMBER	2. GOVT ACCESSION NO. AD-A144 747 / 3. RECIPIENT'S CATALOG NUMBER
4. TITLE (and Subtitle) An Investigation of the Solubility and Diffusivity of Chromium in Gallium Arsenide	5. TYPE OF REPORT & PERIOD COVERED Special Interim Technical 02/07/81 - 01/31/84
	6. PERFORMING ORG. REPORT NUMBER
7. AUTHOR(s) T. J. Magee, G. R. Woolhouse, D. A. Stevensen* and M. Deal* *Stanford University	8. CONTRACT OR GRANT NUMBER(s) N00014-80-C-0482
9. PERFORMING ORGANIZATION NAME AND ADDRESS Advanced Research & Applications Corporation 1223 E. Arques Ave. Sunnyvale, CA 94086	10. PROGRAM ELEMENT, PROJECT, TASK AREA & WORK UNIT NUMBERS
11. CONTROLLING OFFICE NAME AND ADDRESS Defense Advanced Research Projects Agency Materials Sciences Office 1400 Wilson Blvd., Arlington, VA 22209	12. REPORT DATE 05/23/84
	13. NUMBER OF PAGES
14. MONITORING AGENCY NAME & ADDRESS (if different from Controlling Office) Office of Naval Research Code 427, M. Yoder Arlington, VA 22217	15. SECURITY CLASS (of this report) Unclassified
	15a. DECLASSIFICATION/DOWNGRADING SCHEDULE

16. DISTRIBUTION STATEMENT (of this Report)

Approved for public release; distribution unlimited.

17. DISTRIBUTION STATEMENT (of the abstract entered in Block 20, if different from Report)

18. SUPPLEMENTARY NOTES

19. KEY WORDS (Continue on reverse side if necessary and identify by block number)

differential thermal analysis	outdiffusion
diffusion	phase equilibria
Ga-As-Cr	SIMS
indiffusion	solubility
junction diffusion	x-ray diffraction

20. ABSTRACT (Continue on reverse side if necessary and identify by block number)

Phase equilibria in the Ga-As-Cr system have been studied and determined between room temperature and 1300°C by differential thermal analysis and x-ray diffraction. Solubility studies of Cr in GaAs have also been performed together with three types of diffusion experiments: Indiffusion, outdiffusion and junction diffusion. Cr concentration-depth profiles determined by SIMS have been fitted to a diffusion model. Some of the anomalous behavior of Cr in GaAs observed here and in other studies have been explained in terms of the phase equilibria information and the solubility and diffusion results.

DD FORM 1 JAN 73 1473 EDITION OF 1 NOV 65 IS OBSOLETE

Unclassified

SECURITY CLASSIFICATION OF THIS PAGE (When Data Entered)

FOREWORD

This report is a re-formatted version of the Ph.D. thesis of M. Deal describing research carried out under the supervision of Prof. D. A. Stevenson and submitted to Stanford University. The work has been supported under a sub-contract from Advanced Research and Applications Corporation, Drs. T. J. Magee and G. R. Woolhouse, Principal Investigators, under DARPA Contract No. N00014-80-C-0482 (S. Roosild), monitored by ONR (M. Yoder).

FINAL REPORT

AN INVESTIGATION OF THE SOLUBILITY AND DIFFUSIVITY OF CHROMIUM IN GALLIUM ARSENIDE

submitted to

Advanced Research and Applications Corp. (ARACOR)
1223 E. Arques Avenue
Sunnyvale, CA 94086

January 1984

Principal Investigator
David A. Stevenson
Department of Materials
Science and Engineering

ABSTRACT

Recent studies of Cr in GaAs have established that significant Cr diffusion may occur during crystal growth or subsequent processing; however, most work has been done without concern for phase equilibria and, as a result, inconsistent and invalid results are common in the literature. Some investigators were aware of the need for phase equilibria information and stated that their work was limited because the Ga-As-Cr ternary system had not been determined.

This research program concerns the study of phase equilibria in the Ga-As-Cr system and applying this knowledge to the design and implementation of well-defined experiments to study the solubility and diffusion of Cr in GaAs.

The Ga-As-Cr phase diagram (for arsenic a/o $\leq$ 50) was determined from room temperature to 1300°C by differential thermal analysis and x-ray diffraction. Of particular significance to solubility and diffusion studies are: 1) Cr and GaAs are not in equilibrium with each other under any conditions; 2) two and three condensed phase regions are present which would be suitable Cr sources for solubility and diffusion studies; and 3) a Ga-rich liquid is in equilibrium with GaAs which has a very high (up to 10 a/o) Cr solubility.

Well-defined solubility studies of Cr in GaAs have been performed resulting in solubility values for various regions in the ternary phase diagram and distribution coefficients. The Cr solubility in GaAs for the $GaAs_{(s)}$-$CrAs_{(s)}$-$Ga_{(\ell)}$ region ranges from 1.3×10^{16} to 1.2×10^{17} cm^{-3} from 700

to 1000°C; the solubility in the $GaAs_{(s)}$-$Ga_{(\ell)}$ region is lower. Results from these studies confirm the applicability of ternary phase equilibria to these solubility studies and also confirm the phase diagram determinations. The results of Cr solubility studies in doped GaAs confirm the model of Cr as a deep acceptor on a Ga site, and capacitance-voltage measurements confirm that the bulk Cr, measured by secondary ion mass spectrometry (SIMS) is in solution and electrically active.

Three types of diffusion experiments, indiffusion, outdiffusion, and "junction diffusion", have been performed, again utilizing the phase equilibria information. The Cr concentration-depth profiles, determined by SIMS, have been fitted to the "substitutional/interstitial dissociative diffusion" model. Three regimes of the Cr diffusion have been identified - vacancy diffusion controlled, vacancy regeneration controlled, and interstitial diffusion controlled - and values for several key parameters have been determined. Diffusion studies were also done in doped GaAs and in GaAs from different suppliers, and the different diffusion results can be explained in terms of the diffusion model and the defect chemistry of GaAs.

In addition, some of the anomalous behavior of Cr in GaAs observed in this work and in other studies can be explained in terms of the phase equilibria information and the solubility and diffusion results: very fast Cr diffusion observed in some cases is accomplished via fast interstitials; large Cr build-up seen at the GaAs surface after a diffusion anneal is mostly a

result of $Ga_{(\ell)}$ formation; and a depletion of Cr near the surface after Cr indiffusion is due to the surface accumulation of manganese.

Finally, the results from this research have been used in correlating and explaining many of the confusing results in the literature concerning Cr in GaAs. From this work, a much clearer picture of Cr in GaAs has emerged.

TABLE OF CONTENTS

LIST OF TABLES

LIST OF FIGURES

LIST OF SYMBOLS

C	concentration (cm^{-3})
C_i	interstitial conc. (cm^{-3})
C_s	substitutional conc. (cm^{-3})
C_v	vacancy conc. (cm^{-3})
C_i'	equilibrium interstitial conc. (cm^{-3})
C_s'	equilibrium substitutional conc. - "solubility" (cm^{-3})
C_v'	equilibrium vacancy conc. (cm^{-3})
C_i^+	positive charged interstitial conc. (cm^{-3})
C_s^-	negative charged substitutional conc. (cm^{-3})
C_o	extrapolated surface conc. (cm^{-3})
C_1	initial conc. for $x < 0$ (cm^{-3})
C_2	initial conc. for $x > 0$ (cm^{-3})
C_s''	extrinsic solubility (cm^{-3})
c	number of components
D	diffusivity (cm^2/sec)
D_i	interstitial diff. (cm^2/sec)
D_s	substitutional diff. (cm^2/sec)
D_v	vacancy diff. (cm^2/sec)
D_{eff}	effective diff. (cm^2/sec)
D_{fast}	effective diff. which = $D_iC_i/(C_i + C_s)$ (cm^2/sec)
D_{slow}	effective diff. which = $D_vC_v/(C_v + C_s)$ (cm^2/sec)

D_o	pre-exponential diffusion coefficient (cm^2/sec)
E_a	activation energy (eV)
e^-	electron
f	number of degrees of freedom
F	force on atom by stress field (dyne)
g	degeneracy factor
ΔG_f	Gibbs energy of formation (calorie)
h^+	hole
I	impurity atom
I_i	interstitial impurity atom
I_i^+	positive charged interstitial impurity
I_s	substitutional impurity atom
I_s^-	negative charged interstitial impurity
k	distribution coefficient
k_l	vacancy generation rate (sec^{-1})
K	equilibrium constant for V_{Ga} and $As_{2(v)}$
L_i	interstitial lattice atom
L_ℓ	lattice atom (on lattice site)
n	free electron conc. (cm^{-3})
n_i	intrinsic electron conc. (cm^{-3})
p	number of phases
P	pressure
P_{As_2}	partial pressure of arsenic (atm)
T	temperature (K)
T°C	temperature (°C)
t	time (sec)

V	vacancy
V^-	negative charged vacancy
V_{Ga}	gallium vacancy
x	distance (μm)
μ	$x/\sqrt{2Dt}$
μ_j^{α}	chemical potential of species j in phase α (cal.)
Θ	vacancy generation, or "equilibrium", time constant (sec)
γ	activity coefficient

1. INTRODUCTION

The use of chromium in gallium arsenide in microelectronic devices is widespread. Chromium is intentionally introduced into the GaAs substrate material during the initial growth of the bulk single crystal in order to compensate the electrically active residual defects and impurities, and render the substrate semi-insulating. However, there have been problems with the incorporation of chromium in the active region of the devices, either during the epitaxial growth on the substrates, or during the subsequent process annealing of the wafers. This has often resulted in poor device performance and has prompted some device manufacturers to explore other possibilities for semi-insulating substrates, particularly, the use of ultra-pure "undoped semi-insulating GaAs," grown by the Liquid Encapsulated Czochralski (LEC) method (1-3). However, the majority (60 - 80%) of GaAs devices are still being made using Cr-doped GaAs substrates (4).

Because of this problem with Cr-doped GaAs, many studies have been done recently on the redistribution of chromium in gallium arsenide. In many of these studies, solubility and diffusivity values have been cited or used in attempts to explain the behavior. However, in none of these studies had ternary phase equilibria been considered, simply because there was no information on appropriate regions of the Ga-As-Cr phase diagram. Furthermore, only a small percentage of the researchers even mentioned the necessity of considering phase equilibria information in reporting or using other's solubility and diffusivity information, or in performing their

experiments. As a result, many diffusivity and solubility values used in explaining their results are not valid.

The goals in this work have been the following:

1. Experimentally determine the regions of the Ga-As-Cr ternary phase diagram that are appropriate for solubility and diffusion studies of Cr in GaAs;

2. Use this knowledge to perform valid and well-defined solubility and diffusion experiments of Cr in GaAs;

3. Explain other phenomena, such as surface degradation and the anomalous surface build-up of Cr, using the phase equilibria information;

4. Correlate and explain the present literature on the solubility and diffusivity of Cr in GaAs.

The outline for this thesis is as follows:

In chapter 2, I discuss the need to consider ternary phase equilibria, and to know the ternary phase diagram in conducting solubility and diffusion experiments of an impurity in a compound semiconductor and in reporting and using these values. Also, the concept of "equilibrium" is discussed in relation to these studies.

In chapter 3, the Ga-As-Cr phase diagram determination is presented, along with its implications and applications to the solubility and diffusion studies.

Chapter 4 is devoted to the solubility studies of Cr in GaAs. Included is a review of previous work concerning the solubility of Cr in GaAs and how earlier results were in error or were misleading because phase equilibria was not

considered. The results of the present work, including solubility values of Cr in undoped, and doped, GaAs, are presented, as well as results which confirm both the validity of applying the phase equilibria consideration to solubility studies, and of the phase diagram determinations. In addition, the use of Secondary Ion Mass Spectrometry (SIMS) is discussed.

Chapter 5 is devoted to the substitutional/interstitial dissociative diffusion mechanism, including a literature review, the governing equations for the different cases, and its application to real systems.

In chapter 6, I discuss my work on the diffusion of Cr in GaAs. Three types of diffusion experiments - indiffusion, outdiffusion, and "junction" diffusion - have been done, all using the phase diagram and solubility results. From these studies, a previously proposed (5) diffusion mechanism was confirmed, expanded, and quantified. In addition, what has been learned about GaAs itself, and other impurities and defects, from these studies is presented. Previous work concerning the diffusion of Cr in GaAs is also discussed and analyzed.

In chapter 7, studies of various surface phenomena in GaAs are reported. These include: surface build-up of Cr after annealing; surface degradation of GaAs; Cr depletion near the surface, even after indiffusion; and high Cr levels in LPE layers. These are discussed in relation to the previous findings.

In chapter 8, a summary and conclusions of this work will be presented, as well as suggestions for future work.

2. THE NEED FOR THE TERNARY PHASE DIAGRAM

2.1 Introduction

The study of a dopant in a compound semiconductor is more complex than that of a dopant in an elemental semiconductor because of the extra degree of freedom (6). The number of degrees of freedom is the number of intensive variables that must be controlled or measured in order for an equilibrium system to be properly specified or defined. Once the correct number of degrees of freedom in a specific system are specified, then the system is "well-defined". The failure to recognize this has led to confusion, and to erroneous and invalid conclusions, in the past. In order to know the number of degrees of freedom, and to establish if the system is at, or even near, equilibrium, the ternary phase diagram must be known.

The importance of knowing the appropriate ternary phase diagram in diffusion and solubility studies of an impurity in a compound semiconductor has, in the past, only occasionally been espoused. Examples of this are: Shih, Allen, and Pearson's (6) article on "Diffusion in Compound Semiconductors in Terms of the Ternary Phase Diagram"; Tuck's book (7) on Diffusion in Semiconductors; and Casey's review article (8) on "Diffusion in the III-V Compounds Semiconductors". In all these cases, the example of Zn in GaAs is used, mainly because it is the only system that has been extensively studied in this manner, due to its importance in GaAs electronic devices, and to the fact that the Ga-As-Zn system is relatively simple and well-known (9). Casey and Panish's article (10) on Zn in GaAs

is another excellent example of ternary phase considerations in diffusion studies.

A good review of ternary phase diagrams in general is Reisman's Phase Equilibria (11). (Additional references on determining phase diagrams are be given in the succeeding chapter.)

In the present chapter, the basic concepts regarding the relation of ternary phase equilibria to solubility and diffusion are presented first, including the use of the phase rule. Then the need for the ternary phase diagram for establishing well-defined, and for citing and using solubility and diffusion results, is discussed. Finally, the need for the ternary phase diagram for equilibrium conditions will be presented, along with some notes regarding equilibrium, quasi-equilibrium, the determination of the final equilibrium state, and suitable sources for solubility and diffusion studies based on the above considerations.

2.2 Basic Concepts

The number of degrees of freedom needed to define a system is stipulated by the phase rule:

$$f = c - p + 2 \qquad (2\text{-}1)$$

where f is the number of degrees of freedom, c is the number of components (e.g., three for a ternary system, two for a binary system), and p is the number of phases present. A simple derivation of this, taken from R.E. Dickerson (12), follows.

It is a matter of experience that the variables temperature, pressure, and the mole fractions of each component in a phase fix all other macroscopic intensive properties of a

system, including mechanical, thermal, and chemical properties. This means that for p phases, 2 + p c intensive variables are sufficient to define all the intensive properties of the system (assuming temperature and pressure are constant throughout the system). The number of independent intensive variables is the total number of variables minus the number of restraining conditions. There are two types of restraining equations: 1) the sum of the mole fractions in each phase must equal unity - there are p such equations; and 2) the chemical potential of each component must be the same in all phases - for each component, there are p-1 equations ($_j$ = $_j$ = ... = $_j^p$), therefore there are c(p-1) equations of this type. The total number of restraining equations is thus p+p c-c. Therefore, the number of independent variables is: f = 2+p c - (p+p c-c) = c+2-p, as earlier stated.

For ternary phase diagrams, with 3 components by definition:

$$f = 3+2-p = 5-p \qquad (2-2)$$

If the system's total composition lies in a three phase region (two condensed phases plus the ever present vapor phase), then the degrees of freedom are two. Such a system may be defined by specifying the temperature and the vapor pressure. Or alternately, the temperature and the composition of one of the condensed phases may be specified. For a four phase system (three condensed phases plus the vapor phase), there is only one degree of freedom. In this case, specifying only the temperature completely defines the system. In addition, the overall composition of the system (prescribed amounts of

component A, B, and C) lies in a tie triangle region in a ternary phase diagram, which by definition is a region in which 3 condensed phases are present and enclosed by three tie-lines (hence a tie-triangle). As long as the system composition lies within such a region at a given temperature, the system is well-defined; thus, there are no remaining degrees of freedom.

Once a system is well-defined, all intensive variables are fixed, such as the chemical potentials of each component in each phase, the partial pressure of each component, the vacancy concentration in each phase, and such related properties as the solubility and diffusivity. Even if the net composition of the system is changed, as long as the composition remains in the same tie triangle region, the values of all the variables will not change. Similarly, if the system does change from one region in the phase diagram to another (e.g., from a 3-condensed phase region to a two phase region, or to a different 3 phase region), or from one position in a two condensed phase region to another, then the variables mentioned above are expected to change.

2.3 The Need for The Ternary Phase Diagram for Well-defined Conditions

It is obvious, then, that to establish well-defined conditions for studying the behavior of an impurity in a compound semiconductor, one needs the appropriate ternary phase diagram. Without this knowledge, one would not know: 1) if there were any unspecified degrees of freedom, whether it is necessary to control, for example, the exact composition of a liquid phase in the system; 2) if changing such quantities as

the amounts of the components or the volume of the system influence the results; or 3) whether the results of a particular experiment could be compared to another experiment. This last point is an important consideration in presenting results and using results of others. To do these properly, one must have knowledge of the ternary phase diagram since the exact conditions of the experiment may alter the solubility, diffusivity, and partial pressure, and usually do. The person citing results (e.g. the "solubility of C in AB") should report the conditions that led to that result, and if possible, the exact location in the phase diagram. Usually the experimental conditions stipulate at least the first part of this. If those results are then used to explain some other experimental result, such as using solubility results in explaining diffusion behavior, one must make sure that the respective diffusion and solubilty values correspond to the same system, as defined by the phase rule. This is commonly not done, as I will discuss in upcoming chapters. In both cases, the ternary phase diagram is required.

2.4 The Need for the Ternary Phase Diagram for Equilibrium Conditions

Another use of the ternary phase diagram in these studies is to establish whether the system is at or near equilibrium. The best explaination of this is by example. If a dopant is not in equilibrium with the semiconductor material for the specified conditions, and the solubility and diffusion experiments are performed by using the pure elemental dopant as the source material (as is usually done), then during the

course of the experiment, either the source, or the semiconductor material, or both, depending on the position in the ternary phase diagram indicated by the overall composition, will undergo a change in phase. In that case, the results are not valid. This is especially true for the case when the entire semiconductor material itself is changing phase and the desired result is the solubility of a specific dopant in that semiconductor material. But it is also true for the case when the source material is changing because: 1) the activity of the dopant will be changing; and 2) in changing phase, the dopant usually gains components from the semiconductor, and hence part of the semiconductor, usually near the surface and thus critical to the diffusion and/or solubility, many change phase. To know if the initial phases are at equilibrium and stable with respect to each other requires a knowledge of the phase diagram. As will be discussed later, the lack of appropriate phase equilibria was the major limitation in the experiments of chromium in gallium arsenide performed by Tuck and Adegboyega (5), as was indicated by Tuck himself.

2.5 Equilibrium and Quasi-equilibrium

A comment should be made regarding equilibrium and the diffusion process. Diffusion is necessarily a non-equilibrium process. It is, in fact, a process in which equilibrium is approached; i.e., the component concentration approaches the solubility level in the host material for the given source conditions. However, as long as the starting materials are different from the equilibrium phases only by that the amounts of the components ("dopants") in them are different, one may

say that the system is at all times in "quasi-equilibrium" (6). In such cases, the chemical potentials of the diffusing species at the surface may be assumed to remain constant throughout the experiment, and the diffusion experiment is considered valid. This is not the case when the starting materials are different phases from the equilibrium phases (as discussed in the preceding section). In that case, the chemical potentials may undergo a significant change.

Another comment is appropriate regarding the equilibrium of lattice defects, such as vacancies and interstitials, especially deep within the sample. The equilibrium concentrations of lattice defects may take a relatively long time to attain equilibrium, and this must be considered.

Also, equilibrium and phase diagram considerations may affect some aspects of the solubility and diffusion behavior more than other aspects. For example, the solubility of a component in a phase is very dependent on phase considerations, as has been discussed; however, the diffusivity of an impurity by an interstitial mechanism may not be as dependent on the component chemical potentials, as dictated by other phases in the system, and thus may not be as dependent on the phase diagram considerations.

2.6 Determining the Final, Equilibrium State

A point should be made concerning equilibrium in regards to the final, equilibrium state of the system. To determine the final state of a particular experimental system, one usually just determines the overall composition of the system (a/o Ga, As, and Cr, for example) from the starting material,

finds that spot on the isothermal section of the ternary phase diagram for the appropriate temperature, and establishes what phases are stable for that composition. However, one must consider the vapor phase since conventional isothermal sections in ternary diagrams only consider the condensed phases. One must account for the loss of components from the condensed phases to establish the equilibrium vapor pressure. In many cases this will not have any effect on the final state, but in some cases it could. An example of a case where it will not have an effect is in an indiffusion performed with plenty of the source material and a large diffusion sample, and the overall system composition lies well within the interior of a tie triangle. In this case, losing a small amount of one or more of the components to the vapor phase will probably not shift the system to a different region of the phase diagram. (However, it may, as we will see later, affect how much of each phase is present.) An example of a case where losing components from the condensed phase to establish the equilibrium vapor pressure may have a large effect is during an outdiffusion anneal of a doped semiconductor. Here, losing the same amount of a component as in the above case could very well put the system in a new region of the phase diagram just due to the geometry of the phase diagram and the relatively small solubilities of dopants in semiconductors.

In all the considerations mentioned in this chapter, it has been assumed that the system in question is a closed system. Only in that case will equilibrium be achieved. It may take a while, and it may require that some of the

components leave the condensed phases and go into the vapor phase, which can be taken into account without much trouble. But if the system is open, as in the case of open flow tubes commonly used in semiconductor processing and, in some cases, in studying solubility and diffusion, then the system never reaches a final equilibrium state. The components enter the vapor phase to try to achieve equilibrium; however, they are removed before equilibriun is established. As a result, the system becomes very complex to study. Therefore, in our studies, a closed ampoule is used in all cases. (It is possible, though, to qualitatively explain some phenomena reported by others who use open tubes.)

2.7 Suitable Sources

It is obvious from the before-mentioned considerations regarding equilibrium conditions what source materials should be used for valid solubility and diffusion studies. Because you want the material to be in equilbrium - or actually "in quasi-equilibrium"- with the phase you are diffusing the component into, the source material should be made up of phases that all lie in the same region (e.g., a tie-triangle region) as the substrate phase. In practice, one anneals a mixture which has an overall composition in the region so that the proper equilibrium phases are formed. Then the actual solubility or diffusion experiment is done by annealing this source with the undoped substrate.

2.8 Summary

In summary, to have valid solubility and diffusion experiments, one must have a well-defined equilibrium, or

quasi-equilibrium, system. To know if this is the case, one must have a knowledge of the appropriate phase diagram. In the case of an impurity in a compound semiconductor, this means knowing the ternary phase diagram. Further, in citing results, or using other's results, one must be aware of the ternary phase equilibrium considerations.

3. Ga-As-Cr PHASE EQUILIBRIA

3.1 Introduction and Literature Review

As discussed in chapter 2, knowledge of the appropriate ternary phase equilibria is necessary to design and interpret solubility and diffusion studies of an impurity in a compound semiconductor. Since the Ga-As-Cr ternary phase diagram had not previously been determined, this was the first goal of my research.

A logical starting point in determining a ternary phase diagram is the knowledge of the respective binary systems, including a complete description of the compounds, with their melting points, x-ray diffraction patterns (for identification purposes), and, if possible, the Gibb's formation energies of the compounds. With this information, one can predict possible ternary sections. The true sections may then be established by annealing, quenching, and x-raying appropriate ternary compositions at appropriate temperatures. The melting points of the binary compounds establish the temperatures where two or three condensed phase regions may be present, and provide clues to which compounds are the "dominant" ones, with tie lines radiating from them to other compounds and elements; these dominant compounds are usually high melting point compounds which are centrally located along the binary tie lines. The Ga-As-Cr system was particularly difficult because there are nine reported intermediate binary compounds, with incomplete and confusing information concerning many of them.

The Ga-As system, with only one intermediate compound, GaAs, is well known and described in a good review article

(13), and the Cr-Ga system, with 4 intermediate compounds, has been extensively studied (14-16). However, the Cr-As system had not been adequately studied prior to the present work, and there is confusing information in the literature. In 1960, Yuzuri (17) proposed a tentative Cr-As phase diagram for the composition region above 50 a/o Cr, with the following binary CrAs compounds: CrAs, Cr_3As_2, Cr_2As, and Cr_5As. The melting point of each compound was only estimated. In 1967, Boller, Wolfsgruber, and Nowotny (18) reported that the Cr_5As phase was actually Cr_4As. In 1970, Baurecht, Boller, and Nowotny (19) proposed the existence of Cr_4As_3; however, it is not clear from their description whether this compound replaced Cr_3As_2 or is an additional compound. (The latter statement is implied in their paper; however, the fact that their x-ray pattern for Cr_4As_3 is identical to Yuzuri's Cr_3As_2 pattern implies that the former statement is correct.) All references mention CrAs, but there are uncertainties regarding its x-ray pattern. Nowotny and Arstad (20) published an x-ray pattern in 1937; however, many pairs of reflections were grouped together into single d-spacings and 2θ values. (From calculations using their lattice spacing values, I have found that these pairs split into reflections as much as 1° apart. This led to many problems in identifying the compound.) There are also inconsistencies in the reported melting points of some of the compounds. Yuzuri (17) estimated the melting point of CrAs to be ≈800°C; however Baurecht, Boller, and Nowotny (21), in their Cr-As-C phase diagram, show it to be a solid at 1000°C, thus, a melting point of greater than 1000°C. With regard to the

compound Cr_4As_3, it was shown to be present in the Cr-As-C phase diagram at 1000°C (21), but not present in the Cr-As-Ge phase diagram at 800°C (18). This implies a peritectic decomposition of this compound, contrary to all other studies. The compound Cr_4As was shown to be present at 800°C in the Cr-As-Ge system, but not at 1000°C in the Cr-As-C system. This would imply a melting point between 800 and 1000°C; however, Yuzuri estimated its melting point to be greater than 1200°C. The existence of Cr_2As and its x-ray pattern have not been disputed (22). However, its melting point has only been estimated, and low and high temperature forms have been reported, with no transition temperature given. In addition, a high pressure $CrAs_2$ phase on the arsenic side of the phase diagram has been reported (23).

The only study on the Ga-As-Cr system, besides determining the distribution coefficient of Cr in $GaAs_{(s)}$ versus Cr in $Ga_{(\ell)}$ (24-29), was the determination of the arsenic solubility in Cr-doped Ga melt, described by Andre and LeDuc (30). The arsenic and chromium concentrations both ranged from 2 to 10 a/o over a temperature range of 600 to 900°C. They did not say whether 10 a/o was the limiting Cr concentration in the Ga melt, only that it was at least that high.

My initial objective was to confirm the information concerning the Cr-Ga system, and to synthesize the Cr-As compounds and experimentally determine necessary information concerning them, such as their melting points and x-ray diffraction patterns. Then using the annealing, quenching, and x-ray method and differential thermal analysis, I could

determine the important features of the Ga-As-Cr ternary phase diagram. Since I was mainly interested in the Cr and Ga rich portion of the system, and because of the difficulty in annealing arsenic-rich compositions, I limited my work to the arsenic-poor portion of the phase diagram, with a/o As $\leq$ 50.

In the next section, the experimental techniques and procedures used in the phase equilibria studies are discussed, followed by the results of these studies. Then the implications and applications of these findings to solubility and diffusion studies of chromium in gallium arsenide are presented.

3.2 Experimental Techniques

The experimental techniques used in the phase equilibria studies - x-ray diffraction, differential thermal analysis,and sample synthesis and annealing - will be discussed in the following three subsections, in which the basic principles of each will be discussed in addition to the particular experimental methods and operations employed in these studies. Then the specific experimental procedures concerning the Cr-Ga and Cr-As binary systems, and the Ga-As-Cr ternary system will be described.

3.2.1 X-ray Diffraction

Unknown compounds may be identified by x-ray diffraction (XRD). The basic principle of this method is the behavior of diffracted x-ray beams from a crystal in accord with Bragg's law ($\lambda_{beam} = 2d_{hkl}\sin\theta$). The diffraction angles, θ, depend on the d-spacings, and hence on the size and shape of the unit cell of the analyzed sample. In addition, the

relative intensity of each diffracted beam depends on the contents of the unit cell. If a powder sample is analyzed, the proper Bragg angle will be achieved for all possible crystallographic planes. The sample is scanned over a range of θ's, and the intensity of the diffracted beam at each θ is measured. Because of the above considerations regarding unit cell size, shape, and contents, each element or compound will have a characteristic diffraction pattern, or "finger print". Therefore, if one knows the x-ray pattern for a particular element or compound, one may identify that material in an "unknown" sample by matching the positions of the peaks and relative intensities of the obtained diffraction pattern from the "unknown" sample to those in the "known" or "standard" diffraction pattern. If two or more compounds are present in the powder sample, then both diffraction patterns will appear in the obtained pattern, superimposed on each other. Hence, an unknown sample composed of one, two, or more phases may be analyzed, and the constituents identified by obtaining its diffraction pattern and matching the peaks to standard patterns of the different phases. (This assumes, of course, that the pattern of each compound or phase, is already known.)

In this work, a Norelco x-ray diffraction apparatus, using a Cu x-ray source (λ = 1.54178 Å) was used. The beam was operated at 36 KeV and 14 μamps. The samples were treated as follows: they were crushed into powders with a ceramic mortar and pestle; cemented to a microscope slide using a mixture of acetone and colloidion ($\approx$50-50); and slowly heated on a hot plate. (I discovered that this mixture dissolves gallium, so

in the cases that Ga was suspected to be present in the sample, i.e., whenever the composition was in the Ga corner or side of the phase diagram, and when the sample was not easy to crush, indicating a liquid phase present, I would also do an additional XRD analysis using Duco cement to hold the powder on the slide). The usual scan rate was 2°/minute, and in all cases, the scan was done from 2θ = 10° to 85°.

A good review of powder x-ray techniques is found in Schwartz and Cohen's Diffraction from Materials (31).

3.2.2 Differential Thermal Analysis

Differential Thermal Analysis (DTA) was used to determine phase transition temperatures (melting points of compounds, liquidus and solidus temperatures of two and three phase regions, etc.) for various binary and ternary compositions.

In DTA analysis, the sample in question, along with a reference material, is heated slowly to a maximum temperature, and then cooled slowly. The temperatures of the sample and the reference material during the heating/cooling cycle are each measured by separate thermocouples. The output is the difference between those two readings versus the system temperature (measured by a third thermocouple), or sometimes just the temperature of the reference material. As long as no phase transitions are occurring, and the heat capacities of the two materials (sample reference) are similar, the output should yield a straight horizontal line. If there is a slope, it can be electrically adjusted to make up for any difference in heat capacities or masses. But when a phase transition occurs in the sample (such as solid→liquid), then the temperature of the

sample relative to the reference changes. For example, during melting, the temperature of the sample remains constant until the entire phase turns to liquid, while the temperature of the reference material continues to increase. The result in the output in this case is a downward pointing spike, and the temperature (x-axis) at which this begins is the melting point. Similarly, upon cooling, an upward spike or peak occurs upon solidifying. Because of superheating and supercooling, one usually does both heating and cooling runs, and the actual phase transformation temperature is in between, usually much closer to the heating peaks since superheating is usually much less than supercooling. Any phase transition in which the heat capacity of the material changes, or which is endothermic or exothermic, will cause a change in slope of the DTA curve or a peak, thus enabling one to measure the phase transformation temperatures, and hence to obtain melting points, solidus lines, and liquidus lines.

For this work, a DuPont 1090 Thermal Analyzer (controller) with a Dupont 1600°C DTA cell was used. This uses Pt-Pt 13 Rh sample, reference, and control thermocouples. The samples (≈.01 gm) and reference material were sealed in evacuated ($\approx 10^{-6}$ torr) quartz DTA-style ampoules, which were cleaned prior to use with a 10:1 HNO_3/HF solution and rinsed with D.I. water. These were placed in 55 mm. Pt crucibles, which fit over the thermocouples. The reference sample was Al_2O_3, which does not undergo any phase transformation over the temperature range examined (i.e., room temp. to 1400°C). The normal heating rate was 20°/min.; 10°/min. was used occasionally, with

identical results. The cited temperature precision for the instrument is ± 2°C. The phase transition temperatures and melting points determined in this work are conservatively estimated to be ± 5°C. The system was calibrated using a silver sample (m.p. of 960.8°C). Each sample was heated to the maximum temperature (usually 1400°C) and cooled to 300°C, and the cycle was repeated twice to insure complete mixing and reaction of the components.

To ensure that the samples were composed of the correct compositions, a large amount (≈2 gm) of each sample was made from appropriate amounts of GaAs, Ga, Cr, and CrAs, which was annealed in a large quartz ampoule in a annealing furnace at ≈950°C for 8 hours. This was slow-cooled to room temperature (it was found that if it was fast-cooled, or quenched, liquid gallium often formed which made the sample difficult to crush), then crushed, stirred, and ≈.01 gm of it poured into the DTA ampoule, which was evacuated and sealed.

3.2.3 Synthesis and Annealing of Samples

In this section, the general techniques for the synthesis and annealing of the samples are given; the details of the synthesis of the various compounds will be presented in the following section. For both synthesizing the various binary compounds and annealing the different mixtures of Cr, Ga, and As to determine which phases are stable for that composition for the phase diagram determination, the following procedure was used: the material was weighed, placed in quartz ampoules, which were evacuated to $\approx 10^{-6}$ torr, sealed, and placed in a furnace for the appropriate time and temperature. The furnace

used was a one zone tubular Marshall furnace, with a maximum temperature of 1200°C. A sodium heat pipe was used to provide a uniform temperature zone (±1°C along the 12 inch length), and dampened any temperature decrease when placing a cold ampoule in the furnace. The temperature was controlled by a Eurotherm 919 controller, with a 45 amp SCR. A chromel-alumel thermocouple placed right next to the ampoule monitored the temperature. The thermocouple was calibrated by performing cooling curve experiments with silver (m.p. = 960.5°C) and zinc (m.p. = 419.5°C). The quartz ampoules used were constructed by me (made from Amersil and Spectrophysics semiconductor grade quartz tubing), and were cleaned prior to use with a 10% HF in HNO_3 solution, and rinsed in deionized water.

3.2.4 The Cr-Ga System; Experimental

The Cr-Ga compounds, Cr_3Ga, CrGa, Cr_4Ga_3, and $CrGa_4$, were synthesized and analyzed in order to confirm their melting points and x-ray patterns. They were synthesized by annealing appropriate amounts of Cr and Ga (99.9999% pure, from Atomergic) in evacuated quartz ampoules for 24 hours at 950°C, crushing and mixing the contents, and resealing and reannealing for 24 more hours at 950°C. Each was then cooled to 40°C below its reported melting point (except Cr_3Ga, since its melting point is too high for the annealing system), and water quenched at that temperature. Each was x-rayed. Three intermediate compositions, between CrGa and Cr_3Ga_4, between Cr_3Ga_4 and $CrGa_4$, and between Cr_3Ga and CrGa, were annealed, x-rayed, and analyzed by DTA to check the melting points and transition temperatures.

3.2.5 The Cr-As System; Experimental

The Cr-As compounds, CrAs, Cr_4As_3, Cr_2As, and Cr_4As, were synthesized by first synthesizing CrAs and then adding appropriate amounts of Cr to it and annealing to synthesize the others. This minimizes the number of times that elemental arsenic has to be used. The synthesis of CrAs was no easy task, as evidenced by the fact that three commercial chemical companies were unsuccessful at synthesizing it. It was finally necessary to synthesize pure CrAs myself. This procedure consisted of annealing appropriate amounts of powdered chromium (99.99% pure, from Atomergic) and arsenic (99.9999% pure, from Atomergic) in a thick-walled, evacuated and sealed, quartz ampoule. (The arsenic was first heated to 300°C in an evacuated condenser apparatus which removed any oxide layer on the arsenic by depositing the oxide at the cold end of the tube. The pure arsenic was then crushed and added to the chromium, with no excess arsenic.) The temperature in the furnace was ramped to 600°C at a rate of 10°C/ hour and left there for 200 hours. After examining the contents by x-ray diffraction methods, and crushing and resealing the sample, it was returned to the furnace at 600°C and ramped up to 800°C at 10°/hr., and annealed for 200 additional hours. No evidence of elemental arsenic was observed, as evidenced by the absence of yellowish or greenish vapor, characteristic of arsenic. The sample was slowly cooled to room temperature and crushed into a fine powder. Subsequent x-ray analysis produced a clean x-ray pattern of CrAs. The melting point was determined by DTA. The other Cr-As compounds were then synthesized by adding Cr

CrAs and annealing in a similar fashion. Clean x-ray patterns were obtained and are consistent with previously reported patterns. Melting points were determined by DTA. In addition, as intermediate composition between Cr_4As_3 and Cr_2As was annealed, x-ray'd, and analyzed by DTA.

3.2.6 The Ga-As-Cr Ternary System; Experimental

As discussed earlier, once the respective binary systems are known, ternary phase diagrams are usually determined by annealing various three-component compositions at various temperatures and quenched to establish which phases are stable for that composition and temperature. In this manner, appropriate tie lines may be drawn connecting stable phases and enclosing tie-triangle regions. In addition, DTA may be used to determine the transition temperatures of liquidus and solidus lines at various compositions. Using this information along with the binary information, one may construct ternary phase diagrams. The major features of a ternary phase diagram are established by the tie lines between compounds and may be predicted by determining which pairs of compounds have a lowest Gibbs energy at cross-over points. However, one must know the ΔG_f values of all the compounds present in the system. Since only one of these values were known for the Ga-As-Cr system (out of 9 compounds), and because experimentally determining these values is a difficult task, requiring specialized equipment, this method was not used. It is easier to anneal the various compositions and find which phases are present. Good tutorials and discussions of ternary phase diagrams and their determination are found in Rhines' Phase Diagrams in

Metallurgy - Their Development and Application (32) and in Alper's Phase Diagrams (33).

Two hundred samples of various Ga-As-Cr compositions (50 different compositions, shown in figure 3-1), lying below the 50 a/o arsenic composition line, were made up by mixing appropriate amounts of powdered Cr, Ga, GaAs, and CrAs. Some samples of the same composition were made up two or more ways, i.e., using GaAs, Cr, and Ga, or CrAs, Cr, and Ga. The samples were each heated in evacuated quartz ampoules to 1050°C and then annealed at various temperatures (from 600 to 1050°C) for 10 hours. They were then quenched in water. (The "room temp" samples were slow-cooled at ≈100°C/hr. to room temperature, instead of quenching.) The samples were then crushed, x-ray'd, reannealed, and re-x-ray'd. By comparing the x-ray diffraction patterns thus obtained to the known patterns of the elements and compounds, the phases present for each composition and temperature were determined. (Note: no ternary compounds were discovered. All peaks on the x-ray patterns could be attributed to binary compounds or elements.) The presence of the Ga-rich liquid (≈10 a/o Cr, 20 a/o As, and 70 a/o Ga at 700°C, for example) could be identified by the physical condition of the annealed sample (i.e., very malleable and difficult to crush into a powder without using liquid nitrogen to cool it first) and by the presence of very small amounts of Ga and $CrGa_4$ as seen in the XRD pattern; I experimentally determined that this Ga-rich liquid becomes $CrGa_4$, Ga, and GaAs, upon quenching.

Twenty-six compositions were analyzed by DTA (see figure

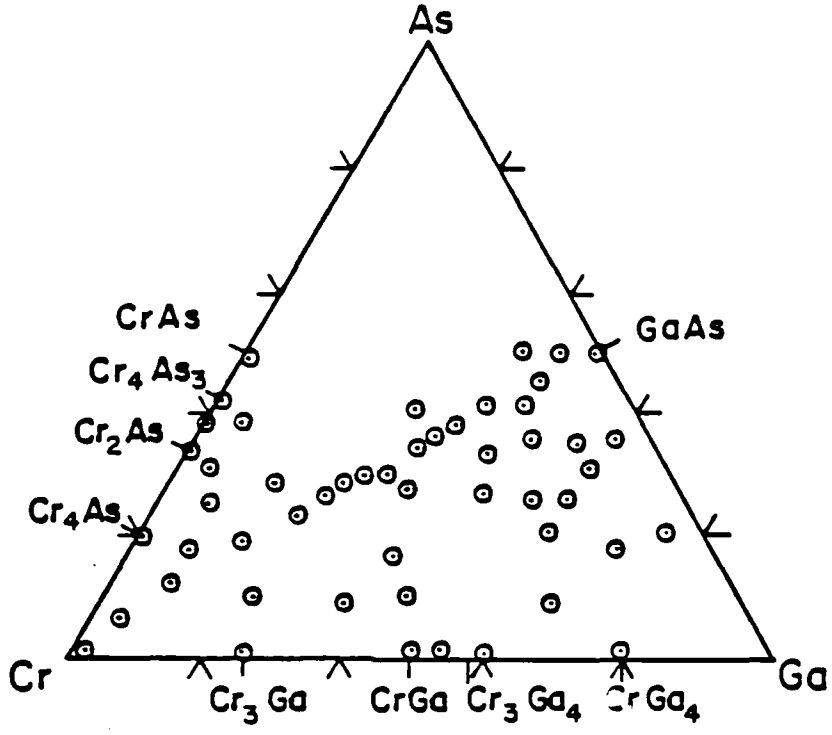

Figure 3-1. Compositions used for anneal, quench, and x-ray experiments.

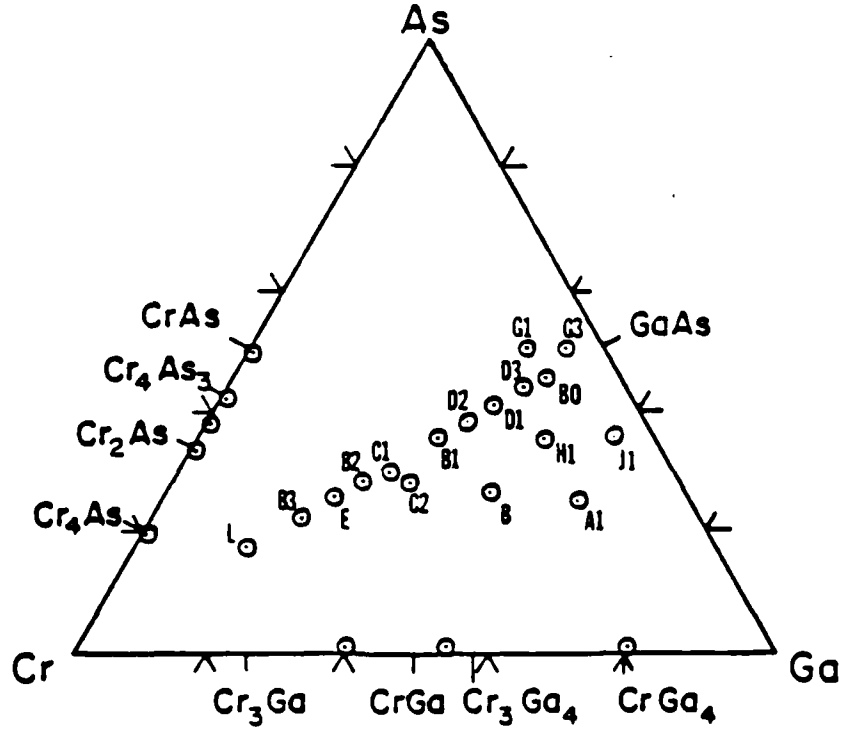

Figure 3-2. Compositions used for differential thermal analysis.

3-2 for the compositions). As mentioned earlier, larger amounts were pre-annealed and x-ray'd before loading them into DTA ampoules. Each went through 3 heat/cool DTA cycles. These were again x-ray'd to make sure that the same phases were present; they were in all cases. In figures 3-3 and 3-4 are shown the DTA curves for two of the samples, H1 and B2, whose compositions are shown in figure 3-2. Table 3-1 lists the transition temperatures, as determined from the DTA work, for the 17 ternary compositions - the remaining 9 were binary compositions.

3.3 Results and Discussion

3.3.1 The Cr-Ga System

The phase diagram, as proposed by Bornand and Feschette (14), and modified slightly by Phillipe et al. (16), was confirmed within experimental error. The x-ray diffraction patterns for the various compounds, as reported in the various references, were confirmed.

3.3.2 The Cr-As System

As stated earlier, the x-ray diffraction pattern of CrAs was reported previously (20), but unambiguous identification of the compound was not possible until after I synthesized the compound and produced a diffraction pattern showing the individual peaks. The diffraction pattern I obtained, shown in figure 3-5, with the corresponding (hkl) indices listed in table 3-2, is consistent with the reported (20) lattice parameters and structure (orthogonal) of CrAs. The lattice parameters of CrAs, as determined from the angles of the various reflections, were found to be:

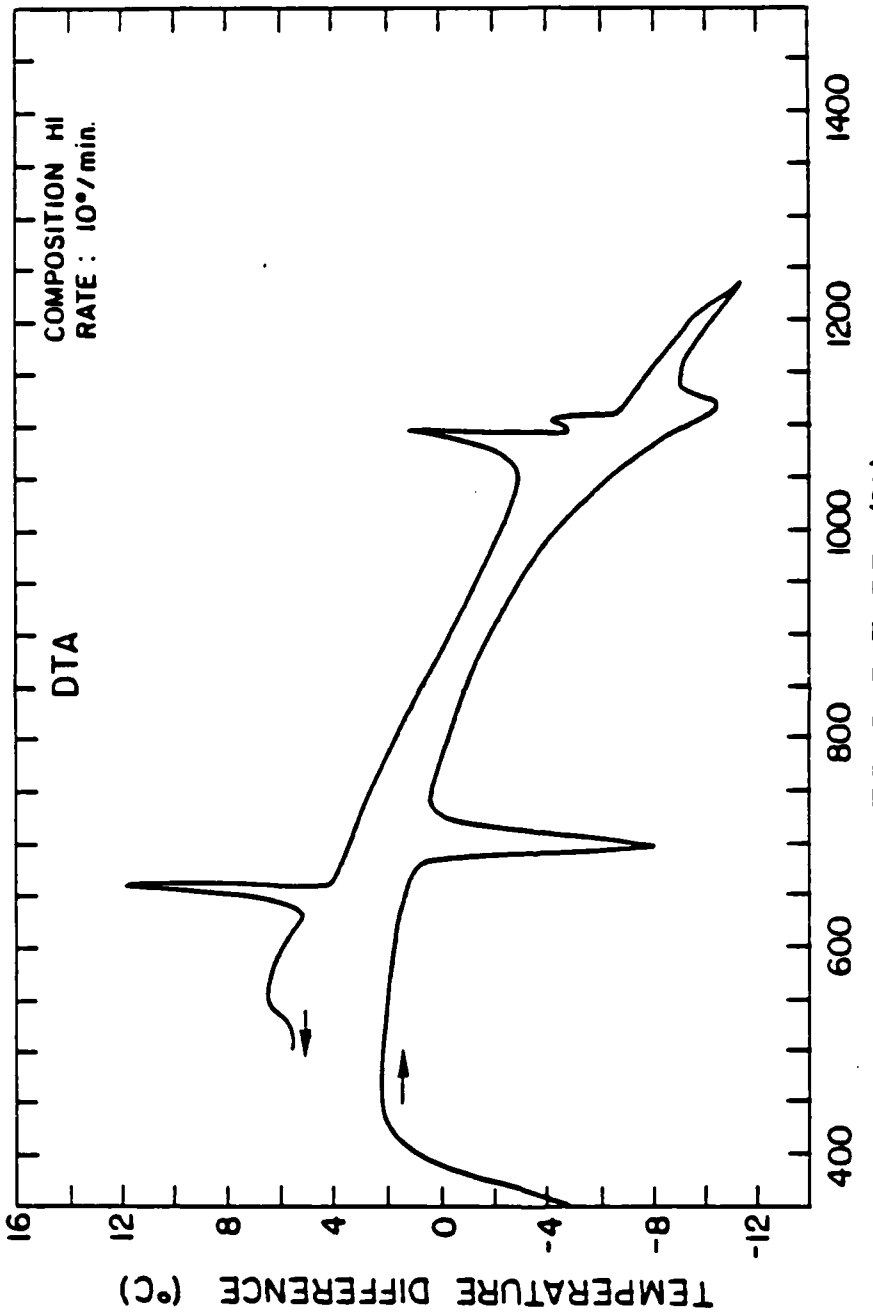

Figure 3-3. DTA curve for composition H1.

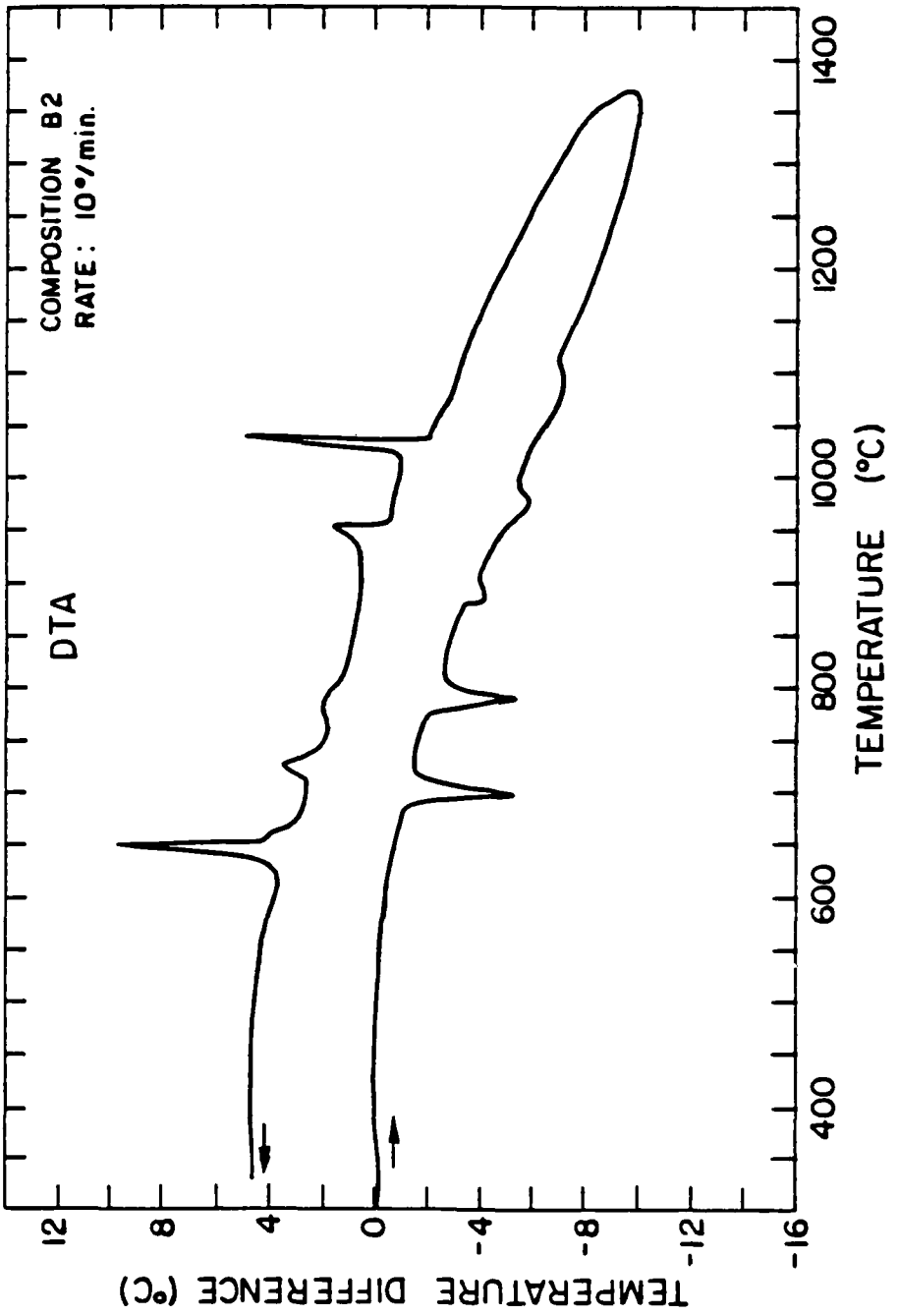

Figure 3-4. DTA curve for composition B2.

Table 3-1. Transition Temperatures for the 17 Ternary Compositions.

Sample Designation	Transition Temps.(°C)
B0	1170, 1125, 670
D3	1140, 1120, 670
D1	1150, 1115, 670
D2	1160, 1060, 670
B1	1160, 970, 670
C1	1070, 910, 870, 770, 675
B2	1040, 960, 880, 770, 740
E1	990, 980, 880, 770, 740
B3	1010, 990, 880, 770, 740
L	1320, 1270, 1015, 880, 740
B	1070, 670
C2	1060, 870, 770, 675
H1	1140, 1100, 670
G1	1190, 1170
A	1050, 975, 670
G3	1220, 1170
J1	1160, 670

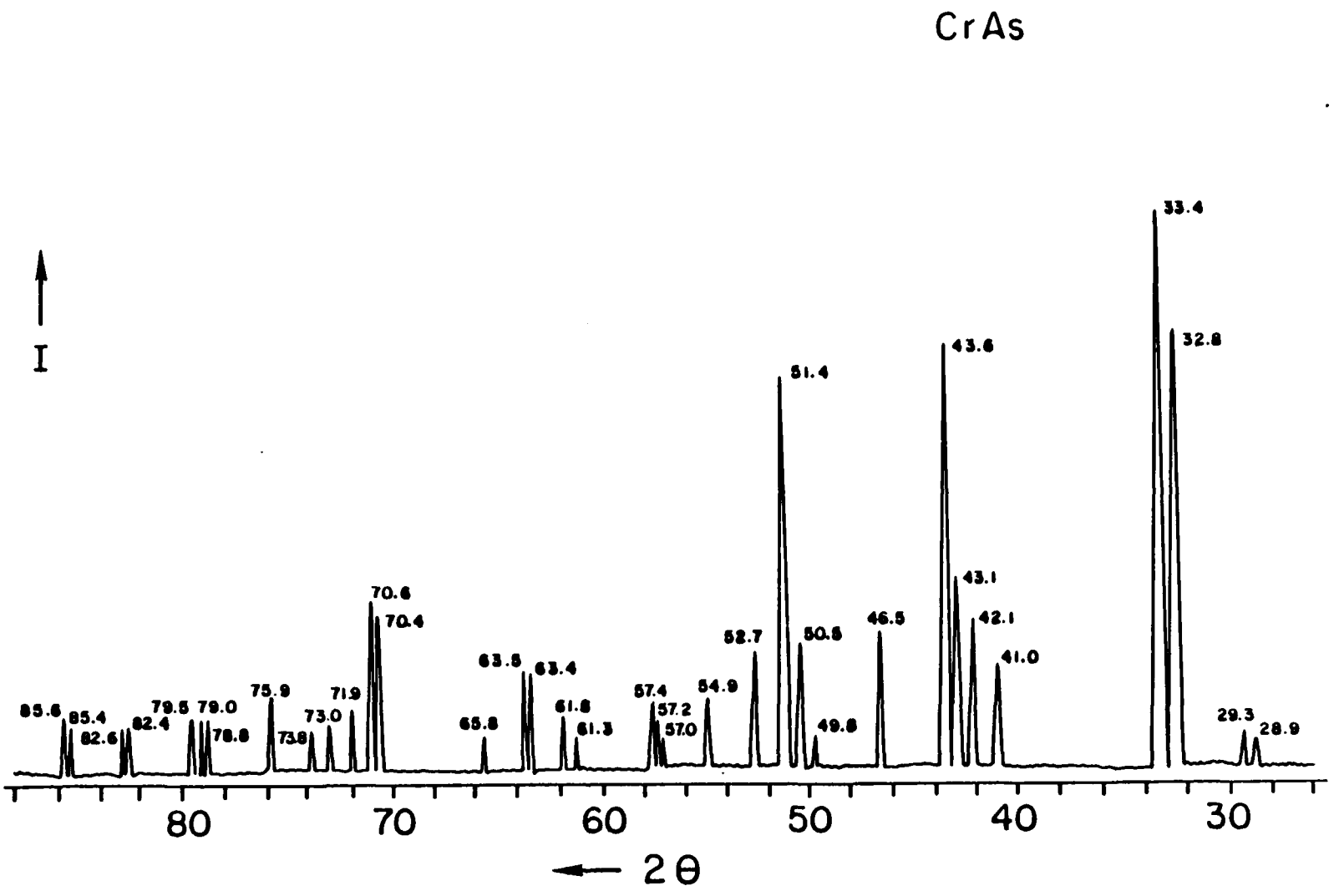

Figure 3-5. X-ray diffraction pattern for CrAs determined in this work (Cu X-ray source).

Table 3-2. 2θ and hkℓ Values for CrAs.

2θ	hkℓ	2θ	hkℓ
28.9	020	61.8	041
29.3	110	63.4	123
32.8	021	63.5	221
33.4	111	65.8	004
41.0	102	70.4	222
42.1	121	70.6	104
43.1	022	71.9	024
43.6	112	73.0	114
46.5	031	73.8	231
49.8	013	75.9	213
50.5	122	78.8	124
51.4	130	79.0	051
52.7	200	79.5	232
54.9	032	82.4	034
57.0	113	82.6	150
57.2	023	85.4	052
57.4	211	85.6	241
61.3	132		

a = 3.48 Å (±0.01 Å)

b = 6.22 Å

c = 5.75 Å

These compare favorably with Nowotny and Arstad's (20):

a = 3.486

b = 6.222

c = 5.741

As mentioned, I did get good separation between peaks; for instance, between the (022) and (112) plane diffractions.

The melting points of the Cr-As compounds were determined to be the following (all ± 5°C):

CrAs: 1360°C

Cr_4As_3: 1185°C (incongruently to CrAs + ℓ)
1300°C (to all liquid)

Cr_2As: 1175°C (no high temperature phase was observed)

Cr_4As: >1400°C (the limit for quartz ampoules)

The diffraction patterns, reported by others, of the other Cr-As compounds were confirmed.

I was unable to determine if "Cr_4As" was Cr_4As or Cr_3As, or if "Cr_4As_3" was Cr_4As_3 or Cr_3As_2, except that in assuming the former stoichiometry in each case (based on the most current reports in the literature), and adding appropriate amounts of Cr to CrAs on that basis, I observed only the single phase after annealing (by x-ray analysis), leading me to suspect that these assumptions were correct.

With regard to Yuzuri's estimated phase diagram, I did agree with him regarding which compounds melt congruently (Cr_4As, Cr_2As, and CrAs) and which incongruently (Cr_4As_3), but

the actual melting points differ considerably. The relatively high melting point of CrAs that I determined would lead one to predict it as being a dominant compound in the Ga-As-Cr system, an unlikely prediction based on Yuzuri's results. Because of this, and because of the problems with the reported XRD pattern of CrAs, it was only after I concluded the work on the Cr-As system that I was able to make sense of my ternary phase diagram results.

3.3.3 The Ga-As-Cr Ternary System

From the 200 anneals and x-ray results, and the 26 DTA results, isothermal sections from room temperature to 1300°C were constructed for the Ga-As-Cr system (for As a/o $\leq$ 50). Several of these are shown in figures 3-6 to 3-15. The liquidus and solidus lines which are dotted are only approximate, as are the sizes of the single solid phase regions and the two-phase tie-lines; the size of the GaAs phase is exaggerated for clarity.

In addition to the isotherms, a vertical section (an "isopleth") was constructed along the GaAs-Cr composition line, from 0 to 70 a/o Cr, and is shown in figure 3-16. The experimentally determined points are included in this figure. This is a vertical slice through the three dimensional ternary phase diagram in contrast to hoizontal slices for isotherms. This paticular vertical section shows what happens as different amounts of Cr are added to GaAs. GaAs is present only in the regions on the right side of the diagram, and Cr and GaAs are never present in the same region. This diagram also illustrates the complexity of the system.

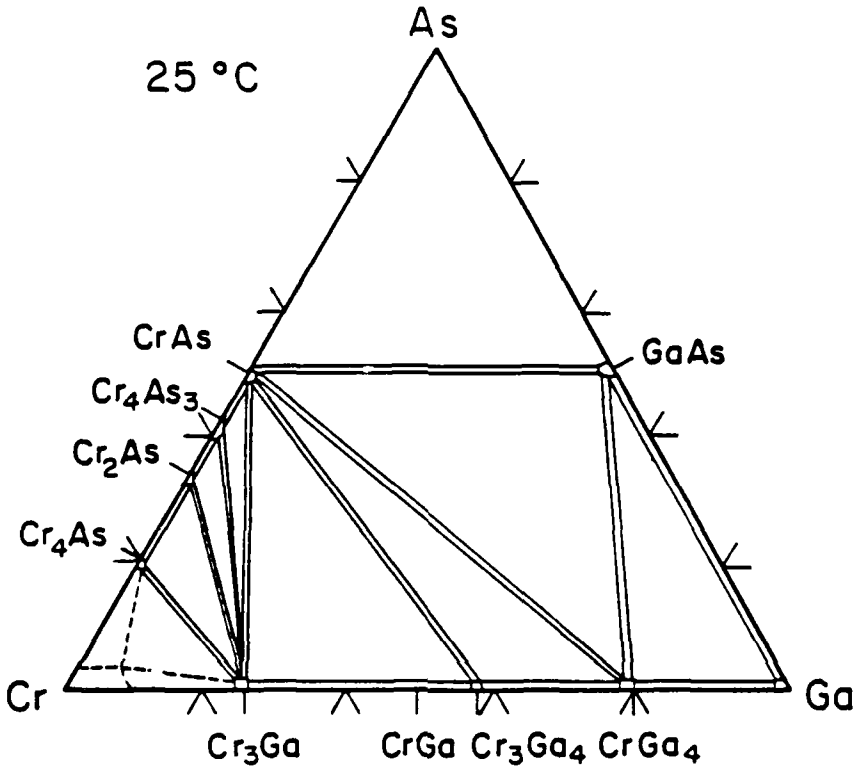

Figure 3-6. Isothermal section of Ga-As-Cr phase diagram for 25°C. Dashed lines indicate estimated features.

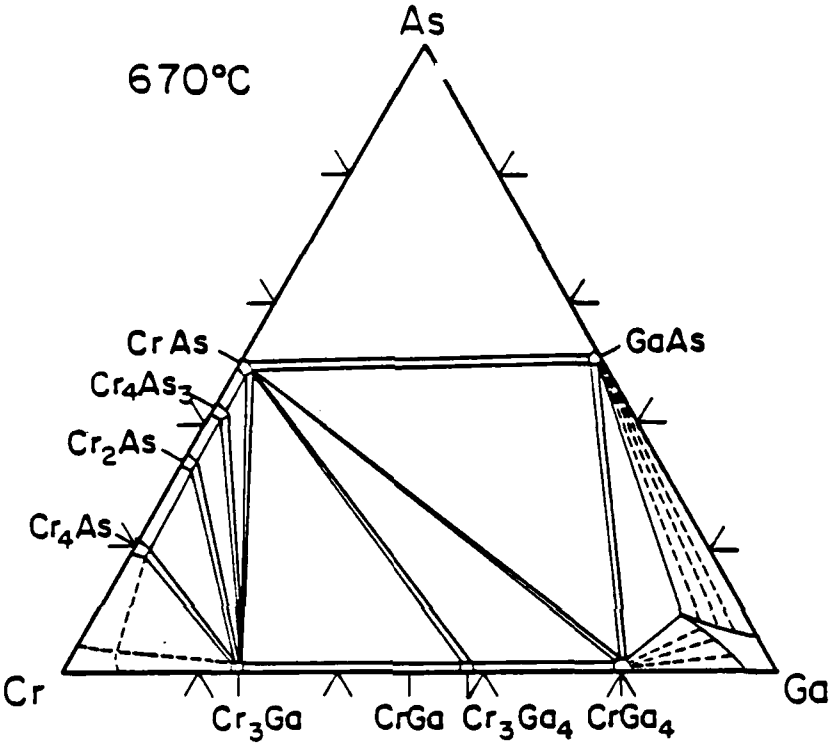

Figure 3-7. Isothermal section of Ga-As-Cr phase diagram for 670°C. Dashed lines indicate estimated features.

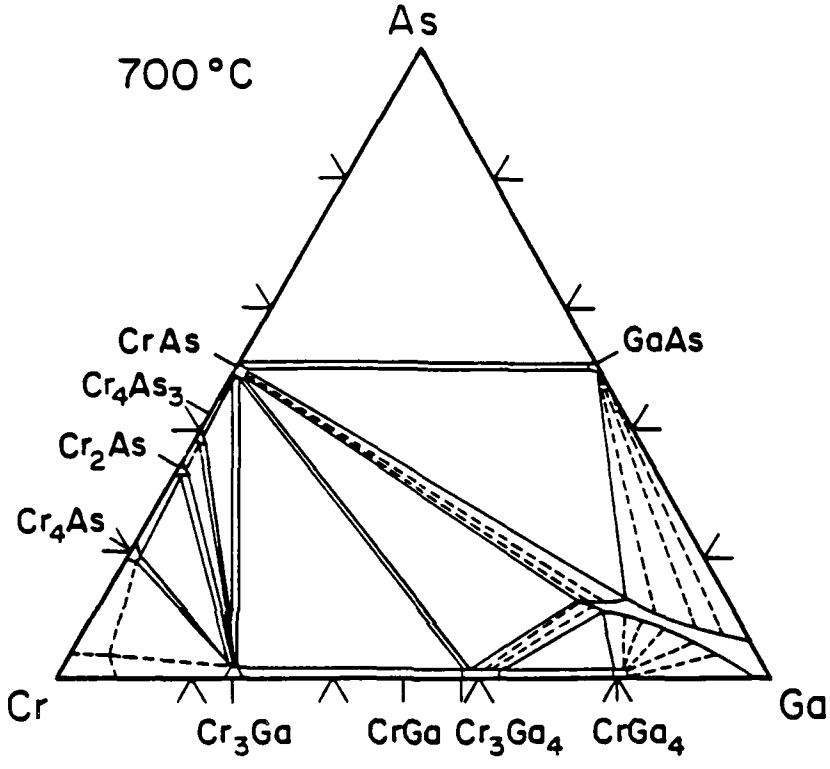

Figure 3-8. Isothermal section of Ga-As-Cr phase diagram for 700°C. Dashed lines indicate estimated features.

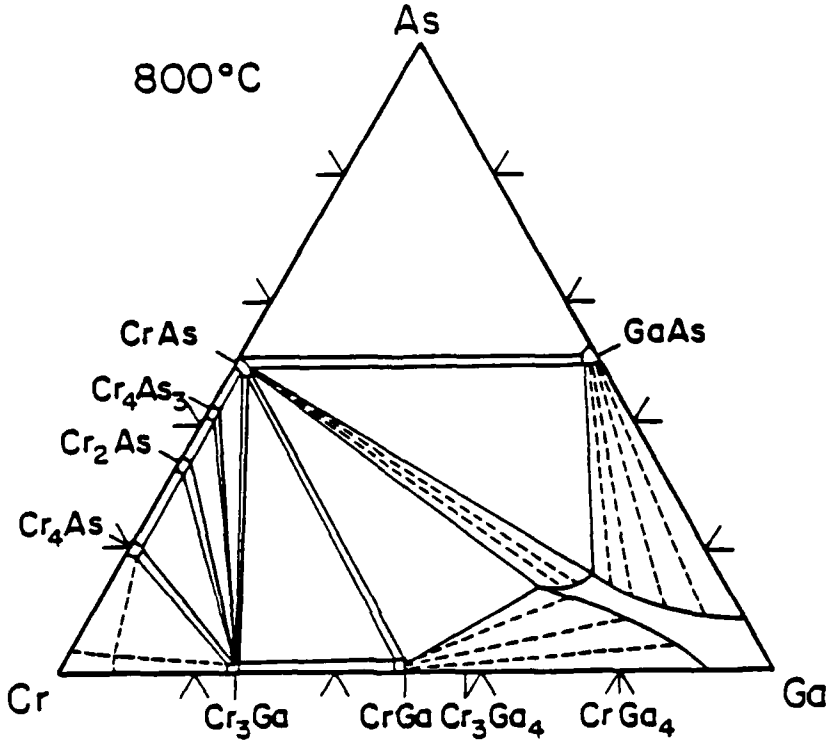

Figure 3-9. Isothermal section of Ga-As-Cr phase diagram for 800°C. Dashed lines indicate estimated features.

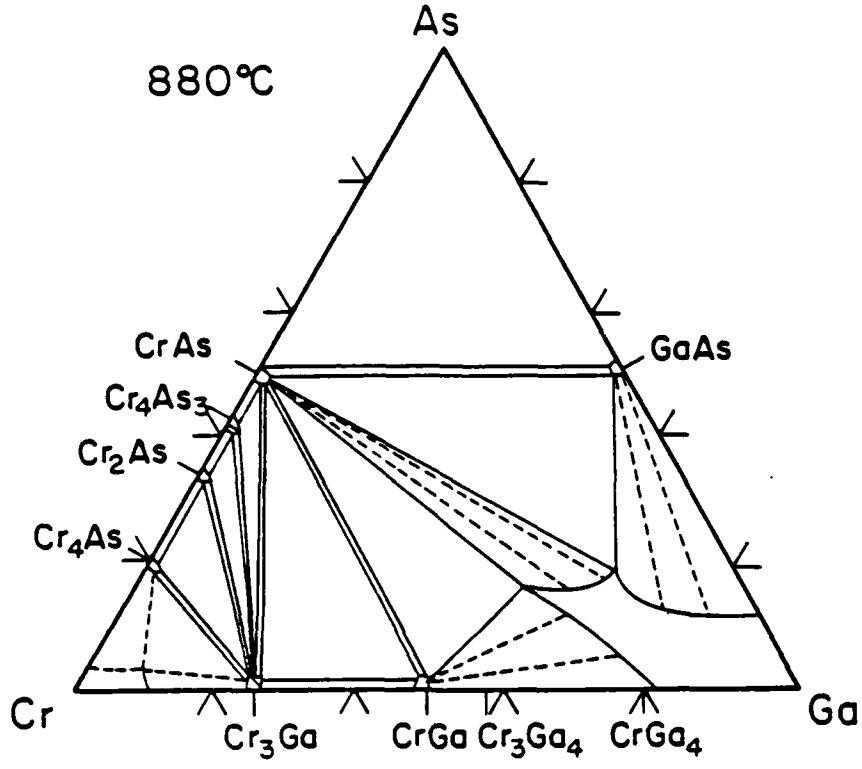

Figure 3-10. Isothermal section of Ga-As-Cr phase diagram for 880°C. Dashed lines indicate estimated features.

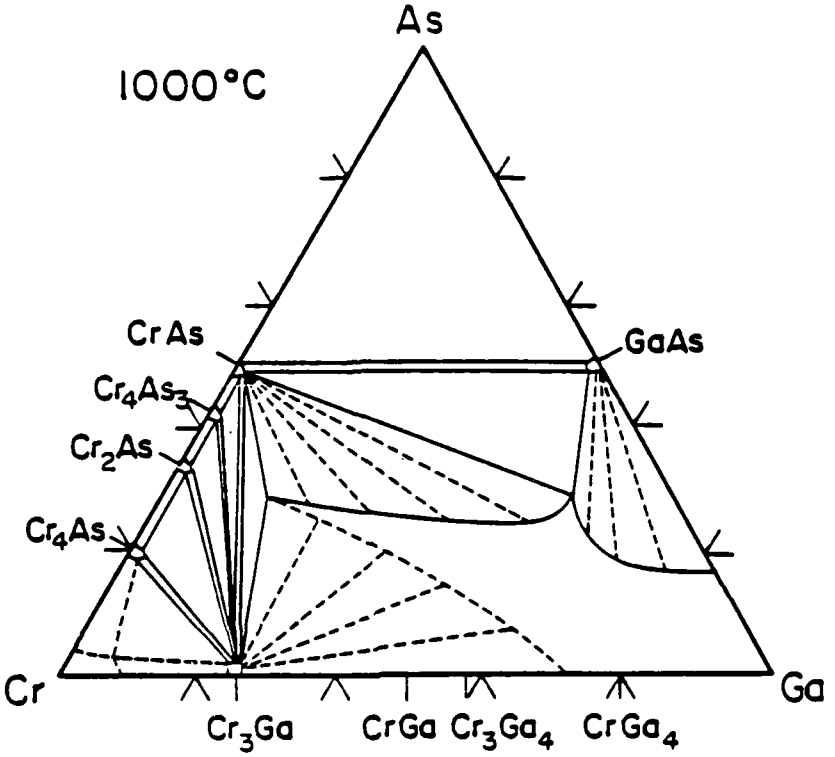

Figure 3-11. Isothermal section of Ga-As-Cr phase diagram for 1000°C. Dashed lines indicate estimated features.

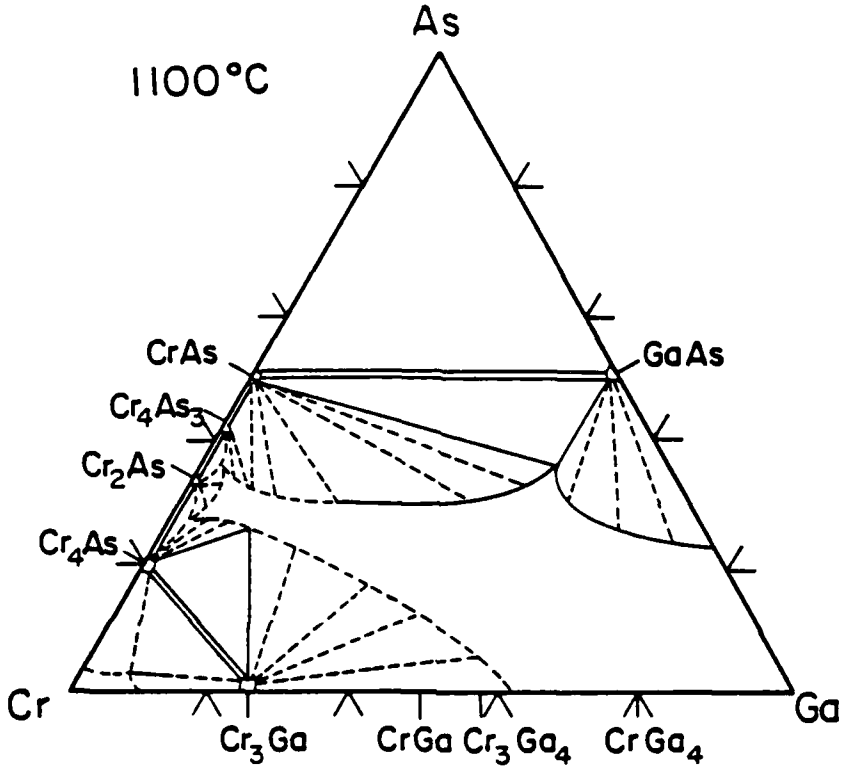

Figure 3-12. Isothermal section of Ga-As-Cr phase diagram for 1100°C. Dashed lines indicate estimated features.

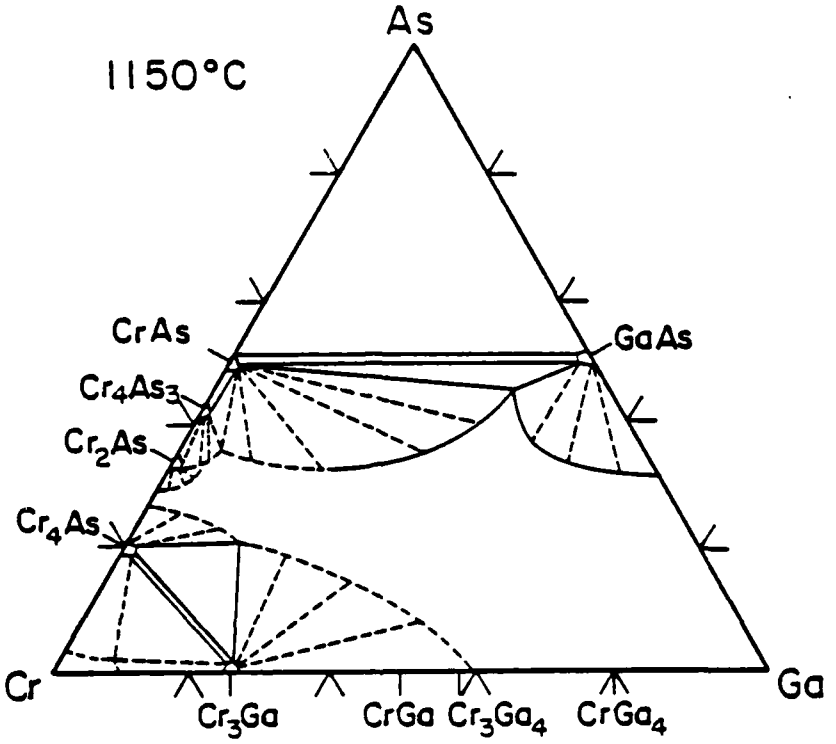

Figure 3-13. Isothermal section of Ga-As-Cr phase diagram for 1150°C. Dashed lines indicate estimated features.

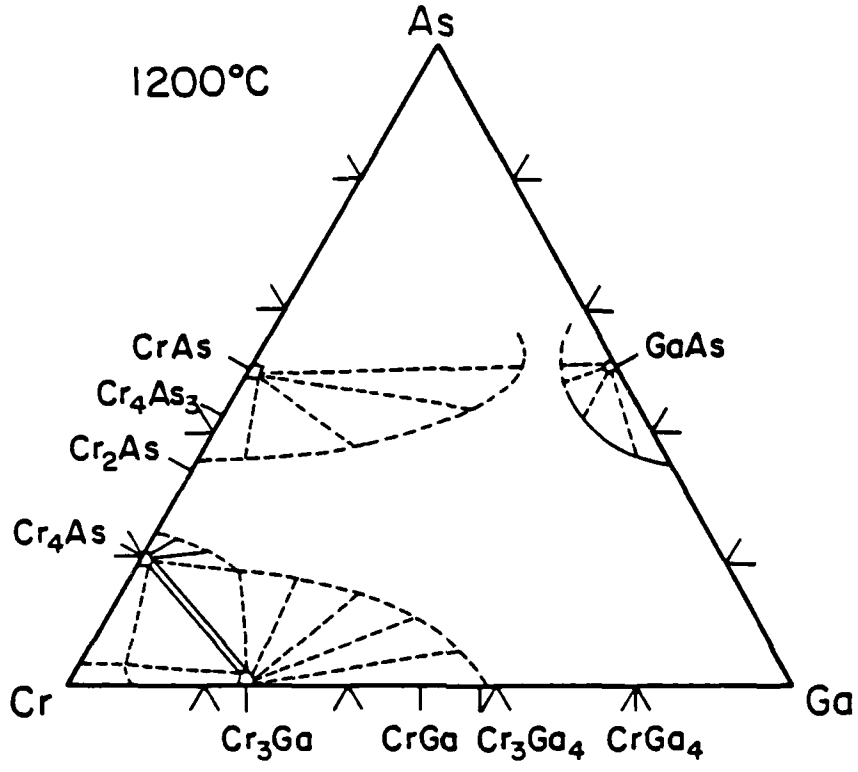

Figure 3-14. Isothermal section of Ga-As-Cr phase diagram for 1200°C. Dashed lines indicate estimated features.

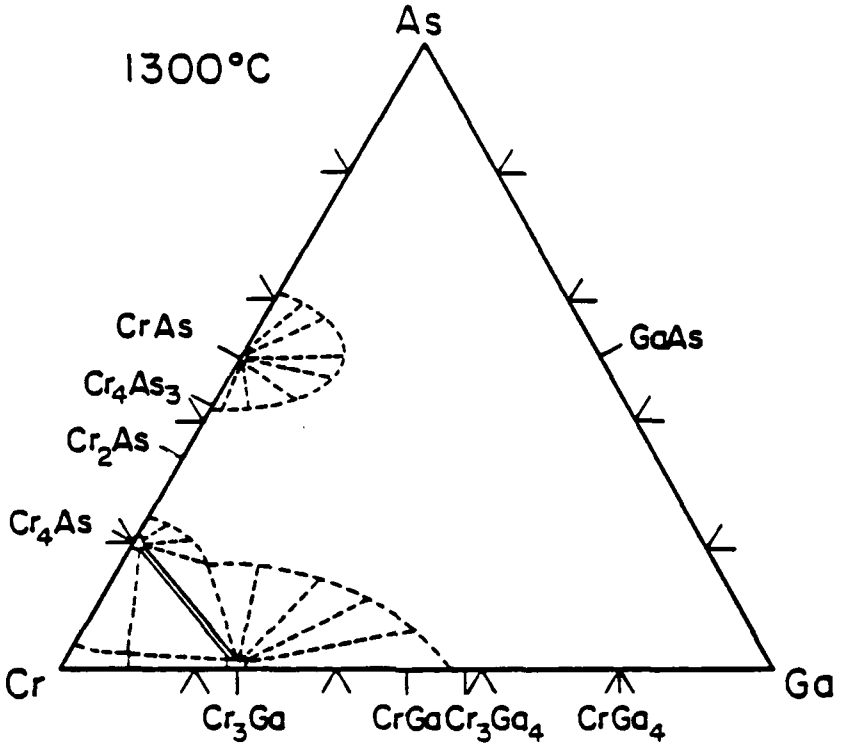

Figure 3-15. Isothermal section of Ga-As-Cr phase diagram for 1300°C. Dashed lines indicate estimated features.

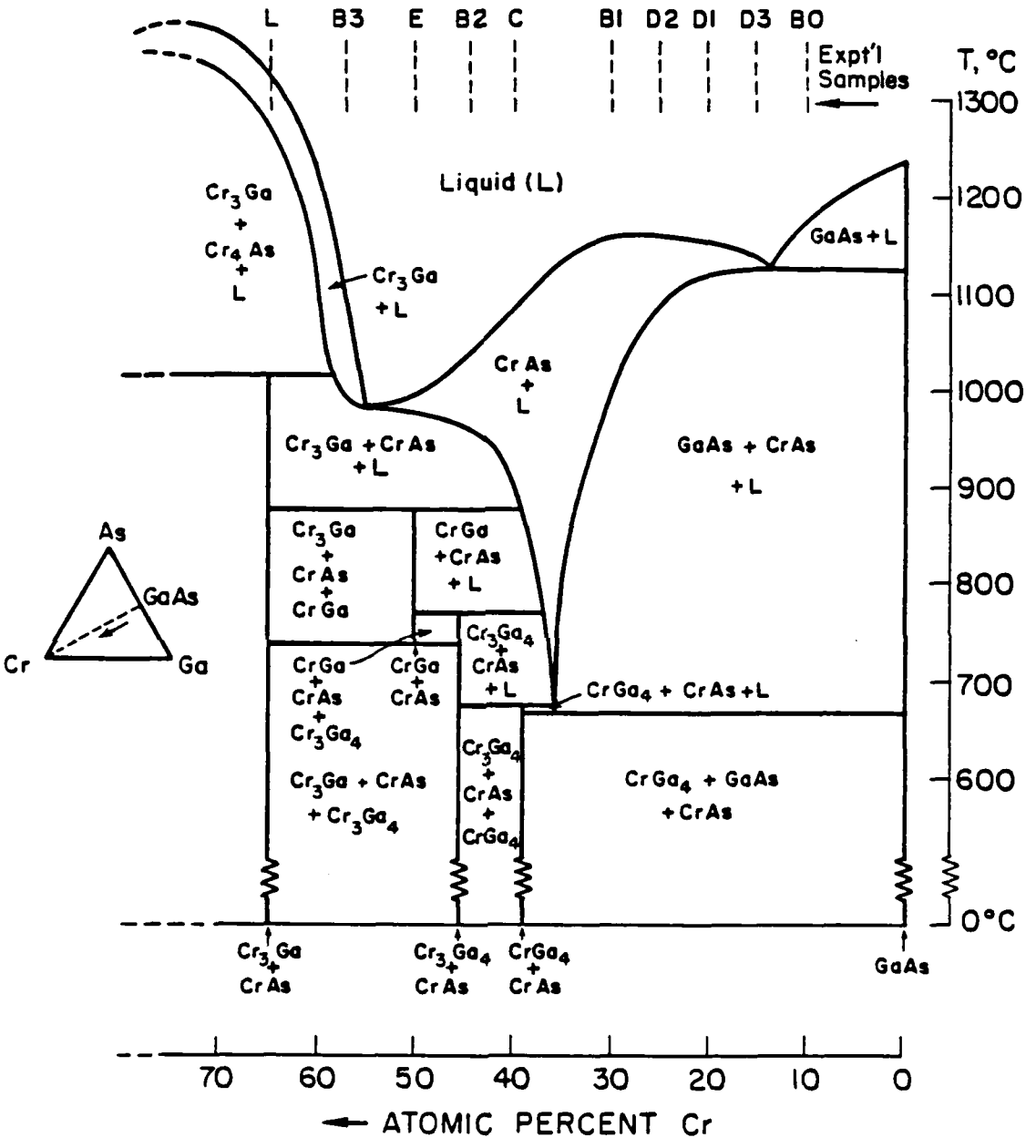

Figure 3-16. Vertical section of Ga-As-Cr phase diagram along GaAs-Cr line. Compositions of DTA samples are indicated at top.

The major significance of how these results relate to solubility and diffusion studies of Cr in GaAs are the following:

1. CrAs and Cr_3Ga, and not GaAs, are the dominant compounds in the Ga-As-Cr system. This means that GaAs is not in equilibrium with nearly as many phases as was previously presumed.

2. Cr and GaAs are not in equilibrium with each other under any conditions; there is no tie line connecting those two phases at any temperature. Therefore, a solubility or diffusion experiment in which Cr and GaAs are placed in contact with each other, or in the same ampoule, would result in either the Cr phase or GaAs phase, or both, depending on where the total composition lies on the ternary phase diagram, ultimately disappearing during the anneal. (This is in contrast to what was done in previous studies (5,34) and which will be discussed in more detail in chapter 6.) This also means that some other phase ($CrAs_{(s)}$ or $Ga_{(\ell)}$), rather than Cr, would precipitate from GaAs if the Cr content exceeds the solubility level.

3. There is a large tie triangle region that includes GaAs, plus $CrAs_{(s)}$ and $Ga_{(\ell)}$; this is a logical choice as a Cr source for solubility and diffusion experiments. As discussed in chapter 2, as long as the entire system (GaAs + Cr source) is anywhere in that region, the system is invarient and well-defined solubility and diffusion experiments are achieved for isothermal conditions. Also, when putting this composition in an ampoule with undoped GaAs (for solubility and diffusion

experiments), the system would initially be removed from the final equilibrium state only by the amount of Cr that can be dissolved in GaAs. This is the "quasi-equilibrium" condition, discussed in the preceding chapter, which is necessary for valid solubility and diffusion studies.

4. A Ga-rich liquid is in equilibrium with GaAs. (This corrosponds to the liquid solvent used in Liquid Phase Epitaxial (LPE) growth of GaAs.) This liquid has a very high Cr solubility, up to ≈10 a/o, which is consistent with the results of Andre and LeDuc (30), as mentioned in section 3.1. The significance of this in my solubility and diffusion studies will be discussed in the upcoming chapters.

3.4 Summary of Phase Equilibria Studies

In this part of the study of chromium in gallium arsenide, the following was accomplished:

1. The various Cr-As compounds were synthesized, melting points were determined, and x-ray diffraction patterns were confirmed or corrected;

2. The Cr-Ga phase diagram, including the same type of information as in the Cr-As system, was confirmed;

3. The Ga-As-Cr ternary phase diagram was experimentally determined for As $\leq$ 50 a/o, from room temperature to 1300°C.

4. Important implications of these results on Cr in GaAs solubility and diffusion studies were deduced, namely:

a) GaAs is not a dominant compound in the Ga-As-Cr system;

b) GaAs and Cr are never in equilibrium with each other;

c) A suitable tie triangle region was found for use in

solubility and diffusion studies;

d) A Ga-rich liquid, which has a high solubility of Cr, is in equilibrium with GaAs at the temperatures of interest.

4. THE SOLUBILITY OF CHROMIUM IN GALLIUM ARSENIDE

4.1 Introduction

Valid and well-defined solubility studies can be performed once the ternary phase equilibria information is known. One can then correctly apply these results to other studies, such as diffusion studies. Failure in the past to recognize the importance of phase equilibria has led to improper determinations and uses of solubility values.

In this chapter, previous reports and uses of "solubility" values of Cr in GaAs are reviewed. Next, a short review of solubility in relation to the phase diagram, as discussed in chapters 2 and 3, is given. Then, the experimental techniques for determining solubility are described, and the results and discussion of the solubility experiments are presented. Finally, the influence of the type of Cr source, and other conditions for the solubility experiments, on the surface morphology of GaAs is described, which provides evidence for the relevance and correctness of the phase equilibrium results.

4.2 Literature Review of the Solubility of Cr in GaAs

In the literature there are numerous invalid and inconsistent results, references to results, and uses of the results regarding the solubility of Cr in GaAs. Most agree (26, 35, 36) that the maximum solubility of chromium in undoped gallium arsenide at, or just below, its melting point (1238°C) is about 2×10^{17} cm^{-3}, but that is where the agreement ends.

The most obvious of the errors committed in measuring the "solubility" of Cr in GaAs are the use of non-equilibrium

techniques. Morkoc et al. (37) propose a solubility of Cr in GaAs of 1 x 10^{16} cm^{-3} at 580°C from molecular beam epitaxy (MBE) experiments. This value is orders of magnitude higher than any others reported for that temperature. Bonnet et al. (38) state that the "solubility limit of Cr in GaAs is around 5 x 10^{16} cm^{-3}" (temperature not known) from their metal-organic chemical vapor deposition (MOCVD) results. Linh et al. (39) point out that their own MBE and MOCVD results for Cr solubility differ from each other as well as from other reported results. Both these methods of layer growth, however, are generally regarded to be non-equilibrium techniques, and are probably not suitable for equilibrium solubility studies.

Even solubility results taken from liquid phase epitaxial (LPE) growth have problems associated with them. Woodard's (29) work on LPE growth of Cr-doped GaAs is an often quoted source for Cr solubility values. Even if those results are accurate, they are only for the particular case of GaAs is equilibrium with a Ga-rich liquid of a particular Cr content (0.83 a/o in Woodard's case). This leads to the most common misuse of Cr solubility values: blindly applying solubility values from one particular experimental system to another, without any understanding and/or concern of ternary phase equilibria considerations. A classic example of this is in two articles by Feng et al. (40,41). They use Cr concentration levels from Tuck and Adegboyega's (5) diffusion results as the Cr solubilities for various temperatures in order to interpret their Cr outdiffusion experiments. They also claim that Woodard's (29) results are consistent with these values.

There are three errors in this. First, Tuck's Cr bulk levels came from diffusing Cr from a pure Cr source into GaAs in a closed quartz ampoule. However, it has been determined in this work that chromium is not in equilibrium with GaAs, at any temperature. Therefore, Tuck's experiments were not performed under either equilibrium or "quasi-equilibrium" conditions, and the concentration levels should not be used as "solubility" levels. Secondly, the Cr levels they interpret as being the Cr in GaAs solubilities at various temperatures are from indiffusions that were not performed long enough to reach the final value in the bulk for all but one temperature; this point was made clear in Tuck's paper. Finally, comparing these results to Woodard's is in error for the reason mentioned above, namely, one must consider the Cr source itself. Another example of inadequate consideration of the Cr source is given by Woodard (29) himself. Woodard cites Huber's (42) outdiffusion results and interpretations as being consistent with his own solubility numbers. In Huber's experiments as in Feng's, however, the GaAs is not in equilibrium with any liquid phase, let alone one with 0.83 a/o Cr. Thus, since the Cr source conditions were different in these studies, the solubility results should not be compared.

There are many examples in which the results are not consistent with Woodard's numbers, and the researchers can not figure out why. For example, Linh et al. (39) look at the Cr levels in their vapor phase epitaxy (VPE) layers and conclude that they are about four times higher than Woodard's results would suggest. They were "unable to resolve this

discrepancy". Again, they assumed that Woodard's solubility values were for all conditions.

These examples show the general lack of concern for ternary phase equilibria when reporting and using Cr-in-GaAs solubility data. It is shown in this thesis how critical it is to have the system at (or near) equilibrium and to be well-defined for meaningful and valid solubility (and diffusion) data.

4.3 Solubility in Relation to the Ternary Phase Diagram

As discussed in chapters 2 and 3, there are several features of ternary phase equilibria that are important in solubility studies of an impurity in a compound semiconductor. In summary, they are: 1) the solubility of a component in a phase (Cr in GaAs in this work) depends on the location of the system on the ternary phase diagram; 2) the solubility is well-defined if the temperature is specified and the system lies in a three condensed phase region (i.e., a tie triangle); and 3) a composition within a three phase region containing GaAs is a suitable source for solubility experiments of Cr in GaAs. Specifically a composition near the middle of the $GaAs_{(s)}$-$CrAs_{(s)}$-$Ga_{(\ell)}$ tie triangle region will be utilized extensively as a Cr source for the solubility studies in this work. Not only does it lead to well-defined conditions, but the region covers a very large composition region around the GaAs phase, therefore the results are applicable to many experimental situations. In addition, the Cr solubility in this region is expected to be greater than anywhere in the $GaAs_{(s)}$ - $Ga_{(\ell)}$ region (which is where the

only other results have come from); therefore, the results one obtains (by SIMS, etc.) will be statistically much more reliable. Finally, it should be reiterated that elemental Cr should not be used as a source for GaAs studies since it is never in equilibrium with GaAs. (The effect of doing this will be demonstrated.)

The above statements apply not only to solubility, but to all the other intensive properties as well, such as partial pressures, equilibrium defect concentrations, and related properties such as diffusivity, and will be applied to the study of the diffusion of Cr in GaAs and also to the defect chemistry of GaAs in the upcoming chapters.

4.4 Experimental Techniques

4.4.1 General Techniques

For most of the experiments, the GaAs used was Cominco LEC high resistivity, undoped GaAs. According to Cominco, the resistivity was $\geq 10^7$ ohm cm. and the dislocation density was $\leq 10^4$ cm^{-2}. This material was used in most cases, rather than Bridgman GaAs, for example, because of its very low impurity level, which is the reason why it is semi-insulating without Cr additions. Other GaAs material used included: Crystal Specialties undoped GaAs (Bridgman); Hewlett-Packard Te-doped and undoped GaAs (LEC); and Morgan semiconductor Si-doped GaAs. The GaAs wafers, 350 to 400 microns thick, were cut into approximately 1 x 1.5 cm squares. Before annealing, the squares were cleaned according to the following schedule which was adapted from Hewlett-Packard's GaAs cleaning schedule:

1. Gently wipe both sides of the wafers with Q-tips in a aquet detergent solution.
2. Rinse substrate with DI water several times.
3. Rinse substrate with acetone and ultrasonic clean for 2 min.
4. Replace acetone with trichloroethane and ultrasonic clean for 2 min.
5. Rinse twice with acetone.
6. Rinse twice with methanol.
7. Ultrasonic clean in acetone for 2 min.
8. Boil in hot trichloroethane for ten minutes.
9. Rinse twice with acetone and agitate in ultrasonic cleaner.
10. Rinse twice with methanol and agitate in ultrasonic cleaner.
11. Boil in HCl for 10 minutes.
12. Pour out most of HCl and replace with cold HCl.
13. Rinse with methanol several times and ultrasonic clean for two minutes.
14. Rinse in isopropyl alcohol and boil for two minutes.

Quartz beakers and wafer holders were used throughout. The first 10 steps are to remove large particles (GaAs dust, etc.), to remove organic impurities, and to degrease the sample. The HCl step is to remove the native oxide that usually forms, and the last two steps remove the HCl.

The Cr sources used were appropriate Ga-As-Cr phases which were made prior to the solubility anneals by mixing appropriate amounts of Cr, Ga, GaAs, and CrAs, and annealing these

mixtures - this was so that the sources were already in their final, equilibrium state before the actual solubility experiments began. The annealing procedure was outlined in chapter 3. The source material was then crushed, and small samples of it were x-rayed to be sure the appropriate phases were present. The ampoules used were made from high purity quartz, and cleaned in the same manner as described in chapter 3. For the solubility (and diffusion) experiments, a constriction was made in the ampoule to keep the powder source material and the the GaAs substrate physically separated. The total interior volume of the ampoule was ≈ 2 ml. A diagram is shown in figure 4-1.

Immediately after cleaning the GaAs wafer, the wafer and source were placed in the ampoule, which was evacuated to $\approx 10^{-6}$ torr, and sealed. The vacuum inside the ampoule was checked by a Tesla coil before and after each anneal. The annealing was done in the furnace system described in chapter 3. After annealing the samples for the appropriate time and temperature, the ampoules were quickly removed from the furnace and quenched in water. The GaAs wafers were then ultrasonically cleaned in methanol and boiled in HCl to remove any loose particles and/or dissolve any precipiates from the surface, and then rinsed in isopropyl alcohol. The GaAs wafers were then analyzed by SIMS. The following section will discuss SIMS in detail, first discussing the basic concepts of SIMS, and then presenting the specific details of the present work.

4.4.1 Secondary Ion Mass Spectrometry

Secondary Ion Mass Spectrometry (SIMS) has become a

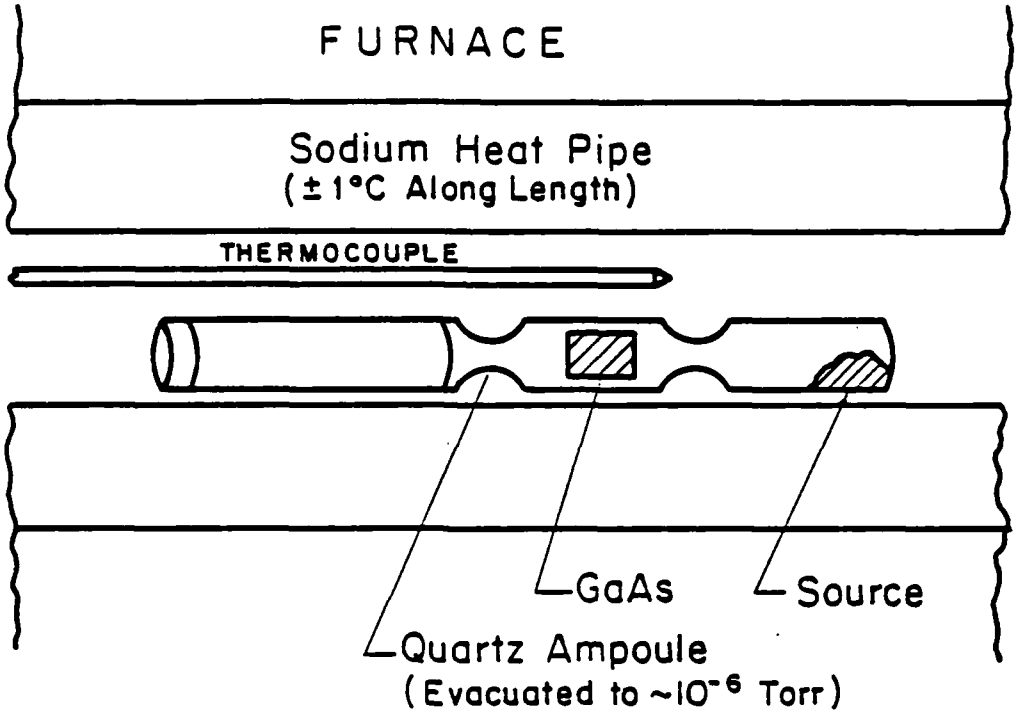

Figure 4-1. Schematic diagram of the annealing system used for the solubility and diffusion experiments.

powerful and popular technique for impurity analysis in semiconductors. Its high sensitivity, allowing one to measure concentrations on the order of 1×10^{14} cm^{-3} (ppb), and its ease of obtaining concentration vs. depth profiles are the main reasons for this. Good reviews of SIMS are found in an article by V.R. Deline (43) and a book by A.W. Czanderna (44). A good review of SIMS applications is an article by E. Zinner (45).

The method uses low energy ionized atoms to bombard a sample surface, and by chemical and kinetic processes, the surface atoms are ionized and ejected (or "sputtered") from the sample. These "secondary ions" (as opposed to the "primary" ions of the bombarding beam) can be analyzed by mass spectrometry. The resulting ion intensity (in counts per sampling time and as measured by the mass spectrometer) versus sputtering time data can then be easily converted to concentration versus depth data by appropriate calibration techniques, as will be discussed later.

Because a mass spectrometer is used, only atoms (or ions) of a specific mass are counted, and because of the great sensitivity of mass spectrometers, one can count very low numbers; therefore, SIMS is a very sensitive and specific analysis. Even if two species have the same mass, such as P and SiH, one can distinguish between them using the "voltage offset" technique, which considers that ions with the same mass usually have different kinetic energy distributions.

The primary beam is usually Ar^+, O_2^+, or Cs^+, depending on the electronegativity of the species to be analyzed, and the energy of this beam is relatively low (1-15

KeV) so that the damage to the matrix material is minimized.

Because of the complexity of the sputtering process, there are several limitations on the resolution of both the concentration and depth determinations, leading to uncertainties regarding the accuracy of the values and profile shapes obtained by this method. However, there are several steps that can be taken to minimize these problems. These will now be discussed.

An easy and effective way to convert ion intensity to elemental concentration - very difficult to do theoretically - is to first analyze standard samples in which the concentration of the desired element in the matrix material is known and obtain a conversion factor for that particular system. This first requires that the concentration in the standard be known. This is easily done using ion implantation. Here the standard is made up by implanting a known total "dose" of the desired element into the matrix material. Then by integrating the SIMS ion intensity - time profile and comparing to the total dose (and knowing the size of the sampling area), one may obtain a counts-to-atom conversion factor. This number is multiplied by the atomic density in the solid of one of the matrix elements (e.g., As in GaAs) and then divided by the ion intensity of that element for that profile to get a modified conversion factor. This takes into account the fact that the ion intensity value - which is in "counts per sampling time" - depends on the sputtering rate of that particular analysis. Therefore, each time an analysis is made, a different conversion factor does not need to be used; one simply

measures the matrix ion intensity value at the end of the sputtering and uses this and the modified conversion factor (or "sensitivity factor") to make the conversion from ion intensity to concentration.

The sputtering rate affects both the concentration results and the depth resolution, and there are several problems associated with it; yet, again, steps may be taken to alleviate them. One problem is a variable sputtering rate which may be caused by such features as inclusions, precipitates, and thin films (e.g., oxides) in the matrix. If, for example, there is a region of enhanced sputtering, then the measured depth in that region will be smaller and the measured concentration will be higher than the actual numbers. There is no reasonable way to correct for this; however, one can tell if this is occurring by simply profiling a matrix element and seeing if it remains constant or not. Another problem is that as the SIMS crater (the hole created by the sputtering process) gets deeper, the primary beam becomes defocused, and the crater area, and hence sampling area, may change. In addition, atoms from the sides of the crater may be sputtered and be counted as coming from much a deeper region. These two effects may be minimized by using a laterally controlled beam which rasters out a large crater, and by using an aperature in front of the detector to sample from a small and uniform sized area.

Other problems include: atoms in the matrix being knocked deeper into the matrix by the primary ions, leading to erroneous profiles; damage created by the primary ions (usually this damage is uniform and hence not important); and

oxide layers at the surface which usually enhance the secondary ion yield by making the atoms easier to ionize. Also, a common observation is a small dip in ion intensity near the surface in the profile, which is believed to be due to the depth being shallower than the projected range of the primary beam. Under normal conditions, this is usually ≈200Å - so for deep profiles this is not a problem.

For this work, a Cameca "IMS 3F" SIMS system, at Charles A. Evans and Associates, was used. For Cr in GaAs, an O_2^+ primary beam was used, with an energy of 12.5 keV. The beam size was either 75 or 150 μm in diameter (it varied from day to day), which rastered out an area of 250x250 μm (or 500x500 μm when the 150 μm was used)), and the sampling area, controlled by an aperature in front of the detector was 75 μm^2 (or 150 μm^2). The usual primary beam current, which determined the sputtering rate, was ≈6 μamps, resulting in a sputtering rate of ≈50 Å/sec.

At the start of each set of analyses, a "low chromium" sample was analyzed by SIMS to determine the background level for that day. This was usually ≈1 x 10^{15} cm^{-3} and sometimes less.

The time-to-depth conversion was determined by measuring the depth of the SIMS crater after each analysis with a Dektak, which uses a very sensitive stylus to measure step distances, and then assuming that the sputter rate is constant throughout the profile (confirmed by periodically profiling of Ga and/or As to establish that they give constant concentration-depth profiles). There is an uncertainly factor in the absolute

depth measurement of 15%. In addition, the depth measurement was taken across the entire SIMS crater, giving a depth vs. distance profile. This showed the crater to be very uniform. Micrographs were also taken (see figure 4-2) which confirm the uniformity of the SIMS sputtering of GaAs, as opposed to some matrix materials, which do not sputter uniformly.

To determine the ion intensity-to-concentration conversion factor, the ion implantation/integration method, as discussed previously, was used. An example of this is shown in figure 4-3. This is a SIMS profile of Cr implanted into GaAs with a dose of 1×10^{14} cm^{-2}. Using the integral of this profile (calculated by the SIMS computer), and knowing the dose, the size of the sampling area, and the arsenic ion intensity, the conversion or "sensitivity" factor was determined. This was done occasionally to ensure that it did not change appreciably over the span of the research (it varied by less than 30%). In addition, one sample (a 12 hr, 800°C Cr indiffusion sample) was occasionally analyzed. The standard deviation (after five Cr analyses over 2 years) was 50%. This was therefore taken to be the maximum expected error in the concentration values obtained in SIMS profiles. (See the appendix for a full discussion on the error analyses.)

4.5 Solubility Studies - Results and Discussion

Anneals of GaAs with a "D source", as shown in figure 4-4, were done at 800°C for 6, 12, and 24 hours in order to determine the length of time needed to reach the Cr solubility level in the bulk of the GaAs (i.e., > 4 μms from the surface); SIMS Cr profiles indicated that 12 hours was sufficient time to

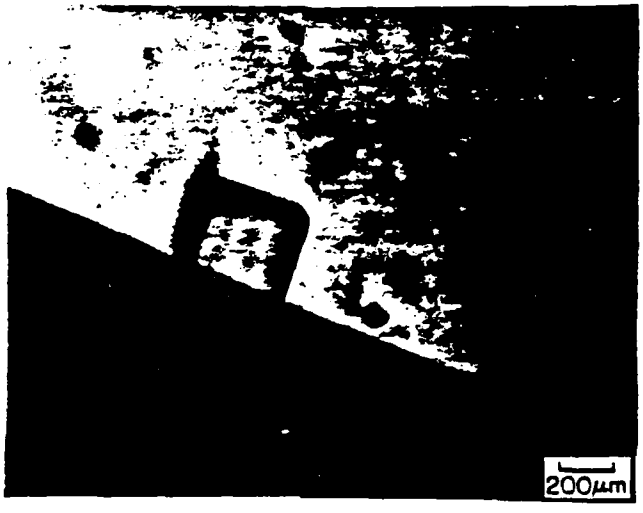

Figure 4-2. Optical micrograph (50X) of a SIMS crater in GaAs (cleaved down the center), indicating uniform sputtering.

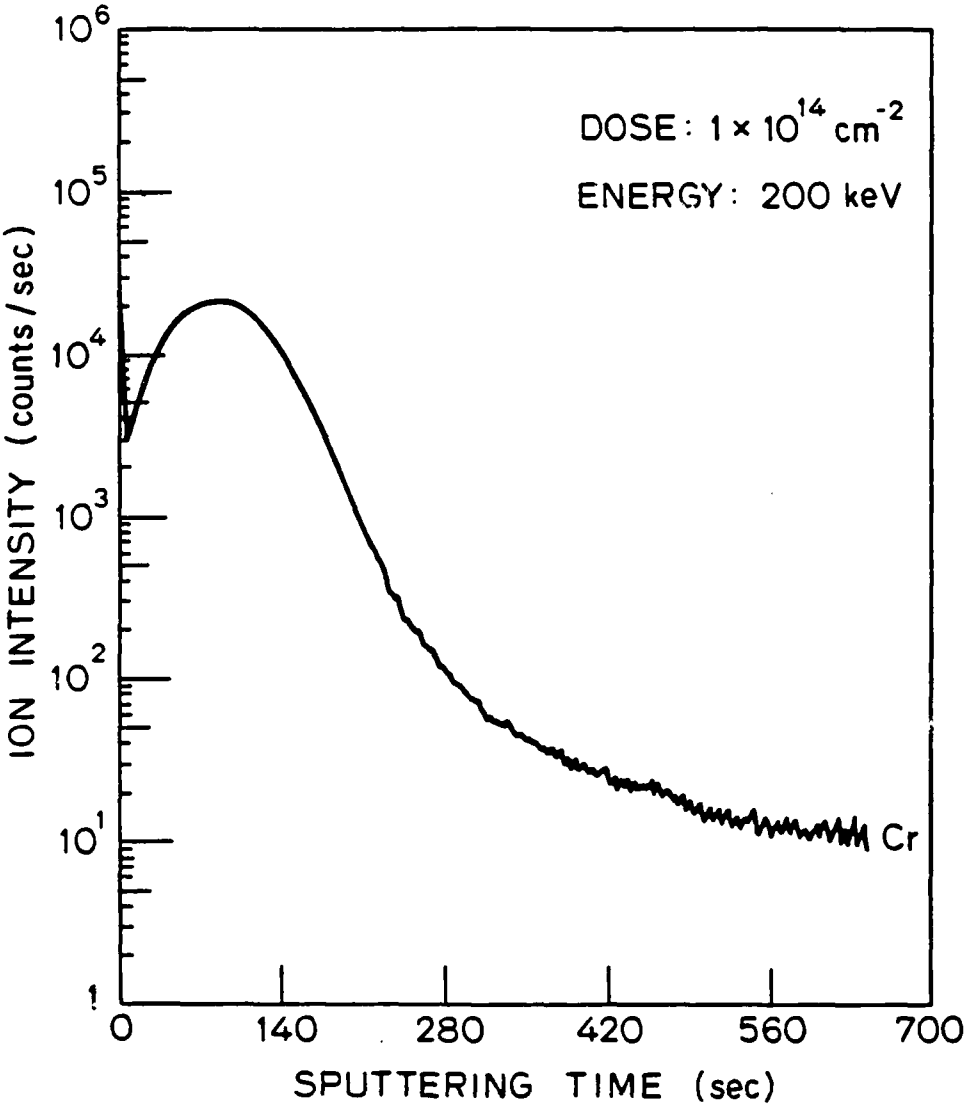

Figure 4-3. Ion intensity versus sputtering time, as determined by SIMS, of GaAs implanted with Cr at the dose and energy indicated above.

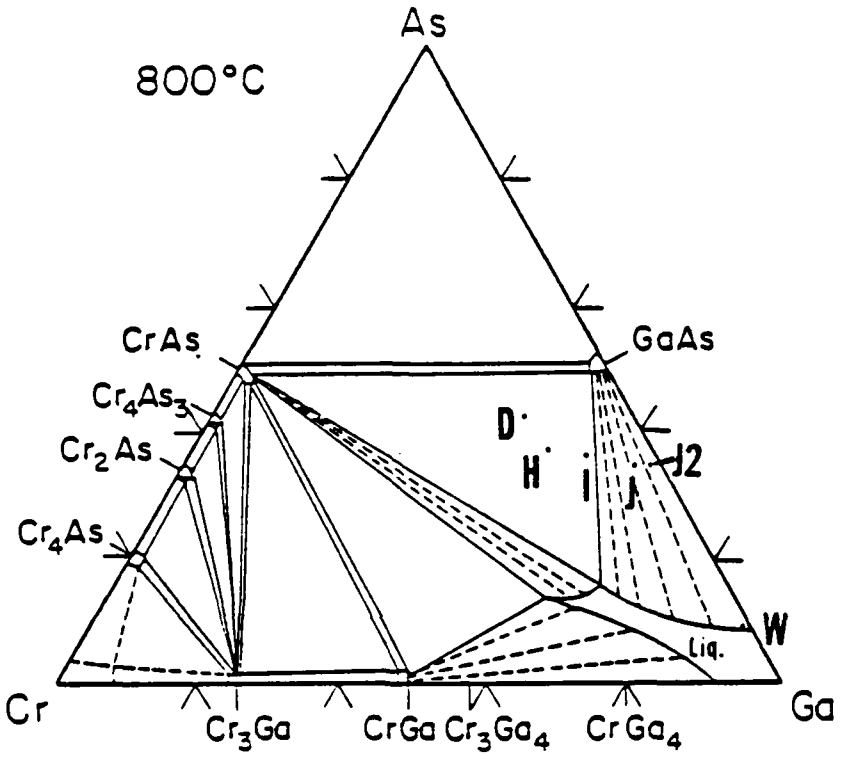

Figure 4-4. Compositions of sources D, H, I, J, J2, and W.

do so at 800°C. The Cr solubility was thus determined to be 3×10^{16} cm^{-3} ($\pm 1.5 \times 10^{16}$ cm^{-3}) at 800°C. Eight anneals were then done at that temperature using sources D, H, I, and J (see figure 4-4) for 6, 12, or 24 hours, as indicated in figure 4-5. As mentioned earlier, according to the phase rule and the Ga-As-Cr ternary phase diagram, GaAs samples in equilibrium with sources D, H, and I should have the same Cr solubility, while a sample in equilibrium with source J should be different, and probably less. The SIMS Cr profiles, shown in figure 4-5, show this to be so. The bulk Cr levels for the D, H, and I samples are all around 3×10^{16} cm^{-3}, while that for J is $\approx 4 \times 10^{15}$ cm^{-3}. (Note: the strange behavior at the surface will be discussed in later chapters.) These results confirm the ternary phase diagram findings of chapter 3 and also confirm the applicability of the phase diagram and the phase rule for this type of study.

These results explain why Woodard's (29) solubility values are low compared to the values obtained for sources D, H, and I. As discussed earlier, his results are for GaAs in equilibrium with $Ga_{(\ell)}$ whose Cr content is 0.86 a/o. This would correspond to approximately point W in figure 4-3. This is to the right of even J in the $GaAs_{(s)}$-$Ga_{(\ell)}$ region, and hence one would expect a lower Cr solubility in GaAs for that case.

Solubility anneals were then done with H source (which tended to result in less surface build-up of Cr) at 700, 750, 900, and 1000°C in order to obtain Cr-in-GaAs solubility values, again, for the $GaAs_{(s)}$-$CrAs_{(s)}$-$Ga_{(\ell)}$ tie

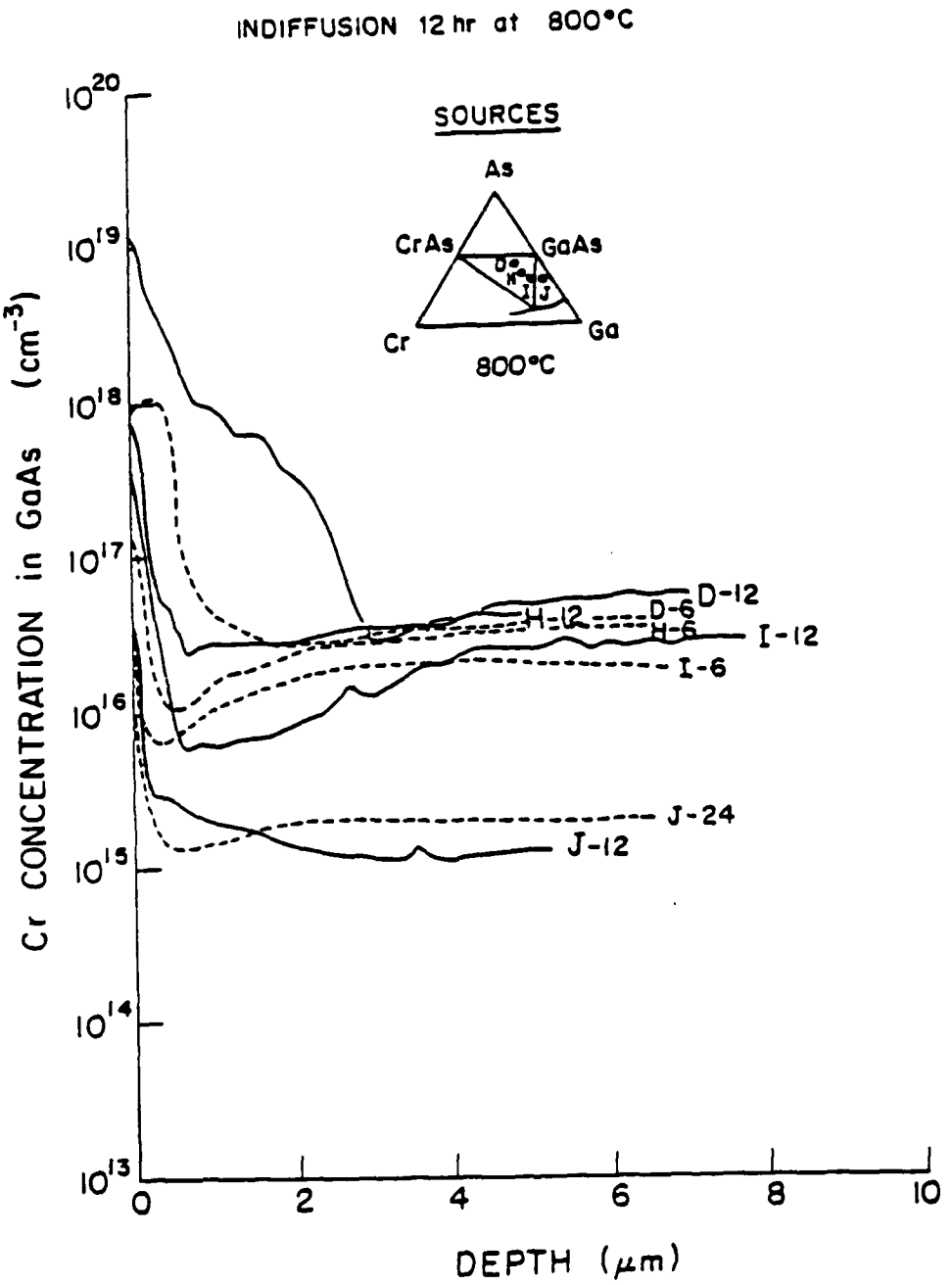

Figure 4-5. Cr in GaAs concentration profiles from 800°C solubility experiments for various times and with various sources, as indicated in the profile designations.

triangle. These were done for 18, 18, 8, and 7 hours respectively - long enough to reach the maximum level in the bulk. The resulting SIMS Cr profiles, including that for 800°C, are shown in figure 4-6. The Cr solubility vs. 1/T is plotted in figure 4-7. As expected, the Cr solubility extrapolates to the maximum Cr solubility of 2×10^{17} cm^{-3} just below the melting point of GaAs.

As is the case with most impurities in semiconductors, Cr exhibits retrograde solubility in GaAs; i.e., the solubility increases with temperature above the eutectic point, 670°C in this case. Swalin (46), using the results of Thurmond and Struthers (47), gives a good review of retrograde solubility, including a good explanation for why it is common in semiconductors. Basically it is due to the large positive heats of solution for the impurities in semiconductors (because of the strong bonding between the lattice atoms, and hence the relatively small solubilities of impurities, compared to solutes in metals). It is shown by Thurmond and Struthers how large heats of solution then lead to retrograde solubility based on the equations for the solidus and liquidus lines.

To confirm that the bulk levels reached in the solubility experiments correspond to equilibrium conditions, an experiment was done in which a GaAs wafer was annealed at 900°C (with H source) for a long time (12 hours), and then annealed at 800°C (again with H source). SIMS analysis was done after each anneal. The Cr profiles are shown in figure 4-8. As one can see, the bulk Cr level after the 900°C anneal (curve A) was at 8×10^{16} cm^{-3}, the determined solubility level for that

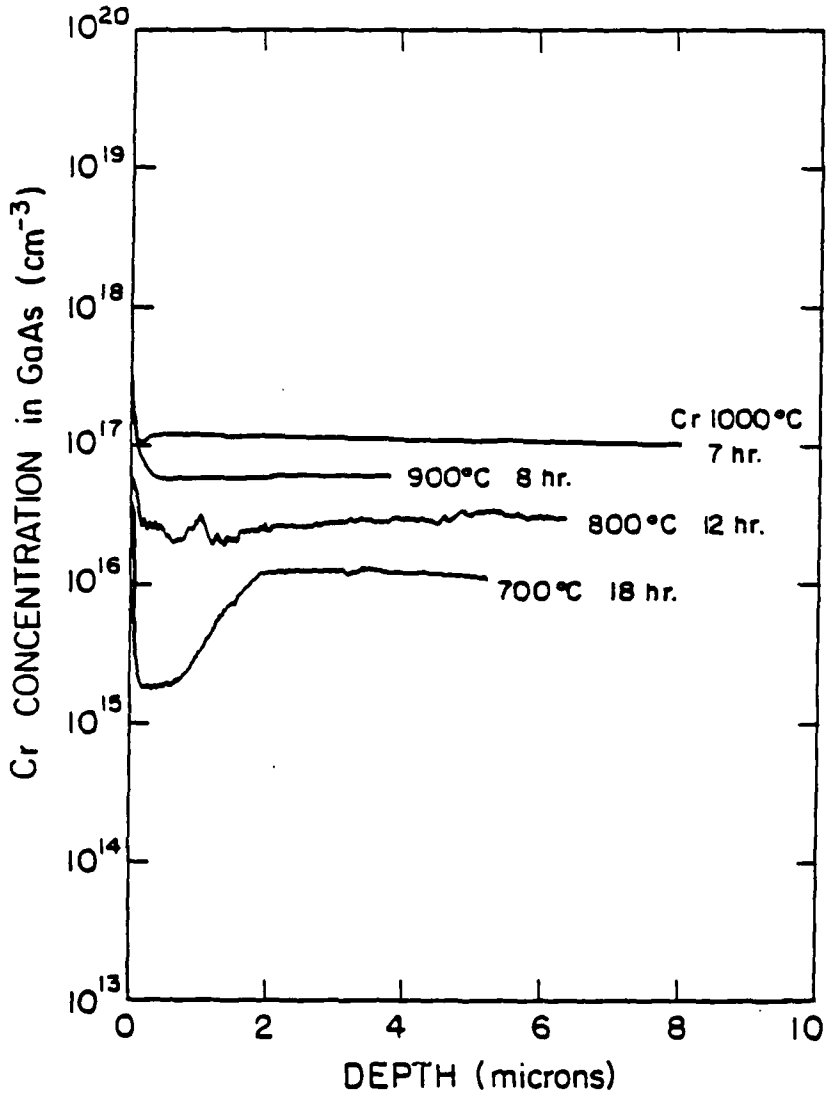

Figure 4-6. Cr in GaAs concentration profiles from solubility experiments for times and temperatures indicated.

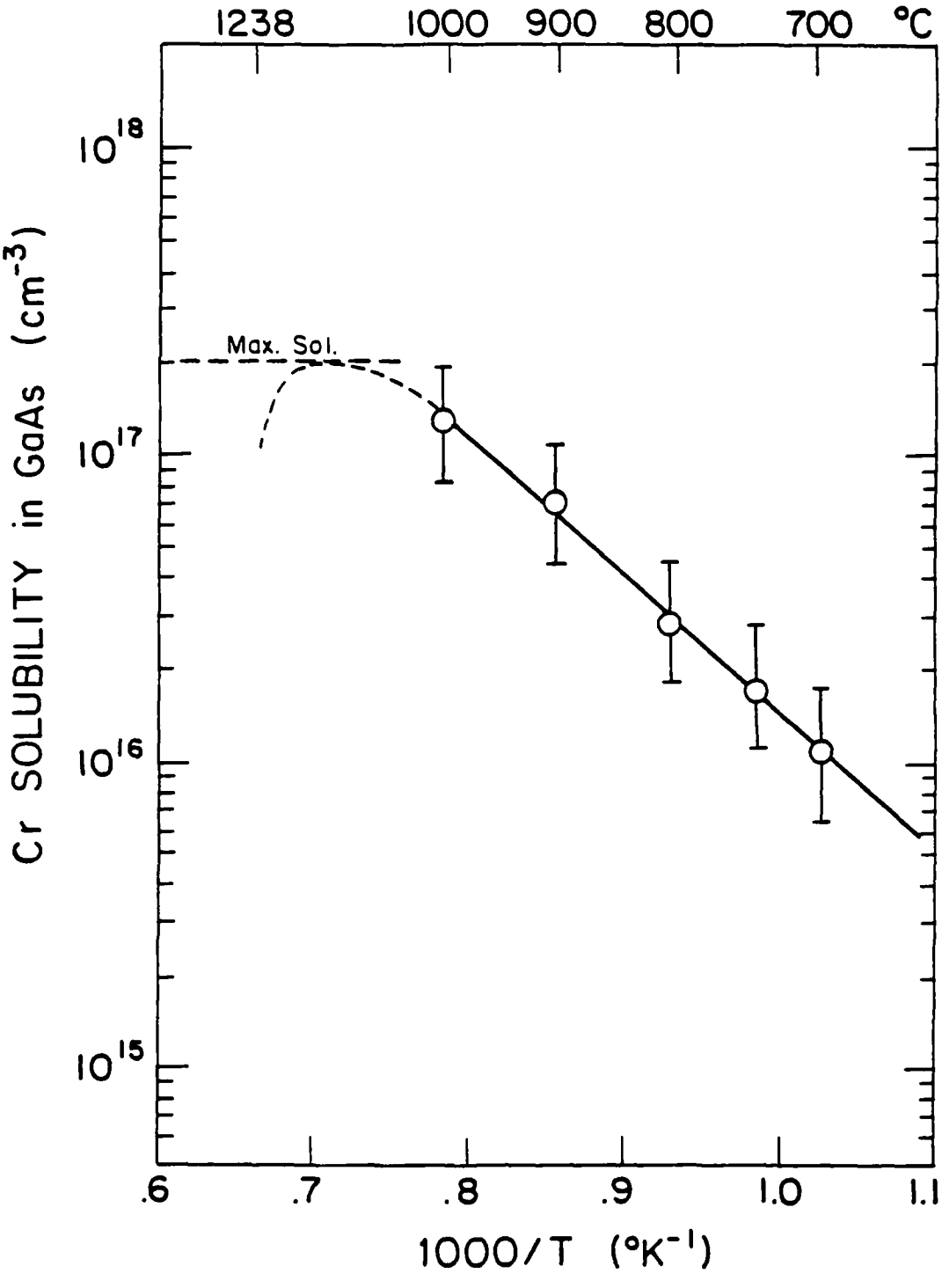

Figure 4-7. Cr solubility in GaAs (for $GaAs_{(s)}$-$CrAs_{(s)}$-$Ga_{(\ell)}$ region), with maximum solubility of Cr in GaAs as indicated.

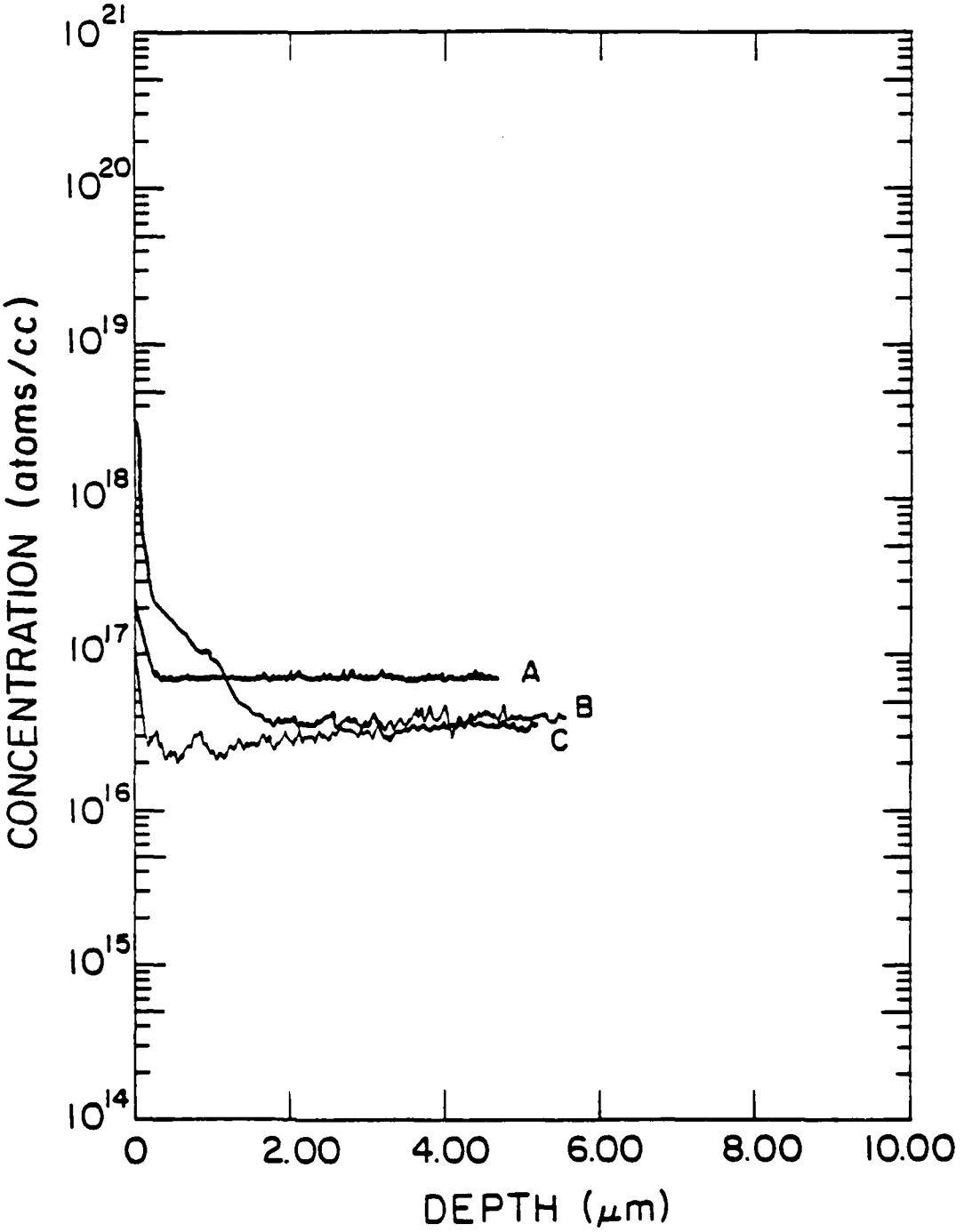

Figure 4-8. Cr in GaAs concentration profiles, from solubility experiments. A: 900°C, 12 hr. indiffusion with H source. B: subsequent 800°C, 12 hour anneal with H source. C: 800°C, 12 indiffusion into undoped GaAs, with H source.

temperature. The bulk Cr level after the subsequent 800°C anneal (curve C) is lower, ≈4 x 10^{16} cm^{-3}. Also shown (curve B) is the profile of the original 800°C solubility determination, with a bulk level of 3.5 x 10^{16} cm^{-3}. This shows that the same Cr concentration (within experimental error) was reached both from above and from below, confirming that it is the equilibrium solubility concentration.

From the solid solubility results, and from the Ga-As-Cr phase diagram results (specifically, the Cr concentration in the Ga-rich liquid in equilibrium with $CrAs_{(s)}$ and $GaAs_{(s)}$), the distribution coefficient, k, of Cr in GaAs was determined for various temperatures; the distribution coefficient equals $[Cr]_s/[Cr]_\ell$, the solid being $GaAs_{(s)}$ and the liquid being $Ga_{(\ell)}$ in this case. These numbers, as well as the liquid and solid solubility numbers from which they were calculated, are tabulated in table 4-1. The distribution coefficients vs. 1/T are plotted in figure 4-9. The distribution coefficient at 800°C was also determined from sample J (GaAs in equilibrium with J source), and is indicated by "J" in the graph. The results show that k does not vary much with Cr concentration; even though the solubilities vary by an order of magnitude between J and D, k varies by only a factor of two. Also plotted in figure 4-9 are the results of Woodard (29), from his LPE studies (which are for $GaAs_{(s)}$ in equilibrium with a Ga-rich liquid of 0.86 a/o Cr concentration). These are very consistent with the results for higher Cr concentrations. Therefore, while the solubilities vary as the total composition moves across the phase diagram,

Table 4-1. Distribution Coefficient, k, of Cr in GaAs (Ga-rich side).

T	$[Cr]_\ell$	$[Cr]_s$	k
700°C	.17	7×10^{15}	9×10^{-7}
800	.16	3×10^{16}	4.5×10^{-6}
800	.05	4×10^{15}	2.5×10^{-6}
900	.15	9×10^{16}	1.2×10^{-5}
1000	.12	1.3×10^{17}	2.5×10^{-5}

$[Cr]_\ell$: Cr concentration (mole fraction) in Ga-rich liquid.

$[Cr]_s$: Cr concentration (cm^{-3}) in GaAs

k: $[Cr_s]/[Cr]_\ell/4.4 \times 10^{22}$

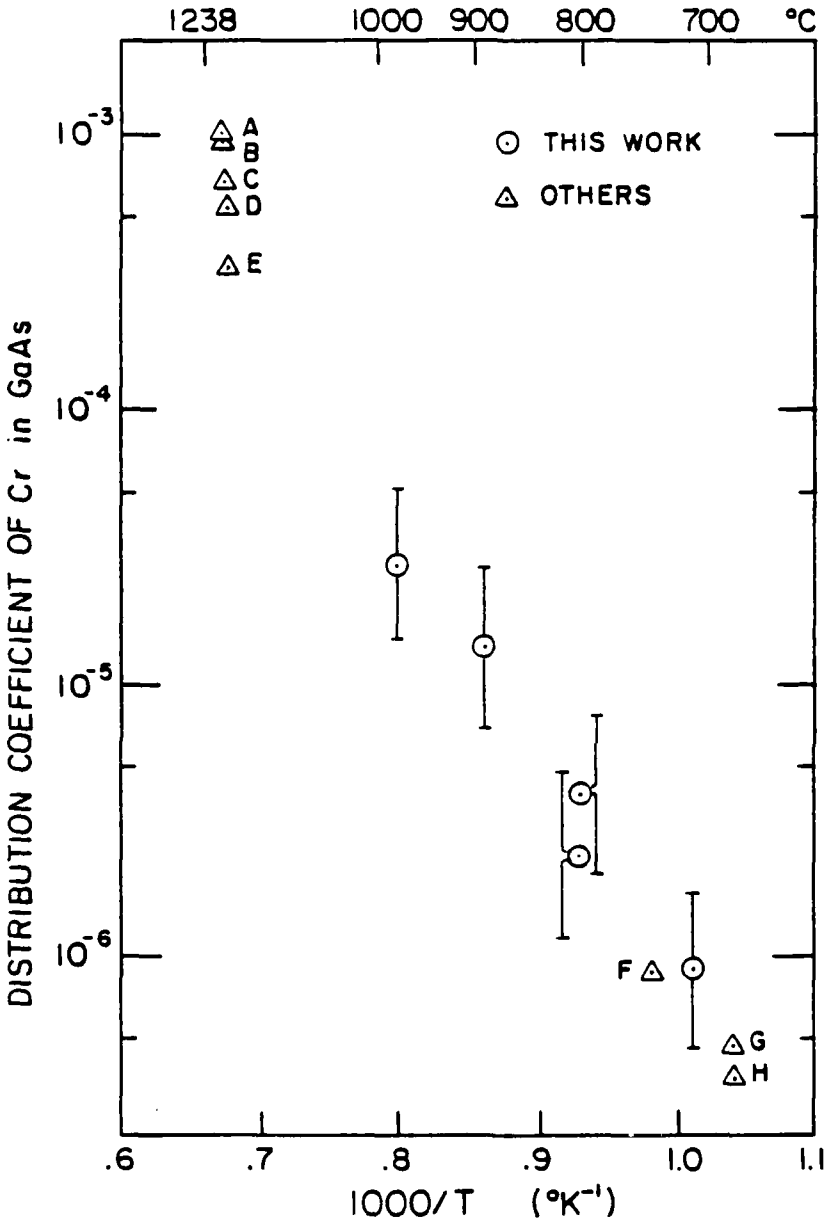

Figure 4-9. Distribution coefficient, k, vs. 1/T for Cr in GaAs. Circled data are from this work; data with triangles are from others: A,C: ref. 25; B: ref. 24; D: ref. 26 and 27; E: ref. 28, and F,G,H: ref. 29.

the ratio of solid solubility to liquid solubility remains approximately constant, as one would expect for dilute solutions. In addition, the distribution coefficients determined from Cr-doped GaAs crystal growth, which are for temperatures just below the melting point of GaAs, are shown (from references 24-29). As one can see, the results of this work fill the gap nicely between the lower temperature results of Woodard for LPE conditions and the higher temperature results from the bulk crystal growers. (Note: upon further examination of the "crystal growth" values, one observes the trend: the more Cr in the melt, the smaller the k value. This makes sense since as the Cr content in the melt increases, the melting point of GaAs decreases, and it is at that temperature at which the distribution of Cr takes place. Therefore, the temperatures for which the k values correspond to for those six cases would be different. Taking this into account, the six points should <u>not</u> be plotted at the same temperature, but for decreasing temperatures, and would follow the trend of k decreasing with decreasing temperature.)

To see if there is a difference in Cr solubility between one type of undoped GaAs and another, solubility anneals were done using GaAs substrates from different suppliers (Cominco, Hewlett Packard, and Crystal Specialties). The differences between the resulting solubilities were within the expected error (± 50%) of the experiments. Therefore, the way the GaAs is produced apparently has no appreciable effect on the final equilibrium solubility.

To see the effect of doping on the solubility of Cr in

GaAs, solubility anneals (at 800°C using H source) were performed in Te-doped (n-type) GaAs. After an 18 hour anneal, 10 μms of the GaAs was etched off each surface (using a 16:1:1 $H_2O:H_2O_2:H_2SO_4$ solution). This was done to ensure that any surface artifacts are removed, in addition to removing any Te depletion region caused by Te outdiffusion. (However, since the diffusivity of Te at 800°C is very small, this was not a problem.) SIMS analysis indicated the Cr solubility to be 8×10^{16} cm^{-3}, almost three times that in undoped GaAs at that temperature. This is consistent with the model of Cr being a deep acceptor in GaAs (on a Ga site)(48-51), since the presence of a donor usually increases the solubility of an acceptor (46,52), based on charge equilibrium considerations. (Likewise, the presence of another acceptor usually decreases the solubility of an acceptor.) These results are consistent with those of Brozel et al. (36) who found in their crystal growth experiments that the Cr solubility increases with increasing Si concentraion, the Si acting as a donor. C-V carrier concentration measurements, using gold contacts to the GaAs surface and an H-P automated C-V measuring system, were made on the Te-doped sample both before and after the Cr indiffusion. Before Cr diffusion, the n-type carrier concentration was 3.8×10^{17} cm^{-3} (consistent with the reported Te doping of $\sim 3 \times 10^{17} cm^{-3}$), whereas after Cr diffusion, it was 2.4×10^{17} cm^{-3}. This means that $1.8 \times 10^{17} cm^{-3}$ carriers were compensated by the chromium. If the Cr acts as a double acceptor, as claimed by Brozel et al. (36), then that means that $1/2 \times (1.8 \times 10^{17})$ cm^{-3}, or

9×10^{16} cm^{-3} Cr atoms are electrically active. This compares very well to the measured 8×10^{16} cm^{-3} chromium (the difference is well within the experimental error). This means that the bulk chromium seen in the SIMS profiles is in solution, and are not precipitates or clusters. It is also good evidence of the accuracy of the SIMS analysis in this work.

Chromium in GaAs is interesting in regards to its electrical properties; Cr is said to be a deep acceptor with an energy level (for the first ionization state) just above midgap and, therefore, above the Fermi level in otherwise undoped GaAs. Therefore Cr-doped GaAs is semi-insulating,and not p-type, even at high temperatures. (Occasionally it is found to be p-type (53); however, that is probably due to other acceptors being present.) But if free electrons are present, due to the presence of n-type impurities or donors, the chromium atoms will accept the electrons (one or two per Cr atom, depending on the electron concentration (36)), and compensate the donors. This is the reason why Cr is put into GaAs in the first place: to compensate the n-type impurities and render the GaAs semi-insulating. Even if too much Cr is added, the GaAs will still remain semi-insulating and not become p-type. It is for these reasons that Cr is sometimes called an "electron trap" in GaAs, rather than an acceptor. And as White (2) points out, the normal models and equations for acceptors, such as those regarding occupancy and the position of the Fermi level, may not apply for a species such as this.

AD-A144 949 AN INVESTIGATION OF THE SOLUBILITY AND DIFFUSIVITY OF CHROMIUM IN GALLIUM ARSENIDE(U) ADVANCED RESEARCH AND APPLICATIONS CORP SUNNYVALE CA T J MAGEE ET AL. 2/3

UNCLASSIFIED 23 MAY 84 N00014-80-C-0482 F/G 7/4 NL

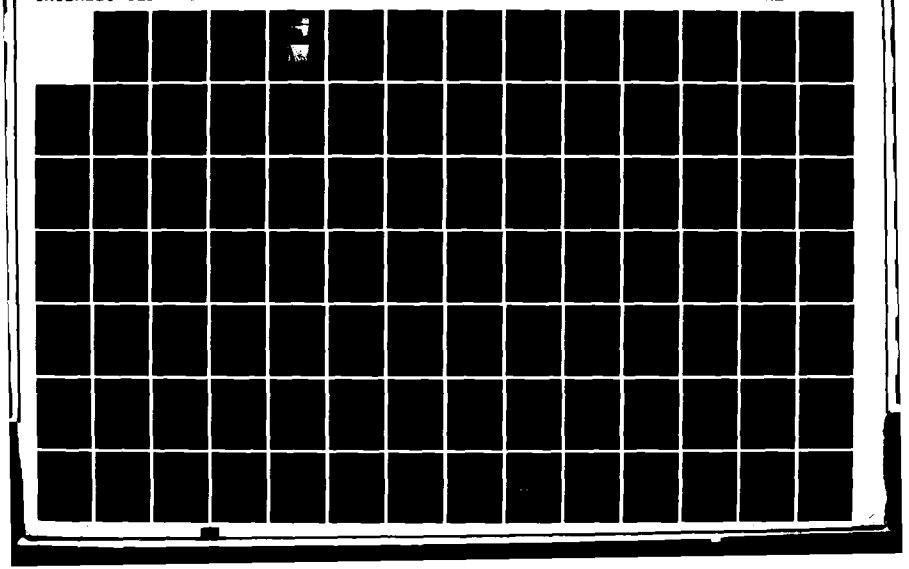

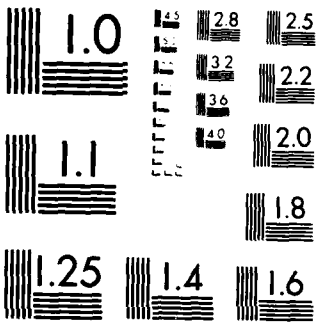

However, in heavily doped GaAs (n-type), all the Cr is probably ionized (36), and acts more like a normal acceptor (e.g., its solubility increases with an increase in the n-type doping level), and the equations that are used to quantitatively predict the increase in solubility may be used as a first order approximation. The increase in the solubility of an acceptor in the presence of a donor is given by (54,46):

$$C_s'' \approx C_s' \, (1 + gn/n_i)/(1 + g) \qquad (4\text{-}1)$$

where C_s'' is the new solubility level, C_s' is the solubility in the intrinsic, or undoped case, n is the electron concentration (due to the doping), n_i is the intrinsic carrier concentration, and g is the degeneracy factor, (which according to Sze (55), is equal to 1/4 for acceptors in Ge, Si, and GaAs). Testing this for the case discussed above, at 800°C (n_i = 7 x 10^{16} cm^{-3} (13)), a Te doping of 3.8 x 10^{17}, and an intrinsic Cr solubility of 3 x 10^{16} cm^{-3}, one would predict from this equation a new solubility of 6 x 10^{16} cm^{-3}. The actual solubility, from SIMS, is 8 x 10^{16} cm^{-3}. A similar calculation at 850°C (with the same Te doping), would predict a solubility of 8 x 10^{16} cm^{-3} for the intrinsic case. A solubility experiment was done at 850°C in the same way as in the previous case, and the SIMS Cr profile indicated a new solubility of 9 x 10^{16} cm^{-3}. As predicted, at high temperatures the % increase is not as great, due to the fact that n_i increases. As a first order

approximation, equation 4-1 is adequate.

A similar experiment was done in n-type Si-doped GaAs at 800°C, for 48 hours. The exact Si concentration was not known (it was believed to be in the low-to-mid 10^{17}'s as with the Te case), but the qualitative result was the same. The Cr solubility was higher than in the undoped case: 7×10^{16} cm^{-3} vs. 3×10^{16} cm^{-3}. So, even though the donor was on a different site (on a Ga site, rather than an As site as is the case of Te), the effect was the same, indicating that it is an electrical effect, rather than a steric and/or lattice stress effect.

4.6 Surface Morphology and Different Sources

Visual observations of the GaAs surface after solubility experiments confirm and nicely illustrate the applicability of the phase diagram studies to these solubility studies. As mentioned in chapter 3, a proper choice of the Cr source, as determined by the ternary phase diagram, is essential for valid solubility and diffusion studies, and the condition of the GaAs surface after such experiments clearly demonstrates this.

All the solubility experiments reported so far in this chapter were done by using a well-defined Cr source which was in equilibrium with GaAs (e.g. H source or J source). An optical micrograph of a typical surface after a solubility anneal is shown in figure 4-10. This was after a 2 hour, 800°C anneal with H source (shown at 500X). In contrast, an anneal was done under the same conditions, except using pure Cr as the source (see figure 4-11). As is obvious, the GaAs surface greatly degraded in the latter case. As predicted by the phase

Figure 4-10. Optical micrograph (500X) of GaAs surface after 800°C, 2 hr. Cr indiffusion anneal with H source.

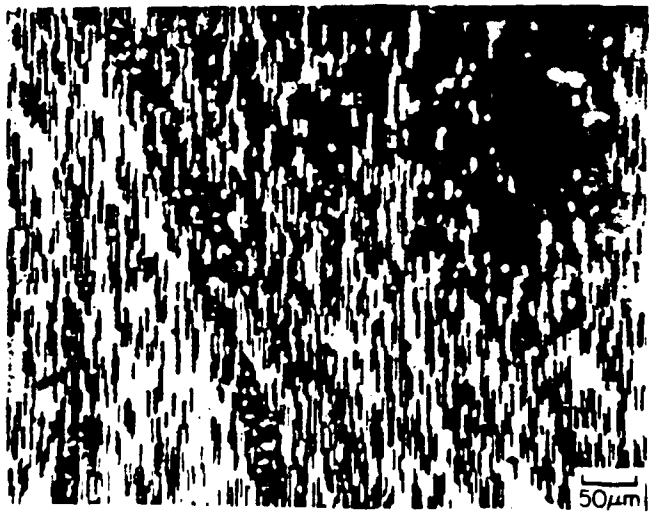

Figure 4-11. Optical micrograph (200X) of GaAs surface after 800°C, 2 hr. Cr indiffusion anneal with elemental Cr source.

diagram, Cr and GaAs are not in equilibrium with each other, and new phases, probably $CrAs_{(s)}$ and $Ga_{(\ell)}$ (which contains Cr and As), will form from the starting materials. (In addition, a SIMS analysis showed a lower Cr level in the bulk of the GaAs than in the H source case, $\approx 5 \times 10^{15}$ vs. $\approx 8 \times 10^{15}$ cm^{-3}; this is perhaps due to the GaAs being in contact with $Ga_{(\ell)}$.) These results confirm the findings of the phase diagram determinations, and show why pure Cr should not be used as the Cr source in GaAs solubility-diffusion studies, as has been done in the past (which will be discussed in chaper 6). More concerning surface phenomena will be presented in chapter 7.

4.7 Summary

In this chapter, the work on the solubility of Cr in GaAs is presented. It was shown that previous studies paid little attention to phase equilibria considerations in regards to solubility values, both in determining them and in using them. Using the information acquired from the phase equilibria experiments, valid and well-defined solubility studies were performed for Cr in GaAs for a range of temperatures and for different regions of the Ga-As-Cr phase diagram. The Cr solubility in GaAs was determined from 700°C to 1000°C for the $GaAs_{(s)}$ - $CrAs_{(s)}$ - $Ga_{(\ell)}$ tie triangle region. In addition, the solubility was determined at 800°C for GaAs in equilibrium with a Ga-rich liquid which contained 5 a/o Cr, for comparison; as expected, the Cr solubility was less for this case. The distribution coefficient was determined for these same temperatures, and the results were consistent with

literature values for lower and higher temperatures and for different Cr concentrations in the Ga-rich liquid. The Cr solubility in Te-doped (n-type) GaAs was measured, which was found to be higher than in undoped GaAs, consistent with the model of Cr acting as an acceptor, or "electron trap". C-V carrier concentration measurements of the Te-doped GaAs, both before and after Cr solubility anneals, confirmed that the Cr acts as a double acceptor for high donor concentration and that the Cr measured by SIMS is in solution and at the levels that the SIMS analyses indicate. Finally, observations of the surface morphology after solubility experiments, using a well-defined, "quasi-equilibrium" source in one case, and pure Cr in another, confirm the findings of chapter 3 concerning phase equilibria and show why such considerations are important in solubility studies.

5. THE SUBSTITUTIONAL/INTERSTITIAL DISSOCIATIVE DIFFUSION MECHANISM

5.1 Introduction

The substitutional/interstitial dissociative diffusion mechanism has been effective in describing diffusion of impurities in semiconductors. In the past, it was used mostly for impurities in compound semiconductors, but it is now being applied to impurities in elemental semiconductors, including silicon. This mechanism has been effective in explaining a variety of complex diffusion profiles which are observed for different impurity/matrix material systems and also for different profiles in the same system that arise for different diffusion conditions. This chapter is a brief tutorial on this mechanism. The motivation for the model and a description of its development is presented in the "History of the Model" section, along with a listing of the systems that are successfully described by the model. The governing reactions and equations, and the different cases - which are used to simplify the rather complex equations - are given, followed by a discussion of how several real systems fit these different cases. In addition, one step of this diffusion process, namely, the substitutional-to-interstitial conversion, is examined, and two mechanisms for this step are presented and discussed. Finally, activation energies and D_o values are examined in order to help one identify the mechanism in a specific system and in determining which is the appropriate case for a particular condition in a system. In chapter 6, this mechanism is used to model the complex behavior of

chromium in gallium arsenide.

5.2 History of the Model

The substitutional/interstitial dissociative diffusion mechanism was conceived and developed in response to unusual diffusion behavior observed in several systems. It not only explains uniform rises or drops in the bulk impurity concentration level, and even "uphill diffusion" at the back side, but also explains what appears to be anomalously high diffusion values for impurities that, according to their electrical activity, are predominantly located on substitutional sites. It also explains different diffusion profiles for different conditions, and even two or more profiles superimposed on each other.

Frank and Turnbull (56), in 1956, first proposed the basic mechanism while analyzing other workers' results of diffusion of Cu in Ge. In the diffusion profiles (concentration vs. depth) of Tweet and Gallagher (57) for Cu diffusing into Ge from one side, it was noted that the distribution corresponded to Fick's Law (normal error function diffusion) only at small depths. At greater depths there was a concentration of copper which was virtually independent of distance and which rose uniformly with time. In addition, the copper that was measured was all electrically active and corresponded to substitutional copper (i.e., acceptors). Frank and Turnbull showed that dislocation pipes could not explain the behavior (which had previously been guessed to be the cause). They proposed the following mechanism. Copper dissolves in germanium in two states, interstitial and substitutional. In interstitial

solution, it has a very high diffusivity, but a low solubility. Conversely, as a substitutional, it has a low diffusivity, but a high solubility. However, they do not diffuse independently as in the normal two-stream model. There is a dissociative mechanism corresponding to the inter-conversion of interstititial and substitutional species. This probably requires a supply of vacancies, which is available only at the free surface or near dislocations. The basic diffusion mechanism begins with copper substitutional atoms dissociating near the surface to vacancies and interstitials, which then diffuse independently. Then, the interstitital atoms convert back to substutitional (to maintain local equilibrium between the two species) by combining with a vacancy which could come either by diffusing from the surface, or by generation in the bulk (from dislocation climb). The first case accounts for the normal error function profile at smaller depths, and the second case accounts for the nearly uniform level in the bulk which rises with time.

Since the mechanism was first proposed, it has been applied effectively to the following impurity/matrix systems: indium in GaAs (58), Ag in InP (59), Zn in InSb (60), Cd in InP (61), Au in InAs (62), Au in Si (63-65), P in Si (66), and most extensively, Zn in GaAs (10, 67-76). In his review of diffusion in III-V semiconductors (77), Kendall concludes, upon a study of the literature, that the following systems also follow this mechanism: Cu, Ag, Au, Mn, Sn, Mg, Cd, and perhaps S, in GaAs, Cu in InSb, and Au in InP. The mechanism has also been proposed for Cr diffusion in GaAs (5,78). Several of

these cases will be discussed in more detail later.

Almost all these diffusing elements are either shallow or deep acceptors in III-V compound semiconductors, and are believed to occupy the group III element site in the compound. There is a structure motivated rationale for a substitutional/interstitial diffusion mechanism impurities in III-V compounds since an impurity on a group III site must travel through a group V plane in reaching another group III site. This is probably done interstitially (79). This mechanism is likely whenever a slower diffusing species has a higher solubility than a faster diffusing species, and there is a finite interconversion rate for the two species. Impurities in semiconductors often have these properties.

5.3 Governing Equations

The substitional/interstitial dissociative diffusion model is described in detail by Tuck in his book, Diffusion in Semiconductors (7), who followed the treatment of Sturge (80). The basic reactions and equations for the model, from these references, are as follows.

As described earlier for this mechanism, the impurity atom enters the diffusion host at the surface where interstitial/substitutional equilibrium is attained and equilibrium solubility values are achieved. These species, along with vacancies, which arise either from the surface or from the vacancy generation attending the formation of the interstitials from substitutionals, diffuse in the material. It is assumed that substitutional diffusion is negligibly slow compared to the interstitial and vacancy

diffusion. The concentrations of the substitutional impurity species, the interstitial impurity species, and the vacancies, will be denoted by C_s, C_i, and C_v respectively, and are functions of x, the distance from the surface. The equilibrium, or solubility, values of these are denoted by C_s', C_i', and C_v'. The basic conversion reaction is:

$$I_i + V = I_s \qquad (5\text{-}1)$$

where I denotes impurity atom, V denotes vacancy, and the subscripts i and s denote interstitial and substitutional, respectively. Inside the material, the interstitials, which have a low solubility, and vacancies can combine by this reaction, resulting in the impurity becoming substitutional. These vacancies can either be the ones diffusing from the surface - or wherever they were created during the formation of interstitials from substitutionals, to be discussed in chapter 6 regarding "junction diffusion" - or can be generated in the bulk. More interstitials can then diffuse in and convert to substitutional species until the high substitutional solubility level is reached throughout the material. Figure 5-1 shows this schematically. (Note: here we are considering uncharged species. For charged species, equation 5-1 would include either holes or electrons. This will be considered later.)

The assumption is made that the equilibrium between substitutional and interstitial atoms is always maintained, so that:

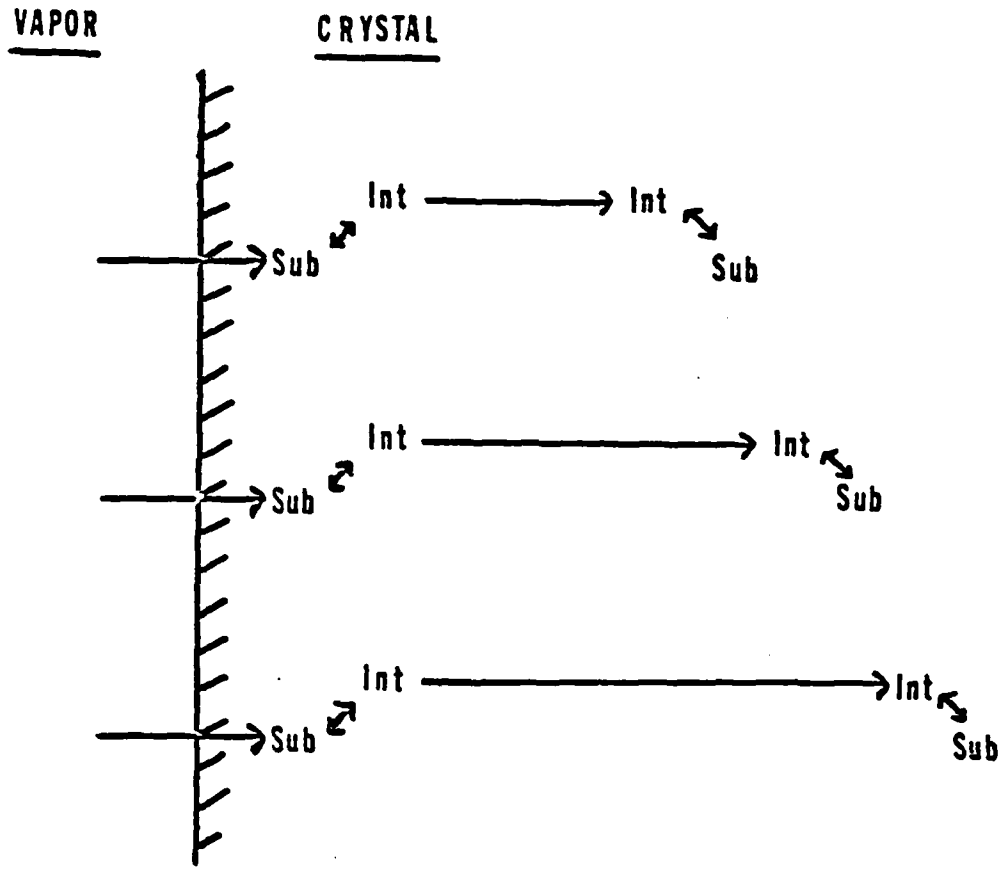

Figure 5-1. Schematic diagram of diffusion mechanism; "Int" indicates interstitial species, and "Sub" indicates substitutional species.

$$C_s = K\, C_i\, C_v \qquad (5\text{-}2)$$

where K is the equilibrium constant for equation 5-1. This, of course, is also true when the concentrations are at their equilibrium, or solubility, values, so:

$$K = C_s'/C_i'C_v' \qquad (5\text{-}3)$$

Fick's Law for two species diffuson is:

$$\frac{\partial C_i}{\partial t} + \frac{\partial C_s}{\partial t} = D_i \frac{\partial^2 C_i}{\partial x^2} + D_s \frac{\partial^2 C_s}{\partial x^2} \qquad (5\text{-}4)$$

where D_i and D_s are the diffusivities for the interstitial and substitutional species respectively.
We assume $D_s = 0$, so

$$\frac{\partial C_i}{\partial t} + \frac{\partial C_s}{\partial t} = D_i \frac{\partial^2 C_i}{\partial x^2} \qquad (5\text{-}5)$$

The continuity equation for vacancies is:

$$\frac{\partial C_v}{\partial t} = D_v \frac{\partial^2 C_v}{\partial x^2} - \frac{\partial C_s}{\partial t} + k_1(C_v' - C_v) \qquad (5\text{-}6)$$

where the first term on the right is the indiffusion of vacancies from the surface, the second term is the loss of

vacancies due to the interstitials converting to substitutionals, and the third term is the bulk production of vacancies by dislocation climb or some other process, assuming that the production of vacancies is proportional to the deviation from the equilibrium value.

The solution to these equations, in order to determine the concentration-depth profiles as a function of time, cannot be solved explicitly. However, several cases can be considered in which appropriate approximations can be made resulting in simple solutions. In each case, it is assumed the total impurity concentration equals the substitutional atom concentration (since $C_s >> C_i$), and therefore we wish to solve for $C_s(x,t)$ in each case.

Case I. Vacancy equilibrium is maintained throughout the crystal. In this case, whenever a vacancy is needed for the interstitial-to-substitutional conversion, it is available. Therefore $C_v = C_v'$ and equation 5-2 becomes: $C_i = C_s/KC_v'$. This is substituted in equation 5-5, leading to:

$$\frac{\partial C_s}{\partial t}(1 + KC_v') = D_i \frac{\partial^2 C_s}{\partial x^2} \qquad (5\text{-}7)$$

Rearranging, and substituting for K from equation 5-3, leads to:

$$\frac{\partial C_s}{\partial t} = D_i \frac{C_i'}{(C_i' + C_s')} \frac{\partial^2 C_s}{\partial x^2} \qquad (5\text{-}8)$$

This is just normal error function-type diffusion, with an

effective diffusion coefficient of:

$$D_{eff} = D_i \frac{C_i'}{(C_i' + C_s')} = "D_{fast}" \qquad (5\text{-}8a)$$

(Designated as such because it is usually much higher than the other effective D to be discussed next).

For indiffusion with constant surface conditions (with $C(x,0) = 0$, $C(0,t) = C_s'$, and a semi-infinite medium), equation 5-8 can be solved, resulting in:

$$C = C_s = C_s' \text{ erfc } (x/2(D_{fast}t)^{1/2}) \qquad (5\text{-}9)$$

Case I would correspond to a high dislocation density (rapid vacancy generation), a high initial vacancy concentration, or long diffusion times (to be discussed in conjunction with Case IV).

Case II. There is no production of vacancies in the bulk ($k = 0$), so that all vacancies for the interstitial-to-substitutional conversion must come by vacancy diffusion. Since this is slow compared to interstitial diffusion, C_i will be assumed to be C_i' for all x. Therefore equation 5-6 becomes:

$$\frac{\partial C_s}{\partial t} (1 + KC_i) = D_v \frac{\partial^2 C_s}{\partial x^2}, \qquad (5\text{-}10)$$

which, upon substitution for K, results in:

$$C_s = C_s' \ \text{erfc} \ \frac{x}{2\sqrt{D_{slow}t}} \qquad (5\text{-}11)$$

for indiffusion, where

$$D_{slow} = D_v \frac{C_v'}{C_v' + C_s'} \qquad (5\text{-}12)$$

This gives the same kind of concentration profiles as in Case I, except $D_{slow} << D_{fast}$ (vacancy diffusion is usually much slower than interstitial diffusion) and therefore the penetration of the impurity is much shallower for any given time. Case II would dominate when the dislocation density is low (little or no vacancy generation) and for short times/low temperatures (before vacancy generation can appreciably replace the vacancies.)

Case III. This is when $k_1 > 0$, but small. Again, the interstitial diffusion is fast enough so that $C_i = C_i'$ for all x. But in contrast to Case II, there is some vacancy generation in the bulk. Equations 5-3 and 5-6 result in:

$$\frac{\partial C_i}{\partial t} = D_{slow} \frac{\partial^2 C_s}{\partial x^2} + \frac{C_s' - C_s}{\theta} \qquad (5\text{-}13)$$

where $\theta = (C_v' + C_s')/k_1 C_v'$. This, and the same boundary and initial conditions for indiffusion, can be solved by Laplace transforms, giving:

$$C = C_s' \ (1-\exp(-t/\theta)) \ \text{erfc}(x/2(D_{slow}t)^{1/2}) \qquad (5\text{-}14)$$

This is plotted for different t/θ values in figure 5-2 (from ref. 7). For small x, this is approximately Case II (vacancy diffusion limited), and for large x, $C \approx C_s'(1-\exp(-t/\theta)$ and the diffusion is vacancy generation limited and independent of x. In finite crystals, vacancies can diffuse in from the opposite side of the crystal as well. According to this model, the interstitials could convert to substitutionals there, and this results in a U-shaped profile, even when the impurity is diffused in from one side only. This "uphill diffusion" has become a test for the substitutional/interstitial dissociative diffusion mechanism, as disscussed by Kendall (81). A classic example of this is Au in Si (7). (Note: this is not uphill diffusion in the sense of diffusing up a concentation gradient while diffusing down an activity gradient, rather, it is uphill diffusion in the sense that the net profile appears to be diffusing uphill; the profile is developed by interstitials actually diffusing down their concentration gradient, andconverting to substitutionals more extensively at the surfaces of high vacancy concentrations.)

Case IV. This is for $k_1>0$, and large (θ small). Here, the generation of vacancies is fast enough so that the interstitial-to-substitutional conversion in the bulk starts to take place before the interstitial concentration is uniform throughout the bulk. If we assume that D_v is so slow that it can be ignored, and also assume a quasi-equilibrium in which $\partial C_v/\partial t = 0$ in the bulk, equation 5-6 becomes:

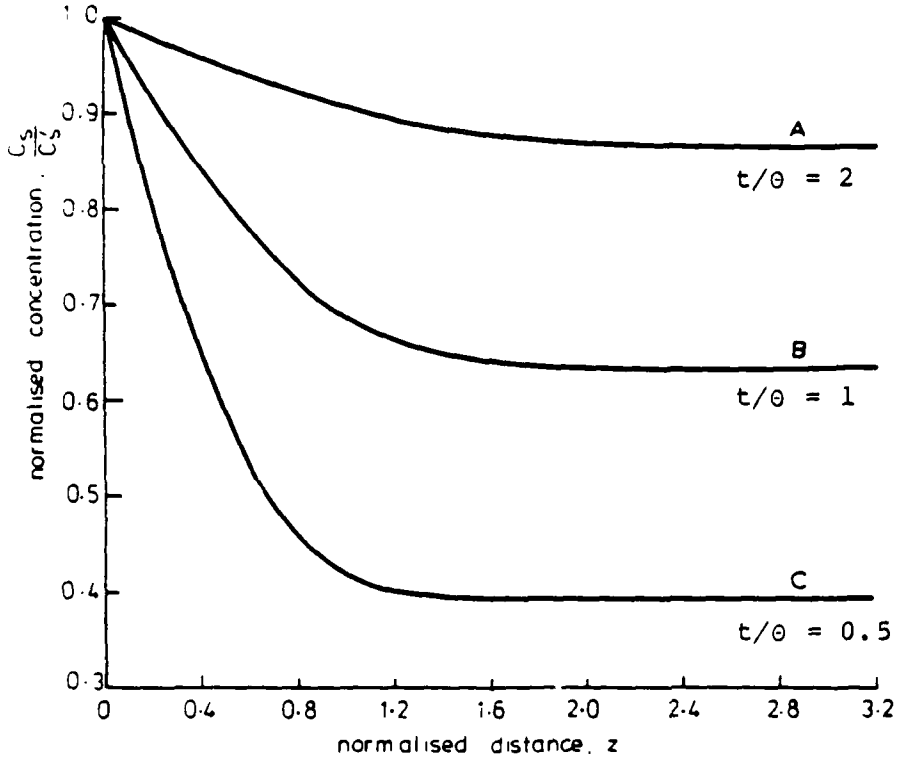

Figure 5-2. Theoretical Case III diffusion profiles, from ref. 7.

$$\frac{\partial C_s}{\partial t} = \frac{k}{KC_i} \left(C_s' - \frac{C_s}{\text{erfc}\,\mu}\right) \qquad (5\text{-}16)$$

where $\mu = x/2(D_{fast}t)^{1/2}$. Using equation 5-3 and approximating θ by C_s'/kC_v', gives:

$$\theta \frac{\partial C_s}{\partial t} = C_s' - C_s/\text{erfc}\ \mu \qquad (5\text{-}17)$$

Simplifying and solving yields:

$$C = C_s'\ \text{erfc}\ \mu\ [1 - \exp(-t/(\theta\ \text{erfc}\,\mu))] \qquad (5\text{-}18)$$

for indiffusion. This is plotted in figure 5-3 (from ref. 7). As t gets large, this approaches Case I. If there is appreciable vacancy diffusion at the surface, then the expression $C = C_S\ \text{erf}(x/2(D_{slow}t)^{1/2})$ would apply near the surface, and would be superimposed on equation 5-18. Or, as Tuck suggests, there may be a region near the surface where vacancy equilibrium is achieved (due to a high dislocation density from surface damage or from the impurity atoms themselves) and Case I would apply for that region, with Case III or IV obeyed in the deeper regions.

Another case, suggested by Asbeck (82), is similar to Case I (where there is no vacancy generation - or vacancy annihilation in the case of outdiffusion), except that both vacancy and interstitial diffusion are both limiting factors. Asbeck derives an effective D of:

$$D = \left[\left(\frac{C_i}{C_s} D_i\right)^{-1} + \left(\frac{C_v}{C_s} D_v\right)^{-1}\right]^{-1} \qquad (5\text{-}19)$$

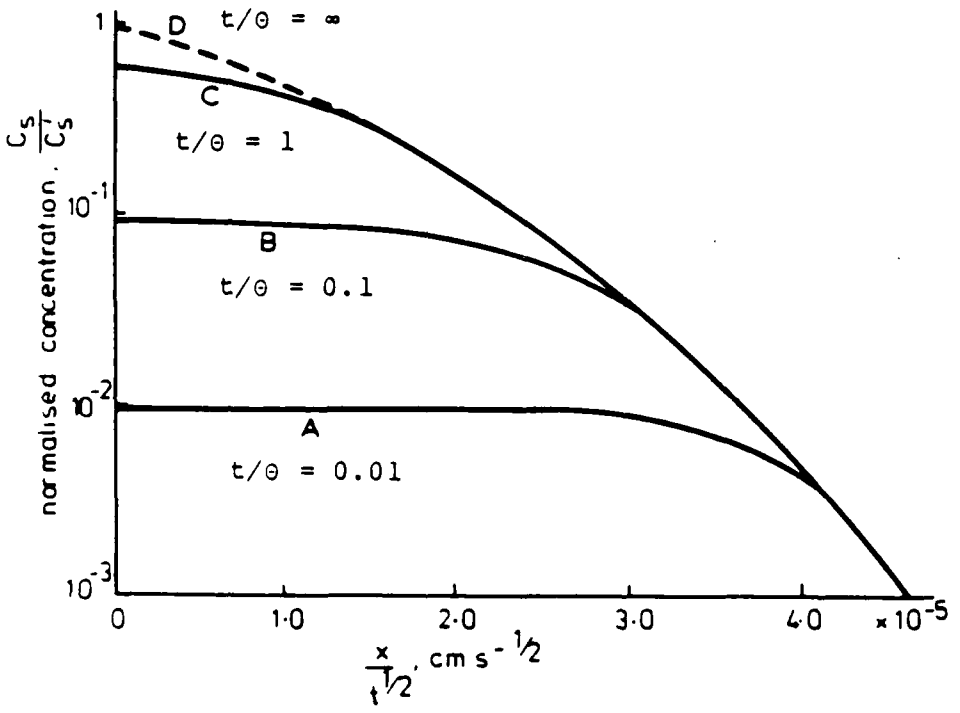

Figure 5-3. Theoretical Case IV diffusion profiles, from ref. 7.

which is smaller than D_{slow} above, and is concentration dependent.

The different cases above can all be easily applied to outdiffusion. The governing differential equation is the same in each case, but with different boundary and initial conditions. The solutions are error functions rather than complementary error functions, and a vacancy annihilation, or sink, term is used rather than a vacancy generation term.

For the four cases described by Tuck, the diffusion coefficients are concentration independent; they are proportional to equilibrium concentration values, which are constants. Implicit in these analyses is the assumption that the activity coefficient of the impurity is constant with concentration and equal to unity (Henry's Law). This is reasonable for most impurities in semiconductors, especially Cr in GaAs, since the concentrations are so low. If the activity coefficient was not constant, concentration dependant D's could result. In the next section, it will be seen how concentration dependent D's can result when the diffusing species are ionized.

5.4 Concentration and Pressure Dependences

The above treatment assumed that the diffusing species are all uncharged and, as a result, the effective diffusion coefficients were independent of concentration. However, if one or more of the species is charged, then concentration dependent diffusion can result. For the case in which the interstitial atom is a singly ionized donor and the substitutional atom is a singly ionized acceptor, for example,

equation 5-1 becomes:

$$I_i^+ + V = I_s^- + 2h^+ \qquad (5\text{-}20)$$

and the mass action law is:

$$KC_i^+ C_v = C_s^- (\gamma p)^2 \qquad (5\text{-}21)$$

where p is the hole concentration and γ is the hole activity coefficient. For high doping ($p>n_i$) and all species ionized, $C_i = C_i'$, $C_s = C_s'$, and $p = C_s$ ($\gamma=1$), which leads to:

$$K\ C_i C_v = C_s^3 \qquad (5\text{-}22)$$

and

$$K\ C_i'\ C_v' = C_s'^3 \qquad (5\text{-}23)$$

which replace equations 5-2 and 5-3. Equations 5-5 and 5-6 would remain the same. For Case I (vacancy equilibrium), this leads to

$$\frac{\partial C_s}{\partial t} = \frac{\partial}{\partial x}\left(D_{eff}\ \frac{\partial C_s}{\partial x}\right) \qquad (5\text{-}24)$$

where

$$D_{eff} = 3\ C_i' D_i C_s^2 / C_s'^3 \qquad (5\text{-}25)$$

Therefore, the diffusion coefficient is concentration dependent (due to the C_s^2 term).

It is important to note that it is possible to have charged species and <u>not</u> have concentration dependent diffusion. This would be the case if in the conversion

reaction equation, $I_i + V = I_s$, the charges on each side of the reaction exactly cancelled each other, and electrons or holes were not necessary to balance the equation. One possibility would be: $I_i + V^- = I_s^-$. Chang and Pearson (83) do suggest that in GaAs, the gallium vacancy is a singly ionized acceptor. However they may have been looking at an impurity-vacancy complex, thus making it appear that the vacancy was charged. Furthermore, when modelling Zn diffusion in GaAs, the gallium vacancy is assumed to be neutral and the theoretical profiles fit the data very well; if the vacancies were ionized, the model would not fit. In regards to substitutional chromium, there is considerable data confirming that substitutional chromium is un-ionized in undoped GaAs. Another possible reaction is: $I_i^+ + V^- = I_s$. The interstitial Zn species is assumed to be a donor (due to the d-electrons that are available), so it is reasonable to think that the interstitial Cr atom might also be. Since no electrons or holes appear in this reaction, this too would result in diffusion that is independent of concentration. One more possible reaction is: $e^- + I_i^+ + V = I_s$. Here, an electron <u>is</u> needed to balance the reaction, but concentration-independent diffusion would probably still occur. This is because the source of electrons would be the interstitials and thus the electron concentration profile would be virtually uniform and the electron concentration level would be very low, probably much less than the intrinsic carrier concentration level, and therefore would not produce concentration-dependent diffusion. Considering all this, impurity diffusion in GaAs

that fits the "uncharged" model rather than the "charged" model probably means that the substitutional species is uncharged.

Another important point is that if the impurity concentration is much below the intrinsic carrier concentration, then concentration-independent diffusion will result no matter if the species are charged or not. The reason for this is because the hole and electron concentrations are dictated by n_i and not by the substitutional impurity concentration.

The presence of charged species not only affects the diffusion by changing the relative concentrations of the different species, but also by creating an electric field. Charged species - both atomic and electronic - diffusing at different speeds, set up an internal electric field which speeds up the slower moving species (usually the atomic species) and slows down the faster moving species (usually the electrons or holes). However, in the following treatments, the electric field term will be assumed negligible (based on the results of Muller et al. (78)).

Weisberg and Blanc (84) numerically calculated the solution for Case I with charged species (from equations 5-24 and 5-25). They did this for three sub-cases, in which the charge difference between the interstitial and substitutional species is 1, 2, and 3, respectively (equation 5-25 is for the second of those three sub-cases; similar equations are easily derived for the other two). These were compared to the uncharged case. The results are shown in figure 5-4. The profiles for the charged species drop off more quickly than the

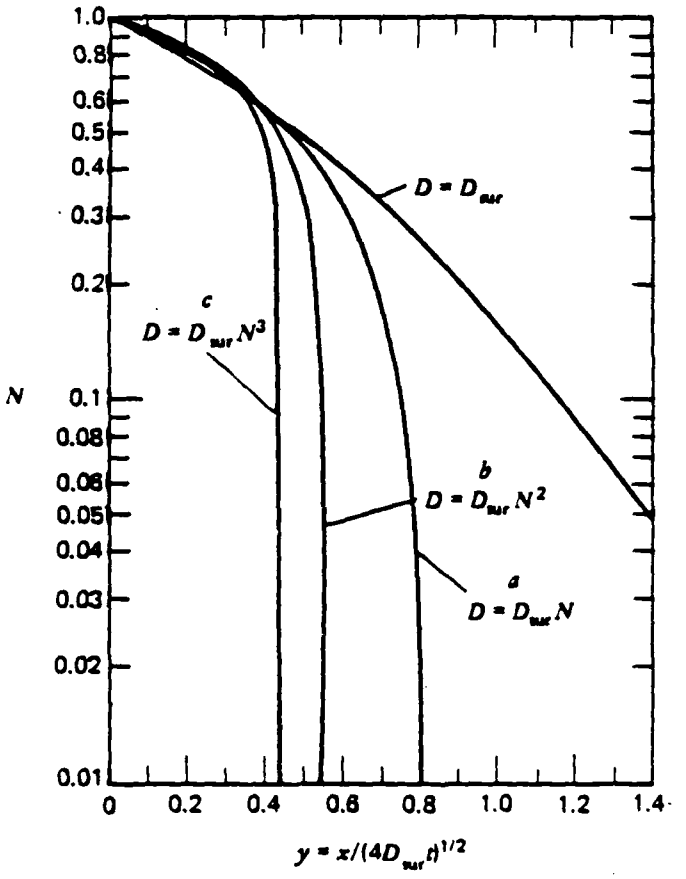

Figure 5-4. Theoretical charged-species diffusion (Case I) profiles, from ref. 84.

uncharged (error function) case due to the concentration dependence of D_{eff}. Another way to look at the effect is to consider the conversion reaction: $I_i^+ + V = I_s^- + 2h^+$. Near the surface, where the substitutional level is high, the hole concentration is high (since for doping > n_i, the source of holes is the acceptor atoms). Therefore, the equilibrium is shifted right to left (relative to low concentration). Since the effective diffusion coefficient is approximately proportional to the C_i/C_s ratio, D_{eff} is higher here. Conversely, for lower substitutional concentrations, (i.e., at the tail of the profile), the equilibrium is shifted to the right relative to high concentrations, and D_{eff} is less there. This same reasoning applies whenever the hole (or electron) concentration is changed, either locally or overall, resulting in a higher or lower D_{eff}. Case II diffusion with charged species would probably also result in concentration dependent diffusion - shifting equation 5-20 to the right or left due to a change in the electron or hole concentration - probably also changes the ratio $C_v'/(C_v' + C_s')$, and hence changes D_{slow} for different concentrations.

It has been suggested by Ghandhi (79) that a concentration-dependent diffusion coefficient might also result for uncharged species if there is a problem in achieving equilibrium between C_i, C_s, and C_v locally. It was assumed in the present work that achieving this equilibrium is no problem.

Tuck utilized Weisberg and Blanc's solutions to solve Case

IV ($k_1>0$ and large) for charged species. His theoretical results for Zn in GaAs, from (73), are shown in figure 5-5. He claims that they fit the qualitative shape of the actual profiles in the bulk.

To estabablish the dependence of the diffusion on the component vapor pressures, we first write equation 5-25 as:

$$D_{eff} = \frac{3\ D_i}{C_v'K} C_s^2 \qquad (5\text{-}26)$$

Then for the case of Cr diffusion in GaAs, in which the impurity is on a Ga site, the value of C_v' can be related to the arsenic vapor pressure by the defect reaction: GaAs + As_2 = GaAs + $2V_{Ga}$; leading to:

$$D_{eff} = \frac{3D_i\ C_s^2}{K_6 P_{As_2}^{\frac{1}{2}} K} \qquad (5\text{-}27)$$

where K_6 is the equilibrium constant between V_{Ga} and P_{As_2}. (According to Arthur (85), As_2 is the dominant arsenic species in the vapor phase on the gallium-rich side; As_4 is dominant on the arsenic side). Equation 5-27 shows the dependence of D_{eff} on the arsenic vapor pressure.

The above treatment regarding vapor pressure dependence was for the charged diffusing species case; similar treatment of the uncharged case (from equation 5-8a, rather than from 5-26), and assuming $C_i' \ll C_s'$, leads to:

$$D_{fast} = D_i/(K_6 P_{As_2}^{1/2} K) \qquad (5\text{-}28)$$

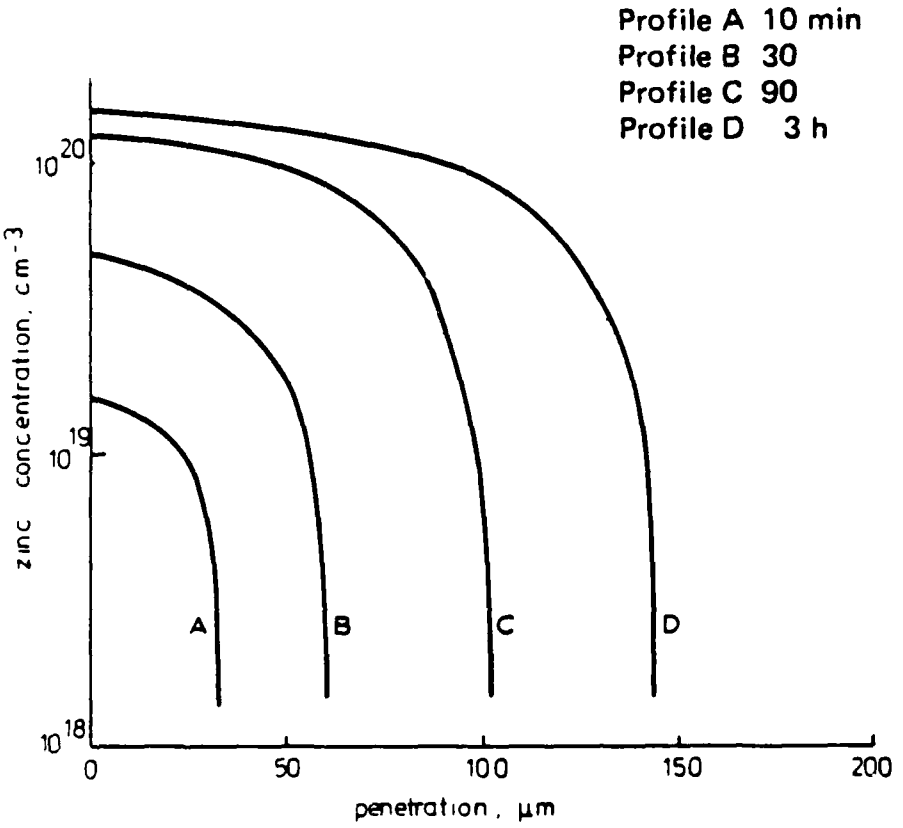

Figure 5-5. Theoretical Zn in GaAs diffusion profiles, from ref. 73.

Expressing D_{slow} as a simple function of arsenic pressure, however, is not possible.

5.5 Applying the Various Cases to Real Systems

Specific systems can now be classified according to their respective categories. For example, the diffusion of Cu in Ge, as described before, would be Case III, with the erfc diffusion (Case II, or vacancy diffusion controlled) at the surface and the uniform levels deep in the bulk building up with time. For shorter times, however, it was observed (56) that the bulk profile did drop off slightly, presumably because of insufficient time for the interstitials to diffuse all the way in prior to the initiation of interstitial-to-substitutional conversion. This is, therefore, Case IV. Van der Maesen and Brenkman's (86) profiles of Cu diffusion in Ge (as shown in Tuck (7)) clearly show this behavior. Tweet and Gallagher (57) found that the rate of increase in the bulk level depends on the number of dislocations in the crystal - the more dislocations, the faster the increase. This is consistent with the model, since k_1 would increase with increasing vacancy sources, leading to a faster rise.

The diffusion of Ag and Cu in InP would be classified the same way as Cu in Ge, and Sn, Mg, Cd, and Zn, at low concentrations, would be vacancy diffusion controlled, or Case II (77). At high concentrations, these would be classified in Cases I, III, or IV; the higher concentrations cause a higher vacancy generation rate. The diffusion of Zn in GaAs has been studied extensively, as previously mentioned. Many have assumed Case I (68, 71, 72, for example). Weisberg and Blanc's

(84) theoretical fitting of Case I (vacancy equilibrium), charged species, to the data of Cunnell and Gooch (72) for various Zn surface concentrations is very good, except for a small inflection or dip in from the surface. Tuck and Kadhim (73), who observe a more pronounced inflection in their profiles (which are for diffusions done for various times), propose that it really follows Case IV, and associate the inflection with the switch of the profile from the vacancy equilibrium region to the vacancy generation region. They show that the build-up with time is consistent with this. Shaw and Showan (69) claim that the idea of "uniform vacancy generation in the bulk" is inappropriate for Zn in GaAs since the levels are too high for normal vacancy generation. They say that diffusion-induced dislocations cause the regeneration of vacancies in the bulk. (This would explain why at a low concentration of Zn, vacancy diffusion would control Zn diffusion.) Chiaretti and Cognetti (75) claim that a certain amount of time (between 1 and 2 hours at 800°C, for example) must elapse before "vacancy equilibrium is maintained" and deep diffusion at relatively high concentrations is achieved (i.e., Case III or IV). Others (87, 88) have made similar statements.

It is clear from this discussion and from the model itself that the initial state of the host material, especially the dislocation density and the initial vacancy concentration, is very important in establishing which case is dominant and therefore the corresponding diffusion behavior. If there are many vacancy sources present, or if the initial vacancy concentration is high (which depends on the history of the

material), the diffusion might be Case I at the outset. Otherwise, it may take some time before that occurs (either Case III or IV). Luckily, however, both these cases ultimately become Case I; therefore the D_{fast} values can be measured accurately no matter what the starting conditions are, as long as enough time is allowed to reach vacancy equilibrium.

5.6 Interstitial to Substitutional Conversion

In the preceding treatment of the diffusion mechanism, the interstitial to substitutional conversion was assumed to take place via the reaction:

$$I_i + V = I_s \qquad (5\text{-}29)$$

This is commonly called the Frank-Turnbull (F-T) mechanism, or sometimes the vacancy mechanism. (This is not to be confused with substitutional dopant diffusion, which is sometimes referred to as "diffusion via vacancies" or "a vacancy model for diffusion". Because of this confusion, the above conversion mechanism will be referred to as the "F-T mechanism", which, like the conversion mechanism to be discussed below, is part of an interstitial diffuson mechanism.) It was assumed that a shortage of vacancies during the diffusion suppresses the bulk concentration levels (resulting in Case III or IV rather than Case I). However, some researchers have recently proposed that in some impurity/diffusion host systems, the interstitial atom does not wait for a vacancy to be formed, but instead creates its own space by "kicking out" a lattice atom, which then becomes an interstitial (this is actually an adaptation of the interstitialcy model of diffusion, this time applied to an

impurity in a host material). This is commonly called the "kickout mechanism." The conversion reaction in this case is:

$$I_i + L_\ell = I_s + L_i \qquad (5\text{-}30)$$

where I and L denote impurity atom and lattice atom, respectively, i denotes interstitial site, ℓ denotes lattice site, and s denotes substitutional site. (Note: a lattice site for a lattice atom is the same position as a substitutional site for an impurity atom). This has recently been applied to the case of gold in silicon by Gösele et al. (89) and Hill et al. (65). Schaake et al. (66, 90) have applied this mechanism to explain anomalous diffusion of phosphorus in silicon, and impurity gettering in mercury cadmium telluride.

For long times, high temperatures, and/or high dislocation densities, the results are exactly the same in both cases: the impurity diffuses with an effective diffusion coefficient equal to $D_i C_i'/(C_i' + C_s')$. However, for short times, low temperatures, and/or low dislocation densities, the diffusion is not limited (the bulk level is not suppressed) by vacancy diffusion or generation, but by the kickout reaction (usually considered to be insignificant) and by removing of the excess interstitial lattice atoms, either by outdiffusion, or by internal interstitial sinks (analogous to internal vacancy sources).

The governing equations of the kickout mechanism are very similar to those of the F-T mechanism. The surface vacancy indiffusion equations are replaced by interstitial lattice atom outdiffusion equations, and the bulk vacancy generation term is

replaced by a combination of the kickout reaction term, the interstitial lattice atom outdiffusion term (sometimes including a surface evaporation term), and the interstitial lattice atom annihilation term (due to sinks - perhaps dislocations). In Hill's (65) analysis of Au in Si, the bulk rise in the impurity level is explained by just the interstitial lattice atom outdiffusion (from a finite crystal so that the bulk level of excess interstitial lattice atoms decreases with time) and the surface evaporation term. In the F-T model, the bulk rise of impurity atoms cannot be reasonably explained by vacancies diffusing into a finite crystal because of the smaller number and slower diffusivity of vacancies (compared to interstitial lattice atoms). However, Hill must still use an interstitial sink to explain Au behavior in previously unannealed Si. And Gosele (89) uses the interstitial sink term in his Au in Si analysis.

Because the governing equations and reactions are so similar, both models predict similar behavior for the different conditions (i.e., high or low dislocation densities, temperatures, etc.), and it is very difficult to distinguish the two in many cases. However, some (65, 89) propose the following distinguishing differences between the two models: (1) the bulk impurity level build-up initially follows a $\sqrt{t}$ dependence (whether the bulk build-up is controlled by interstitial outdiffusion or annihilation), as opposed to a $(1 - \exp(-t/\emptyset))$ dependence for the F-T mechanism. However, as the impurity level approaches the solubility level, the kickout model also follows an exponential approach; (2) the surface

diffusion, which dominates for short times/low dislocation densities, is theoretically governed by a concentration dependent diffusion coefficient proportional to C_s^{-2} in the kickout case, as opposed to $D_{eff} = D_V C_V'/(C_V' + C_s')$, which is independent of concentration, in the F-T mechanism. The first difference, which was used to distinguish the two models in the Au in Si case, is not always easily distinguishable. An initial $\sqrt{t}$ dependence which later becomes an expontential dependence is very similar to a straight exponential, especially when the concentrations are initially low and there is some error in the experimental measuring technique. Even then, Huntley et al. (91) propose that the $\sqrt{t}$ dependence can be explained by the F-T (vacancy generation) model. The second difference has not been proven. For the cases that the kickout model has been proposed, the impurity profiles at the surface were not accurately measured, or other surface effects obscured them. Or in the case of P in Si, neither model's fit to the experimental points was good.

Another difficulty in distinguishing the two mechanisms is that virtually all phenomena explained by one model can just as easily be explained by the other. These phenomena include gettering, enhanced diffusion, and effects of changing the vapor pressure, dislocatiom density, and/or vacancy concentration. The reason for this is that an equilibrium exists between vacancies and interstitial lattice atoms (just as one exists between vacancies and interstitial impurities), with the following reaction:

$$L_i + V = L_\ell \qquad (5\text{-}31)$$

In fact, the reaction for the kickout mechanisms can be converted to the vacancy mechanism by just adding this reaction to it. An example of how either model can explain a phenomenon is as follows: increasing the initial vacancy concentration (by changing the vapor pressure, for instance) would mean that less vacancies would have to be generated in the F-T model, leading to a faster build-up of impurities. Or using the kickout model, increasing the vacancy concentration shifts reaction 5-31 to the right, resulting in fewer interstitial lattice atoms. Therefore, it is easier to remove the excess interstitial lattice atoms, allowing a faster increase in the impurity atom concentration level. Similar arguments can be made for the other phenomena.

Because of these considerations, it is very difficult to distinguish the two models in many cases. As Gosele et al. (89) point out, while some systems, such as Au in Si, can be explained better by the kickout mechanism, and some, such as Cu in Ge, by the F-T mechanism, there is a large body of experimental results which are compatible with both models and are impossible to distinguish. Furthermore, some systems might operate in one manner under some conditions and in the other manner under other conditions.

There are still some problems with the kickout model. The initial reason for proposing the kickout mechanism is the failure of the F-T model to explain such features as anomalously fast: (1) bulk vacancy generation; and 2) vacancy diffusion. (Some investigators (69) have explained these

anomalies with the proposal that high levels of impurities introduce dislocations, which in turn generate vacancies, and also enhance vacancy diffusion.) However, certain phenomena and anomalies in the kickout mechanism are just as difficult to explain. For instance, the interstitial annihilation process, which is needed to explain some phenomena, is not understood, and the equations regarding the process are not known. Also, an extremely wide range of Si interstitial diffusion coefficients are needed to model impurity diffusion in silicon (10^{-17} and 10^{-7} cm^2/sec for P and Au respectively). Also, as mentioned earlier, the fit to experimental data is not extremely good. As one can see, there are still questions regarding both models.

Finally, if one assumes that the vacancy diffuses in an interstitial manner (suggested by Schaake (92)) then the two models are really one in the same. Near the surface, vacancies diffuse in by lattice interstitials diffusing out (which are created by forming a vacancy). The bulk level is limited by vacancy generation which is caused by lattice atoms transforming to interstitial atoms and being annihilated and/or diffusing out. This is, in essence, how Zahre et al. (93) explain the anomalous diffusion behavior of S in GaAs (the same type of behavior seen with P in Si).

To emphasize how similar the two models are in regards to their governing equations and reactions, and since they are, in fact, indistinguishable in many cases, the vacancy regeneration parameter, θ, will from this point on be called the "equilibrium time constant". This parameter, with the same

values which were determined in this research, can then be used with either model, or any other, if necessary. It will be used in describing the final attainment of either vacancy equilibrium or interstitial lattice atom equilibrium, or any other phenomenon that limits the interstitial-to-substitutional conversion in an exponential manner. For instance, just "finding" the vacancies, even if there are enough or more than enough, might limit the conversion, and would probably have an exponential time dependence since the rate of finding the vacancies is probably proportional to how many are left. The equilibrium time constant parameter, and the same values for it, could be used in this case, and equations virtually identical to the ones described earlier would be used to model the diffusion process.

In conclusion, the differences between the two interstitial-to-substitutional conversion models (and perhaps even other conversion models) are extremely subtle, and in fact, may be the same anyway. The important thing is in identifying which general diffusion mechanism, for example, interstitial, substitutional, or substitutional/interstitial dissociative, is operative for a particular system and/or situation. Whether the substitutional/interstitial dissociative mechanism operates via the kickout mechanism or the F-T mechanism, or some other, is not terribly important since both predict virtually the same behavior.

5.7 D_o and E_a Values

The diffusion coefficient can be written in the form:

$D = D_o \exp(-E_a/kT)$ (94), and D_o and E_a values can be easily obtained from ln D vs. 1/T plots. There are correlations between the particular diffusion mechanism and reported D_o and E_a values, thus, these quantities may be used to identify the mechanism for a given system.

For purely interstitial diffusion in compound semiconductors, the E_a values are usually low (e.g., 0.52 eV for Cu in InAs (95)) with D_o values in the 10^{-3} $cm^2/sec.$ range (3.6×10^{-3} cm^2/sec for Cu in InAs). This results in high D values (1.3×10^{-5} cm^2/sec for Cu in InAs at 800°C). At the other extreme, pure substitutional diffusion has high E_a values (4.16 eV for Se in GaAs (96)), and fairly high D_o values (3×10^3 cm^2/sec for Se in GaAs), resulting in very low D values (1×10^{-16} cm^2/sec for Se in GaAs at 800°C). The value of E_a is high for substitutional diffusion because there are two parts: the energy for atom motion and the energy for vacancy formation, the latter depending on bond strength and therefore quite large. On the other hand, E_a for interstitial diffusion depends only on atom motion (squeezing through the other atoms), and is lower.

For atoms which are presumed to diffuse by the substitutional/interstitial dissociative process, the D values usually lie between those of purely substitutional diffusers and purely interstitial diffusers and most have E_a values in the 0.5 to 2.0 eV range. The D_o values are lower than the interstitial diffusers (in the 10^{-4} to 10^{-7} $cm^2/sec.$ range) resulting in D values usually less than interstitial, but higher than substitutional diffusers. The D values are

usually in the 10^{-14} to 10^{-9} cm^2/sec range for 800°C. Therefore, a net D value in that range with a relatively low E_a value is a good indication of the substitutional/interstitial dissociative diffusion mechanism operating.

Further analysis shows that there is also a correlation between the E_a and D_o values and the particular case of the substitutional/interstititial dissociative diffusion mechanism. For vacancy diffusion controled impurity diffusion (Case II), the E_a values are relatively higher (≈ 1 to 2 eV), with corresponding D_o values giving net D values at the lower end of the sub./int. D range. On the other hand, in those case controlled by vacancy generation and interstitial diffusion (Cases I, III, and IV), the E_a values are usually less than 1 eV and with corresponding D_o values that give net D values at the higher end of the range.

Of course, all of this is reasonable when one looks at the equations for the effective diffusion coefficients. $D_{fast} = D_i C_i'(C_i' + C_s')$; therefore, the activation energy should be close to the activation energy for interstitial diffusion, modified slightly by the temperature dependences of the equilibrium concentrations of the interstitials and substitutionals. The D_o value would be less because $C_i'/(C_i' + C_s')$ is usually much less than unity. Similarly, the E_a value for D_{slow} (which equals $D_v C_v'/(C_v' + C_s')$) would be close to the vacancy diffusion value, which according to (83) is 2.1 eV for V_{Ga} in GaAs.

An example of this second correlation is the case of Cu in InSb. For substitutional/interstitial diffusion believed to be

vacancy diffusion controlled, Stocker (97) reported D_o and E_a values of 9 x $10^{-4}cm^2$/sec. and 1.08 eV respectively, leading to a D value of 5 x 10^{-11} cm^2/sec. at 480°C. In addition, Stocker, and also Boltaks and Sokolov (98), observed deeper diffusion branches, with D_o and E_a values of 3 x 10^{-5} cm^2/sec. and 0.37 eV respectively, resulting in a D value of 1 x 10^{-7} cm^2/sec. at 480°C. This was attributed to the interstitial diffusion controlled case.

5.8 Summary

This chapter reviewed the substitutional/interstitial dissociative diffusion mechanism, which is being used with increasing frequency to describe impurity diffusion in semiconductors. The governing reactions and equations, for different rate limiting cases depending on which features of the process dominate, have been given. In this treatment of the model, the Frank-Turnbull, or "vacancy", model for the interstitial-to-substitutional conversion has been assumed. Specific systems which are presumed to follow the substitutional/interstitial model have been considered to establish which of the different rate limiting cases they fit. A new mechanism for the conversion process, the so-called "kickout" mechanism, has been discussed. It has been found that in some cases, this model fits the data better, and in other cases, the Frank-Turnbull model fits the data better; however, in most cases, the two are indistinguishable. It was shown how D_o and E_a values for the effective diffusion coefficients could be used to establish if the substitutional/interstitial diffusion mechanism is operative

for a specific system and if so, establish which is the rate limiting case.

6. CHROMIUM DIFFUSION IN GALLIUM ARSENIDE

6.1 Introduction

Using the same principles concerning ternary phase equilibria that were used in the solubility studies, well-defined chromium diffusion experiments were performed; this chapter reports on those studies. First, a literature review of previous and current work on chromium redistribution in gallium arsenide is presented, emphasizing the following major points: 1) there have been several recent studies on this subject; however, these studies were made without knowledge of, and usually without concern for, phase equilibria; and 2) apparently, there is a complex diffusion mechanism, more complicated than simple interstitial or substitutional diffusion, or even a simple combination of the two. Next, the approach for this work concerning Cr diffusion is outlined and discussed, followed by the experimental procedures. The results are then given, which are shown to fit the substitutional/interstitial dissociative diffusion mechanism, and values for key parameters pertaining to that model are given. In addition it is shown how the defect chemistry (especially concerning vacancies and impurities) of gallium arsenide can be studied using chromium as a "probe". Finally, in this chaper and the next (which deals with several surface phenomena), some of the results of others are explained in terms of the results of this work.

6.2 Literature Review of Chromium Redistribution

In 1972, Khludkov (99) studied the diffusion of several transition elements in n-type GaAs, including chromium, by

depositing each element on a GaAs surface and annealing the sample under an arsenic over-pressure. He calculated the diffusion coefficients by measuring the junction depths (by the stain-etching method) and assuming an error function diffusion profile. For Cr at 900°C, he reported a D of 3×10^{-12} cm^2/sec. However, his results may be in doubt since the Cr concentrations he reports - derived from the junction depths - are much higher than the maximum Cr solubility ((27) and from the present work), in addition to the fact that elemental Cr is not a proper diffusion choice since Cr and GaAs are not in equilibrium with each other.

Sato (34) in 1973 first speculated that surface conversion in n-type GaAs arose from chromium diffusion out of the GaAs (where the chromium presumably compensated the n-type impurities) and into the SiO_2 cap (which is used in GaAs processing to prevent arsenic vaporization during high temperature anneals). Sato calculated a diffusion coefficient at 850°C from an experiment virtually identical to that of Khludkov, with a reported D value of 1.5×10^{-11} cm^2/sec. However, the Cr concentrations were again much higher than the maximum solubility level, and elemental Cr was used as the source. Sato also studied the diffusion of Cr from Cr-doped GaAs into the oxide layer. He calculated diffusion coefficients by performing electrical measurements and fitting a composite medium diffusion solution to the results, again assuming a simple error function profile and that Cr acts as a singly ionized acceptor. The resulting D values were in the 10^{-14} to 10^{-12} range for T = 700°C to 800°C, with an

activation energy of 3.6 eV.

Little work was done on this subject until 1977 when several researchers (100, 101) reported problems with GaAs devices that they attributed to a depletion of chromium near the surface after heat treatments. Deveaud (48), that same year, observed "abnormal" Cr diffusion toward the surface - depletion near the surface and buildup right at the surface - after it was implanted in GaAs and annealed. In 1978, Partin (102) estimated diffusion coefficients from hole lifetime measurements that were two to three orders of magnitude higher than the values previously reported for the same temperatures. This was the first indication that a deep diffusion process might be occurring.

From 1979 to the present, much work has been done studying the "unusual" behavior of chromium in gallium arsenide. Many have reported on Cr gettering to, or building up at, regions of lattice damage or stress, either regions damaged by ion implantation, the damaged and/or stress surface region, or just the free surface (5, 39, 40, 42, 103-120). Many also report on the depletion of chromium near the surface, which may be a result of the gettering to the surface, or simple outdiffusion (and vaporization), or both (41, 42, 50, 78, 105, 107-112, 118, 121, 122). However, there is disagreement regarding the nature and exact cause or causes of the redistribution, which will now be discussed.

The most often reported type of concentration profile of Cr following an anneal of Cr-doped GaAs, is one with a surface

build-up of Cr, as high as three orders of magnitude above the bulk level, over the first few tenths of microns from the surface of the GaAs, and then a Cr depletion over the next two or three microns. (In most of these cases, the Cr profile was obtained using SIMS.) Favennec et al. (105), for example, show a clear example of this behavior. Many investigators believe this is due to gettering of chromium to the encapsulent, which is usually SiO_2 or Si_3N_4 (40-42, 103, 105, 112, 123). Huber et al. (42) and Evans et al. (103) proposed that the Cr preferentially segregates to the strained mismatched region near the cap/GaAs-crystal interface, implying a lowering of the Cr activity there. This is consistent with the observation of Magee, et. al. (123-125) that Cr is preferentially segregated to regions of high dislocation density that could arise from residual stress. However, Magee (125) suggests that the actual gettering may be due to stress-induced diffusion (a field effect). The "cap-gettering" theory, for whatever reason, is supported by the results of Kasahara et al. (112), Feng et al. (41), and Eu et al. (40), who report that when caps are not used, but with an AsH_3/H_2 flow in the ambient to prevent loss of As, the build-up is reduced. In fact, Kasahara (112) reported that the build-up was completely eliminated. Eu (40) suggested that the Cr build-up and depletion associated with the use of caps may occur because the bulk chromium levels are above the solubility limit, and Cr precipitates nucleate at the surface dislocations. He proposed an alternate explanation, that the redistribution may be due to arsenic diffusing through the caps, leaving a Ga-rich phase which getters Cr.

Udagawa (108), who observed a high Cr surface build-up at high temperatures when a cap was not used, suggested that the Cr diffuses into the Ga pools or droplets, which form when the GaAs is annealed (at T > 800°C in a hydrogen atmosphere in his case) and "which have a high Cr solubility." At T < 800°C, no Ga droplets are observed, and no build-up is reported.

Vasudev et al. (109) proposed that the chromium was not gettered to the encapsulent; the build-up was worse when a cap was not used. They proposed that the build-up and depletion is controlled by a balance between the surface solubility limit (a fixed quantity) and the original Cr density in the substrate. Tuck et al. (120) reported even stranger behavior after annealing Cr-doped GaAs in an evacuated closed quartz ampoule (with and without elemental arsenic in the ampoule); they observed a large chromium build-up in the first 40 microns from the surface, and a depletion throughout the rest of the water. They attributed this to a sudden shift in the vacancy/chromium equilibrium after an initial vacancy undersaturation.

Several workers have attemped to model the diffusion behavior. Most have assumed simple error function diffusion profiles, with or without surface evaporation terms, and fit these to measured profiles after annealing uniformly Cr-doped GaAs, or Cr implanted GaAs, or Cr-doped/undoped GaAs junctions (39, 41, 50, 82, 105, 108, 110, 112, 122, 126). Most of the reported D values - determined from the fitting - are in the 10^{-13} to 10^{-10} cm^2/sec range from 700 to 1000°C. Both Udagawa et al. (108) and Kasahara et al. (112) find that while the diffusion coefficient was constant with time for short

annealing times (0 to 45 minutes @ 900°C, for example), it became much larger at longer times.

Just recently, Morkoc et al. (37) and Palmateer et al. (127), who studied Cr redistribution during MBE GaAs growth and processing, claimed that the fast redistribution of Cr observed in their work cannot be explained by a normal diffusion model, and that interstitial Cr and/or Cr segregation may be the driving force.

Several have also studied the effects of changing the arsenic overpressure in the chromium diffusion (5, 40, 108, 112, 122). Kasahara et al. (112) and Udagawa et al. (108) reported that increasing the arsenic pressure apparently increased the Cr diffusion; more Cr depletion was observed after outdiffusion when the P_{As_2} was increased. But Kasahara (112) and Asbeck (82) both suggest that it is the surface concentration that is changing, and not the diffusion coefficient. (If one fits erf diffusion profiles to Kasahara's results, but with a constant D and a varying surface concentration, one sees that they fit virtually perfectly.)

Tuck et al. (5, 120) have been the only ones to study the indiffusion of Cr into GaAs since Khludkov (99) and Sato (34). They did this by annealing GaAs and a piece of radioactive Cr^{51} in an evacuated closed quartz ampoule. (They estimated that the GaAs initially contained $\sim 10^{16}$ cm^{-3} Cr^{52}, perhaps even more.) Using an etch and count method, they obtained Cr profiles for various temperatures and times. The profiles were much like Case III and Case IV diffusion as discussed in chapter 5, and in their articles they suggested

that the substitutional/interstitial dissociative diffusion mechanism was operative. In addition they found that increasing the arsenic pressure, by adding elemental arsenic, decreased the amount of Cr that diffused in.

The fact that for short annealing times and low temperatures (<1000°C) - the conditions at which most of the other workers did their experiments - this complex mechanism reduces to a simple error function diffusion process (Case II) explains why the others got relatively good fits to their results in assuming the simple profile. It also explains why for longer times, the simple model no longer could explain the results.

Others have recently used this model, or models similar to it, in analyzing their results. One example is Asbeck's (128) analysis of outdiffusion as discussed in section 5.3 of chapter 5). Muller et al. (78) assumed a two species diffusion model for Cr when they theoretically predicted the redistribution of Cr and other dopants during LPE growth, in which induced electric field effects were considered. They found that at the impurity levels considered, the electric field had virtually no effect on Cr movement.

In an attempt to explain the results of Tuck's indiffusion experiments and Kasahara's outdiffusion experiments, especially the apparently contradictory results when arsenic pressure is increased (the Cr diffusion apparently increased in one case and decreased in the other), Muller (129) proposed a model similar to the substitutional/interstitial dissociative model, except assuming that the substitutional

chromium species is sometimes complexed with a "D_{As}" species, a residual donor due to an arsenic atom on some unusual site; it is this complexing which supposedly renders the GaAs semi-insulating. According to Muller, the Cr is not complexed in the conditions of Tuck's experiments (indiffusions into GaAs), but is in the conditions of Kasahara's experiments (outdiffusions from semi-insulating Cr-doped GaAs); this difference leads to the different behavior of Cr.

It should be pointed out that Tuck et al. (5, 120) concluded that before their results could be interpreted, the Ga-As-Cr ternary phase diagram must be known. The fact that they found that the Cr source picked up large amounts of Ga and As during the course of the diffusion, and also that Cr concentrations, upon addition of arsenic to the ampoule, decreased instead of the expected increase that would be predicted based on a Cr-on-Ga-site model, suggested to them that perhaps the Cr was reacting with Ga and As and forming a new phase. The need for the Ga-As-Cr phase diagram to study Cr in GaAs is clear.

In summary, much work has been done studying the redistribution and/or diffusion of Cr in GaAs. Many have calculated diffusion coefficients (almost all for short times and low temperatures) based on a simple error function model; yet these cannot explain the deep penetration of chromium seen in some cases. The anomalous Cr build-up at the GaAs surface has been studied, and a few reasons for this have been suggested, including gettering to a damaged or stressed region, or to a Ga-rich region. No one, except for Tuck et al., has

been concerned with ternary phase equilbria considerations. Most experiments were done in open furnace tubes, and hence were not even closed systems. And Tuck's experiments, even though the importance of phase equilibria was known, were done and analyzed without the actual knowledge of it. Finally, a complex diffusion mechanism was suggested for Cr in GaAs, but no detailed quantitative study had been done.

6.3 Introduction to Diffusion Studies

The purpose of this study of Cr diffusion in GaAs was to perform diffusion experiments under well-defined conditions and to fit the results to a diffusion mechanism model. Three types of diffusion experiments were done: 1) Cr indiffusions in evacuated quartz ampoules, with the selection of Cr sources based on the phase equilibria as discussed in chapter 3; 2) Cr outdiffusions, by annealing Cr-doped GaAs in quartz ampoules, with and without well-defined Cr sinks; and 3) Cr "junction" diffusions, which will now be discussed. Because the substitutional/interstitial dissociative diffusion mechanism was strongly suspected - based on Tuck's results (5, 120) as well as the initial results of the present work - a slow, and high concentration, diffusion was expected in the surface region for indiffusion (vacancy diffusion controlled). Likewise, a slow diffusion case was expected at the surface for outdiffusion. However, because of the problems in the GaAs surface region (anomalous Cr build-up and depletion, to be discussed in chapter 7), these diffusion features were obscured. Therefore interdiffusion, or "junction diffusion," experiments were performed in which the diffusion of Cr could

be studied without the surface phenomena interfering. This was done by annealing samples of undoped GaAs LPE layers on Cr-doped GaAs substrates. The "junction sample" (so-called because of the sharp junction with respect to the Cr concentration between the substrate and the epilayer) is ideal for Boltzmann-Matano type diffusion experiments and analysis, and both outdiffusion (out of the substrate) and indiffusion (into the epilayer) are studied, all in one sample. And all this occurs away from the GaAs free surface. These samples were annealed just like the outdiffusion samples, with or without well-defined Cr sources or sinks.

Considerations of ternary phase equilibria are relevant to diffusion studies for the following reasons: 1) only phases which are in equilibrium (or "quasi-equilibrium, as previously discussed) with GaAs should be used as Cr sources or sinks; 2) the Cr solubility (the ultimate level of Cr in the GaAs at the end of a diffusion, and the level of Cr at or near the surface for all times for both indiffusions and outdiffusions) depends on the location of the overall system composition on the ternary phase diagram, which depends on the amounts of the source and sink, and their compositions; and 3) the other intensive variables, such as C_i', C_s', and D_{Cr}, also depend on the location in the phase diagram. However, it will be shown that the values of the diffusion coefficients (both D_{fast} and D_{slow}) were found not to vary (within experimental error) over the range of composition studied. This will be discussed later.

6.4 Experimental Techniques

The techniques and procedures used for the diffusion sutdies were the same as those used in the solubility studies and discussed in chapter 4, i.e., annealing in evacuated, closed quartz ampoules with pre-annealed source material, and profiling the Cr level with SIMS.

The undoped GaAs was obtained from Cominco (LEC, high resistivity), Hewlett-Packard (LEC, high resistivity), and Crystal Specialties (Bridgman, low resistivity). The Cr-doped GaAs was obtained from Crystal Specialties, the Te-doped from Hewlett-Packard and the Si-doped from Hewlett-Packard and Morgan Semiconductor.

The LPE "junction" samples were obtained from James S.C. Chang at Stanford University (see his Ph.D. Thesis (130) for details concerning the growth of these - some discussion of the growth is given in the next chapter).

All samples, including the junction samples, were cleaned prior to each anneal according to the schedule given in chapter 4. Also, each was cleaned with HCl and methanol prior to SIMS analysis to clean away any loose particles or precipitates, except when specifically studying the precipitates.

6.5 Chromium Diffusion Experiments

6.5.1 Introduction

In this section, the results of the the three types of diffusion experiments - indiffusion, outdiffusion and junction diffusion - are reported and discussed. In addition, the implications of the results are discussed, including how the

reports of other investigators can be explained in terms of these results.

6.5.2 Indiffusion Experiments

A series of indiffusion experiments were performed for a variety of times and temperatures, using H source and Cominco undoped GaAs. The temperatures were from 750 to 1000°C at 50 degree intervals, and the times ranged from 1/2 to 12 hours for the lower temperatures and 1/4 to 2 hours for the higher temperatures. The SIMS Cr profiles for the 800°C series, shown in figure 6-1, are the results of sputtering to a relatively shallow depth to show more detail of the surface region. In figure 6-2, several of the profiles of the 800°C samples are shown again, this time profiled to a much greater depth, and figures 6-3 and 6-4 show the deep Cr profiles of the 850 and 900°C indiffusions.

As seen in the shallow profiles of the 800°C series (figure 6-1), the Cr concentration in the bulk is virtually level, and rises uniformly with time. As discussed earlier, this suggests that the substitutional/interstitial dissociative diffusion mechanism is operative. As seen in the deep profiles (figures 6-2, 6-3, and 6-4), the "bulk" Cr levels rise with time, as in figure 6-1, but here one can see that the Cr levels tail off deep in the interior of the GaAs. This strongly resembles Case IV of the diffusion mechanism, as outlined in chapter 5. One sees that the bulk rise (to the final solubility level) is faster as the temperature increases. Also, the chromium penetration is much deeper than one would calculate using the diffusion coefficients reported in most of

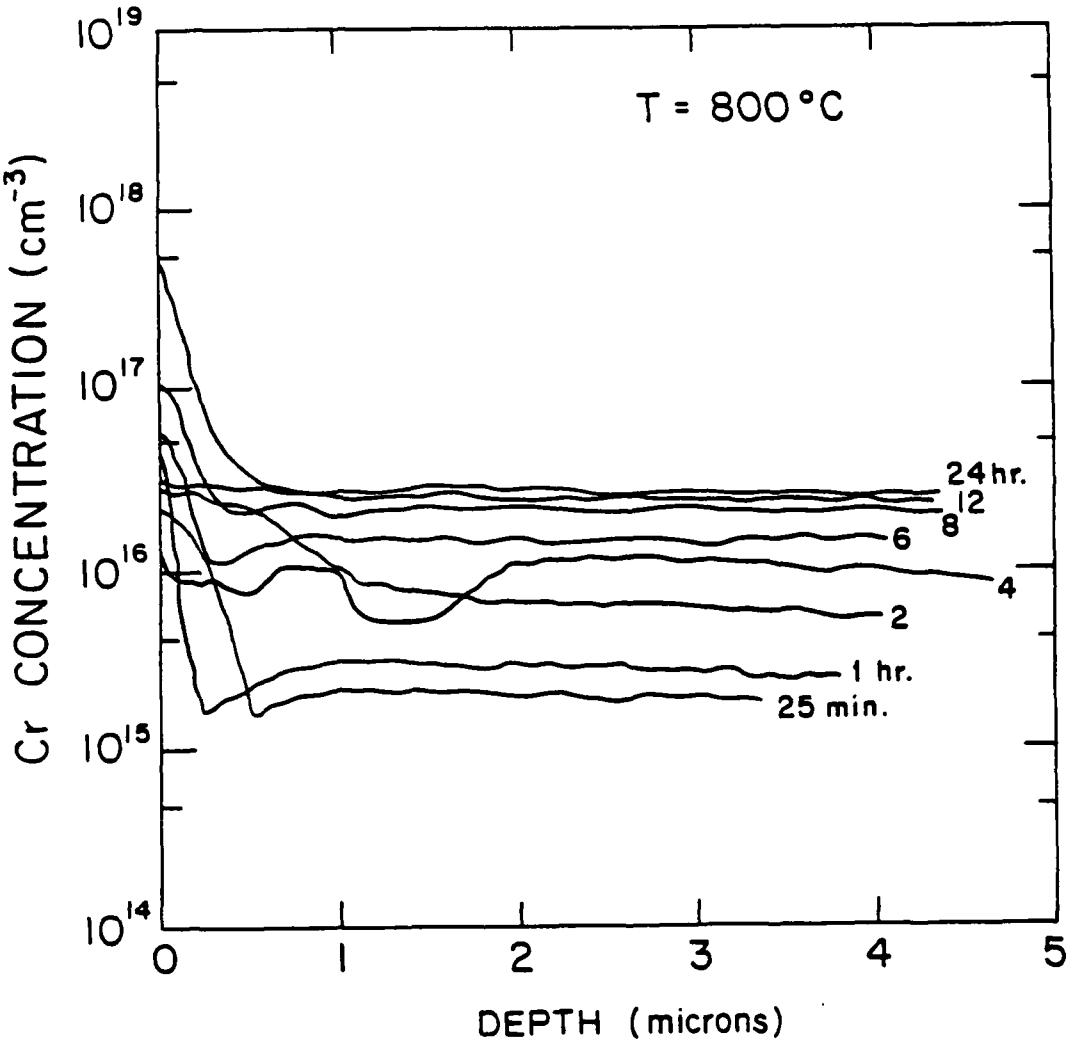

Figure 6-1. Cr concentration profiles from 800°C indiffusion experiments - H source.

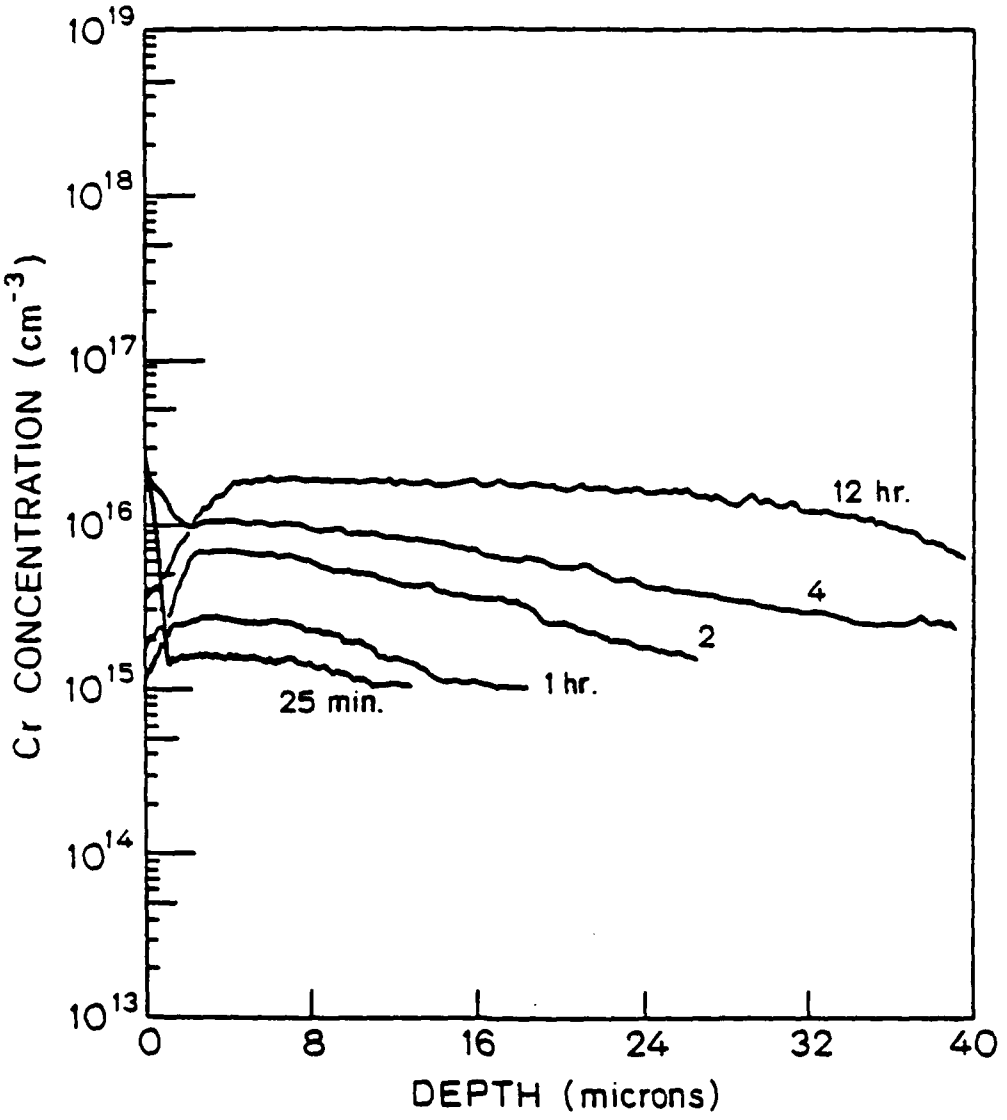

Figure 6-2. Same as figure 6-1, except profiled deeper.

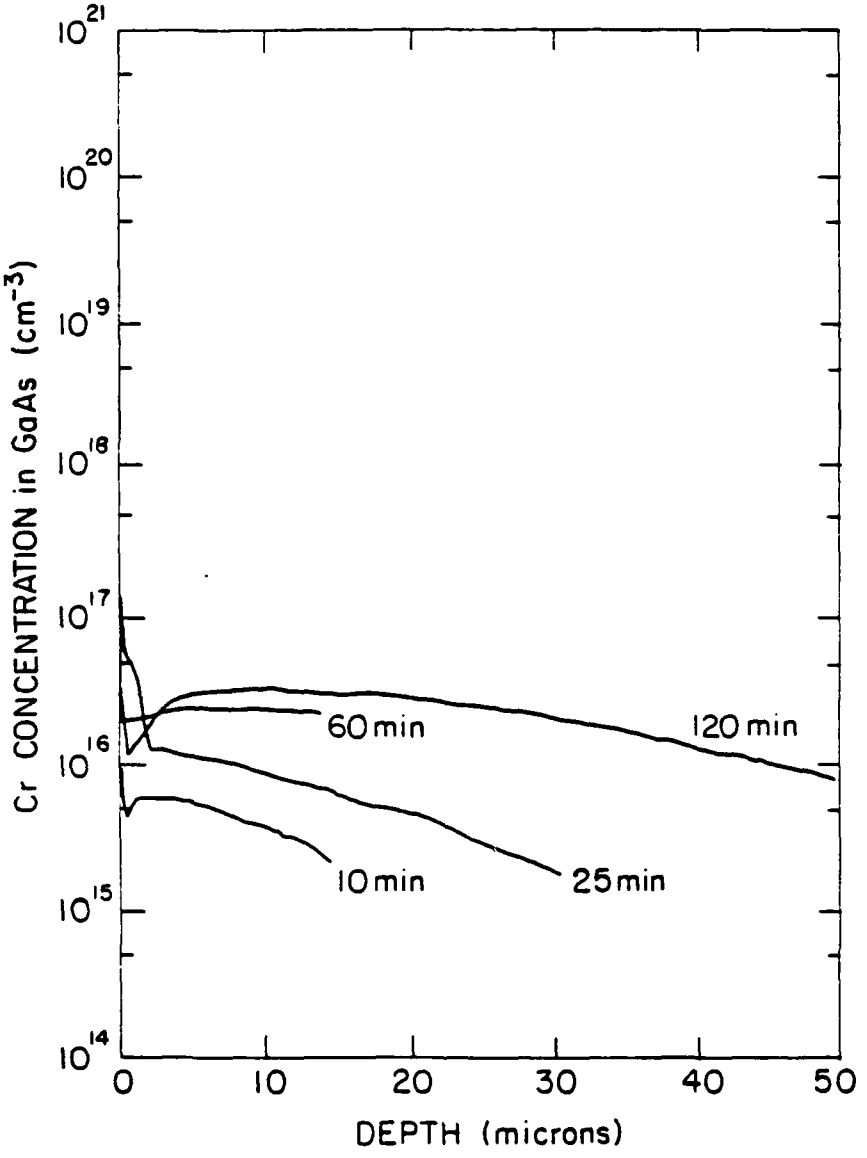

Figure 6-3. Cr concentration profiles from 850°C indiffusion experiments - H source.

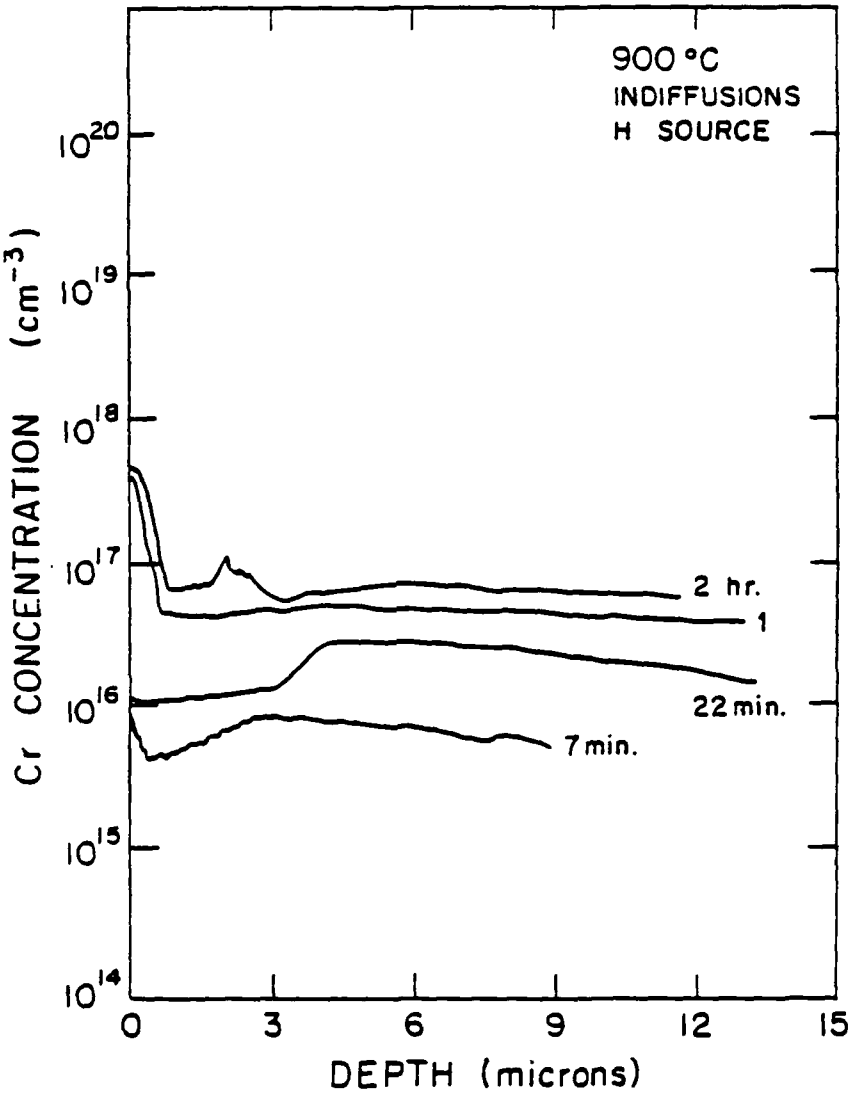

Figure 6-4. Cr concentration profiles from 900°C indiffusion experiments - H source.

the previous work (e.g., $D = 1 \times 10^{-11}$ $cm^2/sec.$ at 900°C according to (112)).

In most of the indiffusion profiles, anomalous features are seen in the surface region (0-4 μms from the surface), as discussed earlier; in particular, a large and erratic build-up of Cr right at the surface and a region in which the Cr level is <u>less</u> than the bulk level just to the right of it in the profiles. These features, which will be examined as to their causes in chapter 7, obscure what is going on at the surface; however, they do not seem to affect what is happening in the bulk. (From this point on, the "bulk" shall be the region that is inside the surface build-up and depletion region.)

Using the equation for Case IV diffusion, uncharged species (equation 5-18) and the C_s' values from the solubility results, the profiles were fit with theoretical curves. For each temperature, D_{fast} and Θ were adjusted to fit the profiles, D_{fast} being the diffusion coefficient that is proportional to the interstitial diffusivity, and Θ being the vacancy generation parameter, or in general, the equilibrium time constant which describes the bulk rise to the vacancy equilibrium case. The values for these two parameters for each temperature were used for all the different profiles, i.e., for the different times. The theoretical curves, plotted on the experimental profiles for those same three temperatures in figures 6-5 to 6-7, show a good fit to the bulk profiles. The D_{fast} values for these and the other temperatures are tabulated in table 6-1 and are plotted in figure 6-8 (the top curve in the figure), showing nice

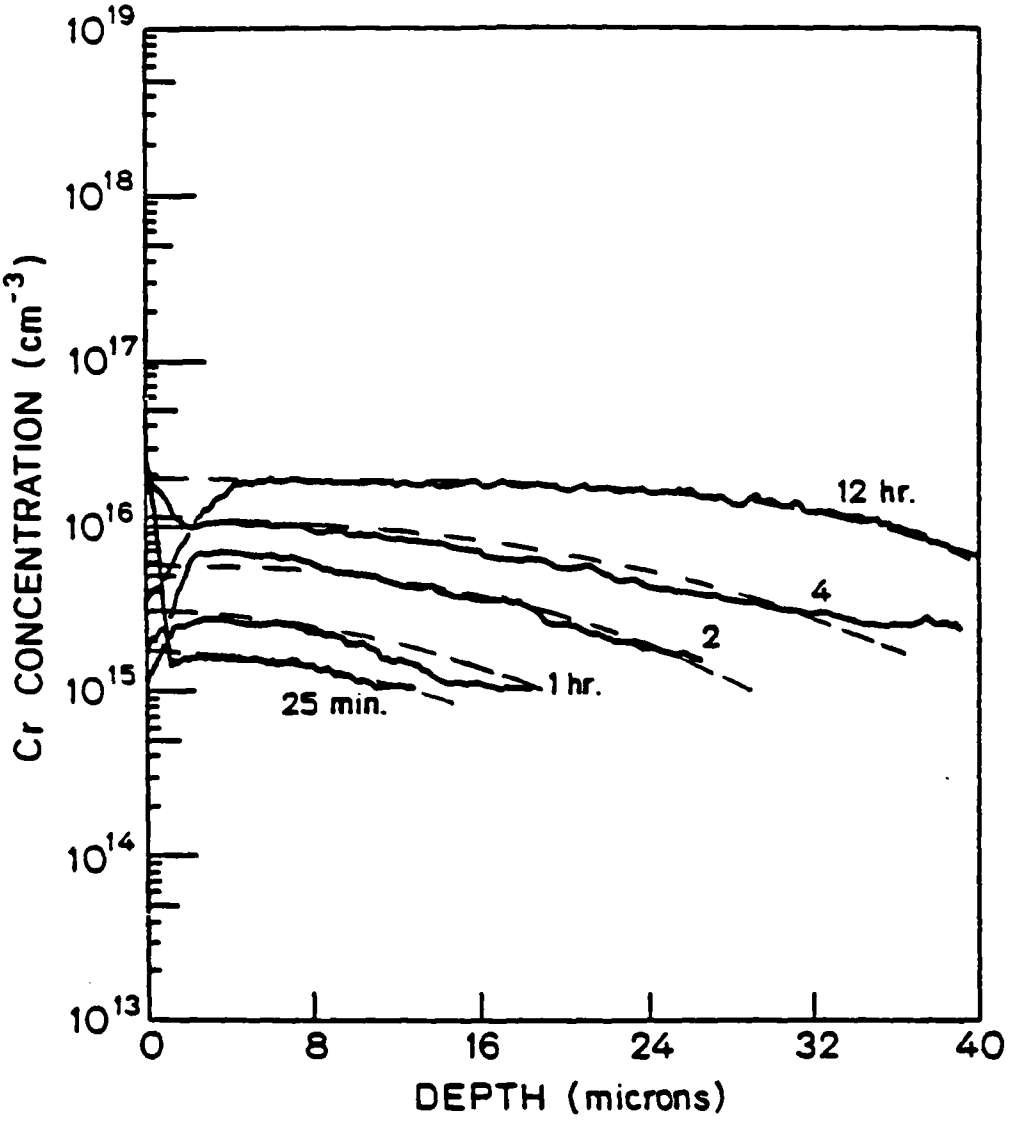

Figure 6-5. 800°C Cr profiles with theoretical profiles (dotted); $D = 2.8 \times 10^{-10}$ cm^2/sec, $\theta = 32,800$ sec.

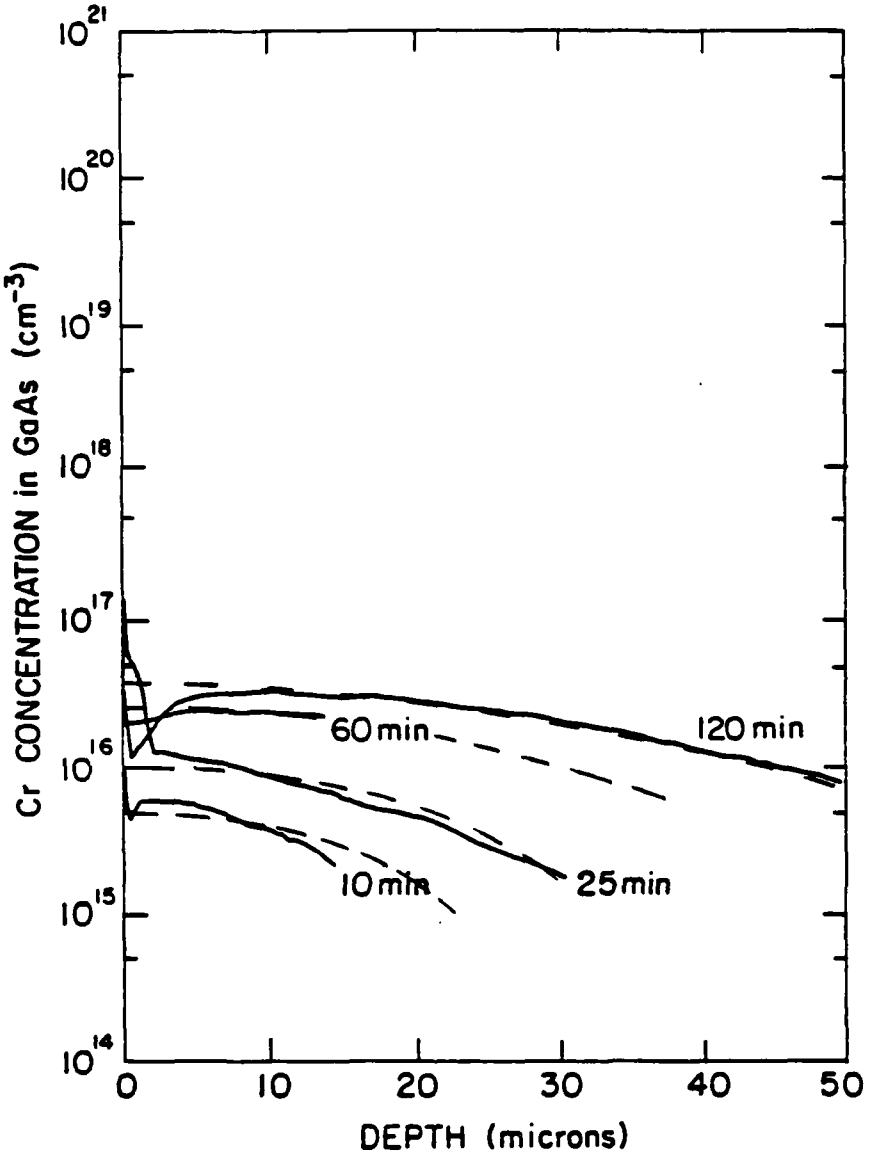

Figure 6-6. 850°C Cr profiles with theoretical profiles (dotted); $D = 4.0 \times 10^{-10}$ cm^2/sec, θ = 6,600 sec.

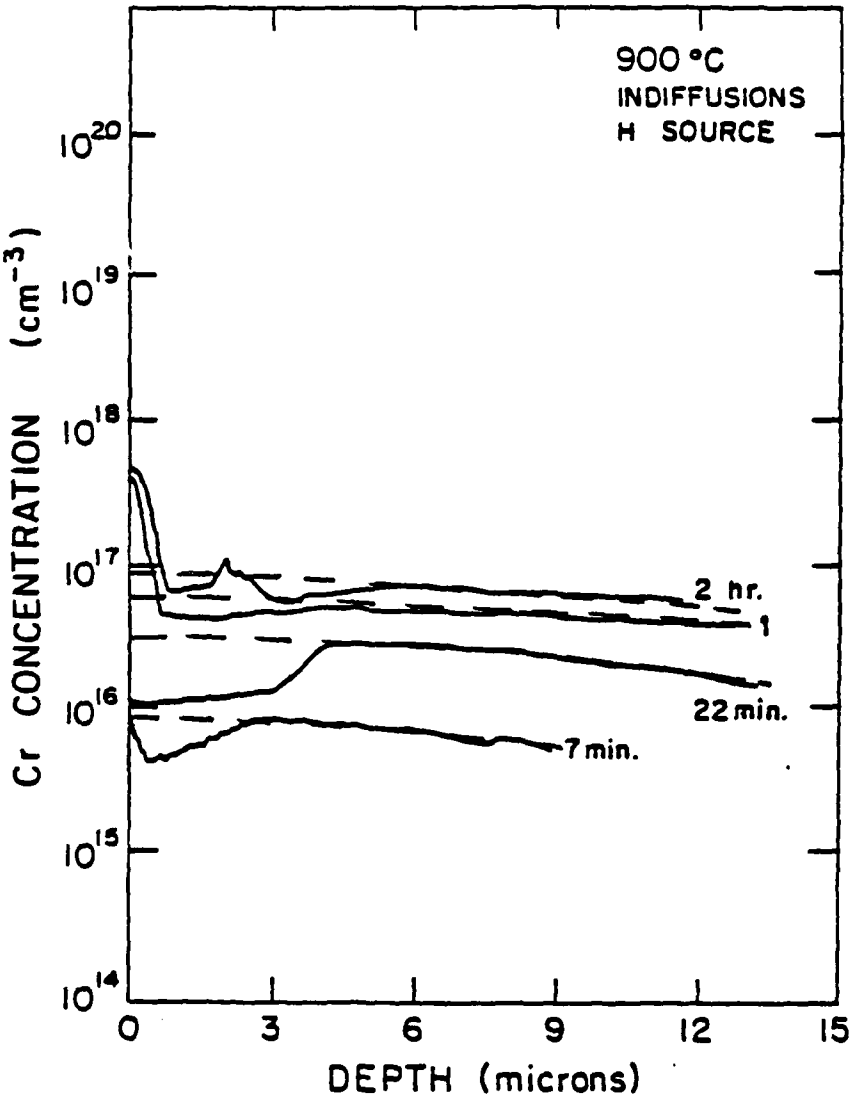

Figure 6-7. 900°C Cr profiles with theoretical profiles (dotted); $D = 5.7 \times 10^{-10}$ cm^2/sec, $\theta = 3{,}000$ sec.

Table 6-1 Chromium indiffusion results (LEC GaAs, H source).

Temp	D_{fast}	Θ
750°C	1.5×10^{-10} cm^2/sec	1.3×10^5 sec
800	2.8×10^{-10}	3.2×10^4
850	4.0×10^{-10}	6.6×10^3
900	5.7×10^{-10}	3.0×10^3
950	7.0×10^{-10}	-
1000	9.1×10^{-10}	-

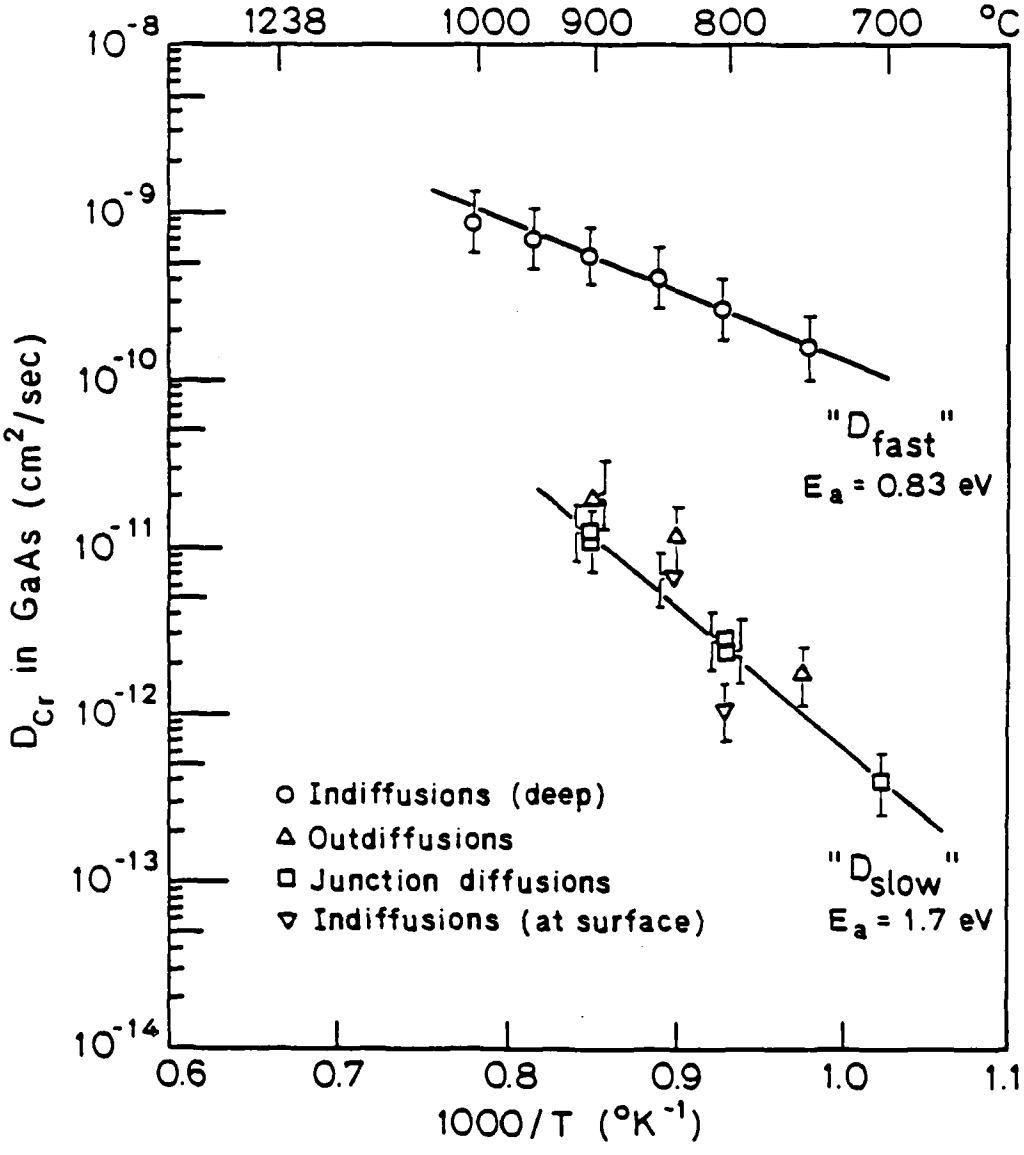

Figure 6-8. D_{fast} and D_{slow} vs. 1/T for Cr in GaAs.

Arrhenius behavior. From this, an activation energy was determined to be 0.83 (± .07) eV and a D_o value of 2.04 x 10^{-6} cm^2/sec. The Θ values are also tabulated in table 6-1 and are plotted in figure 6-9 (the circled points). Again, Arrhenius behavior is observed. In addition, C_o, the extrapolated surface concentration, was plotted vs. time in figure 6-10, along with theoretical C_s' $(1-\exp(-t/\theta))$ curves, which show a good fit. This exponential dependency rather than a $\sqrt{t}$ one is good evidence that the vacancy conversion mechanism is operating rather than the kickout mechanism, as discussed in section 5.6 of chapter 5. (However, the kickout mechanism cannot be ruled out solely by this evidence because it also predicts an exponential time dependency as the concentration approaches the solubility level; however,it is unclear when this transition from $\sqrt{t}$ to exponential behavior occurs.)

As discussed earlier, the models for charged species give much different results than for uncharged species; in this case the uncharged model clearly fits best; the profiles for the charged case would fall off abruptly at about $C = 0.5\ C_o$, as opposed to the gradual, error function-type drop in concentration as the depth increases. This is consistent with substitutional Cr being uncharged in undoped (semi-insulating) GaAs, as discussed in chapter 4.

As mentioned in chapter 5, one must consider the intrinsic carrier concentration, because if it is much higher than the impurity concentration (at the diffusion temperature), then the diffusion process will not be concentration dependent even for charged species. In GaAs, $n_i = 4 \times 10^{16}\ cm^{-3}$ at 750°C,

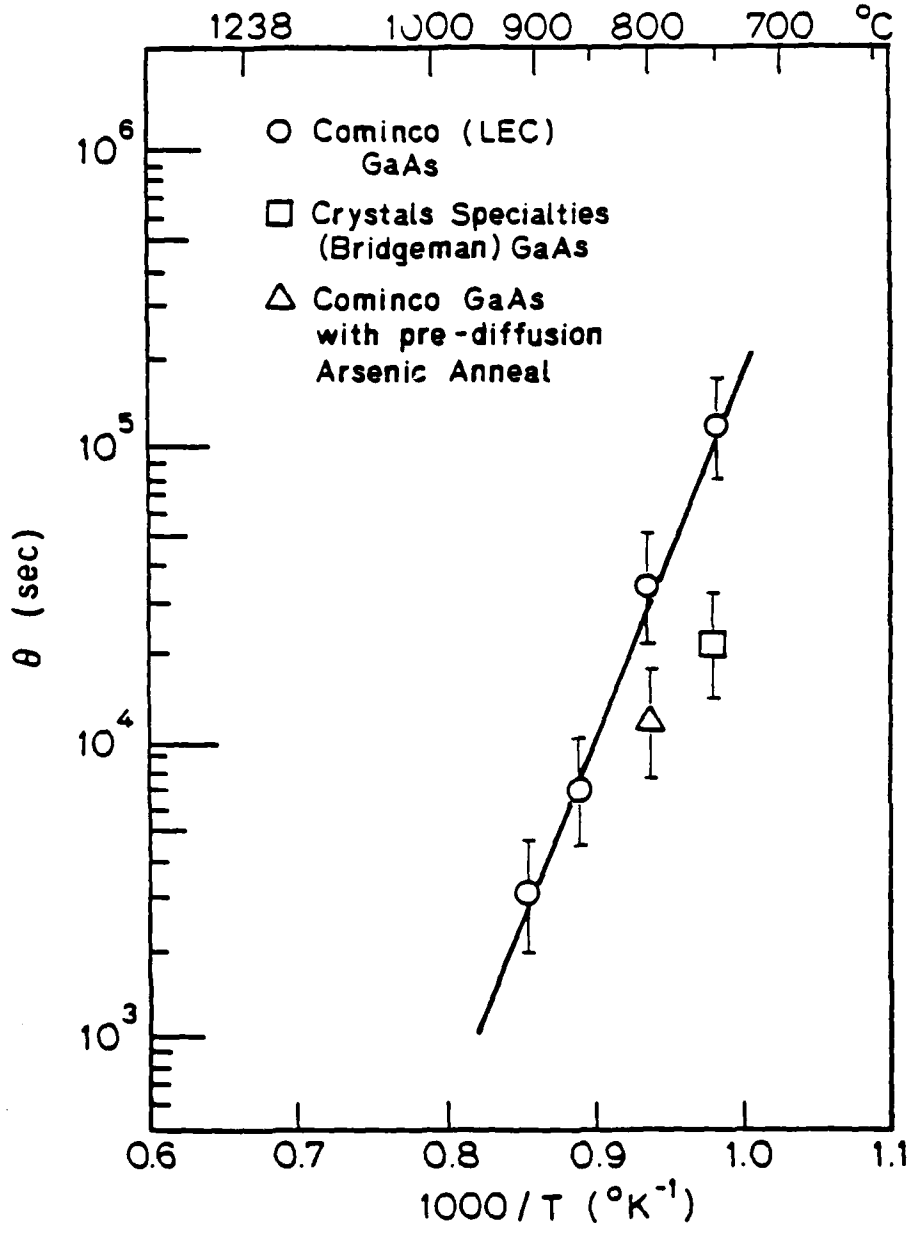

Figure 6-9. Equilibrium time constant, θ, vs. 1/T for Cr in GaAs.

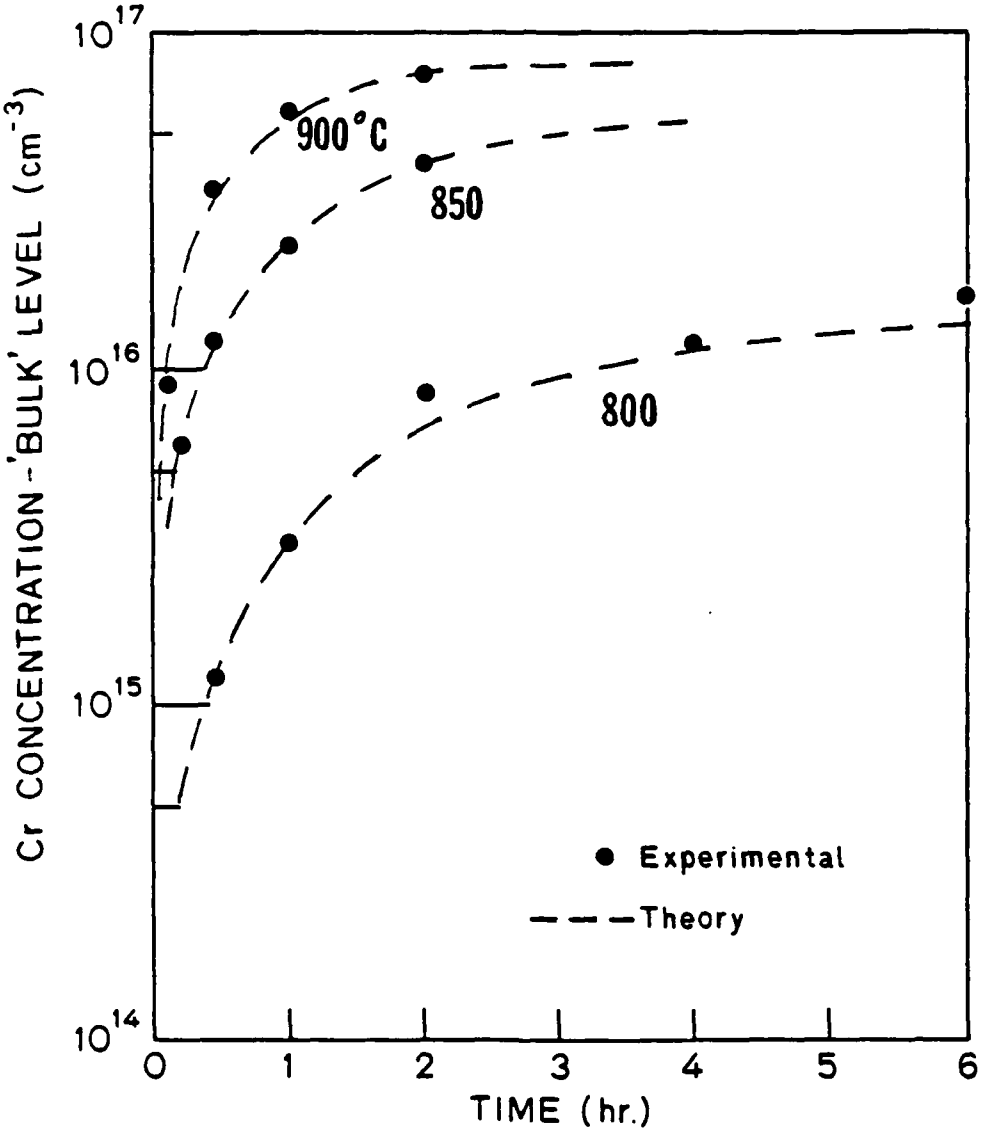

Figure 6-10. C_o vs. time. C_o is the bulk Cr concentration, extrapolated to the surface. Theoretical curves are dotted.

and the solubility of Cr is ≈2 x 10^{16} cm^{-3} at that temperature. Therefore, substitutional Cr could be charged and still not exhibit concentration dependent diffusion. This will be considered again in the junction diffusion samples. In any case, the uncharged model fits very well.

In addition to a good fit of the experimental profiles to the theory, the E_a and D_o values of .83 eV and 2.04 x 10^{-6} cm^2/sec, respectively, provide additional confirmation of the model since they are typical values for the substitutional/interstitial dissociative diffusion mechanism, as discussed in chapter 5. Other results, to be discussed in this chapter and the next, also lend support to this diffusion model for Cr in GaAs.

Since vacancies can diffuse in from the surface, one would expect to see Case II diffusion at the surface, with the Cr concentration right at the surface equal to the Cr solubility value for the temperature in question - 6 x 10^{16} cm^{-3} at 850°C, for example - and a shallow error function profile down to the position where the "bulk Cr" is reached (due to the Case IV diffusion). However, as mentioned, the unusual surface phenomena obscure this. In a couple of profiles (the 25 min., 850°C and the 25 min., 800°C profiles, for instance), this diffusion case is evident. From these, diffusion coefficients for 800 and 850°C were determined, 1 x 10^{-12} and 7 x 10^{-12} cm^2/sec. respectively.

A diffusion was performed in doped GaAs (Te doped, n ≈ 4 x 10^{17} cm^{-3}), to see if doping has an effect on the diffusion of chromium. The SIMS Cr profile for the 2 hr.,

850°C diffusion (with H source) is shown in figure 6-11. Although the extrapolated surface concentration of 9 x 10^{16} cm^{-3} is higher than the Cr solubility in undoped GaAs, as discussed in chapter 4, the effective diffusion coefficient (D_{fast}) of ≈2 x 10^{-10} cm^2/sec. is less than in the undoped case (where D = 4 x 10^{-10} cm^2/sec). This can be explained by the model. By equation 5-9, $D_{fast} = D_i C_i'/(C_i'+C_s')$. In highly doped n-type GaAs, Cr is charged, therefore, the conversion equation is not:

$$I_i + V = I_s \qquad (5\text{-}1)$$

but either:

$$I_i + V = I_s^- + h^+ \qquad (6\text{-}1)$$

or:

$$I_i + V + e^- = I_s^- \qquad (6\text{-}2)$$

Therefore, increasing the electron concentration (by increasing the doping level) shifts equation 6-2 to the right. This decreases the ratio C_i/C_s, and therefore decreases D_{fast}. (This is also the reason why C_s, which is the Cr solubility, increases with n-type doping.)

Next, Cr diffusions were done into Crystal Specialties undoped (Bridgman) GaAs, for various times at 750°C. There were two distinct differences between the results for these and for the Cominco LEC GaAs: 1) θ is much smaller for the Crystal Specialties (2.4 x 10^4 sec. vs. 1.3 x 10^5 sec.) meaning that the solubility level was reached much more quickly; and 2) in some cases, the tail end of the Cr profile dropped off more quickly. Figure 6-12 shows four SIMS Cr profiles for the 750°C, 4 hr. Cr indiffusion, all from the same sample (also

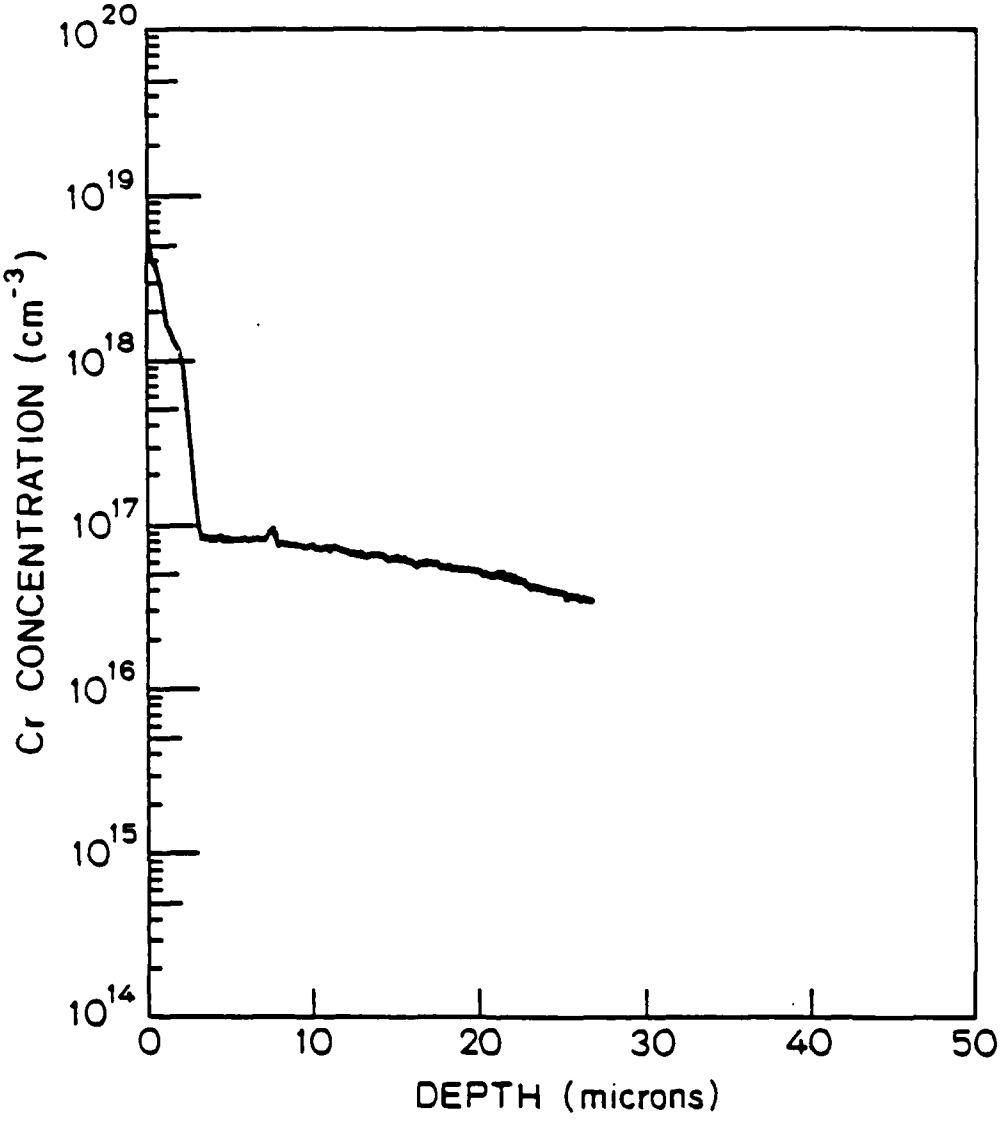

Figure 6-11. Cr concentration profile from 850°C, 2 hr. indiffusion experiment in Te-doped ($n = 4x10^{17}$ cm^{-3}) GaAs - H source.

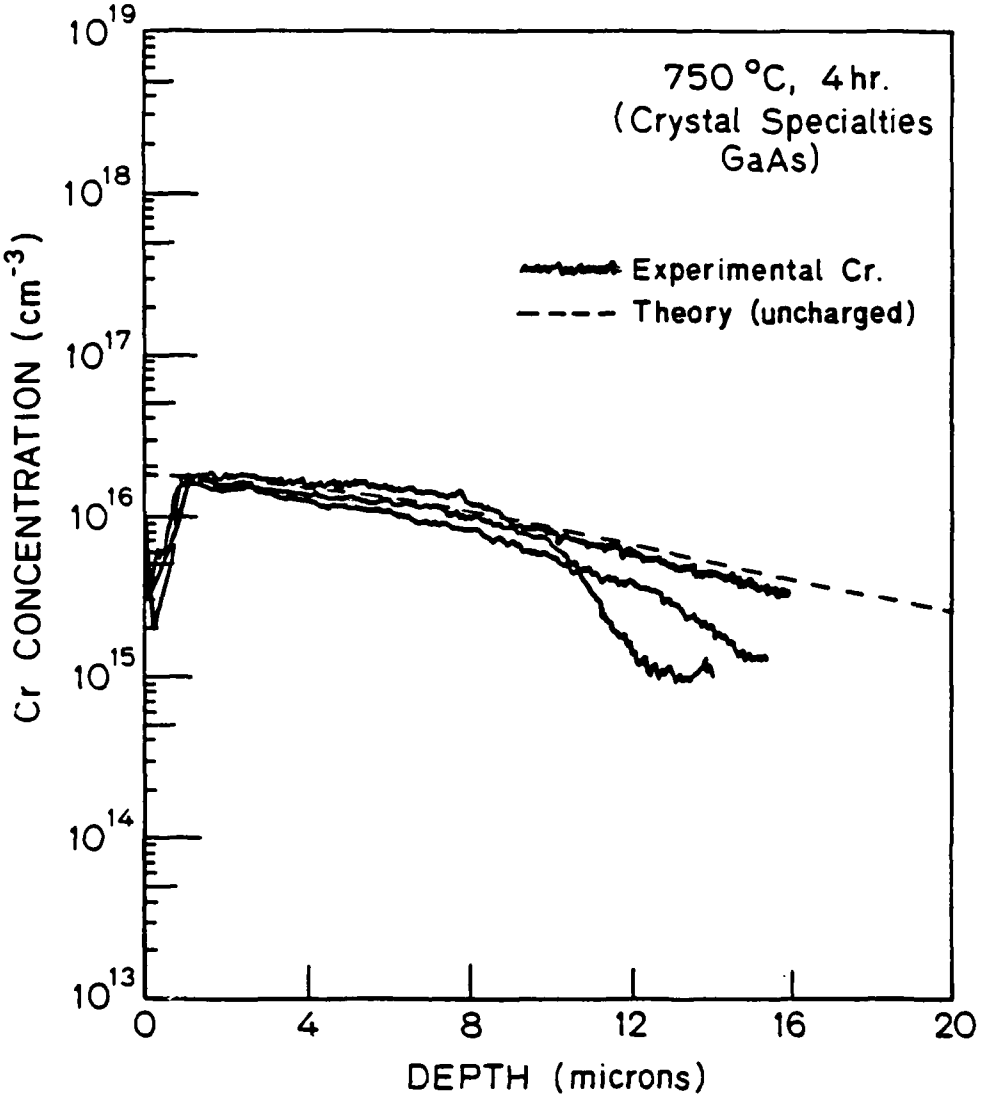

Figure 6-12. Cr concentration profiles from 750°C, 4 hr. indiffusion experiment in Crystal Specialities (Bridgman) GaAs - H source. The three profiles are from different locations on same GaAs wafer.

shown is the theoretical curve for the uncharged case). A hint to the cause for this is the fact that usually Bridgman-type GaAs is not semi-insulating due to impurities (usually oxygen and silicon) and defects, and it is usually n-type (the reason why Cr must be added to it to make it semi-insulating), whereas LEC GaAs is intrinsically semi-insulating. Unannealed Bridgman GaAs was checked by C-V analysis, and it was found that the carrier concentration (n-type) varied from point to point on the wafer, from a value of $\approx 1 \times 10^{14}$ cm^{-3} to the mid 10^{16}'s. These non-uniform carrier concentrations can explain the diffusion profiles in the Bridgman samples. In the regions where the electron density is low, the normal uncharged diffusion occurs. However, in regions of moderate electron density, the diffusion is influenced by the presence of the electrons. Near the surface, where the Cr level is approximately the same as the electron concentration, the Cr compensates the free electrons and the material becomes semi-insulating. However, deeper in the sample, the Cr level is lower and the net electron density is greater than zero. Thus, by the arguments used earlier regarding a shift in the conversion reaction due to a change in the electron or hole concentration, the effective diffusion coefficient is decreased. The extent of the decrease in the diffusivity is directly related to the electron density; hence, for different electron densities, the extent of the diffusion reduction will be different, resulting in different shaped curves. To test this, a Cr diffusion was performed with a Crystal Specialty (Bridgman) wafer at 1000°C. At that temperature, the intrinsic

carrier concentration is $\approx 5 \times 10^{17}$ cm^{-3} (as compared to $\approx 4 \times 10^{16}$ at 750°C) and therefore, any extrinsic electrical affect should be eliminated. Figure 6-13 shows the resulting SIMS Cr profile, along with the profile for a similar run with Cominco LEC GaAs. As one can see, the profiles are virtually identical; the Bridgman sample profile does not exhibit the abrupt drop-off in Cr concentration observed in the lower temperature samples. Therefore, there is good evidence that the difference in Cr profiles observed is related to electrically active impurities or defects in the Bridgman GaAs.

The reason for the smaller value for Θ is not clear. At first one would think that since LEC GaAs is usually grown with a slight excess of arsenic, whereas Bridgman GaAs is usually grown exactly stoichiometric (to avoid high arsenic pressures), that LEC GaAs would have a higher initial concentration of gallium vacancies. Therefore, the build-up to the equilibrium value for that reason should be faster for the LEC material rather than the Bridgman material. This, of course, assumes that Cr is incorporated onto a gallium site rather than an arsenic site. To test this assumption, a piece of LEC GaAs was pre-annealed in an ampoule with a piece of elemental arsenic at 800°C for 24 hours. This should increase the gallium vacancy concentration and decrease the arsenic vacancy concentration. Then a 800°C Cr indiffusion was performed for 4 hours. The bulk level, as determined by SIMS, was indeed higher than in the normal LEC case, with a Θ value of 1/2 the original. Therefore, the original assumptions regarding the diffusion mechanism seem to be good. Another possibility is

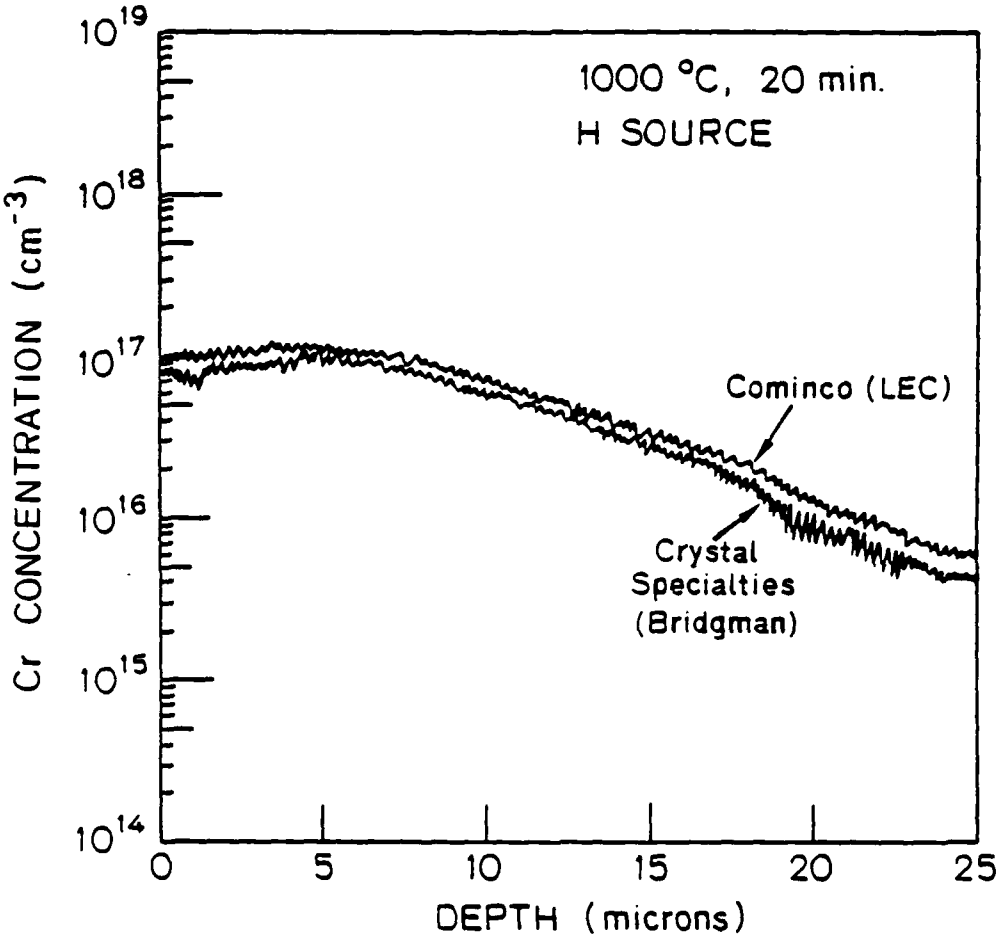

Figure 6-13. Cr concentration profiles from 1000°C, 20 min. indiffusion experiments in Crystal Specialties and Cominco GaAs - H source.

that the dislocation densities might be different; more dislocations would generate more vacancies, and hence Θ would be smaller. But the dislocation densities (as measured by the etch pits), are about the same ($\approx 5 \times 10^4$ cm^{-2} for the LEC and $\approx 2 \times 10^4$ for the Bridgman), if anything, lower for the Bridgman. However, these dislocation densities refer to all types of dislocations, but there are different types of dislocations, such as screw, edge, edge that ends with a Ga atom, edge that ends with an As atom, and not all generate gallium vacancies. Therefore, more of the type that creates gallium vacancies may be present in the Bridgman GaAs than in the LEC GaAs. Another possibility is that whatever is the source of the net electron concentration in the Bridgman material (oxygen impurities, for example) might also affect the Θ value.

At this point, the exact cause of this difference in Cr behavior is not clear. For whatever reason, this difference in Θ for different types of GaAs is good evidence that the rise in the bulk Cr concentration level is associated with processes occuring <u>inside</u> the GaAs, as the model describes, rather than on changing surface conditions due to changing source and/or vapor phase conditions (which could result in similar profiles). In addition, this difference in Cr behavior, as well as the changes in diffusivity, shows how Cr can be used as a probe to study such things as vacancies and other defects and impurities, which are normally difficult, if not impossible, to study directly.

Finally, a Cr indiffusion was done into GaAs (LEC) at 800°C for 12 hours, this time using J source. As discussed

earlier, this results in a lower Cr solubility, i.e., substitutional equilibrium concentration, than using H source; here any difference in diffusion was studied. From the SIMS Cr profile (figure 6-14), a diffusion coefficient of 4×10^{-10} $cm^2/sec.$ was determined. A repeat of this experiment resulted in the same D_{fast} value. This value is just barely within the (large) expected error of the 800°C, H source value of 2.8×10^{-10} (see figure 6-8), and therefore one cannot really say that the value of D_{fast} changed from source H to J. However, a higher value for J <u>is</u> reasonable because as the source changes from H to J, the value for C_s', the substitutional solubility, decreases almost an order of magnitude, and C_i', the interstitial solubility, would probably not change as much. Therefore, D_{fast}, which equals $D_iC_i'/(C_i'+C_s')$, would be expected to slightly increase as the source composition moves towards the Ga corner.

6.5.3 <u>Outdiffusion Experiments</u>

Well-defined Cr outdiffusion experiments were performed by annealing Cr-doped GaAs (Crystal Specialties) in an evacuated closed quartz ampoule, which also contained a large amount of "sink" material. This is the same idea as using the "source" material in the indiffusions, except that the composition of it is such that the Cr solubility in $GaAs_{(s)}$ for that system is <u>less</u> than the initial Cr level in the GaAs. Therefore, Cr will diffuse out of the GaAs and into the sink. An example would be annealing GaAs, with 1×10^{17} cm^{-3} Cr, with J source at 800°C. If there is a lot more sink material than GaAs, then the total system composition will lie near the composition of

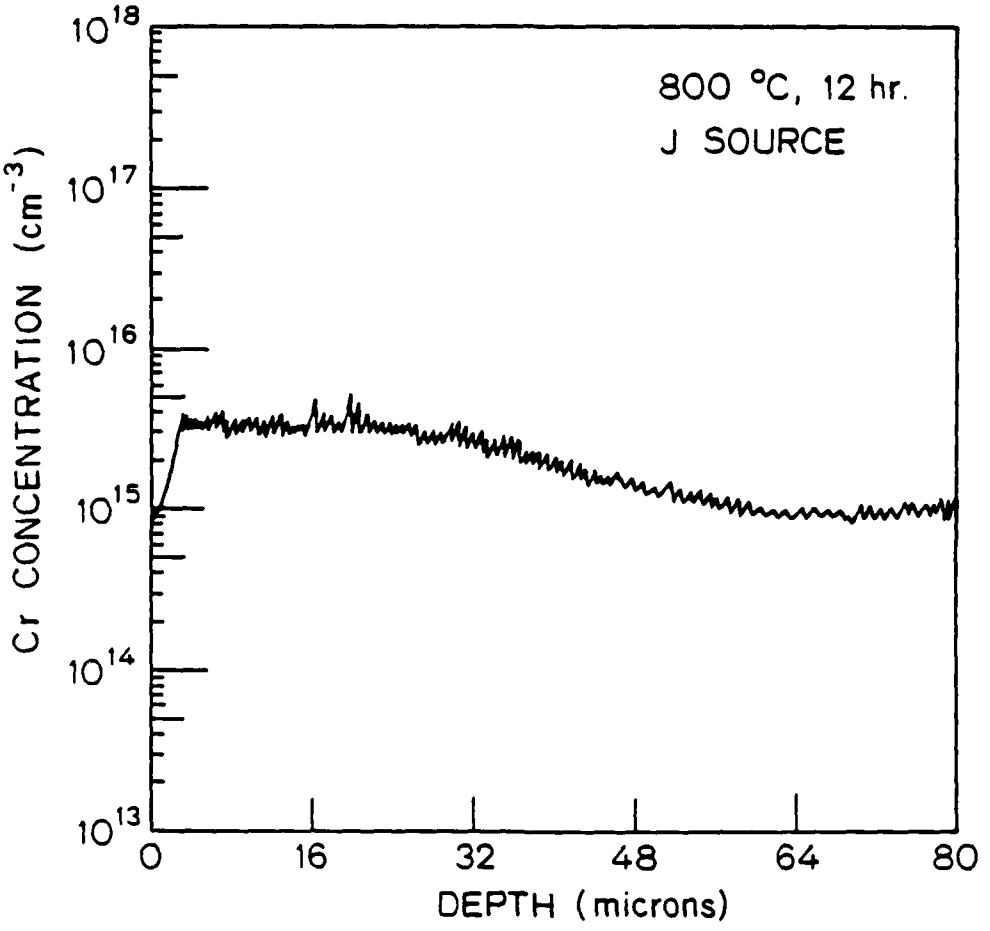

Figure 6-14. Cr concentration profile from 800°C, 12 hr. indiffusion experiment - J source.

J. The GaAs with ≈5 x 10^{15} cm^{-3} Cr is in equilibrium with the sink, and therefore, Cr will diffuse out of the GaAs until that concentration level is reached throughout. During the diffusion, the surface concentration of Cr should be at the solubility limit (5 x 10^{15} cm^{-3} in this case), as is the case with indiffusions as well. The problem with doing outdiffusions without a well-defined sink is discussed a little later.

Outdiffusions were performed using J source at 700, 800 and 850°C (for 2, 1, and 1 hr., respectively), with the corresponding SIMS Cr profiles shown in figure 6-15a. The extent of outdiffusion is similar to that of the assumed Case II for indiffusion (vacancy diffusion controlled); therefore, error function diffusion curves were fitted to the profiles to determine D_{slow} values. As discussed in chapter 5, solving equation 5-10 for outdiffusion conditions leads to the usual outdiffusion equation, $(C-C_1)/(C_2-C_1) = \text{erf}\ (x/(4Dt)^{1/2})$, where D in this case is "D_{slow}" and equals $D_v\ C_v'/(D_v' + C_s')$; C_2 is the initial bulk Cr level, and the surface is maintained at a concentration of C_1, in this case the solubility of GaAs for the J sink. By making the best fit to the profiles, shown in figure 6-15b, D_{slow} values were determined; they are tabulated in table 6-2 and are plotted in figure 6-8. As one can see, they are very close to the D_{slow} values determined from the indiffusion experiments. It should be noted that the fits to the profiles are not perfect, especially for the 850°C profile over the first micron from the surface; this will be discussed later. Also, the build-up of

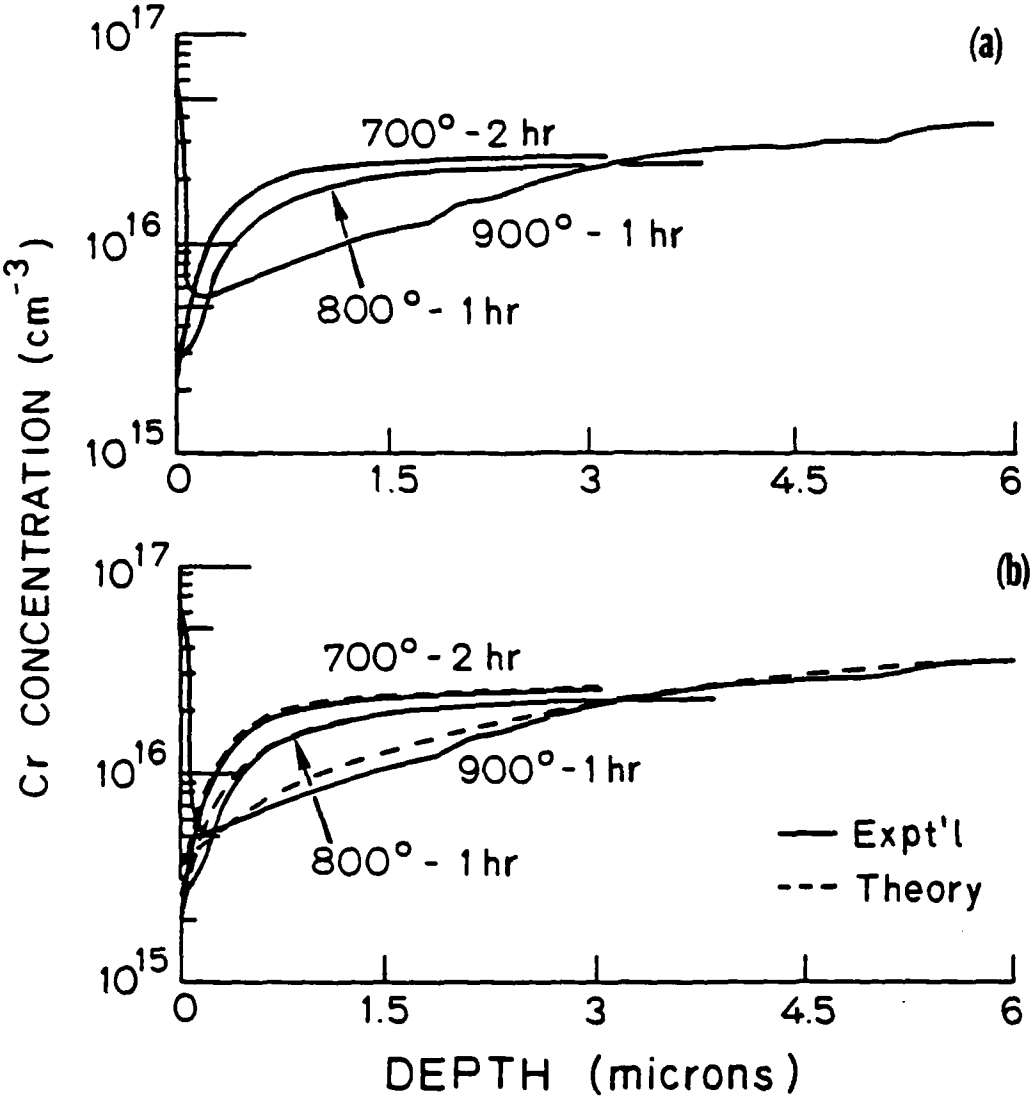

Figure 6-15a. Cr concentration profiles from outdiffusion experiments, with J sink, for various times and temperatures, as indicated.

b. Cr profiles with theoretical curves. See table 6-2 for D values.

Table 6-2. Chromium outdiffusion results.

Temp	Time	Sink	D_{slow}
700°C	2 hr.	J	2×10^{-13} cm^2/sec
750	1	-	1.6×10^{-12}
800	1/2	J	1.4×10^{-10}
	1/2	H	1.4×10^{-2}
	1	J	1.5×10^{-12}
	1	J2	1.6×10^{-12}
	1	D	2.0×10^{-12}
	2	-	2.2×10^{-12}
	2	H	1.8×10^{-12}
850	1	-	1.0×10^{-11}
	4	-	1.3×10^{-11}
900	1	-	2.0×10^{-11}

Cr at the surface was ignored in these analyses; this topic is discussed in chapter 7.

Additional outdiffusion experiments were performed for different annealing times, for example, 1/2 and 2 hours at 800°C, and 4 hours at 850°C. The D_{slow} values determined from these were each within 20% of the other values for those temperatures - within the expected error.

SIMS profiles were obtained from several of the samples before they were annealed, and their bulk levels were compared to the bulk levels of the profiles after the outdiffusions. In each case, the level was within the expected error of the concentration determinations (± 50%); however, in virtually all the cases (90%), the bulk level after the anneal was at or below the initial bulk level. If it was just a random fluctuation, then in more cases than this the bulk level after the anneal would have been greater than the initial level. Therefore, I suspect that the bulk level may drop a little during the anneal.

The mechanism of Cr outdiffusion can be explained in terms of the proposed model. During outdiffusion, as in indiffusion, the atoms diffuse by converting from substitutional to interstitial. A certain number make this conversion initially and can quickly diffuse out. (This could explain the drop in the bulk level.) However, now the GaAs is saturated with vacancies, and no more atoms can convert to interstitial and diffuse out until the vacancies can be disposed of. This can happen either by the vacancies diffusing to the surface, which is a natural vacancy sink, or they can be annihilated in the

bulk, such as by appropriate dislocation movement. This is completely analogous to the indiffusion case, and it is why the same governing equations hold for each case, with only initial and boundary conditions different. The fact that the switchover from Case II dominating to Case I dominating is not observed - even after 4 hours at 850°C - is probably because the bulk vacancy annihilation mechanism is not as effective as the bulk vacancy generation mechanism. (As mentioned, other researchers (112, 108) did observe an abrupt increase in the effective diffusion coefficient after ≈ 1 hour at 800°C, indicating a transition from Case II to Case I, probably due to a different defect state of their starting material.)

Outdiffusion runs were also done at 800°C, for 1 hour each, using different sinks: J1, J2, and D, whose compositions are shown in figure 4-4. (Note: J1 is the same as J, used earlier.) This results in different surface concentrations for the same temperature. In the case of "sink" D, the solubility determined by D is <u>above</u> the initial Cr bulk level, thus an <u>in</u>diffusion would result, and D is a source in this case rather than a sink. The SIMS profiles are shown in figure 6-16. As expected, the surface concentration increases as the sink/source composition goes from J2 to J1 to D. The appropriate theoretical equation (indiffusion or outdiffusion) was fit to each curve, and only C_i was changed from one curve to another, and not D. The fits are quite good. Therefore, while the solubility of Cr in GaAs changes over this range of composition in the ternary phase diagram, D_{slow} does not appear to. Since $D_{slow} = D_v C_v'/(C_v' + C_s')$, and

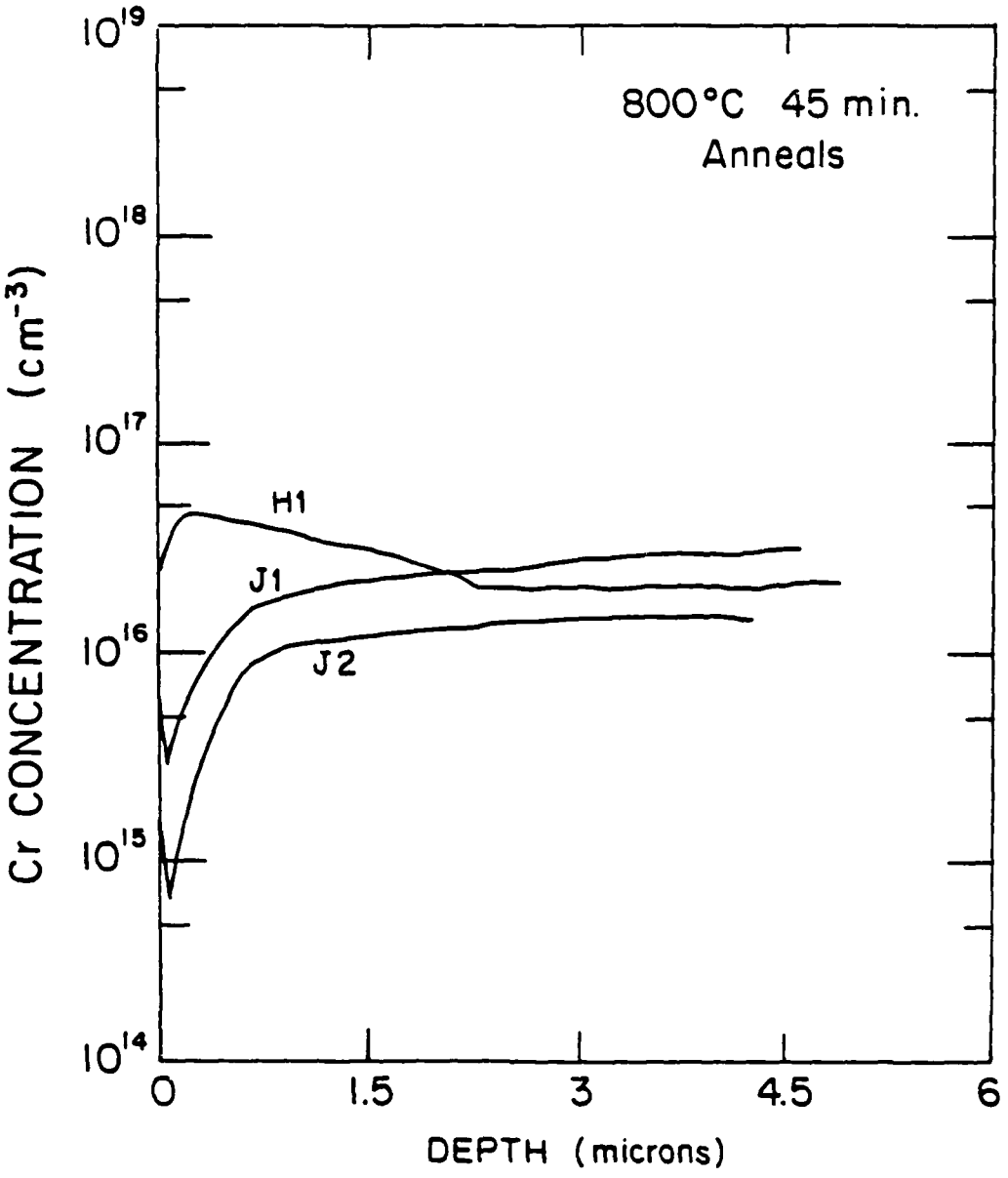

Figure 6-16. Cr concentration profiles from 800°C, 45 min. outdiffusion experiments with various sinks, as indicated.

since C_S' increases when going from J2 to J1 to D, it appears that C_V' increases accordingly so that the net change in D_V is small. This is reasonable since one would expect that the equilibrium gallium vacancy concentration would increase as the composition moves away from the Ga corner of the diagram.

For comparison, some outdiffusion experiments were done without a sink in the ampoule (just annealing Cr-doped GaAs in the evacuated, closed ampoule). The SIMS profile for a 750°C, 1 hr. outdiffusion is shown in figure 6-17. This is very similar to the profile obtained using J1 or J2 sinks. An error function curve was fitted to this (ignoring the surface build-up and assuming a C_1 value of 1×10^{15} cm^{-3}), resulting with a diffusion coefficient consistent with the other outdiffusions. This result is also consistent, both in surface concentration and in the diffusion coefficient, with most of the results of other researchers, who also did short-time outdiffusions without a well-defined sink. This will be discussed further in section 6.6.

The reason why the surface concentration is similar to that for outdiffusing when the J sink is used can be explained in terms of the phase diagram and phase equilibria. At first, one would think that because the system is made up of only Cr-doped GaAs, in which the Cr level is above or at the solubility level for the annealing temperature, then it would lie in the $GaAs_{(s)}$-$CrAs_{(s)}$-$Ga_{(\ell)}$ tie triangle region (see figure 6-18). Therefore, no outdiffusion would occur. However, as mentioned in chapter 2, one must take into account the vapor pressure. Because there is no sink or source, all

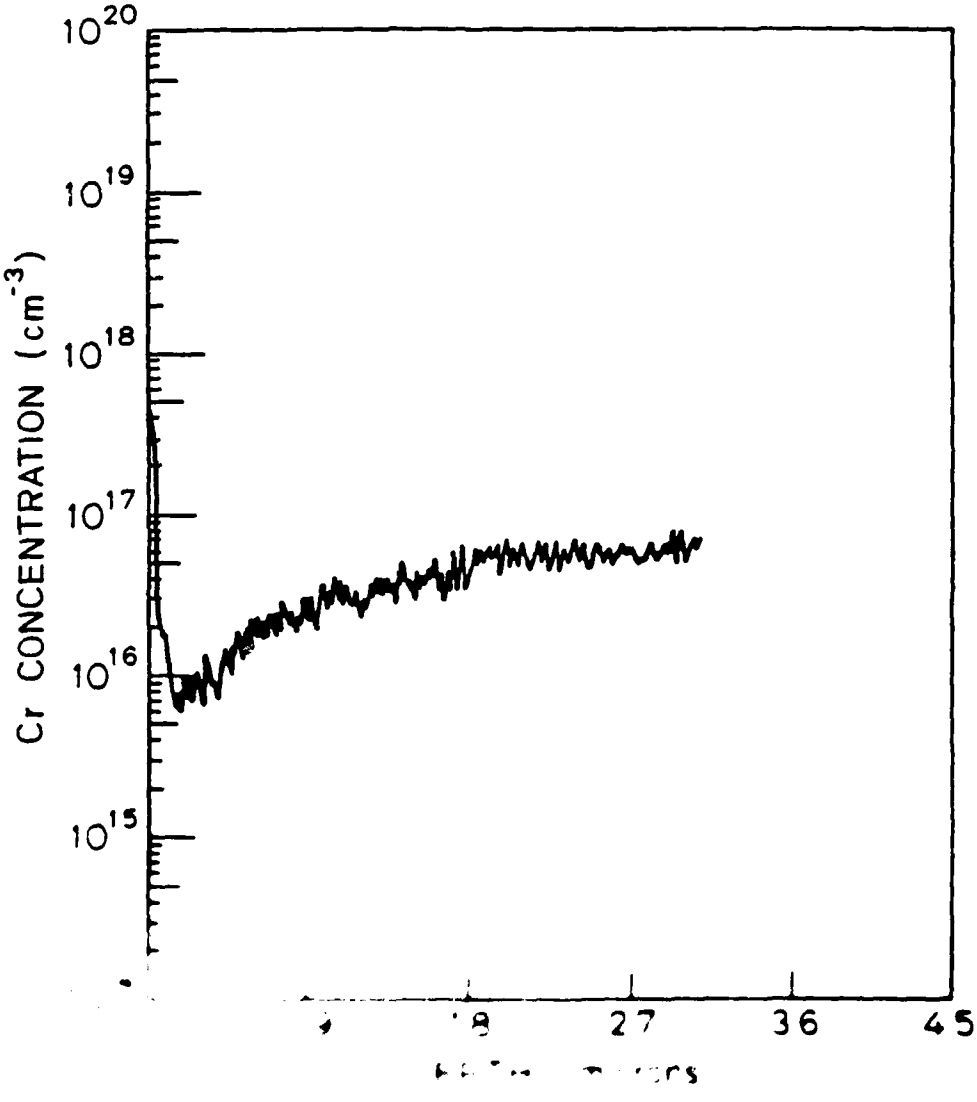
10^{20}
10^{19}
10^{18}
10^{17}
10^{16}
10^{15}
Cr CONCENTRATION (cm^{-3})
9
27
36
45

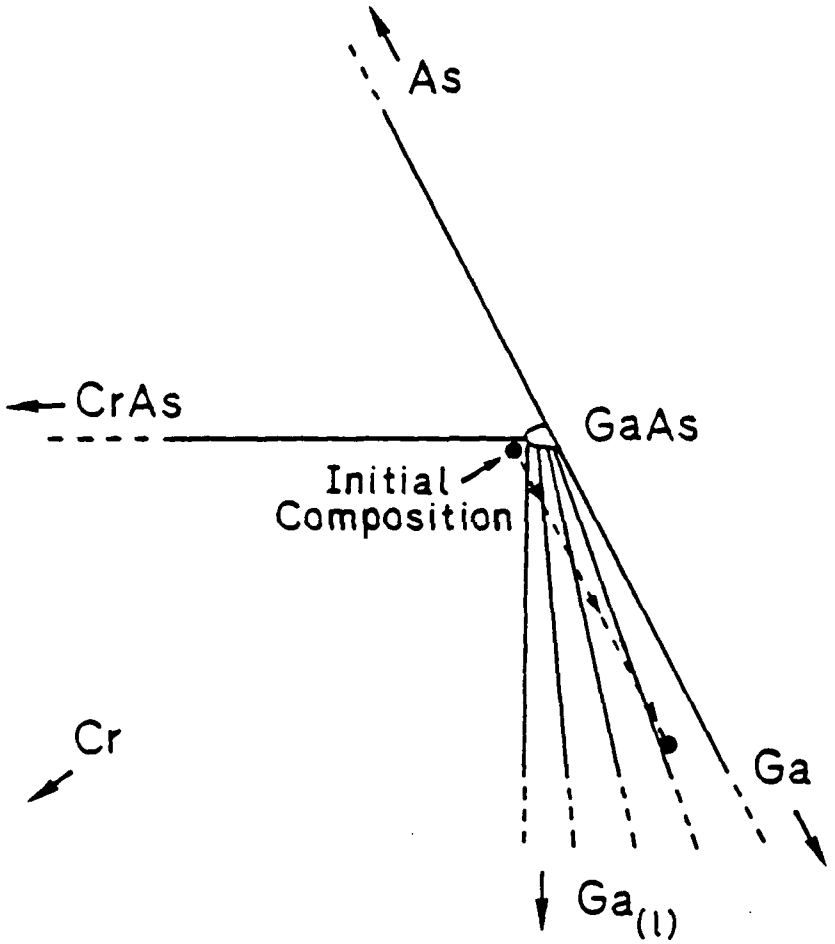

Figure 6-18. Proposed reaction path for outdiffusion experiments.

arsenic (and chromium and gallium) to provide for the vapor phase must come from the GaAs wafer. And because of the extremely small concentrations and the relatively large partial-pressures involved, this is evidently enough to move the system from the tie triangle region to the $Ga_{(\ell)}$ - $GaAs_{(s)}$ region (near J1). Figure 6-18 shows this on the phase diagram.

According to the above theory, some $Ga_{(\ell)}$ should form. Indeed, observation of the surface after the anneals showed little liquid droplets. Furthermore, according to the results of the solubility studies, this phase has a very high Cr solubility and the distribution coefficient is very low, therefore one might expect the Cr to segregate there. Perhaps the surface Cr build-up is due to the Cr in $Ga_{(\ell)}$. This will be examined in chapter 7.

In regards to the surface build-up, in several cases the total amount of Cr in the build-up is much more than the depletion of Cr. This indicates that the bulk level did indeed drop from the original levels, further evidence of the presence of fast Cr intersitials.

6.5.4 Junction Diffusion Experiments

As discussed in section 6.3, junction diffusions were performed to avoid the problems at the surface and to study the vacancy controlled Cr diffusion. Anneals were performed of the undoped LPE GaAs/Cr-doped GaAs substrate samples for various (short) times at 700, 800, and 900°C. The samples, with the temperature and time for each, are tabulated in table 6-3. The [illegible] was obtained from each sample, both before and

Table 6-3. Chromium junction diffusion results.

Temp.	Time	Source	D_{slow}
700°C	1/2 hr.	-	4.0×10^{-13} cm^2/sec
800	1/2	-	3.0×10^{-12}
	1	-	2.0×10^{-12}
	1	J	2.6×10^{-12}
900	1/4	J	1.2×10^{-11}
	1/2	-	1.2×10^{-11}

after each anneal. A typical result is shown in figure 6-19, before and after a 1 hour, 800°C anneal. Three observations are made: 1) there is "normal" Cr diffusion evident from the substrate into the LPE layer (assumed to be the vacancy diffusion controlled case); 2) the bulk level on the substrate uniformly decreases a little, as in the outdiffusion case; and 3) Cr builds up at the surface, which is evidence of fast diffusion of Cr from the substrate, through the LPE layer to the surface. These features are characteristic of all the junction diffusion samples.

The decrease in the bulk level is believed to arise from the same mechanism as seen in the outdiffusion samples: the initial diffusion of interstitial chromium occurs until the vacancy concentration is saturated. The "normal" diffusion at the interface is assumed to be the vacancy controlled Cr diffusion. The proposed mechanism is very similar to the outdiffusion case, except that it includes both outdiffusion and indiffusion - outdiffusion from the substrate and indiffusion into the LPE layer. The fast interstitials quickly diffuse out of the substrate and into the LPE layer (and to the surface, and perhaps even out of the sample). Once the substrate is saturated with vacancies, no more interstitial Cr can be produced until the vacancies are removed. Since there is no evidence for efficient bulk annihilation, this can only occur by vacancy diffusion from the substrate and into the LPE layer. Therefore, the vacancy diffusion controlled Cr diffusion is seen both out of the substrate and into the LPE layer, where the interstitials can recombine with the vacancies

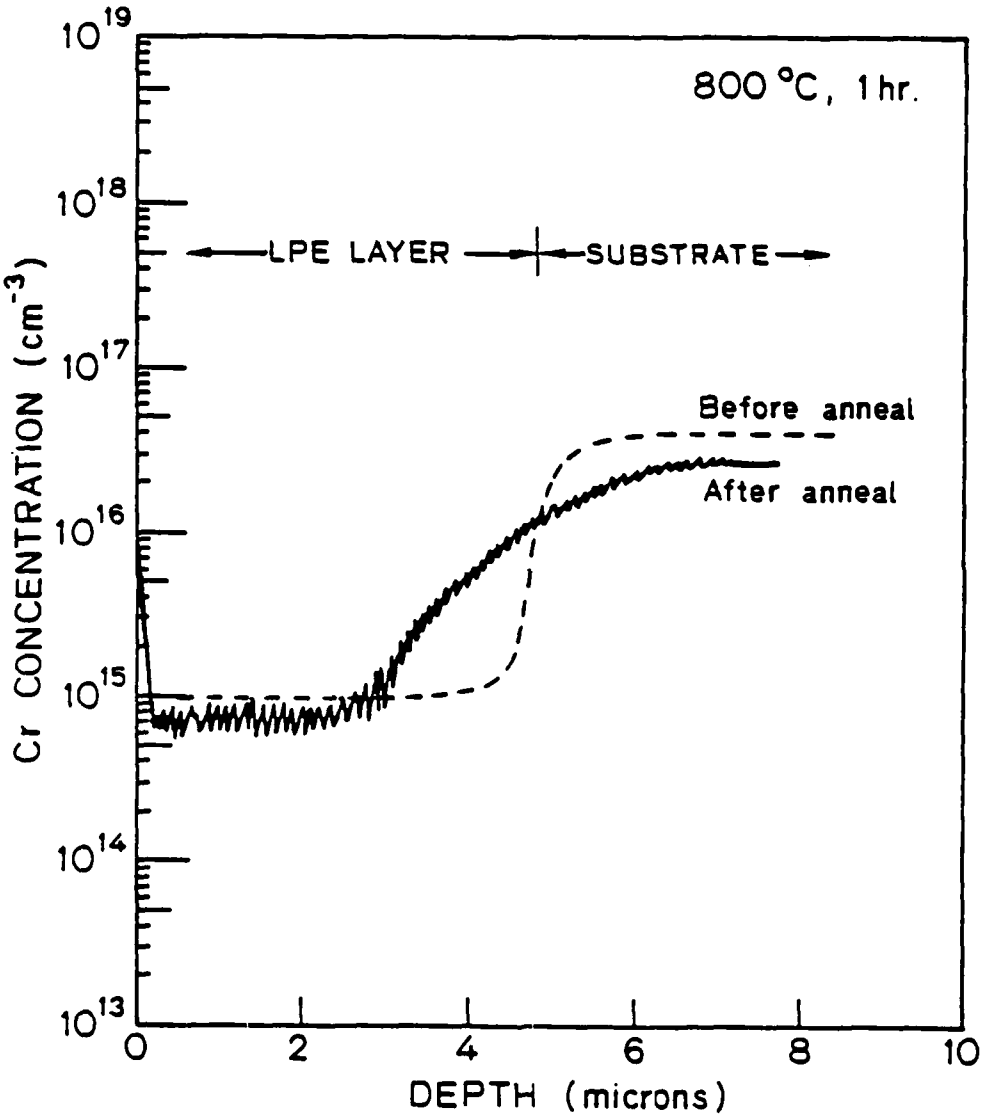

Figure 6-19. Cr concentration profiles - before and after anneal - from typical junction diffusion experiment. This one for 800°C, 1 hr. anneal.

and become substitutionals. This results in one continuous diffusion profile across the junction.

This type of experiment is ideal to measure the effective diffusion coefficient as a function of concentration because, if one assumes a semi-infinite medium on each side, one can use the Boltzmann-Matano analysis to determine D(C) (131, 132). Shewmon (94) gives a detailed review of this graphical technique. The resulting equation for D(C'), for the conditions: $C(x<0,t=0) = C_1$ and $C(x>0,t=0) = C_2$ and semi-infinite media, is:

$$D(C') = \frac{1}{2t} \left(\frac{dx}{dC}\right)_{C'} \int_{C_1}^{C'} x \, dC \qquad (6-3)$$

where x = 0 is defined by

$$\int_{C_1}^{C_2} x \, dC = 0 \qquad (6-4)$$

Therefore, by measuring the appropriate area and slope one may obtain D values as functions of concentration. This analysis was done on all the samples. It was found that, within error of the technique, D does not vary with concentration. The D_{slow} values determined are also tabulated in table 6-3.

In regards to the question of the Cr being charged or not, the diffusion coefficients for the 700°C sample were determined to be within 15% of each other from concentrations levels of 4×10^{15} to 3×10^{16} cm^{-3}, while $n_i = 2 \times 10^{16}$ cm^{-3}, thus indicating that the substitutional Cr is not charged. Therefore, the concentration-independent diffusion can not be attributed to just the n_i effect, since n_i is not >> C_s.

Since the diffusion coefficient was determined to be independent of concentration, then Case II, uncharged, of the diffusion model should apply. This is simple "error function" diffusion applied to the conditions mentioned previously, resulting in:

$$C(x,t) = (C_1-C_2)/2 \cdot \mathrm{erf}(x/2(D_{slow}t)^{1/2}) \qquad (6\text{-}5)$$

This was fitted to each profile with the appropriate D_{slow} value, as determined by the Boltzmann-Matano analysis. Two examples of the fit are shown in figures 6-20 and 6-21. As one can see, the fits are extremely good, indicating that D is independent of concentration, and that the model quite adequately describes the behavior. Furthermore, the fits are much better in these cases than for the outdiffusion experiments, especially at the higher temperatures, indicating that the diffusion at the surface is probably being affected by other phenomena; this confirms the importance of doing these junction diffusion experiments to study the diffusion of Cr in GaAs.

The above analysis assumes an exact step formation of concentration at the junction initially. As seen from the "before annealed" profiles, this is not exactly true. However, one can correct for this initial condition. The final profile may be assumed to be the result of successive diffusions, one during the LPE growth, and one during the junction diffusion. The net Dt simply equals $D_1t_1 + D_2t_2$ (132). In each analysis, the product Dt, is determined. The D of concern (D_2) can thus be determined by determining (D_1t_1) from the initial profile, subtracting that product from

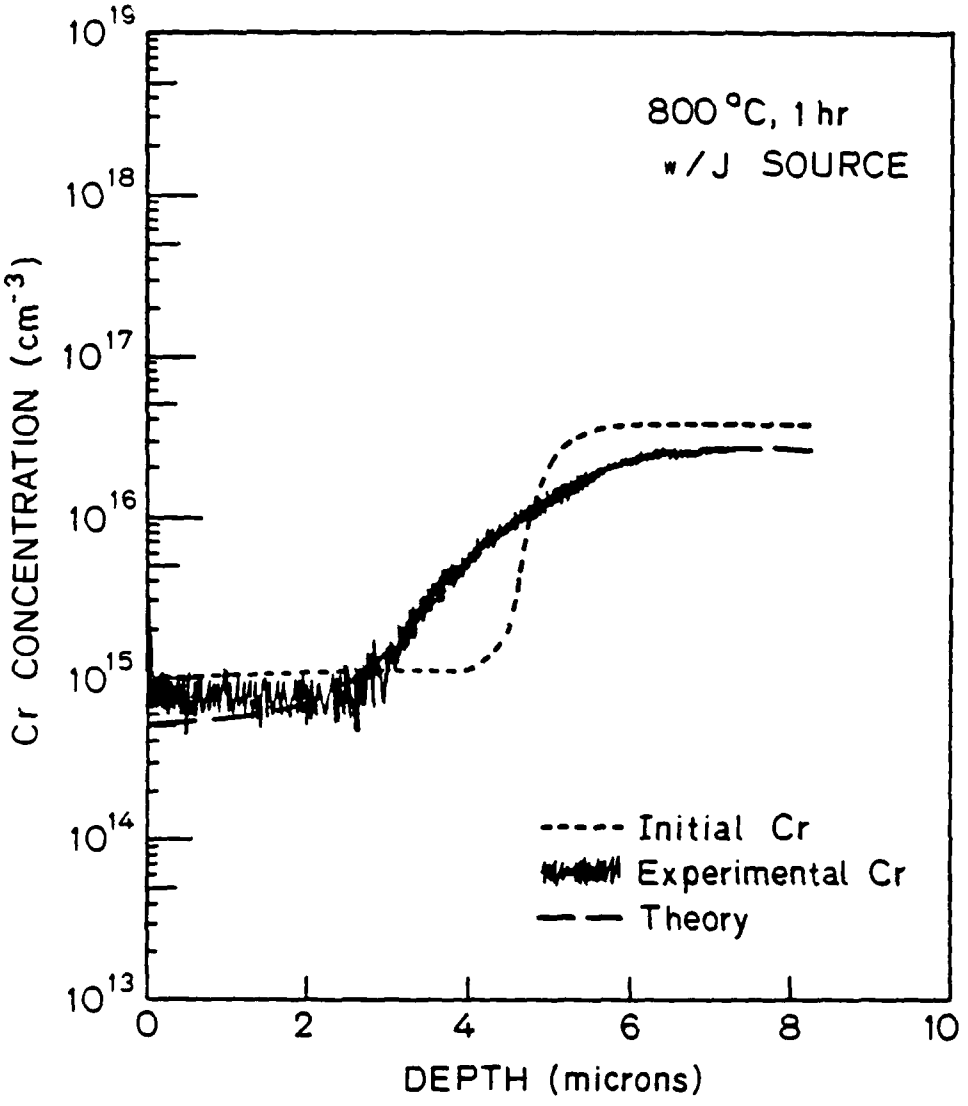

Figure 6-20. Cr concentration profiles - before, after, and theoretical - from 800°C, 1 hr. junction diffusion experiment.

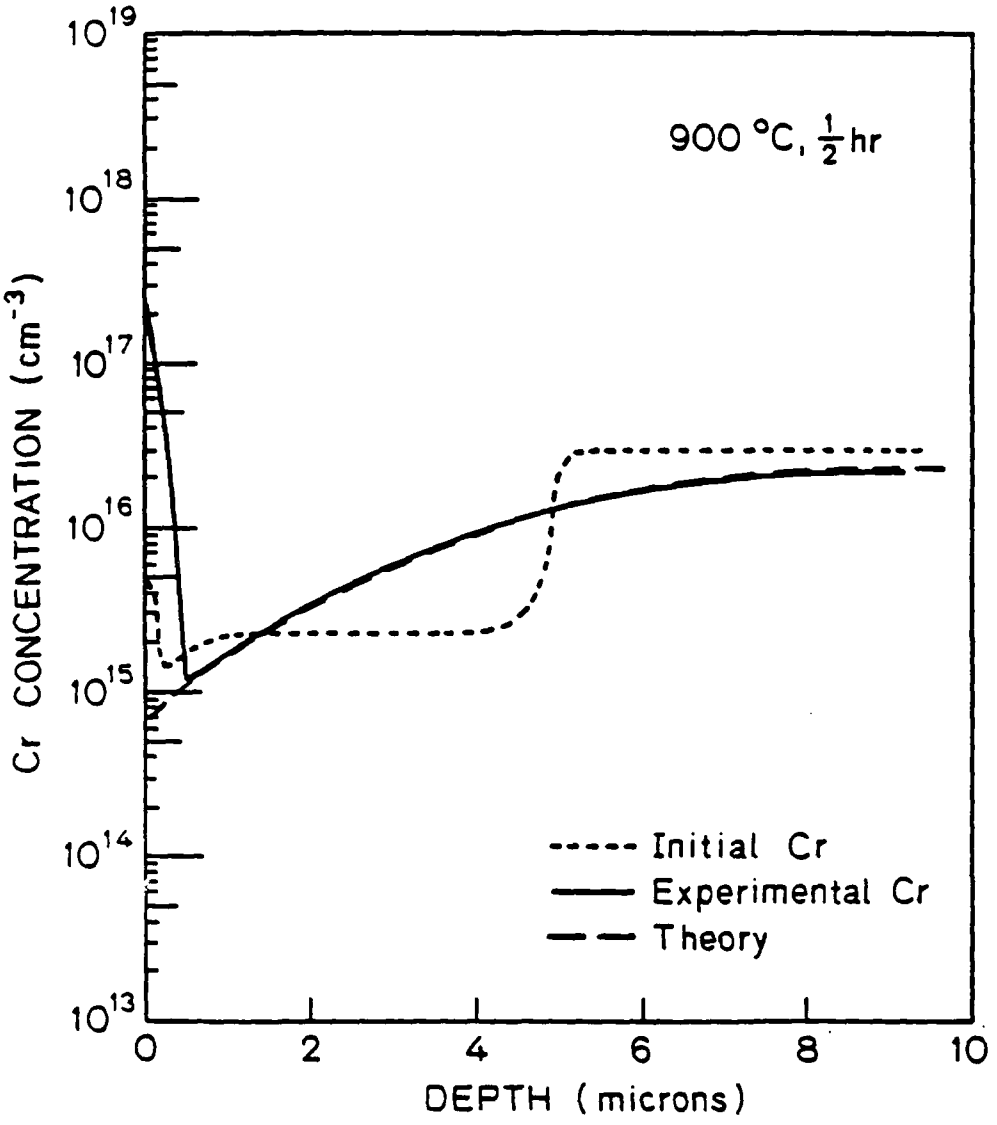

Figure 6-21. Cr concentration profiles - before, after, and theoretical - from 900°C, 1/2 hr. junction diffusion experiment.

the Dt of the final profile, and dividing by the time (and D_1 does not even have to have been constant, or t_1 need to be known, to do this).

This was done for each sample. It is these new corrected D's that are tabulated (the D's for the short time/low temperature anneals are about 35% smaller than the uncorrected values - the D's for the long time/high temperatures are only about 10% smaller).

The diffusion was performed for various times at 800 and 900°C, and the D values determined did not change with time. This indicates that the onset of Case I diffusion did not occur for the times used, and that the diffusion coefficients determined are valid. (The D values would not remain constant with time if, for example, the bulk level changed after the initial drop.)

The average D_{slow} value for each temperature is plotted in figure 6-8. These are quite similar to those determined from the outdiffusions and the indiffusions at the surface, as expected.

From the junction diffusion D_{slow} values for different temperatures, values for E_a and D_o were determined: E_a = 1.7 eV and $D_o = 1.7 \times 10^{-4}$ cm^2/sec. These are very reasonable numbers for the vacancy diffusion controlled diffusion case, as discussed in chapter 5. (The D_{slow} values from the junction diffusions are assumed to be more accurate than the outdiffusion or indiffusion D_{slow} value, which were determined from the profiles at the surface; therefore it was with these values from which E_a and D_o were determined.)

Using equation 5-12 ($D_{slow} = D_v C_v'/(C_v' + C_s')$), one can calculate D_v values for the different temperatures from the following selected values: the present values for D_{slow}, the present solubility values for C_s', and the C_v' values from Chang and Pearson (83). These results, tabulated in table 6-4, are within an order of magnitude of the vacancy diffusivity values determined by Chang and Pearson (83). The activation energy for D_v was determined to be 1.9 eV, very close to the value of 2.1 eV also determined by Chang and Pearson. Therefore, it is reasonable to conclude that this Cr diffusion is limited by gallium vacancy diffusion.

As mentioned previously, evidence for the fast interstitials is seen in the build-up of Cr at the surface, many microns away from the source of Cr in some cases. If the Cr diffusion were just via the normal one-species diffusion (which also usually follows "error function diffusion"), then one would only observe the diffusion profile at the junction. But because there are the fast interstitials, which can concentrate by converting to substitutional or by dissolving in another phase (as will be discussed in chapter 7), a relatively large amount of Cr is seen far away from the Cr source after short annealing times.

Most of the previously mentioned junction diffusion anneals were done with no source or sink in the ampoule. A few were done with J2 sink (for a surface concentration of $\sim 10^{15}$ cm^{-3}), with no observable difference in the results. This is because the Cr concentration in the LPE layer was at that level to begin with and, just like the outdiffusions done without a

Table 6-4. Vacancy diffusion results.

T	D_{slow}	C_s'	C_v' (ref. 36)	D_v
700°C	4×10^{-13} cm^2/sec	1×10^{16} cm^{-3}	3×10^{16} cm^{-3}	5×10^{-13} cm^2/sec
800	2×10^{-12}	3×10^{16}	5×10^{16}	3×10^{-12}
900	1.2×10^{-11}	8×10^{16}	7×10^{16}	2×10^{-11}

+ E_a (D_v) = 1.9 eV

source or sink (as explained in terms of the phase diagram in section 6.5.3), it would remain at that level. That is probably one reason why one did not see an increase in the bulk Cr level in the LPE layer (Case III diffusion), as was seen in the indiffusion experiments; the equilibrium solubility level was already achieved. Another possible reason is that the LPE GaAs might not be able to generate vacancies as effectively due to a smaller number of dislocations. Or perhaps it is because the initial gallium vacancy concentration in the LPE layer, which was grown from a Ga-rich melt, is very low. Any or all of these factors could explain the bulk Cr level in the LPE layer not rising.

The fact that the diffusion coefficient is evidently independent of concentration is further proof that the Frank-Turnbull mechanism for the interstitial-to-substitutional conversion, rather than the kickout mechanism, is operating. As discussed in chapter 5, the kickout mechanism supposedly predicts a C^{-2} dependence for the slow diffusion coefficient, while the F-T mechanism predicts a concentration-independent D_{slow}. The data clearly supports the F-T model over the other in this case. This mechanism is reasonable for Cr in GaAs because: 1) the Cr solubility is very close to the equilibrium gallium vacancy concentration, and therefore relative few, if any, vacancies must be generated; and 2) the effective diffusion coefficient (D_{slow}) measured is very close to the vacancy diffusion coefficient at each temperature. The two main arguments used against this mechanism were that too many vacancies were required to be

AD-A144 949 AN INVESTIGATION OF THE SOLUBILITY AND DIFFUSIVITY OF CHROMIUM IN GALLIUM ARSENIDE(U) ADVANCED RESEARCH AND APPLICATIONS CORP SUNNYVALE CA T J MAGEE ET AL. 3/3

UNCLASSIFIED 23 MAY 84 N00014-80-C-0482 F/G 7/4 NL

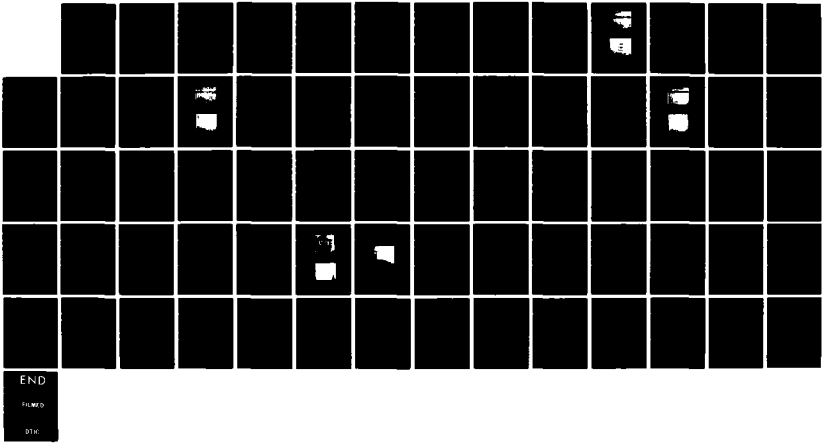

END

FILMED

DTIC

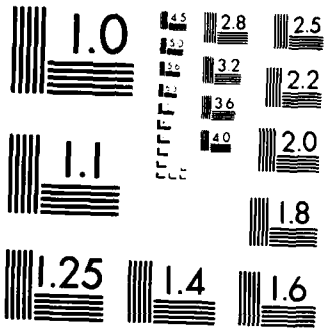

generated and the effective diffusion coefficients were much larger than the reported vacancy diffusion coefficients. These arguments are not valid in the present case, and the F-T model is therefore quite reasonable.

6.6 Chromium as a Probe

Because of its great sensitivity to its environment, as evidenced in the results so far, Cr may be used as a "probe" to study the defect chemistry of GaAs. It has been shown in the present and previous studies that the solubility and diffusion of Cr is greatly affected by other impurities, vacancies, precipitates, and dislocations, and thus by studying the behavior of chromium in GaAs, one can study the defect chemistry of GaAs. In the next chapter it is shown how high levels of another impurity were discovered as a result of studying Cr.

6.7 The Analysis of Previous Studies

These results and the diffusion model can now be used to explain some of the results and observations of other investigators concerning Cr in GaAs.

First, the results and model explain the deep penetration of Cr in GaAs that some have observed (5, 102), penetration much deeper than the "reported diffusion coefficients" could account for. This of course is due to the fast interstitials, which can convert to substitutionals wherever, and whenever, vacancies are available.

The the model also explains why a simple error function diffusion profile fit the results so well, which led to the low "reported diffusion coefficients"; most of these experiments

were done for short times and were outdiffusions, and the rather complex model reduces to a simple error function diffusion model for these conditions. It also explains why for longer times the simple model no longer applied; the proposed model predicts such different behavior for longer times.

The fast interstitials explain the gettering behavior of Cr, specifically, how the Cr move from one place to another so quickly (especially from the bulk to the surface). Magee et al. (123) recently studied the gettering action of Cr, in this case to a mechanically damaged surface. They measured the flux of the gettered Cr (in atoms/cm^2/sec.) versus temperature, from 300 to 400°C. Since the flux due to a stress field equals FDC/kT (from ref. 94), where F is the force exerted on the Cr by the stress field, D is the effective diffusion coefficient, and C is the concentration, which is constant with temperature in this case, a plot of ln(T•flux) versus 1/T results in the activation energy for the diffusion coefficient. From Magee's data, a value of 0.9 eV was determined. The activation energy for the interstitial controlled diffusion, the case that allegedly is responsible for the gettering, was determined in this work to be 0.83 eV, which is within experimental error of Magee's result. If the flux seen in Magee's results is not due to a stress field, but due to concentration gradient diffusion of the interstitials, to a region of lower Cr activity at the surface, then plotting ln(flux) vs 1/T results in a value for E_a. In that case, E_a = .88 eV, even closer to Magee's value. In either case, the results are good evidence that the Cr species that accounts for gettering (as seen by others and

in this work) and the Cr species which accounts for the deep penetration seen in this work (modelled by an interstitial species) are the same.

The low surface concentration of Cr observed when annealing Cr-doped GaAs (without an arsenic overpressure) is explained in terms of the ternary phase diagram, as discussed in section 6.5.3, i.e., by losing arsenic from the GaAs surface and moving to the Ga-rich side of the phase diagram. This is consistent with the results of Kasahara et al. (112) in which the surface concentration of Cr changed from less than 10^{16} to $\approx 5 \times 10^{16}$, and then to $\approx 7 \times 10^{16}$ cm^{-3} (at 850°C), as the arsenic overpressure was increased from 0 to 0.15, and then to 7.6 torr. In the 7.6 torr case, virtually all the arsenic for the vapor phase is externally supplied; therefore, none comes from the GaAs wafer, and the system remains in the $GaAs_{(s)}$-$CrAs_{(s)}$-$Ga_{(\ell)}$ tie triangle region where the Cr solubility in $GaAs_{(s)}$ is $\approx 6 \times 10^{16}$ cm^{-3}. As discussed in section 6.2, Kasahara (112) attributed the different profiles to different diffusion coefficients; however, as mentioned, the curves can be fit better to profiles with the same D value ($\approx 3 \times 10^{-12}$ cm^2/sec.), but with different surface concentrations.

Annealing Cr-doped GaAs with an encapsulent, as reported by others and discussed in section 6.2, also results in Cr profiles with a low concentration of Cr at the surface. As suggested by others, arsenic may diffuse into and through the encapsulents, leaving a Ga-rich phase behind at the surface of the GaAs (40). According to the results of this work, this

would result in a low solubility of Cr in the GaAs, which would explain the low levels of Cr at the surface.

The indiffusion results of Tuck et al. (5, 120), as discussed in section 6.2, can be explained in either of two ways: 1) the Cr at the surface is "built-up Cr", to be discussed in the next chapter, and the maximum bulk level is lower than seen in this work because the GaAs is in equilibrium with a Ga-rich liquid rather than $CrAs_{(s)} + Ga_{(\ell)}$ (because no arsenic source was used); or 2) the Cr at the surface is the "vacancy diffusion controlled case" Cr, and the bulk Cr level doesn't rise as high because the vacancy generation mechanism is not as efficient in their case (due to less dislocations, perhaps, in the GaAs). The fact that the Cr levels were even lower when elemental arsenic was added is probably <u>not</u> due to moving the system from the Ga-rich side to the tie triangle region (which would predict <u>higher</u> levels of Cr), but is probably due to the formation of other Cr-As compounds from elemental Cr and As, which probably changes the chemical potential of Cr.

The phenomenon of the high build-up of Cr at the surface, seen in this and in others' work will be discussed in chapter 7.

6.8 Summary of Chromium Diffusion Studies

In this chapter the studies of the diffusion of Cr in GaAs were presented. The diffusion of Cr in GaAs was studied with well-defined experiments, that used relevant phase equilbria, and using well-defined solubility information, all of which was determined in this research. The diffusion behavior was shown

to follow the substitutional/interstitial dissociative diffusion model, uncharged case. Values for key parameters of this model, including the effective diffusion coefficients for vacancy diffusion controlled Cr diffusion and interstitial controlled diffusion, and the equilibrium time constant (which controlled the rate at which the latter type of diffusion became dominant over the former type), were determined for a large section of the Ga-As-Cr ternary phase diagram from 700 to 1000°C. This diffusion model, and the phase equilibria and solubility information, explain much of the observed phenomena concerning Cr in GaAs during heat treatments, including: deep penetration of Cr into GaAs; the near-uniform increases or decreases of the bulk level of Cr in GaAs; the two different types of diffusion - with different effective diffusion coefficients - seen in various situations; changes in the diffusion profiles due to a change in surface concentration of Cr (and not to a change in diffusion coefficient, as previously assumed); and the gettering behavior of Cr in GaAs, especially from a Cr doped substrate to the surface of the LPE layer many microns away. Also, it was shown that the Frank-Turnbull, or vacancy model, for the interstitial-to-substitutional conversion is probably operating rather than the kickout mechanism. In addition, it was demonstrated how chromium can be used as a probe in GaAs, due to its extreme sensitivity to its environment in regards to its diffusion behavior and solubility, to study the defect chemistry of GaAs.

7. SURFACE PHENOMENA

7.1 Introduction

Of great importance in the study of the behavior of chromium in gallium arsenide is the subject of surface phenomena. There have been two types of unusual behavior exhibited by chromium in the surface region. One is the large surface build-up, which is most evident after outdiffusion. In normal outdiffusion, the concentration level of the impurity decreases to a low value at the surface; however, with Cr in GaAs, the concentration level often increases to a higher value right at the surface, as discussed in chapter 6. As was stated, many causes for this have been proposed, including: stress due to encapsulents, a high dislocation density at the surface, and arsenic evaporation or outdiffusion leading to the formation of gallium droplets. This high and erratic build-up was seen in my studies, both after outdiffusion and indiffusion. In addition, the observation of the Cr level above the solubility level (for the specific conditions of the system) was sometimes observed in the LPE layers grown for the junction diffusion.

The other surface phenomena observed was the depletion of Cr near the surface after indiffusion. A depletion near the surface after outdiffusion is normal; a depletion after indiffusion is quite unexpected and suggests uphill diffusion.

In this chapter, the results of my studies on these phenomena are presented. First, what exactly was observed is presented, followed by a discussion on several topics concerning these phenomena: SIMS analysis effects; phase

diagram considerations; and solubility effects, which might be of help in determining their cause or causes. Next, the experimental testing of some of the theories is discussed, as well as the probable causes based on the results. Next, the implications of these results on the behavior of Cr in GaAs is discussed, especially regarding chromium outdiffusion. In addition, the high Cr levels in some of the LPE layers is explained based on the proposed theories.

7.2 Observations Regarding Cr Build-up and Depletion

Shown in figure 7-1 are two SIMS profiles of Cr in GaAs following 800°C, 12 hour Cr indiffusion runs (using a well-defined Cr source). In these profiles, as in virtually all the indiffusion profiles obtained initially in this research, two characteristics are evident: 1) a high and erratic build-up of Cr at the surface, up to 1000 times higher than the bulk solubility level; and 2) a depletion of Cr 1-4 microns deep for 700-900°C anneals. Both of these phenomena increase with annealing temperature and time. In addition, these two phenomena appear to be totally unrelated; there is no correlation between the occurrence and magnitude of them. However, there does seem to be a correlation between the Cr build-up and the occurence of certain surface features observed by optical microscopy; these are small (10-200 microns across) solidified droplets of a silver appearing material sitting in rectangular recesses. Examples are shown in figures 7-2 and 7-3 (after 12 hour, 900°C anneals). Features such as these have been reported quite often and are believed to be gallium droplets which form when arsenic preferentially vaporizes from

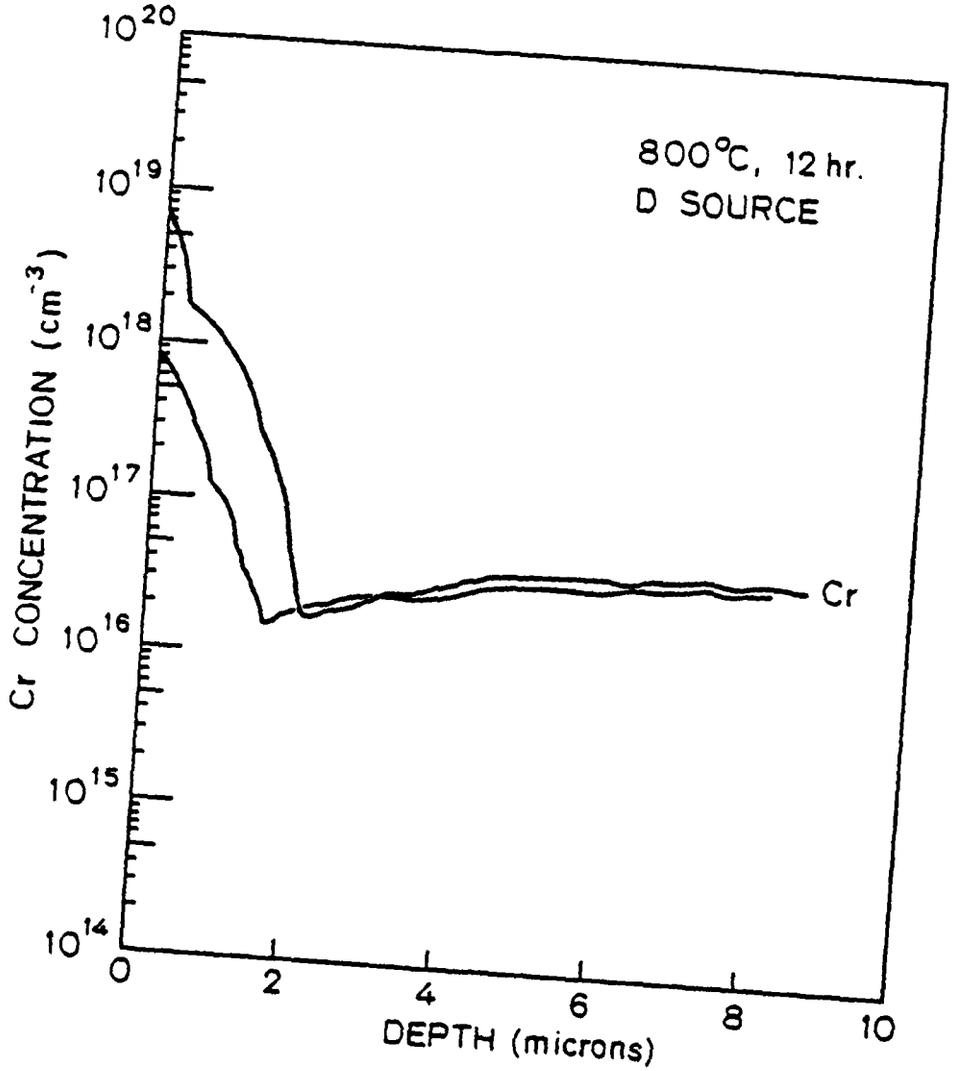

Figure 7-1. Cr concentration profiles for typical indiffusion experiments showing surface build-up and depletion. These are from 800°C, 12 hr. anneals using D source.

Figure 7-2. Optical micrograph (200X) of GaAs surface after 900°C, 12 hr. anneal.

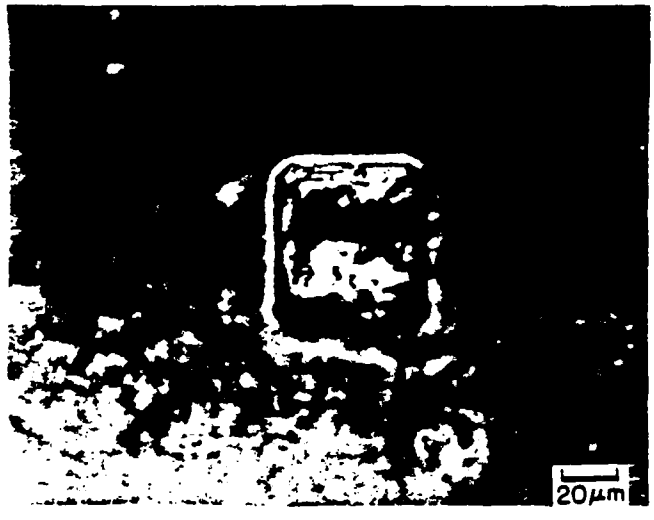

Figure 7-3. Optical micrograph (500X) of GaAs surface after 900°C, 12 hr. anneal.

the surface (108, 133).

The Cr surface build-up is also observed after indiffusion. Sometimes this is over a very narrow region (0.01 to 0.04 microns), but other times it is much deeper (up to 0.5 microns).

7.3 Discussion of Possible Causes of Cr Anomalies

7.3.1 SIMS Effects

One must consider the possibility that the Cr build-up and/or depletion seen in the profiles may by due to the profiling process itself - SIMS. In chapter 4, several SIMS phenomena were discussed, including enhanced secondary ion yield due to the presence of oxides, and the "artificial dip" near the surface related to the projected range of the primary ion. As discussd previously, these effects are far too small to explain the depletion and large build-up seen. However, the enhanced yield due to an oxide layer (which usually is present on the surface of GaAs) may be the cause of the very high, yet extremely shallow (≈0.01 - 0.04 microns deep) build-up of Cr usually present in the SIMS profiles. This is present even in the Cr profiles of unannealed GaAs (see figure 7-4), leading one to suspect that it is a SIMS artifact.

The other possibility for the large build-ups and/or depletions is that uneven sputtering near the surface could result in the anomalous profiles. This was easily checked by profiling the arsenic and gallium concentrations. If the sputtering rate changes, then the As and Ga concentrations would change. Figure 7-5 shows the As and Ga profiles, as well as the Cr profile, for an indiffusion sample (12 hr. @ 800°C).

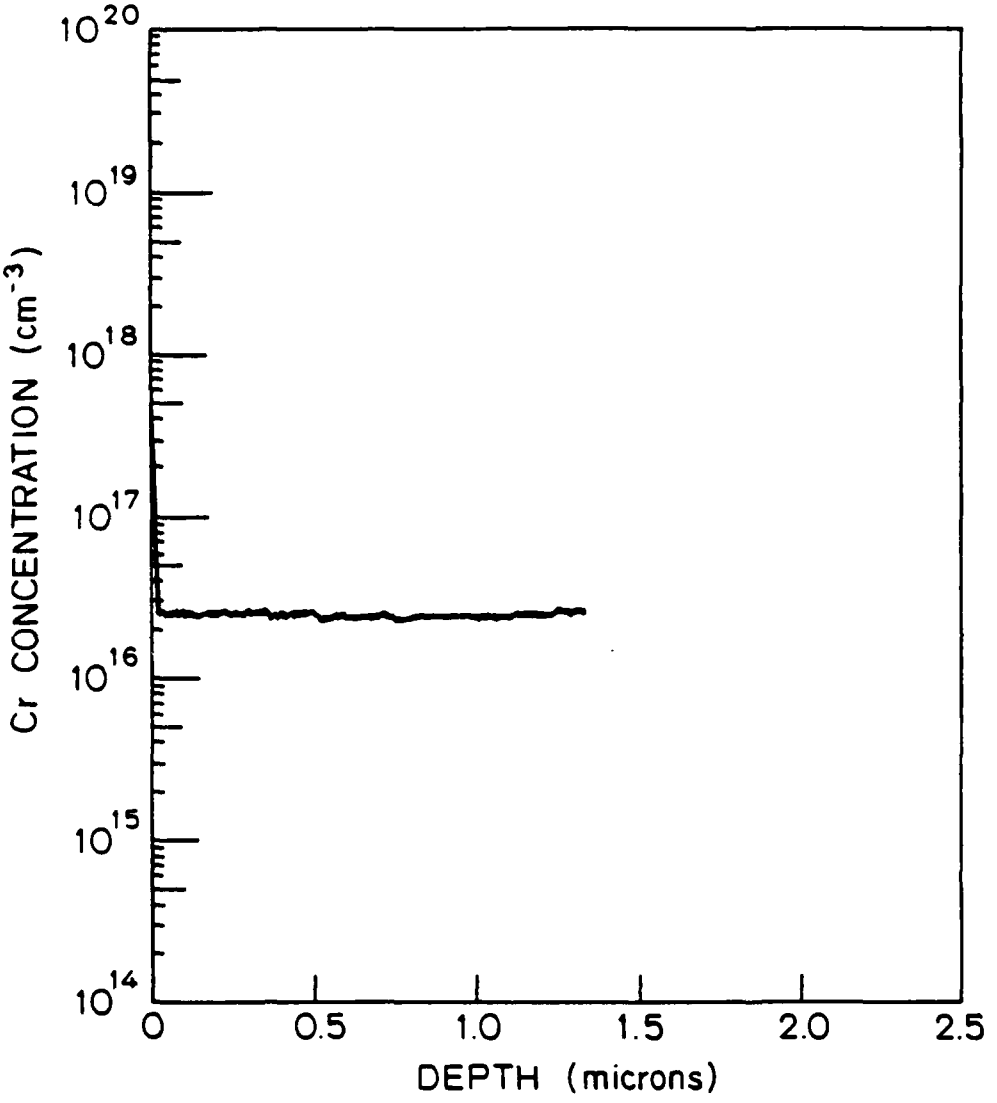

Figure 7-4. Cr concentration profile from unannealed, Cr-doped GaAs.

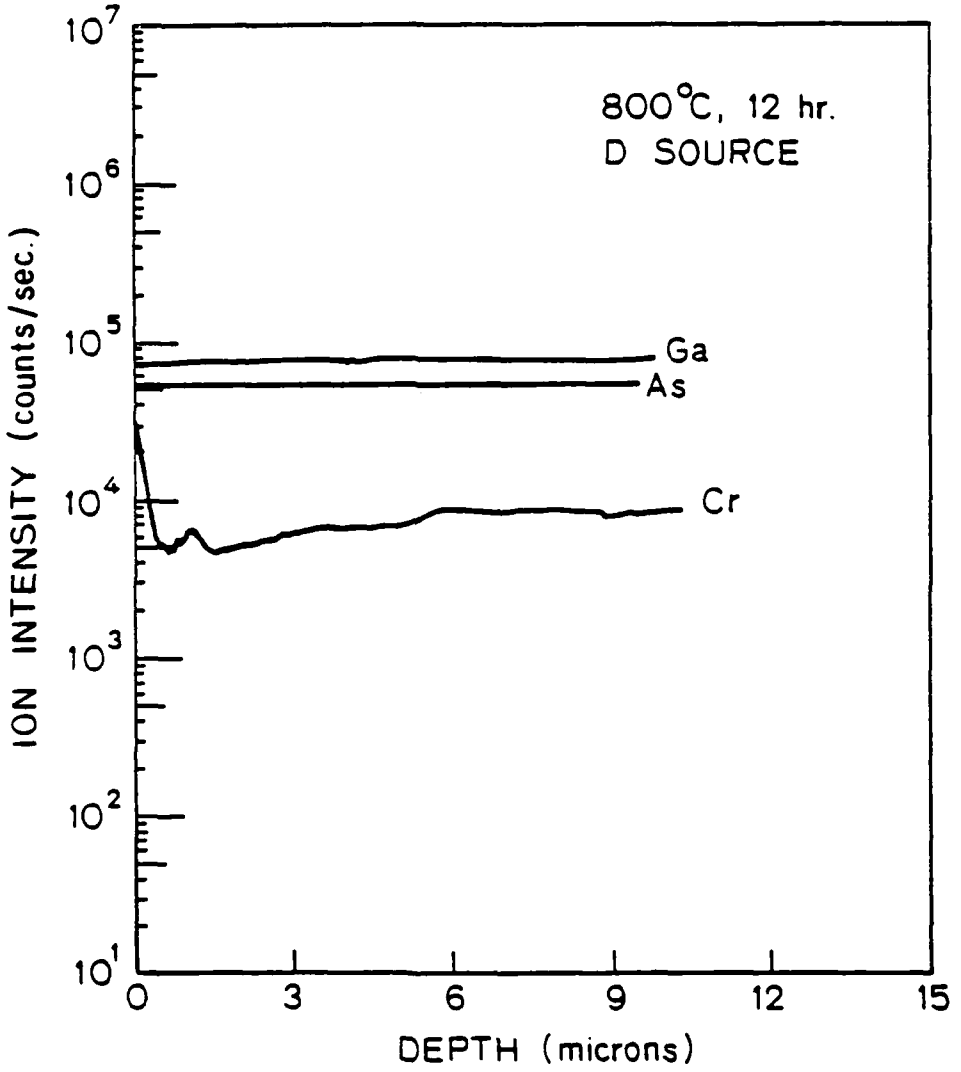

Figure 7-5. Cr, Ga, and As ion intensity profiles from 800°C, 12 hr. indiffusion experiment.

As one can see, the As and Ga levels are uniform, indicating that the Cr depletion is not a SIMS artifact. In figure 7-6, the arsenic profile is shown with the Cr profile for a different sample. In this case, the arsenic level is slightly lower in the region where the Cr build-up occurs. However, the fact that the percent change in the As level is nowhere close to the percent change in the Cr level means that the Cr build-up is not merely due to a change in sputtering rate; rather, whatever is causing the change in arsenic rate is probably also changing the Cr level. This will be made more clear later. In conclusion then, the phenomena in question do not appear to be due to anomalous profiling by SIMS. However, a clue has been given regarding the build-up of Cr at the surface, i.e., a slight depletion of arsenic there.

7.3.2 Phase Diagram Considerations

As discussed in chapter 3, one of the results of the phase diagram determinations is that a Ga-rich liquid is in equilibrium with GaAs for the temperatures of interest. It is, in fact, one of the phases in the source material and one of the phases present in the final, equilibrium state of the solubility or diffusion system. In addition, the $Ga_{(\ell)}$ phase has a high Cr solubility (≈10 a/o at 900°C), and the distribution coefficient between Cr in $GaAs_{(s)}$ and in the $Ga_{(\ell)}$ phase is quite low (in the 10^{-3} range). Therefore, if some $Ga_{(\ell)}$ should be present in the system, it would dissolve a considerable amount of Cr, and at a much higher concentration than in $GaAs_{(s)}$. If, for some reason, the $Ga_{(\ell)}$ phase should be present on the surface of the GaAs

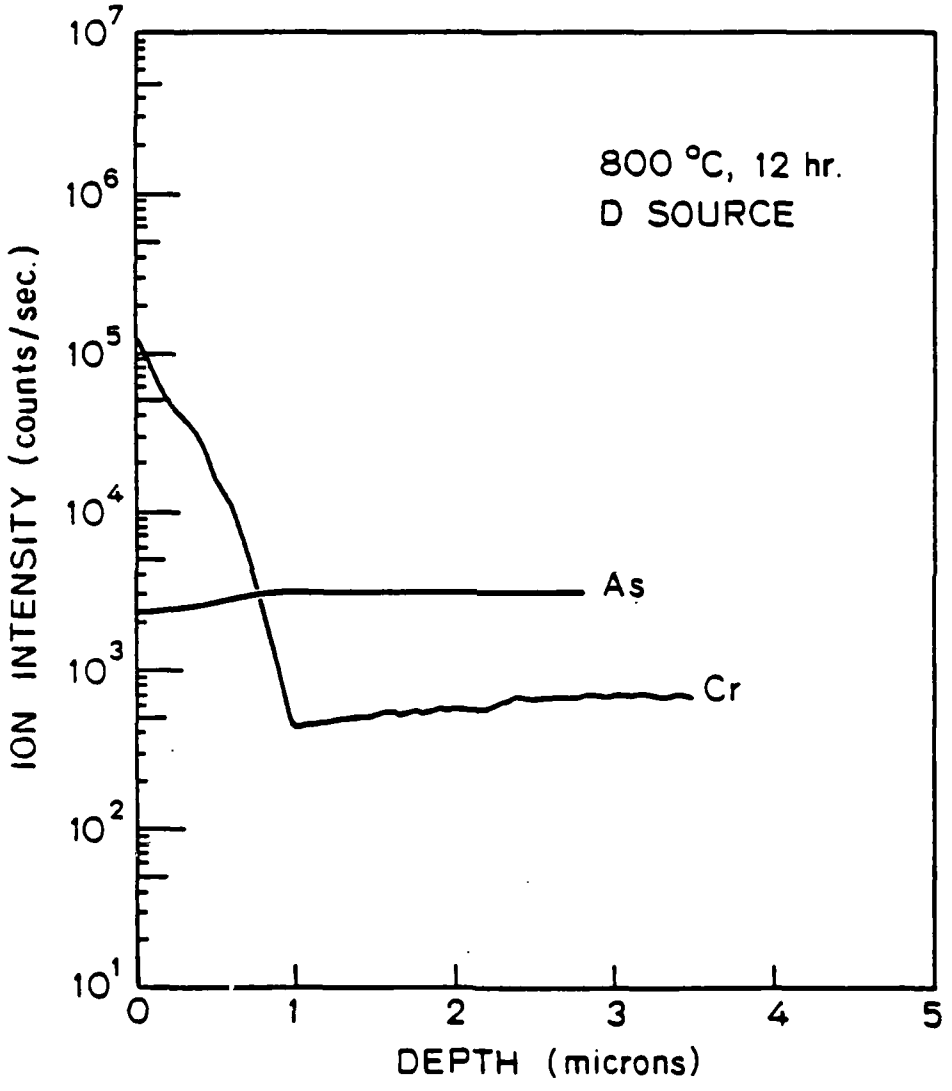

Figure 7-6. Cr and As ion intensity profiles from 800°C, 12 hr. indiffusion experiment.

wafer during a diffusion or solubility anneal, then as equilibrium is approached, more and more Cr would be dissolved in the liquid phase until the high equilibrium liquid solubility level is reached.

The formation of Ga droplets on the surface of GaAs, as previously discussed, is commonly observed. As discussed in chapter 2 regarding reaching the final equilibrium state, achieving the equilibrium vapor pressure of all the components must be taken into account. In the case of annealing pure GaAs in an ampoule at 900°C, the equilibrium partial pressure of arsenic is $\approx 10^{-5}$ atm (134), while that of gallium is $\approx 10^{-7}$ atm. This explains the formation of Ga pools on GaAs; much more arsenic leaves the surface than Ga in order to achieve the equilibrium vapor pressure and, therefore, regions of pure Ga are left behind (135). This behavior is illustrated in figure 7-7 which shows the surface of a GaAs wafer which was annealed in an ampoule at 1000°C for 2 hours. Also shown, in figure 7-8, is the surface of a GaAs wafer annealed with enough elemental arsenic added to the ampoule so that the partial pressure of arsenic is ≈1 atm., greater than the equilibrium pressure of arsenic over GaAs, and hence large enough to prevent dissociation of the GaAs wafer. (Annealing in an arsenic overpressure is common practice in GaAs processing (136).)

It is a reasonable to assume that the partial pressure of arsenic in the three condensed-phase tie triangle region containing $GaAs_{(s)}$, $CrAs_{(s)}$, and $Ga_{(\ell)}$ is high relative to the partial pressures of Cr and Ga. Therefore, one would

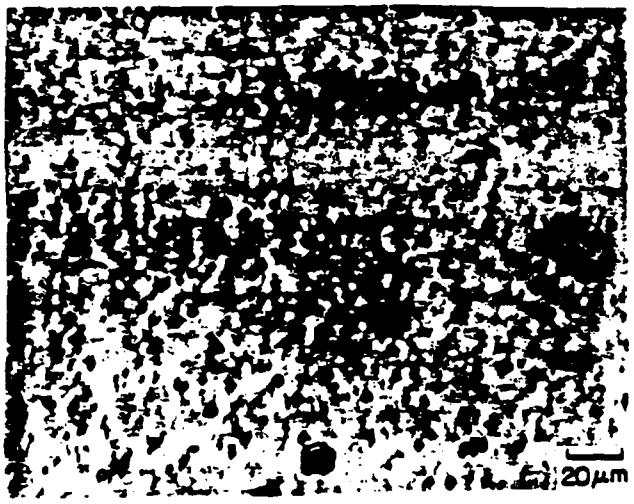

Figure 7-7. Optical micrograph (500X) of GaAs surface after 1000°C, 2 hr. anneal.

Figure 7-8. Optical micrograph (500X) of GaAs surface after 1000°C, 2 hr. anneal - with elemental arsenic added to ampoule.

expect that more arsenic than gallium would leave the starting material (both the GaAs wafer and the source material) in order to achieve the equilibrium vapor pressure. This would leave Ga droplets on the GaAs surface, which would then dissolve Cr to its solubility level.

This process is shown schematically using a "reaction path" diagram in figure 7-9. Initially, the GaAs surface is at point A. Upon heating, arsenic selectively vaporizes from the surface, leaving Ga droplets. The composition of these droplets is represented by point B. However, in attaining equilibrium, the composition of the droplets moves towards point C with an increase in Cr content. Therefore, the total system at equilibrium consists of $GaAs_{(s)}$, $CrAs_{(s)}$, $Ga_{(\ell)}$ (at point C), and the vapor phase, with some $Ga_{(\ell)}$ on the $GaAs_{(s)}$ surface, as well as in the source.

Because of the high Cr solubility in the $Ga_{(\ell)}$ phase compared to in $GaAs_{(s)}$, even a small amount of the $Ga_{(\ell)}$ phase on the surface could lead to a large Cr level as measured by SIMS. Even if only 1/1000 of the area analyzed by SIMS was $Ga_{(\ell)}$, the Cr level could increase by 100 times just because of the relative solubilities. Because of these considerations, and because of the correlation between the occurrence of the Ga droplets and the Cr build-up, it was suspected that this was the main cause for the Cr build-up at the surface seen in these studies.

7.3.3 Discussion on Solubility in Regards to Cr Depletion

Another consideration regarding solubility is the effect that other impurities have on the solubility of chromium in

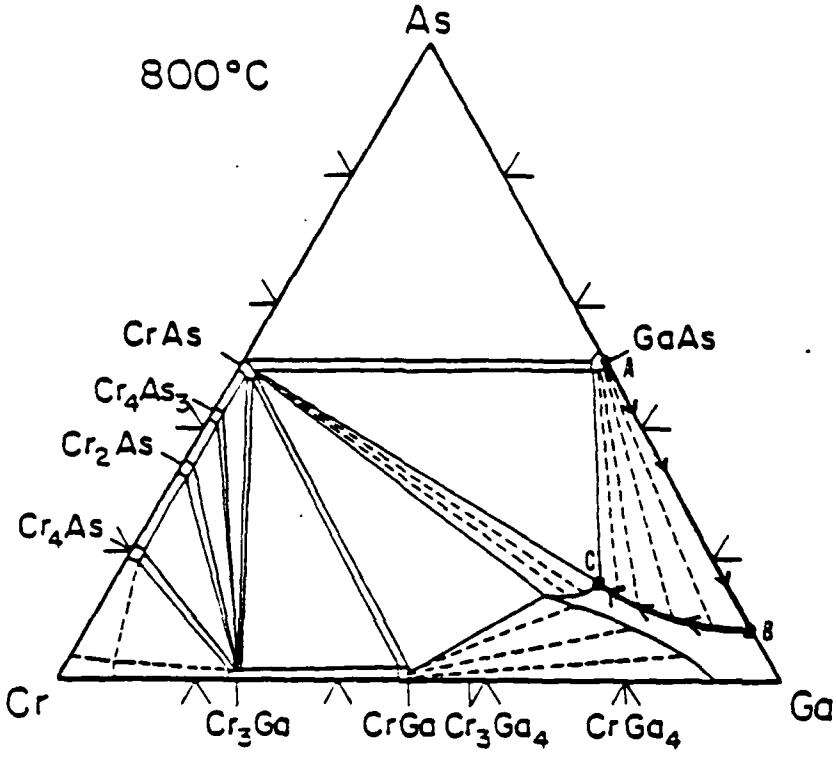

Figure 7-9. Schematic diagram of reaction path of GaAs surface regions.

GaAs. As discussed in chapter 4, the presence of other acceptors in GaAs would decrease the solubility of an acceptor, such as Cr, and the presence of donors would increase the solubility of an acceptor. This latter effect was shown to be true for the case of chromium in Si and Te doped GaAs. Therefore, a build-up of Cr in GaAs above the normal case (i.e., in undoped GaAs) might be due to the presence of a donor impurity; likewise, a depletion could be due to the presence of an acceptor.

As discussed in chapter 4, chromium in undoped GaAs is probably uncharged and only becomes an acceptor when n-type impurites are introduced. Therefore, it might not act as a normal acceptor in the presence of another acceptor and decrease in solubility due to electronic effects. However, since most acceptors occupy the same site as Cr does (Ga sites), then site (or vacancy) competition could likewise lead to a decrease in the amount of each. This would especially be true if there is a kinetic problem with the impurity atoms incorporating into the site, such as is the case for Cr and other impurities incorporating into a Ga site in GaAs by finding a vacancy. The decrease in the Cr level in GaAs due to the presence of other impurity atoms has been reported by Asbeck (82), who observed a decrease in the Cr level when Zn and Cu atoms were introduced into the GaAs.

Another cause of increased or decreased solubility is an appreciable change in defect density and/or structure. A region that has an abnormally high concentration of dislocations, vacancies, stress fields, etc., could change

the basic structure of the crystal enough so that the "solubility" of an impurity in it could be different than that of the crystal in the equilibrium state. By definition, the true solubility of an impurity in a substance is the solubility when the substance is in the equilibrium state (with the equilibrium density of vacancies, etc.). However, depending on the history of the material, higher or lower numbers of these defects may be frozen in. There are three ways to check this: perform the solubility anneal for a "long" time to see if the effect decreases or not; pre-anneal the substrate at a high temperature; or remove regions such as surfaces with polishing or slicing damage.

The last two effects, the site competition and defect effects, are kinetic effects and will therefore disappear in time. In contrast, the electrical effect applies even for equilibrium conditions. Another way one impurity can change the solubility of another is by producing stress fields in the matrix material which in turn influence the solubility of the other impurity. This, like the electrical effect, is an "equilibrium effect" and, therefore, will not anneal out.

An additional phenomena is that of impurity segregation to the substrate surface, which is occasionally observed. It is believed to occur when the impurity lowers the surface tension and hence minimizes the energy of the system (137). Therefore, for some impurities, its "solubility" is higher at the surface than in the bulk, whereas, some impurities have <u>lower</u> solubilities at the surface because they <u>raise</u> the surface tension. However, either case would result in reproducible

levels at the surface (for a given temperature), which is clearly not the case for Cr build up in GaAs. Also, a lowering of the surface concentration usually occurs for cases in which the impurity increases the melting point of the substrate (137), which is not the case for Cr in GaAs; therefore the depletion is probably not a direct result of this.

7.4 Experimental Testing To Find Causes of Phenomena

7.4.1 Chromium Build-up

First to be considered is the large chromium build-up seen at the surface following Cr solubility and diffusion anneals. As mentioned, a likely explanation for this is the formation of gallium droplets which have a high Cr solubility. Two observations, previously discussed, are consistent with this theory: 1) there is a correlation between the number and size of the droplets and the magnitude of the Cr build-up as measured by SIMS; and 2) the build-up increases with increasing annealing time and temperature, both in concentration level and in depth into the GaAs.

To test the theory, two indiffusion runs were done at 800°C, for 12 hours, using H source. Sample E was in an ampoule with a small volume ($\approx$ 2 cm^3 total), with a large amount of source material, and the GaAs wafer was large. Sample L was a small GaAs wafer, had a small amount of source material, and was in a large ampoule ($\approx$6 cm^3). If the build-up is due to Cr in $Ga_{(\ell)}$, which forms when arsenic leaves the GaAs surface to provide for the equilibrium arsenic vapor pressure in the ampoule, then sample E should result in less Cr build-up. The reason for this is that less $Ga_{(\ell)}$

will form on the surface because less arsenic is needed in the ampoule due to the smaller volume. Also, because of the larger size of wafer and larger amount of source material, less arsenic will leave per square cm. of surface. The resulting SIMS Cr profiles are shown in figure 7-10. As predicted, sample E shows a much smaller Cr build-up. Shown in figures 7-11 and 7-12 are micrographs of the two surfaces. Again as predicted, the surface of sample E has much less $Ga_{(\ell)}$ present.

Another experiment was done to confirm the fact that the Ga droplets on the GaAs surface do contain large amounts of Cr. A GaAs wafer was annealed in an ampoule, with H source, at 1000°C for 12 hours, and quenched. Many Ga droplets were observed. A typical one was analyzed by an electron microprobe (sampling size of $\approx 1\ \mu m^2$). The results were: 68.7 a/o Ga; 14.9 a/o As; and 16.4 a/o Cr. According to the 1000°C ternary isotherm, these numbers are within 5% of what the $Ga_{(\ell)}$ composition should be. In addition, a spot next to the Ga droplet (in the GaAs matrix) was analyzed to check the accuracy of the analysis. The results were: 50.01 a/o Ga; 49.99 a/o As, and 0.000 a/o Cr, i.e., below the detection limit for Cr; these values confirmed the accuracy of the analysis.

Finally, a GaAs wafer was annealed, again at 1000°C for 12 hours, with H source, but this time slow cooled to room temperature. According to the phase equilibria studies, the $Ga_{(\ell)}$ phase, upon cooling, should convert to $CrGa_{4(s)}$ and $Ga_{(\ell)}$ (with less Cr), plus a little $CrAs_{(s)}$ and $GaAs_{(s)}$. The sample was crushed and analyzed by XRD. The diffraction

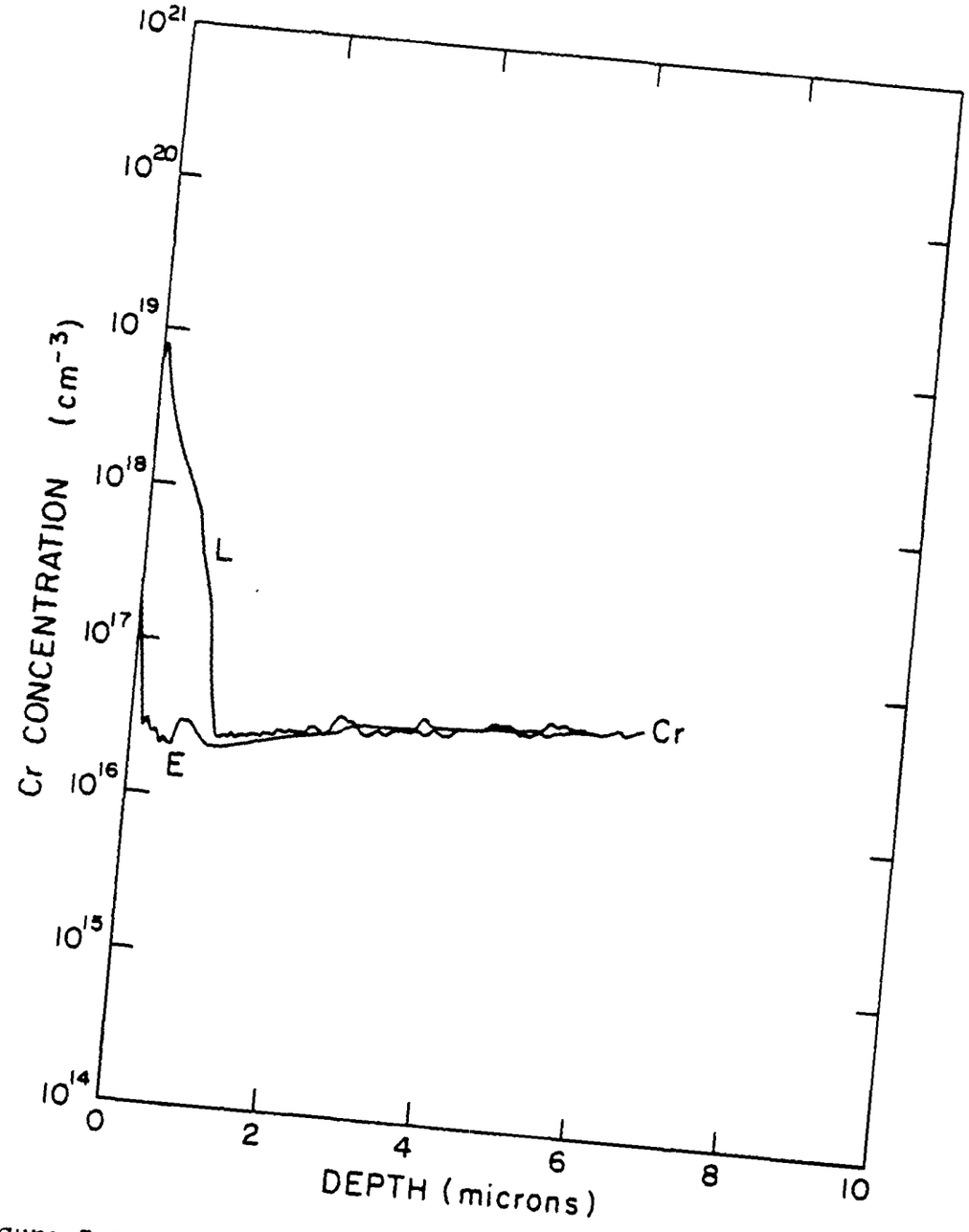

Figure 7-10. Cr concentration profiles from 800°C, 12 hr. indiffusion experiments. Sample L conditions: large volume ampoule, small source and GaAs. Sample E conditions: small volume ampoule, large source and GaAs.

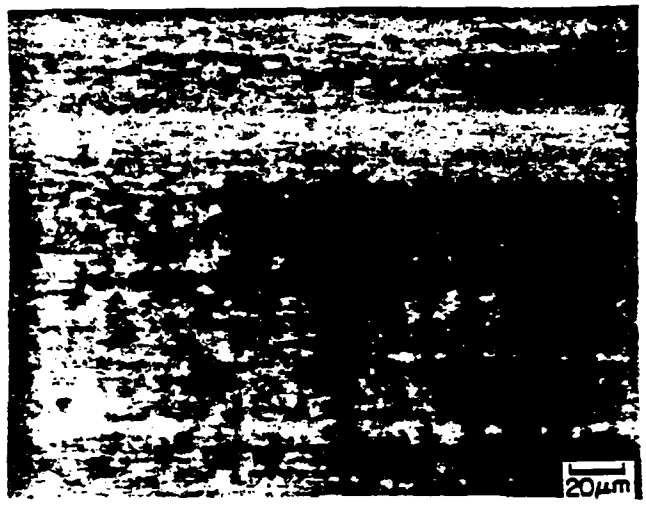

Figure 7-11. Optical micrograph (500X) of GaAs surface of experiment L.

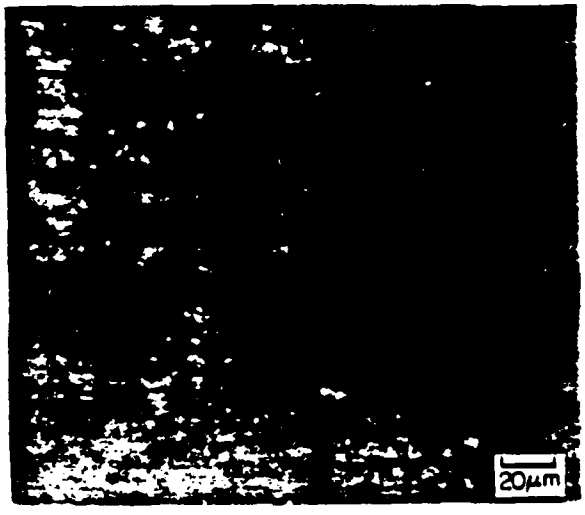

Figure 7-12. Optical micrograph (500X) of GaAs surface of experiment E.

pattern indicated that there was some $CrGa_{4(s)}$ present.

One final observation was that evidence, or "artifacts", of Ga droplets could be seen in the interior of the SIMS crater in many cases when there was Cr build-up at the surface. The actual Ga droplet was gone by the time the entire SIMS profile was completed since it was only in the surface region; however, small areas of uneven morphology resulting from slightly uneven sputtering of that phase could be seen.

The SIMS arsenic profile, which shows the the As level to be slightly less in the region where the Cr build-up occurs, can now be explained: the sputtering rate may be a little different there due to the second phase present; in addition, that phase ($Ga_{(\ell)}$) has less arsenic than the matrix.

In conclusion, the major cause of the Cr surface build-up is the formation of the Ga-rich liquid phase which forms when arsenic selectively vaporizes in order to establish the equilibrium arsenic vapor pressure. Even with small volume ampoules, the surface build-up was not always eliminated, especially during the higher temperature anneals. However, it was believed to have had a negligible influence on the actual diffusion process.

7.4.2 Chromium Depletion

In contrast to the chromium build-up phenomenon, the cause of the Cr depletion, after indiffusion, was not quite so easy to determine. However, after many experiments, and a little luck, a cause was discovered.

Initially, a few theories of its origin were considered, but none of these were appropriate. One of these theories was

the uneven SIMS sputtering rate. But, as previously discussed, uniform gallium and arsenic concentration levels in that region disproved that. Another theory proposed that Cr outdiffused during the quench, because the Cr solubility is lower at lower temperatures. This was the reason given for similar profiles for Au in InAs (62) and Cu in InAs (138). Tuck et al. (59), who made the same observation with Au in InP, did not accept this theory for all those systems, saying that the results were not consistent with one another. This theory was tested with Cr in GaAs by me by changing the quench rate. However, no change was seen in the profiles. Besides, the diffusion coefficients for these times and temperatures are far too low to account for that much depletion.

It was therefore concluded that the Cr depletion seen is not an artifact of the profiling, but is real and occurs during the indiffusion. This suggests "uphill diffusion", diffusion up the concentration gradient. However, in light of the proposed diffusion mechanism, this type of behavior can be explained, as discussed in section 5.3 of chapter 5, without using normal uphill diffusion arguments. Cr atoms diffuse in interstitially, down the interstitial concentration gradient. They then convert to substitutional atoms, and more interstitials diffuse in. The concentration of the substitutional atoms builds up to the substitutional solubility level, whatever it is in that region. If a region, such as a region near the surface, has a lower Cr solubility than adjacent regions, the final Cr concentration will be lower; this situation could lead to profiles such as we have seen.

Therefore, it was presumed that the cause of the Cr depletion near the surface was a lower Cr solubility near the surface. The cause of the lower solubility was not easy to determine.

Initially it was presumed that surface damage and/or stress at the surface, caused by slicing and polishing, might cause the lower Cr solubility. The fact that the depletion did not occur after very high temperature anneals ($\geq$ 1000°C), except for very short times, suggests that the damage was annealed out at the high temperatures. To test this theory, three experiments were conducted. One was pre-annealing the wafer before the actual indiffusion to reduce the damage and/or stresses. This was done at 1000°C for 6 hours, with either elemental arsenic in the ampoule to prevent arsenic vaporization, or with J source (which would introduce only a very low level of Cr into the GaAs, and yet provide a source of arsenic). In each case, after doing subsequent normal indiffusions at 800°C for 12 hours with H source, the depletion region was still present and, if anything, worse. Another experiment was pre-etching the wafer to physically remove the surface region. This was done using various etching solutions, e.g., 16:1:1 $H_2O:H_2O_2:H_2SO_4$, and etching off from 1 to 20 μms. Subsequent indiffusion again resulted with depletion regions. The third experiment was simply to do the indiffusion for long times and see if the depletion is reduced with time. However, after 12, 18, and 14 hours at 900°C, there was still a depletion in each case, and it actually increased in depth with time. From these experiments, it was concluded

that a damaged or "non-equilibrium" surface region was not the cause of the Cr depletion there.

Another cause for a change in solubility or expected concentration level locally, is the presence of other impurities, as discussed previously. It was therefore considered that an acceptor or an impurity on a Ga site might be present in the surface region. Using SIMS, the various common impurities - Si, Cu, Fe, O, and C - were searched for. However, none showed high levels near the surface. It was then discovered that Klein and Nordquist (139) proposed that p-type surface conversion occurred in undoped GaAs, after annealing in a H_2 atmosphere, due to high levels of manganese at the surface. The Mn levels reached the mid 10^{17} cm^{-3} range over the first four microns after a 20 minute 740°C anneal. Virtually all of it was electrically active. Klein concluded that the Mn was gettered to the surface from the bulk of the GaAs (which normally has levels of 10^{14} to 10^{15} cm^{-3}) and didn't come from outside the wafer. Others (41, 127, 140, 141) have also recently studied this phenomena. Palmateer et al. (127), like Klein, found that the Mn accumulation decreased after successive anneal/polishing cycles, consistent with the theory that the Mn comes from inside the GaAs. Klein suggested that it is the indiffusion of gallium vacancies that causes this. However, when annealing in an argon atomosphere rather than in hydrogen, Klein found that no Mn accumulated at the surface, the reason for which is not known. It appears that there is a complex relationship between the atmosphere (and/or surface) and the Mn accumulation phenomena. For whatever

reason the Mn does accumulate at the surface, if it is coming from the bulk, it strongly suggests that the substitutional/interstitial diffusion mechanism is again at work.

In any case, manganese, a known acceptor in GaAs, was analyzed by SIMS. In many indiffusion samples, Cr and Mn were simultaneously profiled. Three examples are shown in figures 7-13, and 7-14. As one can see, the Cr depletion and Mn build-up complement each other in each case. This was true for all the cases that Mn was profiled (15 in all). In addition, Cr and Mn were profiled in several of the LPE junction samples after various anneals, with and without J sources in the ampoules. In each of these there was Mn build-up at the surface, but not in the interface (junction) region. This explains why "normal" Cr diffusion in the junction region can be observed (the vacancy diffusion controlled Cr diffusion), whereas this cannot usually be seen at the surface in the indiffusion samples. From all these observations it is concluded that the decrease in Cr concentration near the surface after indiffusion is due to the build-up of Mn there.

As stated earlier, it appeared that the depletion did not occur at higher annealing temperatures (1000°C and above). The SIMS analysis was done on a sample annealed at 1000°C, again profiling both Cr and Mn. The results are shown in figure 7-15. As one can see, the Mn is still there; however, the Cr profile does not appear to be affected by the presence of the Mn. This is explainable if the lowering of the Cr level is due to an electrical effect. At 900°C, the intrinsic

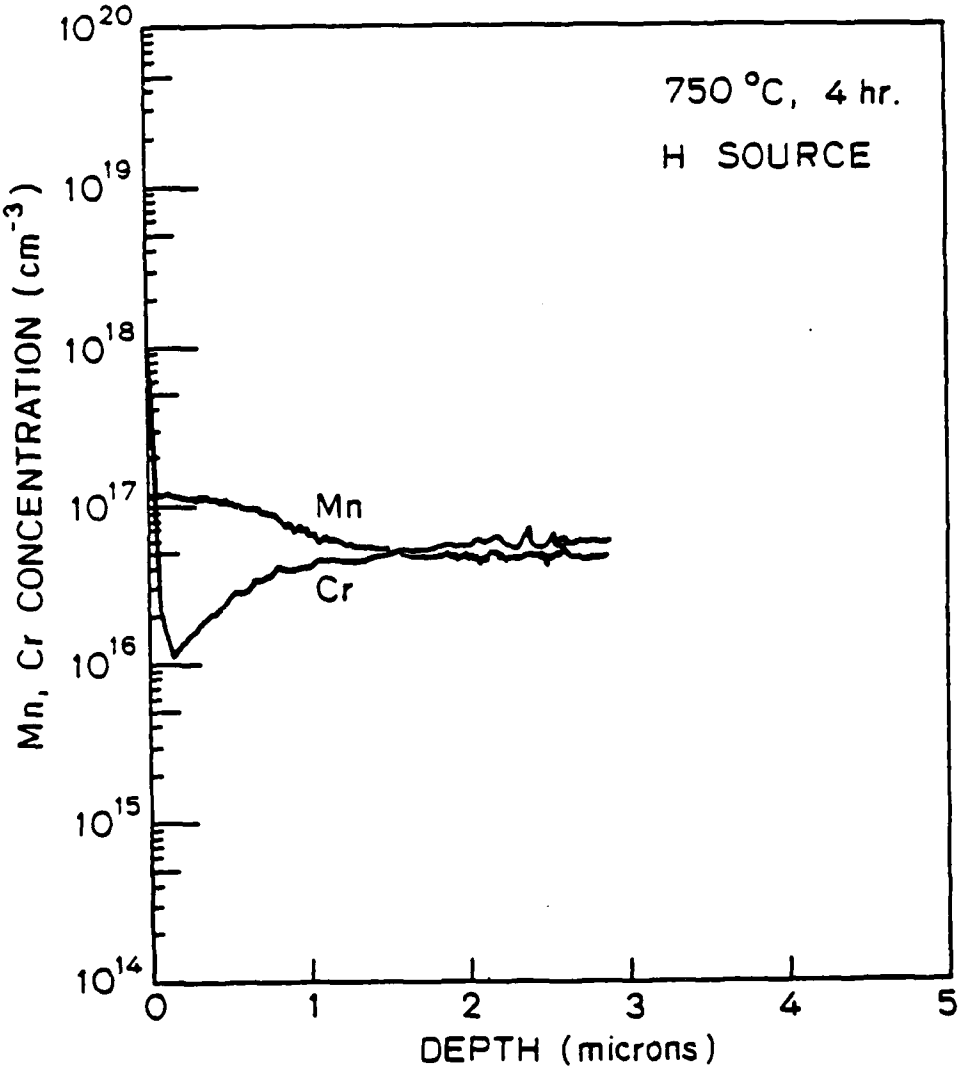

Figure 7-13. Cr and Mn concentration profiles from 750°C, 4 hr. indiffusion experiment.

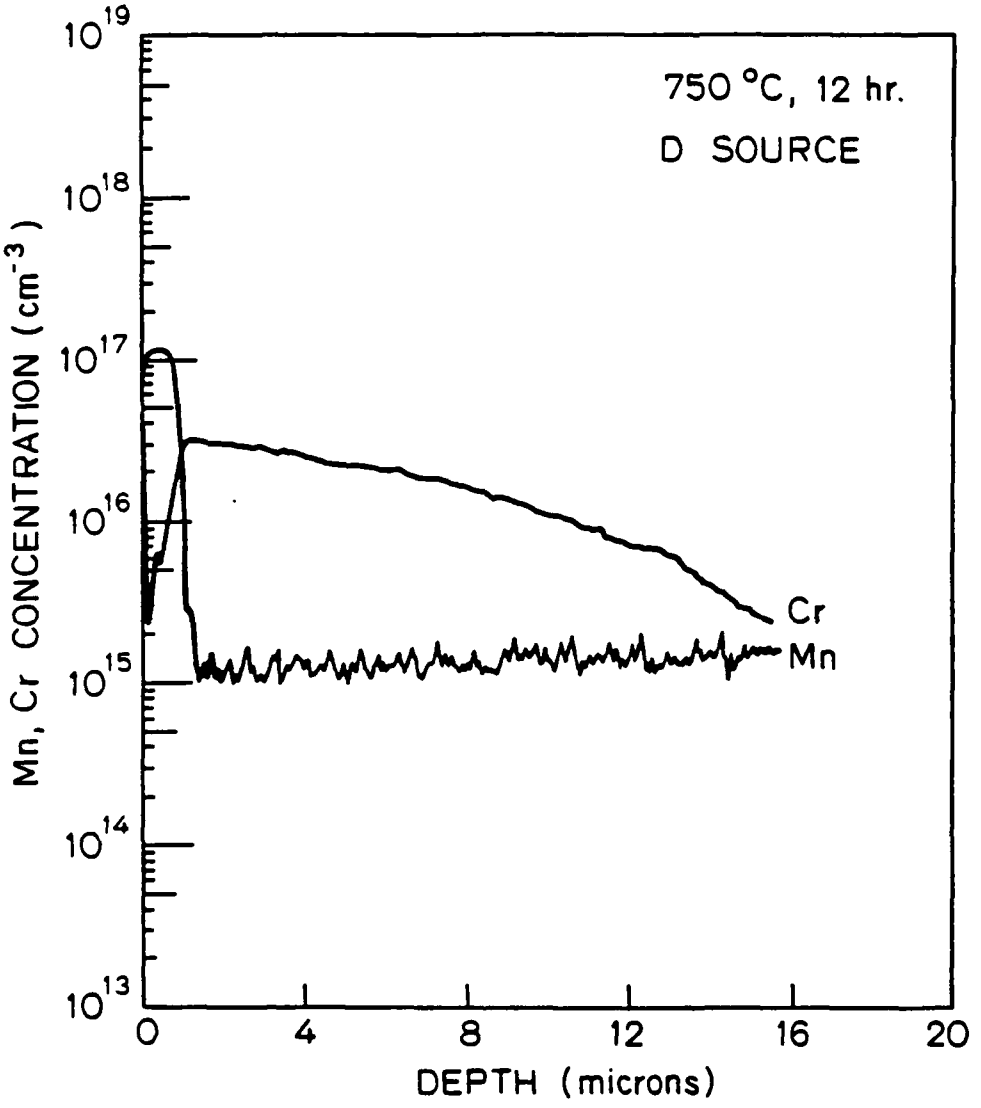

Figure 7-14. Cr and Mn concentration profiles from 750°C, 12 hr. indiffusion experiment.

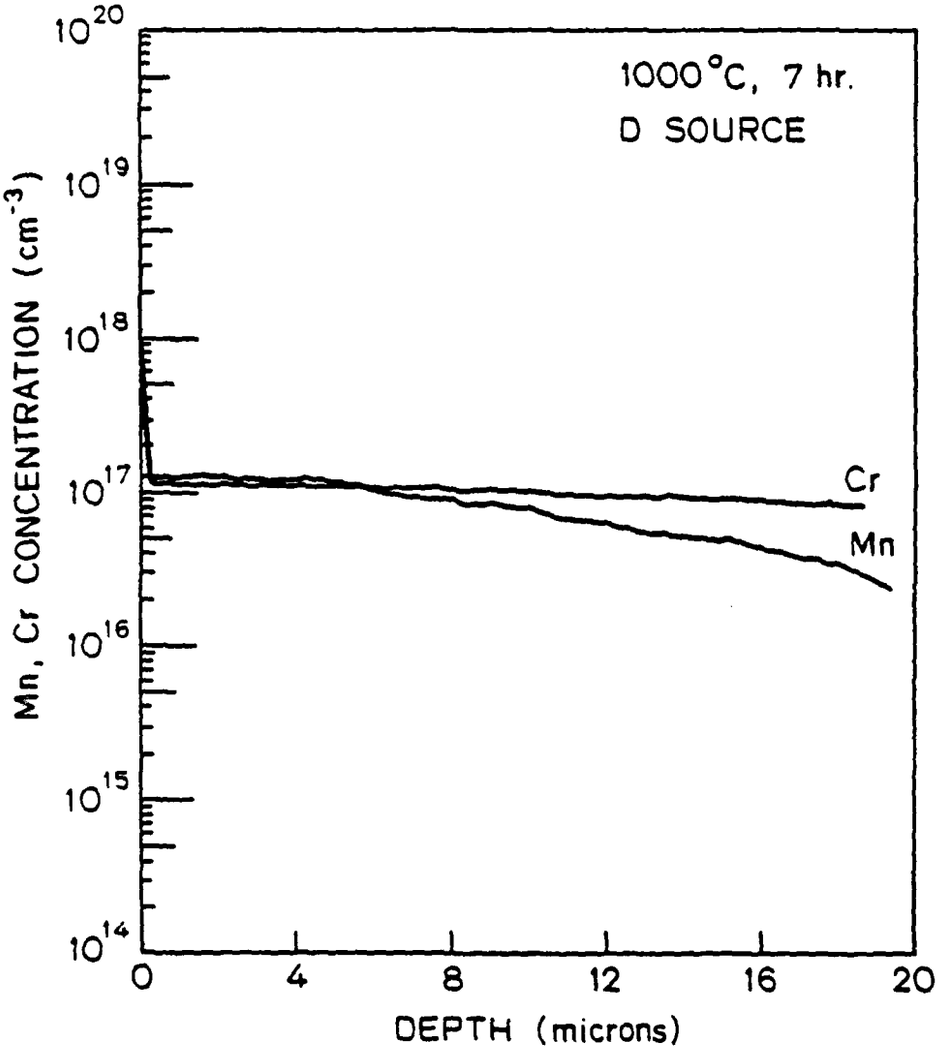

Figure 7-15. Cr and Mn concentration profiles from 1000°C, 7 hr. indiffusion experiment.

carrier concentration is $\approx 2 \times 10^{17}$ cm^{-3} (13), while at 1000°C it is $\approx 5 \times 10^{17}$ cm^{-3}. Therefore, as the temperature is increased, the electrical effect of the Mn is swamped out by the intrinsic carrier concentration, and the Mn has little or no effect on the Cr; the presence of Mn would not change the hole or electron concentration in the GaAs. Also, in the two Te-doped GaAs (n-type) indiffusion samples, only small depletions are observed. This is consistent with the electrical effect theory, since the electrons from the Te would compensate the holes from the Mn.

However, one can not rule out the possibility that it is not entirely an electrical effect - the presence of the Mn might also have an effect on the Cr level just because it is on the same site and it may change the state of the crystal by mechanical or crystallographic effects, as discussed earlier. The GaAs might only be able to accommodate so many impurity atoms on the gallium sites, whether they are Mn atoms or Cr atoms, and since Mn and Cr are both transition elements and right next to each other in the periodic table, they may not be very distinguishable. The fact the Cr level is affected even when the Mn level is below the n_i level in some of the profiles would suggest that it is not entirely an electrical effect. And even the vacancy or site competition theory, closely related to this, is not impossible. It was ruled out because it was believed that <u>eventually</u> the Cr would reach its equilibrium solubility level which it did not do for the times measured. However, if the Mn is constantly arriving at the surface, then the Cr level might be kept low there for long

times. The observation that the final solubility of Cr in Si-doped (n-type) GaAs is higher than in undoped GaAs, but that the rise to the solubility level is slower (Si is on a Ga site) shows that both electrical and "mechanical" effects are important. At this point, the exact reason or reasons why Mn causes the Cr depletion is not known; however, it is clear that it is the cause.

An attempt was made to get rid of the Mn by pre-annealing a GaAs wafer in 0.1 atm arsenic overpressure (using elemental arsenic in the ampoule) for 24 hours at 750°C, then etching the surface. However, the arsenic anneal did not produce any Mn build-up at the surface. The reason for this is not known. If the Mn builds up at the surface by gallium vacancies diffusing in, one would expect an even greater tendency for this to occur in an arsenic atmosphere because the gallium vacancy concentration would be higher. But this did not occur.

7.3 Advantages of Having Mn Present

Even though the presence of manganese at the surface of the GaAs wafer did obscure some aspects of the chromium diffusion (especially the vacancy diffusion controlled Cr diffusion at the surface for indiffusions), there were three benefits of having it there and affecting the chromium. First, it is a good confirmation of the substitutional/interstitial dissociate diffusion mechanism. If the diffusion was the "normal" type (interstitial and/or substitutional diffusion down a concentration gradient), and the surface concentration was lowered (due to the Mn), then that would be the maximum level throughout. However, the "uphill diffusion" seen can

easily be explained by the sub./int. dissociative mechanism, as discussed earlier. And as Kendall (77) points out, this "uphill diffusion" is a good indicator of this type of diffusion. Secondly, the depletion in the Cr level is a good indication that that Cr is in solution. In many of the Cr profiles, some Cr build-up due to the Ga droplets still occurred to some extent, and it might have been difficult to distinguish the "build-up Cr" from the Cr in solution. However, the Mn only affects the Cr in solution. Therefore, the "solution Cr" always had a small depletion zone near the surface, while the "build-up" Cr did not, and the two were easily distinguishable. Thirdly, because the Cr level in the depletion region is lower than the bulk level (which can be quite low for short time/low temperature diffusion), we know that the level in the bulk (which is often very low and flat) is above the background level of the SIMS.

Therefore, there were actually some benefits to having the Mn there and affecting the chromium. Luckily, neither the Mn or the Cr build-up had any apparent affect on the other parts of the diffusion process, such as the deep, interstitial controlled diffusion, as evidenced by how well the model fit the profiles.

7.6 Application of Surface Phenomena Results to Other Cr Behavior

The results of these surface phenomena studies can now be used to explain some of the "anomalous" behavior of Cr in GaAs seen by others and in the present work. For outdiffusion, a high Cr build-up at the surface is usually observed, as

mentioned earlier. Part of this (0 to .04 microns deep) can be attributed to the enhanced yield due to an oxide layer, or some other SIMS artifact. However, in many cases, the build-up goes much deeper into the wafer, and this can be explained, in part, by gallium droplet formation. As was the case with the Cr indiffusion, this build-up could be reduced by using a smaller volume ampoule (see figure 7-16).

The fact that others have shown rather conclusively that the presence of dislocations, stress, and lattice damage (due to ion implantation, for example) does result in a redistribution of Cr in the regions where the defects are present (usually with increasing Cr level concentrations in these regions) suggests that these factors may also be responsible for some of the Cr build-up at the surface. Perhaps the dislocations, damage, and/or stresses, or whatever causes them (encapsulents, etc.), cause the formation of gallium droplets or inclusions, which then results in the high levels of Cr. As mentioned earlier, it has been suggested that arsenic diffusion into or through the encapsulents may result in Ga inclusions at the GaAs surface (40, 142). Gyulai et al. (143) claim, from their backscattering measurements, that gallium does accumulate at the encapsulent/GaAs interface for both SiO_2 and Si_3N_4 encapsulents following 700-800°C anneals. Also, Morkoc (37) reports that no electrically active Cr is detected in the regions of high Cr build-up at the surface. This implies that the Cr is not in solution there, consistent with it being in a gallium precipitate.

An extreme example of Cr surface build-up is shown in

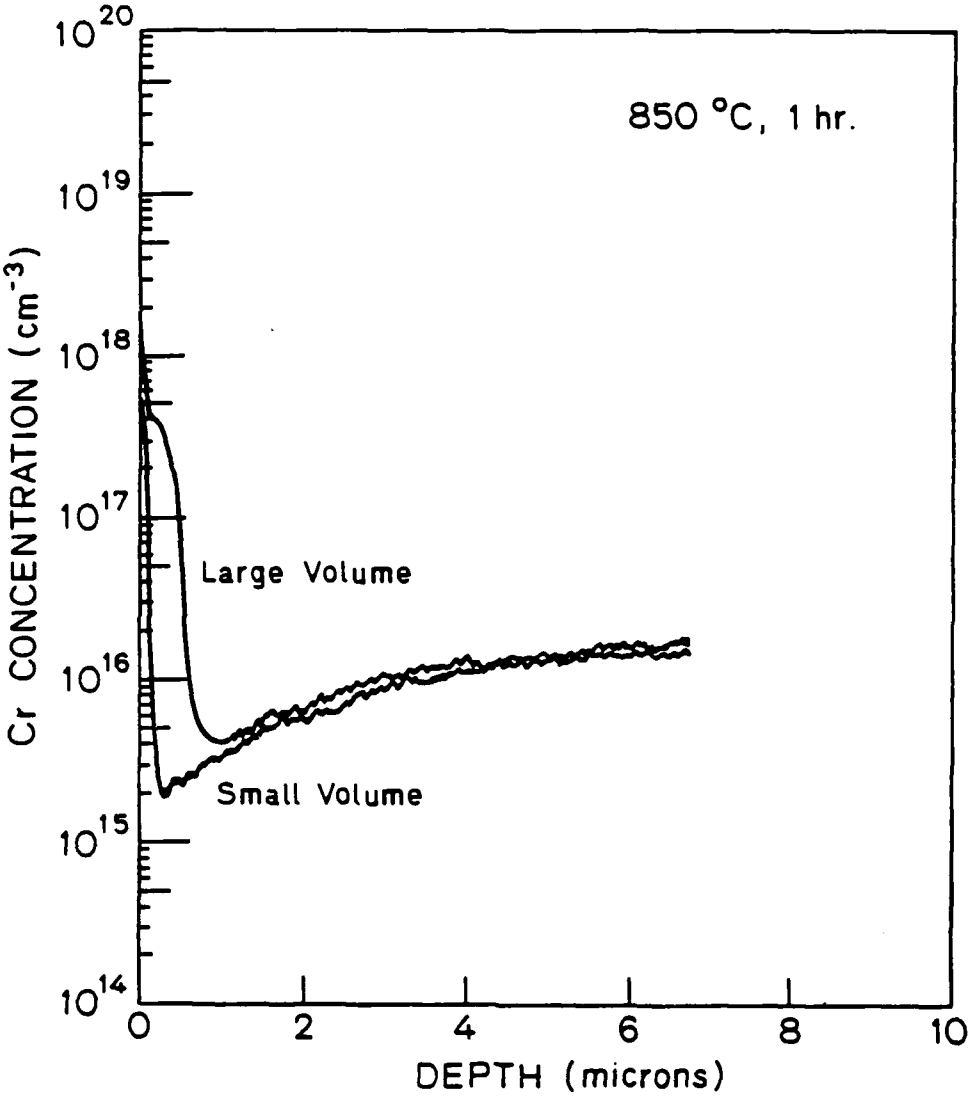

Figure 7-16. Cr concentration profiles from 800°C, 1 hr. out-diffusion experiments. A: small volume ampoule, B: large volume ampoule.

figure 7-17. This is a result of annealing Cr-doped GaAs (1 hr. @ 800°C) in an evacuated ampoule after a "different" cleaning technique. The same cleaning schedule as outlined in chapter 4 was followed, except no wafer holder was used; rather, the GaAs wafer was allowed to "slosh" around in the bottom of the cleaning beaker. As one can see, much more Cr build-up occurs than when the GaAs is kept in the wafer holder. It is presumed that this is due to the damage that is produced on the surface and/or gallium inclusions that form. This illustrates how critical the handling of the material is and how sensitive the behavior of impurities are to the state of the crystal.

It is not clear whether or not the presence of Mn affects the outdiffusion of Cr. Mn surface accumulation does occur during the Cr outdiffusions, as evidenced by SIMS. However, a depletion of Cr in the surface region is expected anyway as it is a normal result of the outdiffusion as discussed earlier. The manganese might be expected to enhance the depletion and result in higher measured effective D values. The fact that most of the D_{slow} values for the outdiffusion experiments are slightly higher that those for the junction diffusion experiments (which were not affected by Mn) suggests that the Mn is affecting the outdiffusion experiments.

The surface build-up of Cr in the junction samples after annealing (see figure 7-18 for an example of this) can also be attributed to the formation of gallium droplets and/or damage. This is a little different than the normal outdiffusion cases in that the surface, and hence Cr build-up, is removed from the

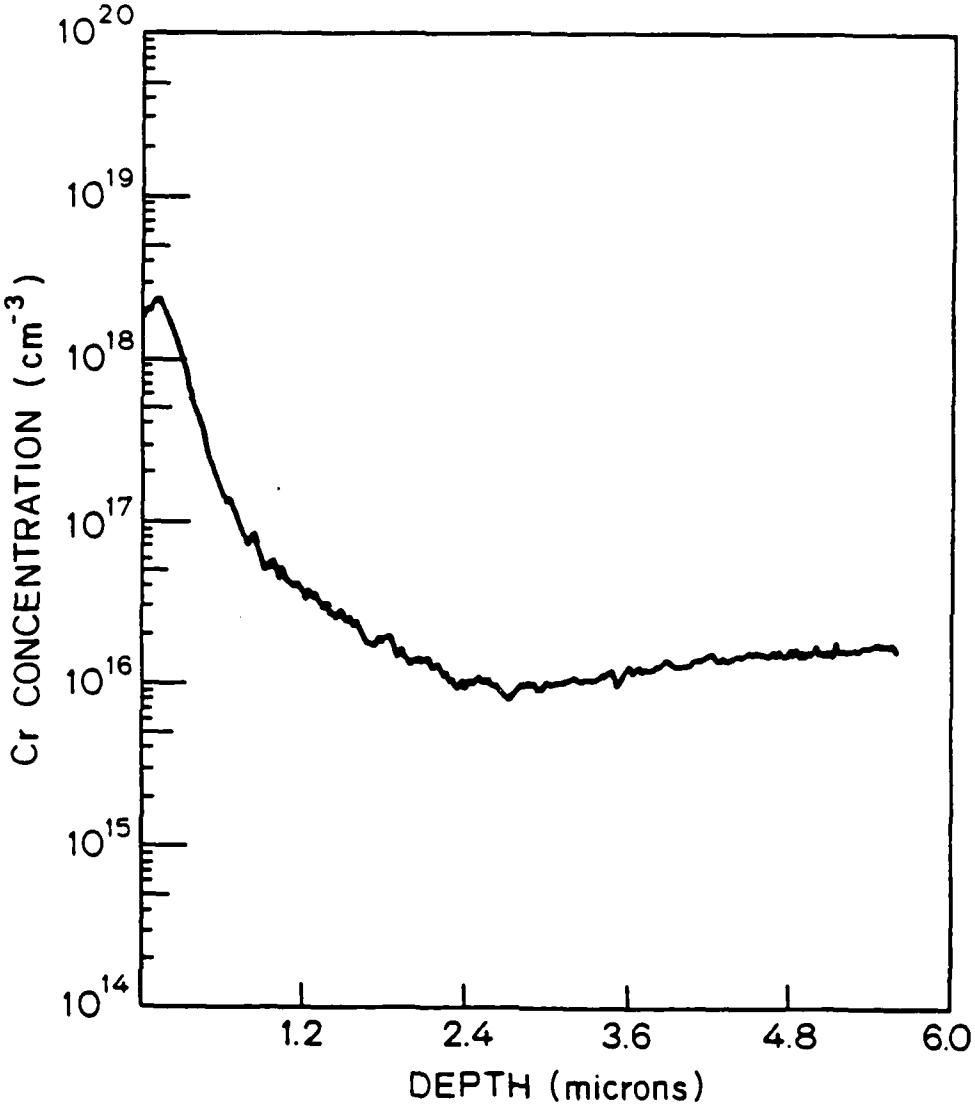

Figure 7-17. Cr concentration profile from 800°C, 1 hr. out-diffusion experiment, using different cleaning technique.

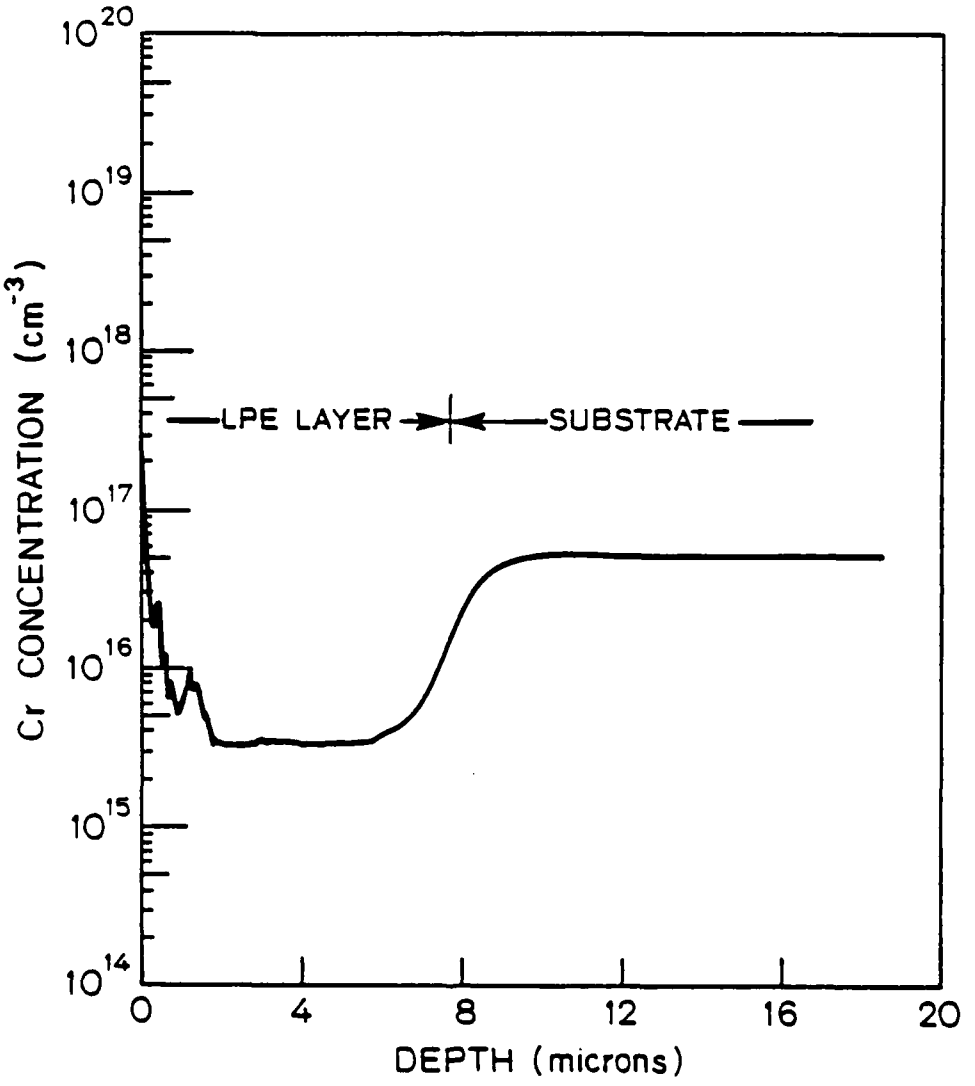

Figure 7-18. Cr concentration profile from 800°C, 1 hr. junction diffusion experiment, showing Cr build-up at surface.

source of chromium, sometimes by as much as 20 microns. But the substitutional/interstitial dissociative diffusion mechanism can easily explain this, as discussed in chapter 6; the fast interstitial Cr species can quickly diffuse from the substrate to the surface. (This is the answer to the researchers who could not explain how Cr got to the surface so fast based on the reported diffusion coefficients; the "reported" D values are the vacancy diffusion controlled Cr D values and only apply to the diffusion seen at the GaAs substrate/LPE layer interface.) Once the Cr interstials get to the surface, they can dissolve in the gallium phase, incorporate into the stressed or damaged surface region, or perhaps become subtitutional by reacting with excess vacancies diffusing in from the surface. Therefore, why the chromium can be at high concentration levels at the surface can be explained (dissolving in the Ga phase, etc.) as well as how it can get there so fast (interstitial diffusion).

Another use of the results of this section, and of earlier chapters, to explain other observations concerns Cr levels in LPE layers. For the junction diffusion experiments, as discussed earlier, undoped LPE GaAs on Cr-doped GaAs samples were desired. However, the first two samples obtained (from S.C. Chang) showed relatively high levels of Cr in the LPE layers, as measured by SIMS (see figures 7-19 and 7-20 for the SIMS profiles of such samples). In these samples, the meltback procedure was used just prior to growth of the LPE layer in order to remove any residual damage and/or impurities at the surface. (This is done by slightly raising the temperature

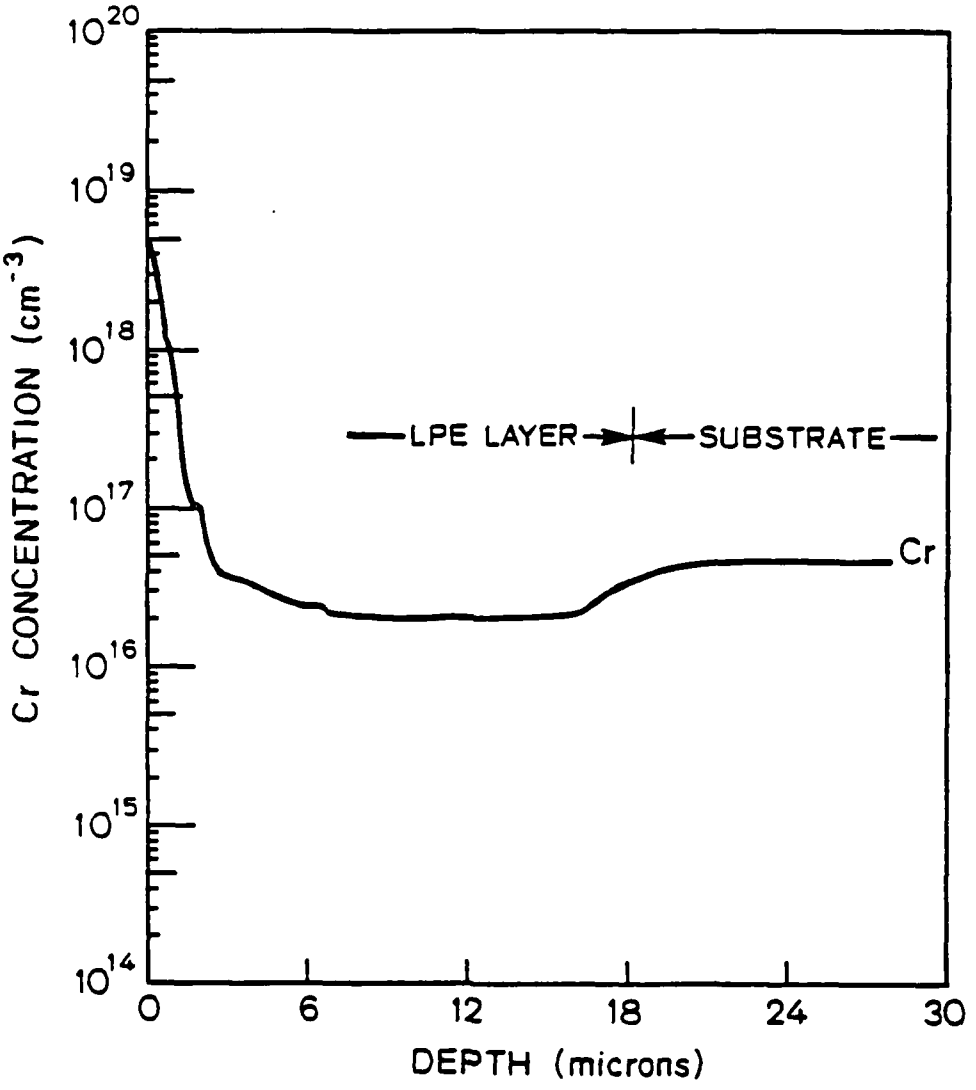

Figure 7-19. Cr concentration profile from junction diffusion sample, before diffusion anneal, grown with melt-back step.

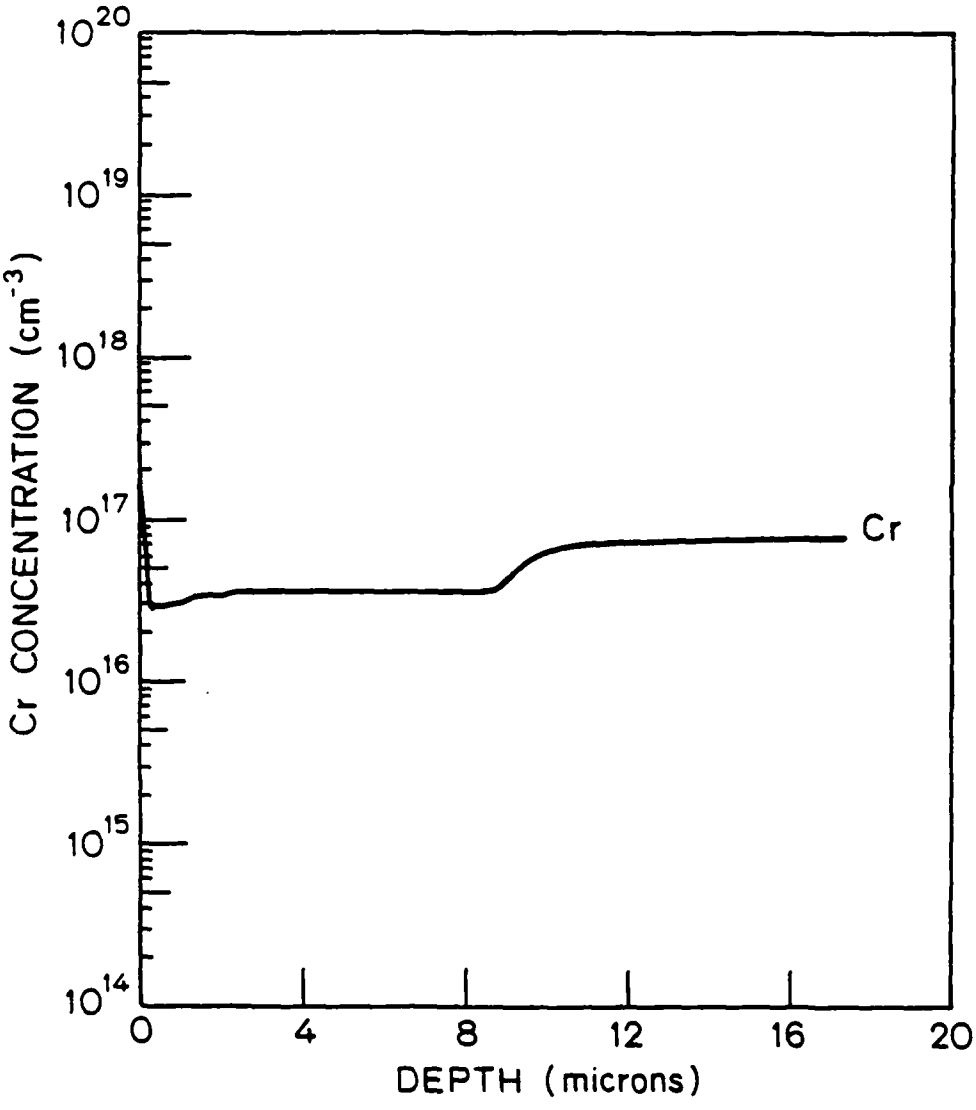

Figure 7-20. Cr concentration profile from junction diffusion sample, before diffusion anneal, grown with meltback step.

when $GaAs_{(s)}$ and $Ga_{(\ell)}$ (saturated with $GaAs_{(s)}$) are first in contact with each other, which results in some of the GaAs substrate melting and becoming part of the melt.) Because of the high Cr concentration in these LPE layers, these samples could not be used for the junction diffusion experiments. Samples were then produced without the meltback step. In these, the Cr level is very low in the LPE layer, as measured by SIMS (see figure 7-21). An explanation for the high level of Cr in the LPE in the first samples was sought.

Because the Cr level in the LPE layer is fairly uniform, it was initially assumed that the Cr that was detected was in solution. However, based on the solubility results, this was not possible. For a GaAs layer to be grown with these levels of Cr, it must be in equilibrium with a gallium-rich liquid or with ≈ 1-2 a/o Cr (based on distribution coefficient results). However, the gallium melt used had no Cr in it to begin with, and diffusion of Cr into the liquid during the growth procedure could not account for that much chromium in the melt. The only explanation was that the Cr was not in solution (i.e., not in GaAs). It was therefore presumed that the Cr was in $Ga_{(\ell)}$ inclusions. Optical micrographs were taken of the SIMS craters (see figures 7-22, 7-23, 7-24), which show evidence of $Ga_{(\ell)}$ inclusions in the SIMS craters of the meltback samples, while the craters of the other (low Cr level) samples show no such inclusions. Electron microprobe analysis revealed that the features are indeed mostly gallium (91 a/o Ga and 9 a/o As, which is exactly the composition of gallium, saturated with $GaAs_{(s)}$, for the growth temperature. (No chromium was

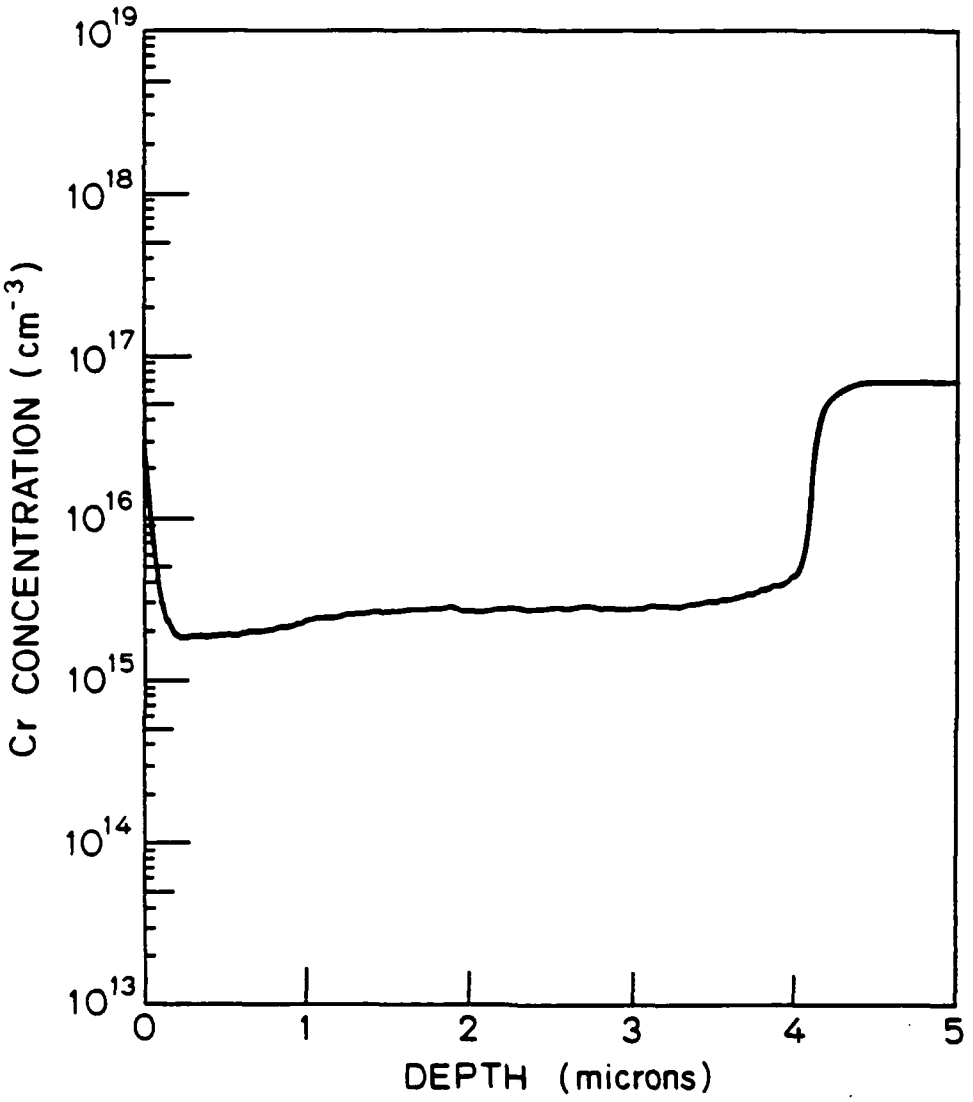

Figure 7-21. Cr concentration profile from, junction diffusion sample, before diffusion anneal, grown <u>without</u> melt-back step.

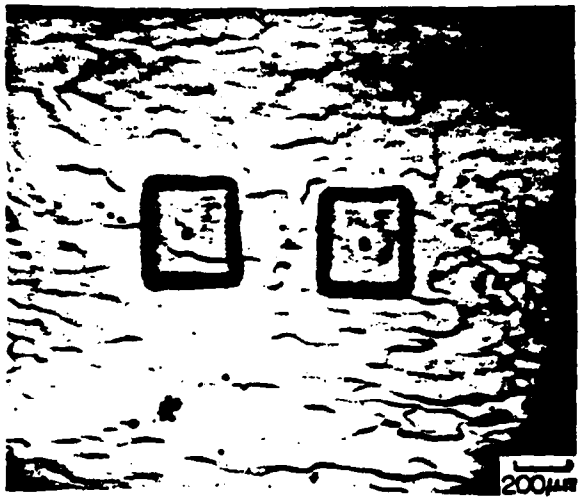

Figure 7-22. Optical micrograph (50X) of GaAs surface of melt-back sample, showing SIMS craters.

Figure 7-23. Optical micrograph (200X) of GaAs surface of melt-back sample, showing SIMS crater.

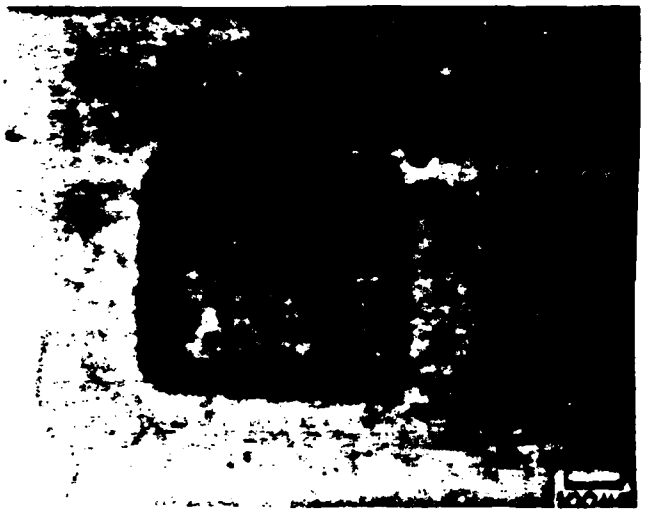

Figure 7-24. Optical micrograph (100X) of GaAs surface of non-meltback sample, showing SIMS crater.

detected, but for these levels in the LPE layer, none would be expected based on the detectability of the analysis technique.) Therefore, it was concluded that during the LPE growth, some $Ga_{(\ell)}$ inclusions remained imbedded in the GaAs layers, with substantial Cr dissolved in the $Ga_{(\ell)}$ which was then measured in the SIMS analysis. To test this theory, a SIMS Cr analysis was done on another area of one of the samples which showed the high Cr level. If the Cr was in solution in the $GaAs_{(s)}$, then all SIMS analysis should show the high Cr level; but if the Cr is concentrated in the few, and small, Ga inclusions, then some areas (which did have an inclusion in it) should show low levels of Cr on the LPE layer. Figure 7-25 is such a SIMS profile. As one can see, the Cr level in the LPE layer is very low (at the background level of Cr in GaAs by SIMS analyses), consistent with the theory.

The results suggest that perhaps it was just luck that the SIMS analyses of the two meltback samples just happened to hit areas with the Ga inclusion, while the others did not. However, it does appear that the meltback samples do have a somewhat larger number of these inclusions than the non-meltback samples (≈ 30 cm^{-2} vs. ≈ 15 cm^{-2}). The reason why the $Ga_{(\ell)}$ inclusions would be present in larger numbers after the meltback procedure is not known; however, others have observed this same phenomena (144).

The above treatment is a good illustration of how phase equilibria considerations and information are used in explaining observed phenomena.

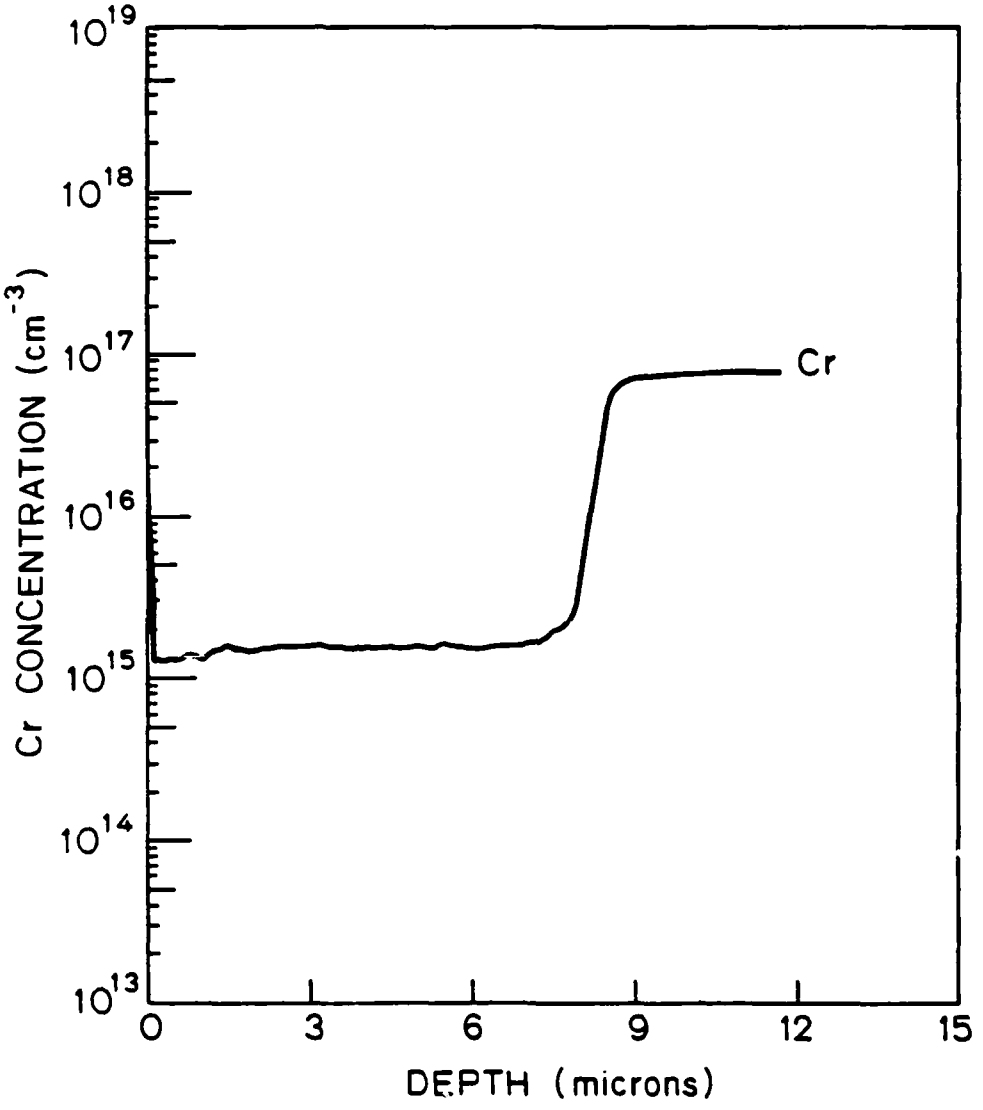

Figure 7-25. Cr concentration profile from meltback sample, but from different location than figure 7-19.

7.7 Summary of Surface Phenomena Studies

In this chapter, the unusual behavior of Cr seen in this work and in previous studies was examined and explained with the help of information learned from the phase equilibria, solubility, and diffusion sections of this work. In particular, the large Cr surface build-up after both indiffusion and outdiffusion is to a large part due to the formation of $Ga_{(\ell)}$ droplets or inclusions which have a high Cr solubility. The Cr depletion is due to the surface accumulation of manganese. It was also shown how substantial levels of Cr in LPE layers are a result of the presence of $Ga_{(\ell)}$ inclusions and not Cr in solid solution. In addition, the proposed diffusion mechanism for Cr in GaAs explains how the Cr can get to the surface region so quickly, i.e., via fast interstitials.

8. SUMMARY AND CONCLUSIONS

In this chapter a review of this research is given, followed by the major conclusions of the work. In addition, suggestions for further work in this area are presented.

The present research concerns the phase equilibria of the Ga-As-Cr ternary system and its application in solubility and diffusivity studies of Cr in GaAs. Using the anneal, quench, and x-ray diffration method and differential thermal analysis, the Ga-As-Cr ternary phase diagram was determined from room temperature to 1300°C for As a/o $\leq$ 50. This information was used to perform well-defined solubility and diffusion experiments, which were done by annealing GaAs and an appropriate Ga-As-Cr composition - as the Cr source or sink - for various times and temperatures in an evacuated closed quartz ampoule, and measuring the Cr concentration vs. depth in the GaAs using SIMS. The solubility of Cr in GaAs was determined as a function of position in the ternary phase diagram from 700 to 1000°C, and the results were checked by C-V measurements. Using these values and the solubility of Cr in $Ga_{(\ell)}$, as determined in the phase diagram studies, the distribution coefficient of Cr in GaAs was determined for this same temperature range. In addition, the solubility of Cr in doped (n-type) GaAs was studied. The diffusion of Cr in GaAs was studied by performing three types of diffusion experiments - indiffusion, outdiffusion, and junction diffusion - again under well-defined conditions. The diffusion behavior was modelled by a complex diffusion mechanism, and values for key parameters pertaining to the model were determined, including

two types of diffusion coefficients corresponding to two different regimes of the diffusion. In addition, unusual behavior of Cr in the surface region of GaAs was studied, specifically, the large build-up of Cr at the surface after all types of diffusion and depletion of Cr near the surface after indiffusion, and the causes for such behavior were determined. The results of these studies were applied to some of the results reported by others, which explained much of the observations of others concerning Cr in GaAs. Finally it was shown how Cr can be used as a probe to study the defect chemistry of GaAs, especially concerning other impurities and vacancies.

The major conclusions are summarized below:

(1) CrAs and Cr_3Ga, and not GaAs, are the dominant phases in the Ga-As-Cr ternary system, thus, most other phases are in equilibrium with them and not with GaAs.

(2) GaAs and Cr are not in equilibrium with each other under any condition; therefore, when heated together they will react with each other to form Cr-Ga and Cr-As phases.

(3) A large tie triangle region, containing $GaAs_{(s)}$, $CrAs_{(s)}$, and $Ga_{(\ell)}$, is a suitable source or sink for solubility and diffusion studies for Cr in GaAs; elemental Cr is not.

(4) The solubility of Cr in GaAs for the tie triangle region mentioned above increases from 1.2×10^{16} to 1.3×10^{17} cm^{-3} as the temperature increases from 700 to 1000°C. The solubility of Cr at a given temperature decreases considerably as the overall composition of the

system moves toward the Ga-rich corner.

(5) The distribution coefficient increases from 9×10^{-7} to 3×10^{-5} from 700 to 1000°C, but is virtually independent of Cr concentration at a given temperature.

(6) The Cr solubility increases with n-type doping in GaAs and decreases with p-type doping, consistent with Cr being a deep acceptor in GaAs.

(7) The diffusion of Cr in GaAs follows the substitutional/interstitial dissociative diffusion mechanism. In this, there are three regimes: the vacancy diffusion, the interstitial diffusion, and the vacancy regeneration controlled cases. The first first case dominates at shorter annealing times and lower temperatures, the second case dominates at longer annealing times and higher temperatures (and presumably for high dislocation densities), and the third case describes the behavior in between. The effective diffusion coefficient for the first case ranges from 4.0×10^{-13} to 1.2×10^{-11} $cm^2/sec.$ for 700 to 900°C, with an activation energy of 1.7 eV, and for the second case, ranges from 1.5×10^{-10} to 9.1×10^{-10} cm^2/sec from 750 to 1000°C, with an activation energy of 0.8 eV. The equilibrium time constant (or the vacancy regeneration rate), which describes the transition from the first case to the second, decreases from 1.3×10^5 to 3.0×10^3 sec. from 750 to 900°C, for LEC GaAs. It is considerably less at each temperature for Bridgman GaAs.

(8) The Cr diffusion and solubility is affected by defects in

GaAs, especially other impurities and vacancies. For example, donor impurities increase the Cr solubility but decrease the diffusivity - acceptors do the opposite, and increasing the gallium vacancy concentration decreases the time it takes for the extrapolated surface concentration of Cr to reach the solubility level. In addition, such defects as dislocations introduced by polishing, etc., probably affect Cr behavior.

(9) The anomalous build-up of Cr at the surface of GaAs is mostly due to the presence of a second phase - $Ga_{(\ell)}$ - which forms upon the incongruent vaporization of arsenic and which has a very high solubility of Cr (≈10 a/o at 700°C). Similarly, the large Cr concentration seen in LPE layers after growth using the meltback technique is due to the incorporation of Cr in $Ga_{(\ell)}$ inclusions that remain in the layer.

(10) The depletion region of Cr observed near the surface after indiffusion is due to uneven Mn distribution, which lowers the solubility of Cr in that region.

(11) The gettering of Cr to the surface is accomplished via fast Cr interstials.

The following are suggestions for further work in this area:

(1) Continue the use of Cr as a probe to study the defect chemistry of GaAs. As discussed earlier, since the behavior of Cr is very sensitive to the presence and behavior of defects in GaAs, the defects can be studied by

studying Cr. This would be particularly useful in investigating vacancies and dislocations, which are inherently difficult to study directly. Therefore, more work could be done studying the effects of dislocations and vacancies on the behavior of Cr in GaAs.

(2) The same types of studies done in this research on the Ga-rich side of the phase diagram can be done on the arsenic-rich side. Since many GaAs device manufacturers are going to the use of arsenic overpressure rather than encapsulents to prevent surface degradation, this would have practical applications.

(3) To study Cr diffusion in the absence of a concentration or activity gradient, one can do isoconcentration diffusion experiments. This also eliminates any non-uniform electrical effects on non-equilibrium effects. This can easily be done without the use of radioisotopes by diffusing Cr^{53}, a non-radioactive isotope, in Cr^{52}-doped GaAs, and using SIMS to measure the Cr^{53} concentrations (SIMS is mass specific). However, since: 1) the concentration of Cr in GaAs is so small (ppb), the activity coefficient is probably constant with concentration and virtually equal to unity anyway; 2) the diffusion in most cases follows the uncharged model; and 3) equilibrium is achieved rather quickly, especially at high temperatures, not much difference is expected for the behavior of Cr in isoconcentration conditions compared to concentration gradient conditions, except at low

temperatures (where the concentrations of Cr and electrically active defects are less than n_i) and for crystals with a large number of defects present.

(4) Study the interaction between Cr and the other materials present in GaAs devices, especially the materials used to make electrical contacts to GaAs. These include Au, Ge, Sn, Se, and Zn. Since Cr has a tendency to end up in the surface region of GaAs and to react with other materials, this could be a major problem in GaAs devices. Not only must the binary phase equilibria between Cr and the other elements be considered, but also the multi-component phase equilibria between all the elements present must be considered. The same concepts used in the present study can be, and should be, applied to these cases.

(5) Now that the mode of Cr diffusion in GaAs and the phase equilibria are known, one might now attempt to determine a way to keep Cr from adversely affecting the performance of GaAs devices. This may include preannealing the Cr-doped substrate under conditions such that it is saturated with gallium vacancies, thus reducing the tendency for conversion of Cr to the interstitial state and thus reducing the fast interstitial diffusion. Another possibility is using backside gettering or internal gettering, such as are used in silicon I.C. processing, to keep the Cr from getting into the active region.

APPENDIX - ERROR ANALYSIS

Error bars indicating the maximum expected error for the particular determinations have been included with each data point in figures 4-7, 4-9, 6-8, and 6-9. The reasoning behind such determinations for each case is as follows:

Cr Solubility, Figure 4-7

As discussed in Section 4.4.1, the reported maximum expected error for the SIMS analyses of Cr in GaAs is a factor of 1.5 to 2, and the standard deviation of several sample results is $\pm$ 50%. The solubility values were taken directly from SIMS Cr profiles after appropriate anneals, and therefore the error in the solubility is just the error in SIMS analysis (the error in extrapolating the profile to the surface was trivial in comparison to the error in SIMS). Thus, the maximum expected error for the solubility values is determined to be "a factor of 1.5". This means that for a reported value of 2×10^{16}, for example, the true value could be from 1.3×10^{16} to 3×10^{16}. This type of expected error, rather than $\pm$ 50 percent, is much more suited to data that is presented on a log scale.

Distribution Coefficient, Figure 4-9

The distribution coefficient, k, was calculated by dividing the solid solubility of Cr in GaAs by the liquid solubility of Cr in the Ga-rich liquid. The error in the solid solubility is determined to be "a factor of 1.5", as discussed above. The error in the liquid solubility, from the phase

diagram determinations, is estimated to be a factor of 1.3, resulting in an overall total expected error of a factor of 2.

Diffusion Coefficients, Figure 6-8

The diffusion coefficients were determined by fitting the diffusion model profiles to the actual profiles. The value of the diffusion coefficient depends on three parameters: 1) the relative concentration; 2) the depth; and 3) the annealing time. The relative concentration refers to the ratio of the impurity concentration at a given depth to either the surface concentration (for indiffusion results) or the bulk concentration (for outdiffusion results). In SIMS analysis, while the error in the absolute concentrations are somewhat large, the error in relative concentration are regarded as very small. This is especially true when the matrix atom profiles are very uniform, indicating uniform sputtering, as is the case in this research. Thus, this error is considered negligible. The depth determination, as measured by a DEKTAC instrument, has a reported error of 15%. Since D is proportional to the square of the depth, this results in an error of 1 - (1.15 x 1.15), or 32%. Finally, the error in annealing time, which also takes into account that it takes some time for the sample to reach the desired temperature, is estimated to be 10%. D is inversely proportional to t, so the net error is determined to be 1-(1.32 x 1.1) = 50%. In order to place this on a log scale, error bars representing a factor of 1.5 error are used.

Equilibrium Time Constant, Figure 6-9

The equilibrium time constant, Θ, for each temperature was determined from the ratio of the extrapolated surface concentration to the solubility concentration at that temperature, and the annealing time through the equation: $\Theta = -t/\ln(1-C_o/C_1)$. The best way to determine the maximum error for this is by taking the standard deviation of the results at each temperature for the various annealing times (the value for Θ should be the same for all times at each temperature). The maximum expected error is thus determined to be a factor of 1.5.

Error in Temperature

In all of the above mentioned graphs, the values are plotted against temperature. The absolute error in the temperature is estimated to be $\pm$ 5°C, or ≈0.5%, while the relative error, from one experiment to the next, is only $\pm$ 1°C, or ≈ 0.1%. The vertical error bars for this were not included in the graphs; however, one should be aware of this error in addition to the others.

REFERENCES

1. R.L. Van Tuyl, V. Kumar, D.C. D'Avanzo, T.W. Taylor, V.E. Peterson, D.P. Hornbuckle, R.A. Fisher, and D.B. Estreich, IEEE Trans. Electron Dev., ED 29, 1031 (1982).

2. A.M. White, in "Semi-Insulating III-V Materials; Nottingham 1980," G.J. Rees, Editor, pg. 3, Shiva Publ., London (1980).

3. R.N. Thomas, H.M. Hobgood, D.L. Barrett, in "Semi-Insulating III-V Materials, Nottingham 1980," G.J. Rees, Editor, pg. 77, Shiva Publ., London (1980).

4. Jeff Woolhouse, private communication.

5. B. Tuck and G.A. Adegboyega, J. Phys. D; Appl. Phys., 12, 1895 (1979).

6. K.K. Shih, J.W. Allen, and G.L. Pearson, U.S. Army Signal Corp. Contract NONR 225(83) and NASA Grant Ns6-555.

7. B. Tuck, "Introduction to Diffusion in Semiconductors," Peter Peregrinus Ltd., Stevenage, England (1974).

8. H.C. Casey, Jr. in "Atomic Diffusion in Semiconductors," D. Shaw, Editor, Plenom Press, N.Y. (1973).

9. M.B. Panish, J. Phys. Chem. Solids, 27, 291 (1966).

10. H.C. Casey and M.B. Panish, Trans. Metall. Soc. of AIME, 242, 406 (1968).

11. A. Reisman, "Phase Equilibria," Academic Press, N.Y. (1970).

12. R.E. Dickerson, "Molecular Thermodynamics," W.A. Benjamin, Inc., Menlo Park (1969).

13. J.S. Blakemore, J. of Appl. Phys., 53 (10), R123 (1982).

14. J.D. Bornand and P. Feschette, J. Less Common Metals, 29, 81 (1972).

15. V.H. Meissner and K. Schubert, Z. Metalk., 56, 523 (1965).

16. M. Phillipe, Acta Cryst., B31, 477 (1975).

17. M. Yuzuri, J. Phys. Soc. of Jap., 15(11), 2007 (1960).

18. H. Boller, H. Wolfsgruber, and H. Nowotny, Monatsch Chem., 98, 2356 (1967).

19. H. Baurecht, H. Boller, and H. Nowotny, Mh. Chem., 101, 1696 (1970).

20. H. Nowotny and O. Arstad, Z. Physik. Chem. B38, 461 (1938).

21. H. Baurecht, H. Boller, and H. Nowotny, Mh. Chem., 102, 373 (1971).

22. H. Wolfsgruber, H. Boller, and H. Nowotny, Mh. Chem., 99, 1230 (1968).

23. W. Jeitschko and P.C. Donohue, Acta Cryst. B29, 783 (1973).

24. G.M. Martin, J. Appl. Phys., 50, 467 (1979).

25. M.R. Brozel, B. Tuck, D. Rumsby, and R.M. Ware, submitted for Publication.

26. G.R. Cronin and R.W. Haisty, J. Electrochem. Soc., 111(7), 874 (1964).

27. R.K. Willardson and W.R. Allred, Inst. Phys. London, 35 (1967).

28. T. Udagawa and T. Nakanisi, Jap. J. of Appl. Phys., 20(8), 579 (1981).

29. D.W. Woddard, Ph.D. Thesis, Cornell U. (1979).

30. E. Andre and J.M. LeDuc, Mater. Res. Bull., 4, 149 (1969).

31. L.H. Schwartz and J.B. Cohen, "Diffraction from Metals," Academic Press, New York (1977).

32. F.N. Rhines, "Phase Diagrams in Metallurgy," McGraw Hill, New York (1956)

33. A.M. Alper (ed.), "Phase Diagrams, Theory, Principles, and Techniques," Academic Press, N.Y. (1970).

34. Y. Sato, Jap. J. Appl. Phys., 12, 242 (1973).

35. R.W. Haisty and G.R. Cronin, "Proc. of 7th Intl. Conf. of Phys. of Sem." p. 1161, Dunod, Paris (1974).

36. M.R. Brozel, J. Butler, R.C. Newman, A. Ritson, D.J. Stirland, and C. Whitehead, J. Phys. C: Solid State Phys., 11, 1857 (1978).

37. H. Morkoc, C. Hopkins, C.A. Evans, Jr., and A.Y. Cho, J. Appl. Phys., 51(11), 5986 (1980).

38. M. Bonnet, J.P. Duchemin, A.M. Huber, and G. Morillot, in "Semi-Insulating III-V Materials, Nottingham 1980," G.J. Rees, Editor, pg. 68, Shiva Publ., London (1980).

39. N.T. Linh, A.M. Huber, P. Etrenne, G. Morillot, P. Duchemin, and M. Bonnet, in "Semi-Insulating III-V Materials, Nottingham 1980," G.J. Rees, Editor, pg. 206, Shiva Publ., London (1980).

40. V. Eu, M. Feng, W.B. Henderson, H.B. Kim and J.M. Whelan, Appl. Phys. Lett. 37(5), 473 (1980).

41. M. Feng, V. Eu, H. Kamber, and W.B. Henderson, J. Electron Mat., 10(6), 973 (1981).

42. A.M. Huber, G. Morillot, N.T. Linh, P.N. Favennec, B. Deveaud, and B. Toulouse, Appl. Phys. Lett., 34(12), 858 (1979).

43. V.R. Deline, U. of Illinois Ph.D. Thesis (1978).

44. A.W. Czanderna, "Methods of Surface Analysis," Elsevier Scientific Pub. Co., New York (1975).

45. E. Zinner, J. Electrochem. Soc., 130(5), 199C (1983).

46. R.A. Swalin, "Thermodynamics of Solids," John Wiley and Sons, New York (1962).

47. C.S. Thurmond and J.S. Struthers, J. Electrochem. Soc., 57, 831 (1953).

48. B. Deveaud and P.N. Favennec, Sol. State Commun., 24, 473 (1977).

49. G.H. Stauss and J.J. Krebs, Inst. Phys. Conf. Ser., 33a, 84 (1977).

50. P.M. Asbeck, J. Tandon, B.M. Welch, C.A. Evans, Jr., and V.R. Deline, IEEE Elect. Dev. Lett., 1(3), 35 (1980).

51. U. Kaufmann and J. Schneider, Appl. Phys. Lett., 36(a), 747 (1980).

52. F.A. Kroger, "The Chemistry of Imperfect Crystals," John Wiley and Sons, Inc., New York (1964).

53. G.M. Martin, in "Semi-Insulating III-V Materials, Nottingham 1980," G.J. Rees, Editor, pg. 13, Shiva Publ., London (1980).

54. R.A. Swalin, in "Atomic Diffusion in Semiconductors," D. Shaw, Editor, pg. 65-112, Plenum Press, New York (1973).

55. S.M. Sze, "Physics of Semiconductor Devices," John Wiley and Sons, New York (1981).

56. F.C. Frank and D. Turnbull, Phys. Rev., 104(3), 617 (1956).

57. A.G. Tweet and C.J. Gallagher, Phys. Rev., 103, 828 (1956).

58. D.L. Kendall, Appl. Phys. Lett., 4(4), 67 (1964).

59. B. Tuck and P.R. Jay, J. Phys. D: Appl. Phys., 11, 1413 (1978).

60. K. Nighitani, K. Nagahama, and T. Murotani, J. Electronic Mat., 12(1), 125 (1983).

61. B. V. Dutt, A.K. Chin, and W.A. Bonner, J. Electrochem. Soc., 128(a), 2014 (1981).

62. S.I. Rembeza, Soviet Phys. - Semiconductors, 1(4), 516 (1967).

63. O.J. Sprokel and J.M. Fairfield, J. Electrochem. Soc., 112, 200 (1965).

64. F.A. Huntley and A.F.W. Willoughby, Solid-State Electronics, 12, 1231 (1970).

65. M. Hill, M. Lietz, and R. Sittig, J. Electrochem. Soc., 129 (7), 1579 (1982).

66. H.F. Schaake, "The Diffusion of P in Si From High Surface Concentrations," to be published.

67. R.L. Longini, Solid-State Elec., 5, 127 (1962).

68. K.K. Shih, J.W. Allen, and G.L. Pearson, J. Phys. Chem. Solids, 29, 379 (1968).

69. D. Shaw and S.R. Showan, Phys. Stat. Sol., 32, 109 (1969).

70. D.L. Kendall and M.E. Jones, Sol. State Device Res. Conference, Stanford, 1961.

71. L.C. Chang and G.L. Pearson, J. Phys. Chem. Solids, 25, 23 (1964).

72. F.A. Cunnel and C.H. Gooch, J. Phys. Chem. Sol., 15, 127 (1960).

73. B. Tuck and M.A.H. Kadhim, J. of Mat. Sci., 7, 585 (1972).

74. M.A.H. Kadhim and B. Tuck, J. of Mat. Sci., 7, 68 (1972).

75. G. Chiaretti and C. Cognetti, J. Electrochem. Soc., 128(10), 2199 (1981).

76. A.J.N. Houghton and B. Tuck, Solid State Elect., 75 (6), 441 (1982).

77. D. L. Kendall, in "Semiconductors and Semimetals, Vol. 4," Willardson and Beer, Editors, Academic Press, New York (1968).

78. H. Rohdin, M.W. Muller, and C.M. Wolfe, J. Electronic Mat., 11 (3), 517 (1982).

79. S.K. Ghandhi, "VLSI Fabrication Principles, Si and GaAs," John Wiley and Sons, New York (1983).

80. M.D. Sturge, Proc. Phys. Soc., London, 73, 297 (1957).

81. D. L. Kendall, Ph.D. Thesis, Stanford U. (1965).

82. P.M. Asbeck, AIME Electronic Materials Conference, Santa Barbara, June, 1981.

83. S.Y. Chiang and G.L. Pearson, J. Appl. Phys., 46, 2986 (1975).

84. L.R. Weisberg and J. Blanc, Phys. Rev., 131 (4), 1548 (1963).

85. J. R. Arthur, J. Phys. Chem. Solids, 28, 2257 (1967).

86. F. Van der Maesen and J.A. Brenkman, J. Electrochem. Soc., 102, 229 (1955).

87. M. Maruyama, J. Appl. Phys. Japan, 7, 476 (1968).

88. J.F. Black and E.D. Jungbluth, J. Electrochem. Soc., 114, 189 (1967).

89. U. Gösele, W. Frank, and H. Seeger, Appl. Phys., 23, 361 (1980).

90. H.F. Schaake, J.H. Tregilgas, J.D. Beck, and M.A. Kinch, "Observation of a New Gettering Mechanism in Semiconductors," to be published.

91. F.A. Huntley and A.F.W. Willoughby, J. Electrochem. Soc., 120, 414 (1973).

92. H.F. Schaake, private communication.

93. M.D. Zahari and B. Tuck, J. Phys. D: Appl. Phys., 15, 1741 (1982).

94. P.G. Shewmon, "Diffusion in Solids," McGraw-Hill, New York (1963).

95. C.S. Fuller and K.B. Wolfstirn, J. Electrochem. Soc., 114, 856 (1967).

96. B. Goldstein, Phys. Rev., 121, 1305 (1961).

97. H.J. Stocker, Phys. Rev., 130, 2160 (1963).

98. B. Boltaks and B. Sokolov, B.I.B. and V.I. Sol. Fiz., Tuerg. Tela, 6, 771 (1964).

99. S.S. Khludkov, G.L. Prikhod'ko, and T.A. Karelina, Izu, Akad. Nauk. SSSR, Neorg. Mater., 8, 1044 (1972).

100. H.B. Kim and D. Barrett, Inst. Phys. Conf. Series, 33b, 136 (1977).

101. J.P. Donnelly, C.O. Bozler, and W.T. Lindley, Solid State Electronics, 20, 273 (1977).

102. D.L. Partin, A.G. Milnes, and L.F. Vassamillet, J. Electron. Mater., 7, 279 (1978).

103. C.A. Evans, Jr., V.R. Deline, T.W. Sigmon, and A. Lidow, Appl. Phys. Lett., 35(3), 291 (1979).

104. C.A. Evans, Jr., C.G. Hopkins, J.C. Norberg, V.R. Deline, R.J. Blattner, R.G. Wilson, D.M. Jamba, and Y.S. Park, in "Semi-Insulating III-V Materials, Nottingham 1980," G.J. Rees Editor, pg. 138 Shiva Publ., London (1980).

105. P.N. Favannec and H. L'Haridon, Appl. Phys. Lett., 35(a), 699 (1979).

106. P.N. Favennec, M. Gauneau, H. L'Haridon, B. Deveaud, C.A. Evans, Jr., and R.J. Blattner, Appl. Phys. Lett., 38(4), 271 (1981).

107. P.N. Favannec and H. L'Haridon, in "Semi-Insulating III-V Materials, Nottingham 1980," G.J. Rees, Editor, pg. 130, Shiva Publ., London (1980).

108. T. Udagawa, M. Higashiura, and T. Nakanisi, in "Semi-Insulating III-V Materials, Nottingham 1980," G.J. Rees, Editor, pg. 108, Shiva Publ., London (1980).

109. P.K. Vasudev, R.G. Wilson, and C.A. Evans, Jr., Appl. Phys. Lett., 36(10), 837 (1980).

110. R.G. Wilson, P.K. Vasudev, D.M. Jamba, C.A. Evans, Jr., and V.R. Deline, Appl. Phys. Lett., 36, 215 (1980).

111. R.G. Wilson, J. Appl. Phys., 52(6), 3954 (1981).

112. J. Kasahara and N. Watanabe, Jap. J. of Appl. Phys., 19(3) L151 (1980).

113. T.J. Magee, H. Kawayoshi, and R.K. Ormond, L.A. Christel, J.F. Gibbons, C.G. Hopkins, C.A. Evans, Jr., and D.S. Day, Appl. Phys. Lett., 39(11), 906 (1981).

114. T.J. Magee, R.D. Ormond, C.A. Evans, Jr., R.J. Blattner, R.M. Malbon, D.S. Day, and R. Sankaron, Appl. Phys. Lett., 38(7), 473 (1981).

115. T.J. Magee, K.S. Lee, R. Ormond, C.A. Evans, Jr., R.J. Blattner, and C. Hopkins, Appl. Phys. Lett., 37(7), 635 (1980).

116. H. Yagita and T. Onuma, J. Appl. Phys. 53(2), 1218 (1982).

117. D.K. Sadana, J. Washburn, T. Zee, and R.G. Wilson, J. Appl. Phys., 53(a), 6413 (1982).

118. F. Simondet, C. Venger, G.M. Martin, and J. Chaumont, in "Semi-Insulating III-V Materials, Nottingham 1980," G.J. Rees, Editor, pg. 100, Shiva Publ., London (1980).

119. M.N. Yoder, in "Semi-Insulating III-V Materials, Nottingham 1980," G.J. Rees, Editor, pg. 281, Shiva Publ., London (1980).

120. B. Tuck, G.A. Adegboyega, P.R. Jay, and M.J. Cardwell, Conf. Ser. Inst. Phys., 45, 114 (1979).

121. J. Kasahara, M. Arai, and N. Watanabe, J. Appl. Phys. 50(12), 8224 (1979).

122. J. Kasahara and N. Watenabe, in "Semi-Insulating III-V Materials, Nottingham 1980," G.J. Rees, Editor, pg. 115, Shiva Publ., London (1980).

123. T.J. Magee, J. Hung, V.R. Deline, and C.A. Evans, Jr., Appl. Phys. Lett., 37(1), 53 (1980).

124. T.J. Magee, J. Peng, J.D. Hong, C.A. Evans, and V.R. Deline, Phys. Stat. Sol., 55, 169 (1979).

125. T.J. Magee, J. Peng, J.D. Hong, Charles Evans, Jr., V.R. Deline, and R.M. Malborn, Appl. Phys. Lett., 35(3), 277 (1979).

126. B.V. Kozeikin and I.A. Frolov, Izu. Akad. Nauk. SSSR Neorg. Mater., 13, 1515 (1977).

127. S.C. Palmateer, W.J. Schaff, A. Galuska, J.D. Berry, and L.R. Eastman, Appl. Phys. Lett., 42(2), 183 (1983).

128. M. Binet, Electronics Lett., 11(24), 580 (1975).

129. N.W. Muller, private communication.

130. S.C. Chang, Ph.D. Thesis, Stanford University (1983).

131. L. Boltzmann, Ann. Physik, 53, 960 (1894).

132. C. Matano, Japan Phys., 8, 109 (1933).

133. J. Kasahara, M. Arai, and N. Watanabe, J. Appl. Phys., 50(1), 541 (1979).

134. C.D. Thurmond, J. Phys. Chem. Solids, 26, 785 (1965).

135. A. Lidow, Ph.D. Thesis, Stanford U. (1977).

136. R.M. Malbon, D.H. Lee, and J.M. Whelan, J. Electrochem. Soc., 123, 1413 (1976).

137. M.M. Mandural, Ph.D. Thesis, Stanford U. (1981).

138. B.I. Boltaks, S.I. Rembeza, and M.K. Bakhadyrkhanov, Soviet Phys. Sol. State, 10(2), 432 (1968).

139. P.B. Klein, P.E.R. Nordquist, and P.G. Siebermann, J. Appl. Phys., 51(a), 4861 (1980).

140. R. Zucca, Inst. Phys. Serv., 33(b), 228 (1977).

141. J. Hallais, A. Mircea-Roussel, J.P. Farges, and G. Poibleud, Inst. Phys. Conf. Ser., 33b, 220 (1976).

142. A. Lidow, J.F. Gibbons, T. Magee, and J. Peng, J. Appl. Phys., 49(10), 5213 (1978).

143. J. Gyulai, J.W. Mayer, I.V. Mitchell, and V. Rodriquez, Appl. Phys. Lett., 17, 332 (1970).

144. B.L. Mattes, personal communication.

CONTRACT N00014-80-C-0482

Office of Naval Research 1
Code 414
Arlington, VA 22217

Naval Research Laboratory
4555 Overlook Avenue, S.W.
Washington, DC 20375
Code 6820 1

Defense Documentation Center 12
Building 5, Cameron Station
Alexandria, VA 22314

Dr. D. Shaw 1
Texas Instruments
Central Research Lab
M.S. 134
13500 North Central Expressway
Dallas, TX 75265

Dr. F. Eisen 1
Rockwell International
Science Center
P.O. Box 1085
Thousand Oaks, CA 91360

Dr. R. Bell, K-101 1
Varian Associates, Inc.
611 Hansen Way
Palo Alto, CA 94304

Professor L. Eastman 1
Cornell University
Phillips Hall
Ithaca, NY 14853

Professor C. Wolfe 1
Washington University
Semiconductor Research Laboratory
St. Louis, MO 63130

Professor August F. Witt 1
Massachusetts Institute of Technology
Room 13-4134
Department of Material Science
and Engineering
Cambridge, MA 02139

Dr. C. Krumm 1
Hughes Research Laboratory
3011 Malibu Canyon Road
Malibu, CA 90265

Dr. Sven Roosild 1
DARPA/DSO
1400 Wilson Blvd.
Arlington, VA 22209

Dr. Harvey Nathanson 1
Westinghouse R&D Center
1310 Beulah Road
Pittsburgh, PA 15235

Dr. Richard A. Reynolds 1
Deputy Director, Defense
Sciences Office
Defense Advanced Research
Projects Agency
1400 Willson Blvd.
Arlington, VA 22209

Dr. Joseph A. Saloom 1
MACOM, Inc.
Corporate Components
Technology Center
South Avenue, Building 7
Burlington, MA 01803

Dr. Jeff Woolhouse 1
Advanced Research and
Applications Corporation
1223 E. Arques Avenue
Sunnyvale, CA 94086

Professor James Harris 1
Stanford University
Stanford Electronics Laboratories
Department of Electrical Engineering
Standford, CA 94305

END

FILMED

2-85

DTIC